Assessment of cardiopulmonary function by contrast-enhanced echocardiography

Assessment of cardiopulmonary function by contrast-enhanced echocardiography

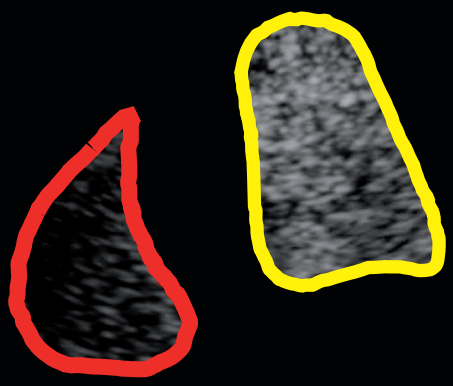

Ingeborg H.F. Herold

Trans-thoracic contrast-enhanced four chamber view, regions of interest were drawn in right (red) and left (yellow) ventricle. Acoustic intensity dilution curves were obtained from backscattered ultrasound by the microbubbles within the regions of interest (lower panel).

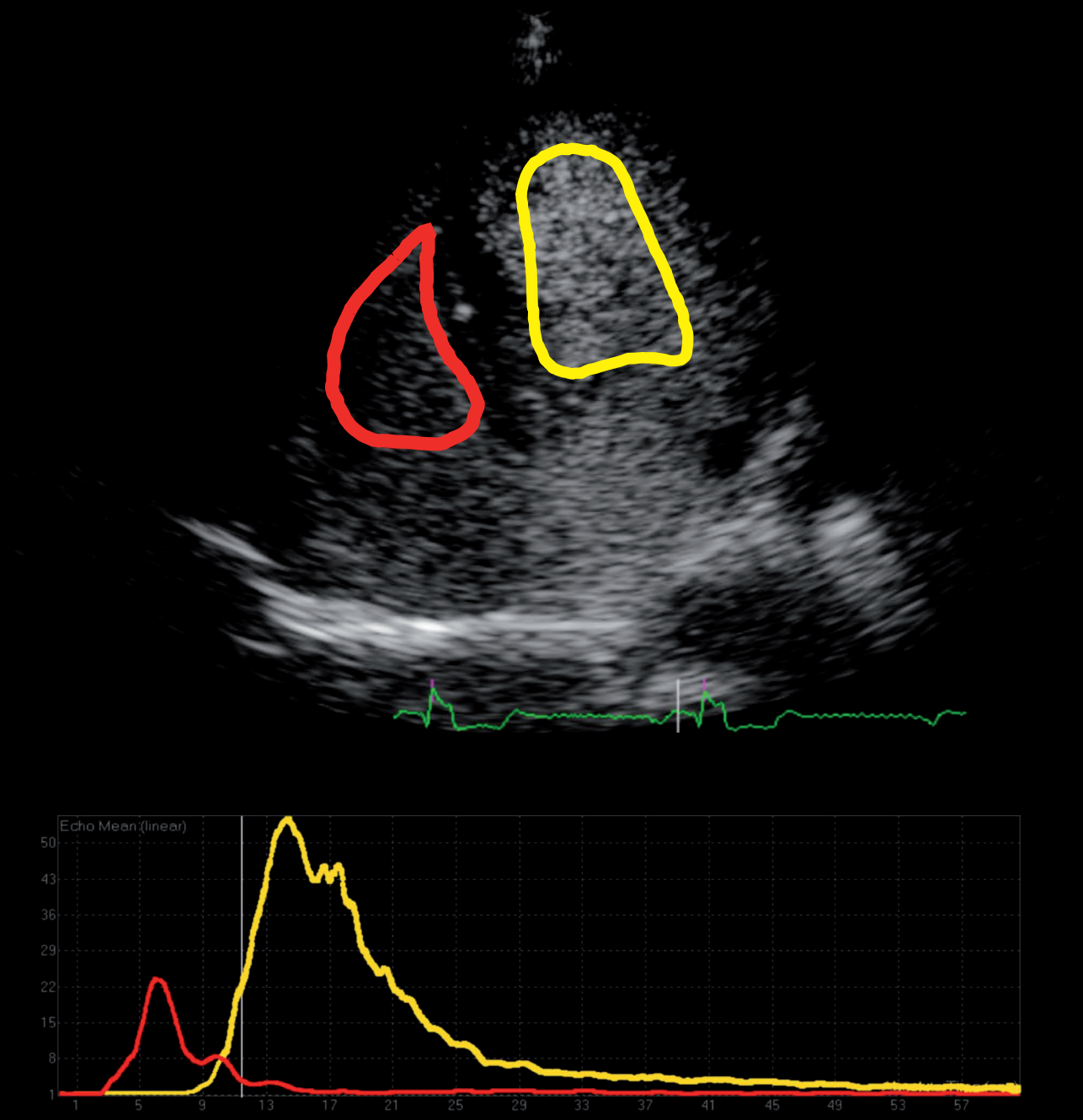

Assessment of cardiopulmonary function by contrast-enhanced echocardiography

Ingeborg Henriëtte Franziska Herold

Layout of this thesis was financially supported by:
Philips Healthcare, Bracco Imaging en Catharina ziekenhuis Eindhoven.
Printing of this thesis was financially supported by Eindhoven University of Technology.

Layout and printed by: Optima Grafische Communicatie, Rotterdam, the Netherlands

ISBN: 978-94-6169-925-1

Assessment of cardiopulmonary function by contrast-enhanced echocardiography

Proefschrift

ter verkrijging van de graad van doctor aan de Technische Universiteit Eindhoven, op gezag van de rector magnificus prof.dr.ir. F.P.T. Baaijens, voor een commissie aangewezen door het College voor Promoties, in het openbaar te verdedigen op donderdag 17 november 2016 om 16:00 uur

door

Ingeborg Henriëtte Franziska Herold

geboren te Utrecht

Dit proefschrift is goedgekeurd door de promotor en de samenstelling van de promotiecommissie is als volgt:

voorzitter:	prof.dr.ir. A.C.P.M. Backx
1e promotor:	prof.dr. H.H.M. Korsten
copromotoren:	dr.ir. M.Mischi
	dr. R.A. Bouwman
leden:	prof.dr.ir. J.W.M. Bergmans
	prof.dr. W. Buhre
	prof.dr. J.Kesecioglu
adviseur:	prof.dr.N.H.J. Pijls

Het onderzoek of ontwerp dat in dit proefschrift wordt beschreven is uitgevoerd in overeenstemming met de TU/e Gedragscode Wetenschapsbeoefening.

Voor mijn ouders

Summary

ASSESSMENT OF CARDIOPULMONARY FUNCTION BY CONTRAST-ENHANCED ECHOCARDIOGRAPHY

In daily practice, cardiologists and intensivists need estimates of cardiac preload and cardiopulmonary performance. Methods used to obtain these estimates require either central catheterization or complex imaging facilities; the latter is unsuitable for critically ill patients. For the assessment of the cardiopulmonary condition, pulmonary and intrathoracic blood volumes are valuable parameters that have been correlated in the literature with cardiac preload and different classes of heart failure. In particular, pulmonary blood volume can be indirectly estimated by the transpulmonary transit time of an indicator bolus. This parameter is referred to as pulmonary transit time (PTT).

This thesis describes the estimation of PTT by contrast-enhanced ultrasound (CEUS). The transit times were estimated using the indicator dilution theory, by fitting proper dilution models to the measured indicator dilution curves. To this end, the relationship between the concentration of ultrasound contrast agents (UCA, the adopted indicator) and the backscattered acoustic intensity was established. The acoustic backscatter from the diluted UCA was recorded using an ultrasound scanner. A dedicated in-vitro setup was realized and employed to validate the adopted dilution models and signal analysis. Recording of the passage of an UCA bolus was investigated and quantified in regions of interest in order to generate indicator dilution curves. In-vitro, the measurement was performed along tubes with a controlled flow.

The resulting indicator dilution curves were fitted according to the local density random walk model, which gives a physical description of the bolus transport process. The model describes the indicator dilution curve by the mean transit time (μ), skewness of the curve (λ), and area under the curve. The skewness of the curve is proportional to the ratio between convection and diffusion. In-vitro volumes were estimated by multiplying the flow by the difference in mean transit time at two different sites. In-vivo, the regions of interest were drawn in the cardiac chambers. The PTT was estimated as the difference in mean transit time between the left and right heart chambers.

In the first part of the thesis, the estimated volumes using CEUS and thermodilution were compared in-vitro with an absolute reference. Thermodilution uses cold saline as indicator and is frequently applied in clinical practice. In addition, in the second part, a validation study was performed in patients measuring pulmonary blood volumes using transesopageal CEUS and transpulmonary thermodilution. Thermodilution showed some drawbacks due to heat loss, therefore another comparison study was performed in patients

by estimating PTTs with dynamic contrast-enhanced MRI (DCE-MRI), using gadolinium as indicator. The transpulmonary dilution response was estimated by system identification techniques and evaluated by comparing λ in healthy volunteers and heart failure patients using DCE-MRI. In the third part, reliability, repeatability, and reproducibility of the PTT estimate was investigated in fifteen patients who received three different doses of UCA. Eight raters received the fifteen echoloops and drew twice regions of interest within the endocardial borders at two time moments. PTTs by automatically obtained regions were also estimated and compared with manually obtained PTTs. Additionally, in the last part; PTT was correlated with different echocardiographic heart failure parameters in patients and with NT-proBNP, which is a biomarker for acute heart failure. In a large observational study over two years, the effect of cardiac resynchronization therapy on the PTT was investigated. Moreover, the ability of PTT to predict response to cardiac resynchronization therapy was investigated.

The main results showed that CEUS-estimated PTT could accurately measure volumes in an in-vitro model. Pulmonary blood volumes estimated by CEUS in patients showed a good correlation with thermodilution, and the volumes measured by CEUS agreed better with the volumes presented in the literature. PTT estimated by CEUS and DCE-MRI correlated strongly. The correlation of PTT with different echocardiographic parameters was moderate to strong. PTT by both DCE-MRI and CEUS correlated strong with NT-proBNP. The transpulmonary dilution response using DCE-MRI showed a significant difference in the skewness parameter, λ, between healthy volunteers and patients; moreover, the λ estimates were highly repeatable. The reliability, repeatability, and reproducibility of PTT was strong. Furthermore, the automatically obtained PTT also showed a strong correlation with the manual obtained PTTs. The effect of cardiac resynchronization therapy resulted in a general PTT improvement (reduction). Within the responder group PTT decreased significantly, whereas the PTTs of non-responders related to changes in end-systolic volume, showed no significant change. In addition, PTT measured before cardiac resynchronization therapy was significantly lower in patients who responded to the therapy than those who did not respond.

In conclusion, CEUS is a minimally-invasive imaging procedure, which shows low dependency on image quality and is bedside applicable. PTT correlated with echocardiographic and biochemical heart failure parameters. The effect of cardiac resynchronization therapy on PTT was significant and showed possible predictive value for the selection of responders to the therapy. PTT can therefore provide an additional valuable parameter to assist clinicians in diagnosis, prognosis, and therapy of cardiopulmonary dysfunction.

Samenvatting

Evaluatie van de hartfunctie is belangrijk in de cardiologie, intensive-care (IC) en de operatiekamer (OK). De beschikbare technieken om de hartfunctie te evalueren, vereisen vaak plaatsing van catheters in de grote bloedvaten rond het hart (longslagader of bovenste holle ader) of complexe beeldvormingstechnieken, zoals een magneetscan (MRI) of nucleaire scan. Deze laatste technieken zijn ongeschikt voor een kritiek zieke patiënt op de IC of OK. Echocardiografie is veel minder belastend en overal toepasbaar (beddenhuis, OK, IC). Door gebruik te maken van echocontrast (CEUS = Contrast-enhanced Ultrasound) kan niet alleen de hartfunctie in veel gevallen beter worden geëvalueerd, maar kunnen ook andere metingen minimaal invasief worden uitgevoerd. Eén van die metingen is het pulmonale bloedvolume. Voor het beoordelen van de cardiopulmonale functie zijn intrathoracale- en pulmonale bloedvolumes waardevolle parameters, die in de literatuur gerelateerd zijn aan de voorbelasting van het hart en de ernst van hartfalen. Deze parameter wordt indirect gemeten door de tijd te meten die een bolus echocontrast nodig heeft om de longen te passeren. Deze parameter wordt de pulmonale transittijd (PTT) genoemd.

Dit proefschrift beschrijft de bepaling van de PTT met CEUS. De transittijden worden gemeten door gebruik te maken van de indicator-dilutie theorie en de juiste dilutie modellen toe te passen op de geregistreerde indicator-dilutiecurven. Hiervoor werd eerst de relatie tussen de concentratie echocontrastvloeistof en de teruggekaatste akoestische intensiteit onderzocht. De teruggekaatste akoestische intensiteit van het verdunde echocontrast werd gemeten met behulp van een echomachine. In een speciaal ontwikkeld in-vitro model werd vervolgens het toegepaste dilutiemodel en de signaal analyse gevalideerd. Vervolgens kon, in-vitro, de passage van een bolus echocontrast in een netwerk van buizen worden geregistreerd met echo-opnames. Indicator-dilutiecurves werden verkregen door op aangemerkte plaatsen in de opstelling, de zogenoemde "regions of interest", de akoestische intensiteit te meten.

Het "Local Density Random Walk model" (diffusie met drift verdeling), wat een fysische beschrijving geeft van het transportproces van een bolus indicator in een vloeistofstroom, gebruikten we voor de interpretatie van de gemeten curves. Dit model beschrijft de indicator-dilutiecurve, met de gemiddelde transittijd (μ), de scheefheidsfactor van de curve (afhankelijk van de symmetrie van de curve) (λ) en de oppervlakte onder de curve. De scheefheidsfactor is rechtevenredig met de verhouding tussen convectie en diffusie van de bolus in de vloeistofstroom. In-vitro werden volumes bepaald door het verschil tussen de gemiddelde transittijden (μ) van twee "regions of interest" te vermenigvuldigen met de vloeistofdoorstroomsnelheid en dit resultaat werd vergeleken met het werkelijk aanwezige vloeistofvolume. In-vivo, werden de "regions of interest" in de beiden kamers

van het hart getekend. De PTT werd berekend als het verschil tussen de gemiddelde transittijd van de linker en rechter hartkamer.

In het eerste deel van het proefschrift wordt in een in-vitro model verschillende vloeistofvolumes volgens de CEUS en thermodilutie methode gemeten en vergeleken met elkaar en het absolute vloeistofvolume. Thermodilutie gebruikt een koude injectievloeistof als indicator en wordt veel toegepast in de klinische praktijk. In het tweede deel wordt in een studie bij patiënten tijdens hartoperaties, het pulmonale bloedvolume gemeten met CEUS en transpulmonale thermodilutie. Thermodilutie kent tekortkomingen door onder andere warmte- (koude-) verlies. Bovendien vonden we bij de in-vitro metingen een overschatting van de vloeistofvolumes volgens de thermodilutie methode. In een vervolg onderzoek vergeleken we daarom transittijden gemeten met zowel CEUS als dynamische contrast-versterkte MRI (DCE-MRI), wat gebaseerd is op hetzelfde principe, maar dan met gadolinium als indicator. De transpulmonale dilutierespons werd bepaald door systeemidentificatie technieken en hierbij werd λ in gezonde vrijwilligers vergeleken met λ van patiënten met hartfalen door DCE-MRI. In het derde deel wordt de betrouwbaarheid, herhaalbaarheid en reproduceerbaarheid van PTT onderzocht in een groep van vijftien patiënten, die drie verschillende doses echocontrast kregen. Acht beoordelaars hebben echo-opnames beoordeeld door indicator-dilutiecurves te meten in de linker en rechter kamer, waarbij dezelfde procedure één keer herhaald is. Daarnaast werd PTT ook automatisch bepaald en vergeleken met manueel verkregen PTTs. In het laatste deel van het proefschrift wordt PTT gecorreleerd met verschillende echografische hartfalenparameters en NT-proBNP, wat een biomarker is voor acuut hartfalen. In een observationele studie werd gedurende twee jaar het effect van cardiale resynchronisatie therapie (biventriculair pacen) gemeten op de PTT. Daarbij is onderzocht of de duur van PTT een voorspeller kan zijn voor respons op cardiale resynchronisatie therapie.

De belangrijkste bevindingen in dit proefschrift zijn dat CEUS vloeistofvolumes nauwkeuring kan meten in het in-vitro model, terwijl thermodilutie deze vloeistofvolumes overschat. Daarnaast komen, vergeleken met transpulmonale thermodilutie, de met CEUS gemeten pulmonale bloedvolumes in patiënten beter overeen met de volumes beschreven in de literatuur. Ook toonden we aan dat PTTs gemeten met CEUS sterk correleren met de PTTs gemeten met DCE-MRI en vonden we een matige tot sterke relatie tussen PTT en verschillende echografische parameters. Daarnaast correleert PTT gemeten met CEUS en DCE-MRI beiden sterk met NT-proBNP. De λ bepaalt met de transpulmonale dilutierespons en DCE-MRI toonde een significant verschil aan tussen de gezonde vrijwilligers en hartfalenpatiënten wat duidt op een verschil tussen de convectie/dilutie ratio. De betrouwbaarheid, herhaalbaarheid en reproduceerbaarheid van de PTT bepaling was sterk. Daarbij correleerden de automatisch berekende PTT ook sterk met de handmatig berekende PTT. Het effect van cardiale resynchronisatie therapie leidde tot een afname van de PTT, wat duidt op een klinische verbetering. Zo toonden we aan dat patiënten,

die verbeterden na cardiale resynchronisatie (responders) op basis van een afname van het eind-systolisch linker ventrikelvolume, ook een significante daling van PTT lieten zien. In de patiënten die niet reageerden op deze behandeling zagen we deze daling in PTT niet. Daarnaast waren de PTT's gemeten vóór de cardiale resynchronisatie lager in patiënten die respondeerden dan in patiënten die niet-respondeerden op resynchronisatie therapie. Dit is een belangrijke bevinding, omdat het voorspellen van het succes van deze intensieve behandeling in de klinische praktijk moeilijk is.

Concluderend, CEUS is een minimaal-invasieve beeldvormingstechniek, die weinig afhankelijk is van de beeldkwaliteit en aan bed kan worden toegepast en waarmee intrathoracale bloedvolumes middels transittijden geschat kunnen worden. Pulmonale transittijden correleren met echografische en biochemische parameters van hartfalen. Het effect van cardiale resynchronisatie op de PTT was significant en mogelijk heeft PTT een voorspellende waarde voor de selectie van responders. Op basis van deze bevindingen concluderen we dan ook dat PTT een belangrijke aanvullende en waardevolle parameter voor de klinische praktijk kan zijn bij het stellen van de diagnose, het evalueren van de behandeling en het bepalen van de prognose van de cardiopulmonale functie bij patiënten thuis en in het ziekenhuis.

CONTENTS

Chapter 1

Introduction

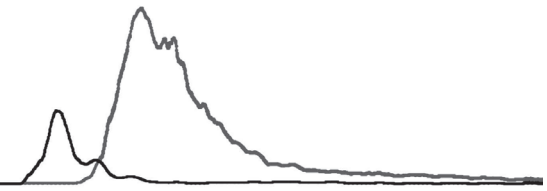

In every patient-physician contact, where assessment of the circulation is needed for diagnostic and therapeutic guidance an evaluation of the cardiac performance is essential. In our critically ill and high-risk surgical patients, cardiac performance is often evaluated (semi-) continuously, usually invasively by arterial and central venous catheterization.

This thesis describes the in-vitro validation and the first clinical results of a recently developed technique based on the indicator dilution technique, which enables the user to quantify cardiac performance in a minimal-invasive manner.[1-2] This technique comprises contrast-enhanced echocardiography and can be performed at the bedside or even in the out-patient clinic.

HEMODYNAMIC MONITORING USING INDICATOR DILUTION METHODS

Cardiac performance can be assessed by cardiac output measurements and central blood pool estimations. Cardiac performance and in particular the relation between cardiac output and central blood volumes (e.g. preload) is described by the Frank Starling curve (Fig. 1), which is the cornerstone of treatment in the critically ill patient in clinical practice. Adolf Fick was the first to describe, in 1870, the cardiac output estimation using oxygen concentrations in arterial and venous blood samples of dogs. He stated that "the rate of indicator in is the rate of indicator out plus the rate of indicator added". A few years later in 1897, the indicator dilution theory was introduced by Stewart. A bolus

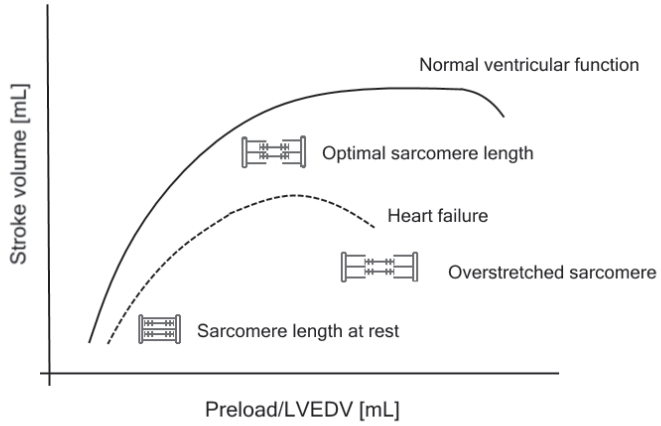

Figure 1. The Frank Starling curve (FS) can be presented during normal left ventricular function and heart failure and describes the interaction between preload and stroke volume (cardiac output). The preload dependent ventricle is at the ascending part of both FS curves and the preload independent ventricle is at the horizontal part of the normal ventricle. In the horizontal part extra fluid administration will not lead to an increase in cardiac output.

of sodiumchloride was injected in the central circulation and the subsequent estimation of the concentration change over time in the femoral artery allowed calculation of cardiac output in dogs.[3] Using a similar approach in humans, Hamilton was able to calculate cardiac output by measuring the area under the curve of the recorded indicator dilution curve (IDC) (Fig. 2).[4] Subsequently, the Stewart-Hamilton equation was formulated which is still used today in clinical practice.

$$\varphi = \frac{m}{\int Ci\, dt} \qquad (1)$$

The cardiac output φ is defined by the amount of injected indicator [m] divided by the area under the IDC [$\int Ci\, dt$] (Eq. 1).

The indicator dilution theory relies on a few important assumptions; [5-7]

- the indicator is inert, soluble, and non-toxic.
- the indicator is instantaneously injected, homogeneously mixed, and diluted in the circulation
- no indicator is lost during the measurement
- the mixture is transported downstream to a detection point, with a constant flow and through a constant volume
- the indicator should be detected only once (no recirculation)
- the indicator concentration change in time is recorded at the detection point

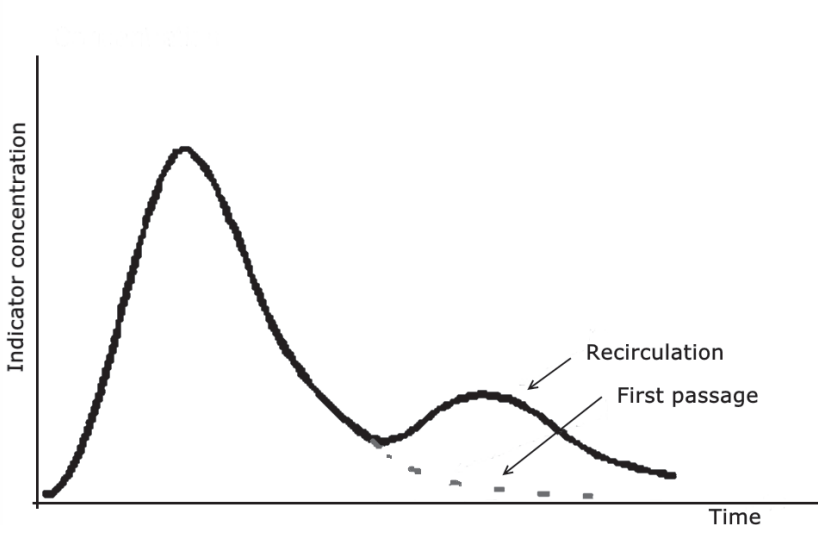

Figure 2. The blood circulation is a closed system implicating the indicator passes the detection point more than once, this is called recirculation. Therefore, a model is necessary to fit the indicator dilution curve to estimate its first passage curve.

Although several indicators can be used, indocyanine green, which is inert, non-toxic, measureable, and rapidly metabolized by the liver, meets most of the above described conditions and is considered as gold standard. To obtain an IDC, indocyanine green is injected into a peripheral vein and subsequently measured in the arterial blood with a infra-red photocell that records changes in light absorption at wavelength of 805 nm reflecting the change in concentration of indocyanine green. The obtained IDCs are robust and devoid of artefacts due to recirculation, indicator loss etc. and as such, cardiac output measurements are reliable and accurate at both low and high cardiac output.[8] However, the method is laborious and requires a lot of material, which was a drawback for its use in routine clinical practice. In the meanwhile, Swan and Ganz developed the pulmonary artery catheter in 1970 (Fig. 3).[9] The introduction of the thermo-indicator-dilution technique in the pulmonary artery catheter (1954) by Fegler enabled easier intermittent – and later also continuous cardiac output measurements in high-risk patients.[10] Since then the Swan Ganz catheter has been extensively used in anaesthesiology, cardiology, and intensive care.[9] Cardiac output is estimated by injecting 10 or 20 ml cold saline (T_0) in the right atrium after which the temperature change over time (T_B and $\int_t \Delta T_B dt$) is measured at the catheter tip (Fig. 1) in the pulmonary artery. (Eq. 2).[11]

$$\varphi = \frac{V_0 (T_B - T_0) K_1}{\int_t \Delta T_B dt} \qquad (2)$$

- V_0 is volume injected
- T_B is blood temperature at time of injections
- T_0 is temperature of indicator
- K_1 is the heat capacity factor (=1.08 for glucose 5%)

However, insertion of the pulmonary artery catheter is not without risk. Complications like heart rhythm disturbances, infection, pulmonary infarction, perforation of the pulmonary artery, and knotting are described.[12] Furthermore, treatment based on the measured results (cardiac-output and pressure readings in the pulmonary circulation) do not always

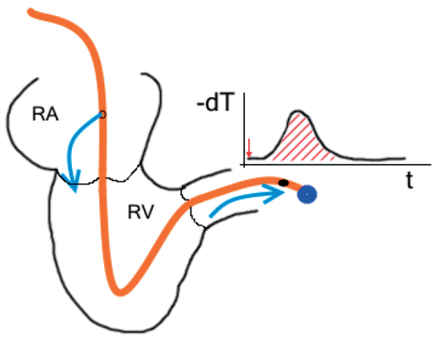

Figure 3. A schematic overview of pulmonary artery catheter (PAC); a bolus of cold saline is injected in the right atrium and detected at the thermistor at the tip of the PAC catheter (black dot). A thermodilution indicator curve is registered and cardiac output is measured by the Stewart-Hamilton equation.

lead to better survival or outcome.[13-14] Therefore, the pulmonary artery catheter is nowadays mainly applied in a specific patient category i.e., right ventricular dysfunction, pulmonary hypertension, and conditions which demand right ventricular function monitoring. Transpulmonary thermodilution, a less invasive technique using an arterial line with a thermistor, has replaced its abundant use in the critically ill patients.[15]

TRANSPULMONARY THERMODILUTION

Originally, the thermal-dye dilution technique was adopted to measure cardiac output and extravascular lung water (EVLW) by the simultaneous injection of indocyanine green (intravascular agent) and cold saline (intra- and extravascular agent due to diffusion through the vascular wall).[16] Indocyanine green is a strictly intravascular indicator and therefore measures the intravascular volume (central blood pool) of distribution. In contrast to cold saline, which is a thermal indicator and distributes to the extravascular compartments hence, the intra- and extravascular volumes of distribution are measured. The IDCs of each indicator can be described in terms of area under the curve, mean transit time (MTT), and downslope time (DSt). The latter is determined by the monoexponential extrapolation of the descending limb of the IDC and reflects the largest mixing intrathoracic volume i.e. pulmonary volume (Fig. 4 en 5). Intrathoracic distribution volumes can be estimated by multiplying the transit times by the cardiac output. The product of the difference in MTT of cold saline and indocyanine green and cardiac output represents the EVLW or – more correctly, the extravascular thermal volume (Fig. 5). However, these measurements are demanding as it requires a continuous blood withdrawal system with an extracorporeal densitometer. In the earlier 1990s, the COLD-system (Pulsion Medical, Munich, Germany) was introduced containing a thermistor and fiberoptic fibers in one catheter.[16] Still, two indicators had to be used and in 1999 single-injection transpulmonary thermodilution was introduced, which allowed easier assessment of cardiac output and central circulatory volumes.[17-18] The intrathoracic blood volumes, formerly measured by indocyanine green, were estimated by dedicated analysis of a single transpulmonary thermodilution IDC, which estimates the intrathoracic blood volume (ITBV), EVLW, and pulmonary blood volume (PBV) (Fig. 4 and 5).[19] Therefore, transpulmonary thermodilution can be used to guide fluid management and optimize cardiac output without increasing EVLW (e.g. pulmonary edema). Transpulmonary thermodilution proved to be a reliable hemodynamic monitor in different conditions like; cardiopulmonary surgery, heart failure, septic shock, transplantation patients, and pancreatitis patients.[20-23] It has been shown that fluid therapy based on transpulmonary thermodilution reduces time to extubation, length of stay, and hospital costs.[24-26]

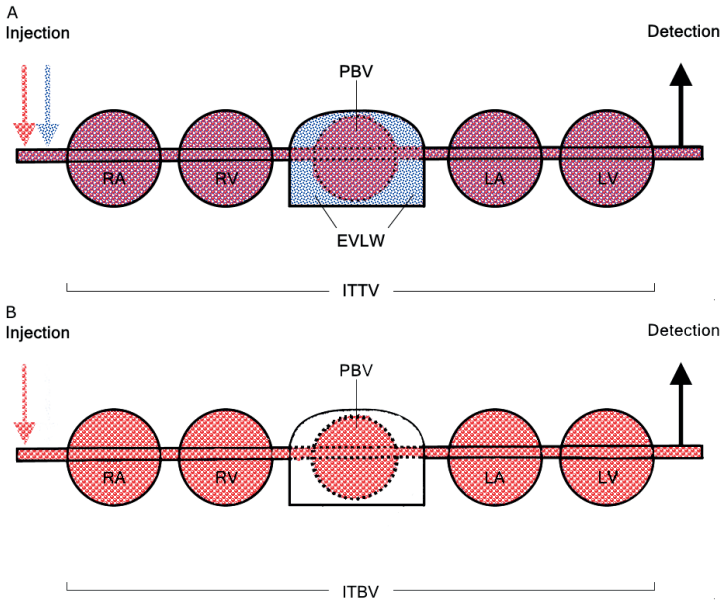

Figure 4. Transpulmonary double indicator dilution technique. Panel A Intravascular indicator (red) and extravascular indicator (blue) are injected in a central vein. The moment of injection is registered and both indicators are detected at detection point. Red indicator stays intravascular and measures intrathoracic blood volume (ITBV) (Panel B). Blue indicator measures intravascular bloodvolume and extra vascular lung water (EVLW) by passing the pulmonary capillary membrane. Blue indicator measures the intrathoracic total volume (ITTV). The difference between the ITTV and ITBV represents the EVLW.

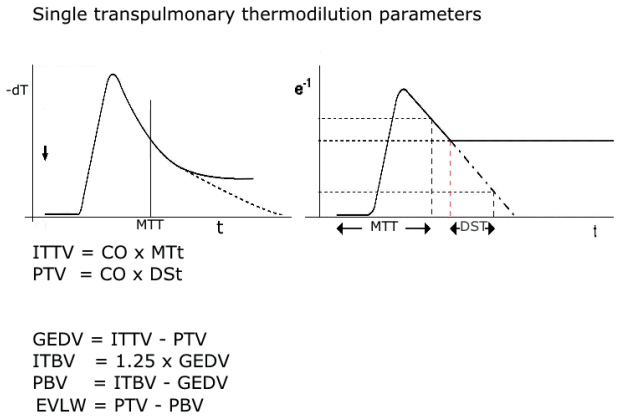

Figure 5. Left IDC is transpulmonary thermodilution curve. MTT is derived from the IDC. From the natural logarithm of the IDC (right panel) the downslope time (DST) is estimated and describes the time needed to pass the largest circulating volume (i.e. pulmonary circulation) presenting the pulmonary total volume (PTV).

PULMONARY TRANSIT TIME AND PULMONARY BLOOD VOLUME

As described above, cardiac output, cardiac transit time, and cardiopulmonary blood volumes are closely related to cardiopulmonary performance.[27] In the sixties, cardiac performance was evaluated by estimating PBV. Indocyanine green was injected in the pulmonary artery and left atrium (by insertion of a catheter through the intra-atrial septum). The difference in MTTs was measured at a peripheral artery and considered as an estimate of the pulmonary transit time (PTT).[28] The PBV was calculated by multiplying cardiac output by PTT. These PBVs correlated well with the severity of mitral stenosis and congestive heart failure.[28-29] Moreover, a correlation was observed between the amount of PBV and the NYHA classification.[30] These relationships between transit time and cardiac performance have also been confirmed using angiocardiograms and radionuclides as indicator.[31-32] This methodology allowed easier assessment of cardiac output and transit times without arterial sampling. Although considered less invasive, the technique required ^{99m}Tc pertechnetate injections and scintigraphy, which is not bedside applicable.[33]

The development of dynamic contrast-enhanced MRI (DCE-MRI), opened the possibility to measure the transit time of gadolinium in the pulmonary artery and left atrium without the use of radionuclides.[34] The transit times estimated by DCE-MRI correlated well with previous values and with different parameters of heart failure.[34-35] However, MRI is not bedside applicable and is not available, in most cases, for patients on mechanical ventilation. Therefore, the development of a method to estimate for cardiac performance like cardiac circulation times and PBV, which is minimally invasive and bedside applicable, could be of great clinical value.

ULTRASOUND CONTRAST AGENTS AS MINIMAL INVASIVE INDICATOR

The idea for contrast echocardiography was born in 1968, when a "cloud of echos" was observed from the aortic root after injecting saline through an intra-aortic catheter.[36-37] As air is an excellent acoustic reflector, gas-filled bubbles are easily detected by ultrasound machines. In the eighties, commercial microbubbles were developed. These microbubbles were used for left-right shunt assessment and left ventricle opacification to quantify ejection-fraction in poor quality transthoracic echograms. The first microbubbles, like agitated saline, were too large and had half-lives of a few seconds, and therefore did not pass the pulmonary circulation. Next generation microbubbles were smaller, consisting of less diffusible, high-molecular-weight gas stabilized with elastic shells.[38] The majority of the first encapsulated smaller microbubbles reached the left atrium and resulted in opacification of left atrium and left ventricle.[37] They consisted of diffusible air

and albumin (Albunex®, Molecular Biosystems Inc, San Diego, Calif.) or a suspension of galactose and fatty acid (Levovist®, Schering AG, Berlin, Germany). Albunex and Levovist were used for ventricular opacification and Doppler profile optimization. Due to pressure dependence and a short lifetime, Albunex® did not visualize the myocardium itself. The lifetime of the microbubbles had to increase and therefore, less diffusible gases were required. The so called second generation microbubbles were developed with focus on stability and size by using insoluble gas encapsulated by a protein, lipid, or polymer shells to improve durability.[39] SonoVue® (Bracco Imaging S.p.A, Milan, Italy) (2001) consists of sulphur hexafluoride gas with a phospholipid shell.[40] The gas is lipophilic and shows low solubility in plasma. The microbubble size is between 1 and 10 μm in diameter, with an average value of approximately 2.5 μm, which is in general smaller than a red blood cell (6-8 μm) and therefore the majority of the bubbles do pass the pulmonary circulation.[41] The microbubbles are too large to migrate through the vessel wall and, therefore are considered a pure intravascular indicator. They are used to visualize the endocardial border of the left ventricle, for perfusion-studies of the myocardium and other organs, and imaging cancer angiogenesis.[38, 42-43] Furthermore, drug and gene delivery by microbubbles is a promising new development.[44-45]

The injection of microbubbles is considered to be safe, although not completely without risk. Side effects vary from headache, injection pain, to chest pain with an incidence between 0.5 to 2.1%.[38] Serious allergic reactions are reported but at a very low incidence.[38] In 2007 the FDA imposed a black box warning to the use of Bracco's SonoVue® microbubbles. This warning followed reports of patient deaths and serious cardiopulmonary reactions after UCA administration, however not clearly caused by UCAs. One and a half year later, the FDA relaxed the black box as studies showed that the incidence of severe reactions was extremely rare (1 in 10000), which is comparable to low- to iso-osmolar ionic intravenous contrast media with an incidence of 0.04%.[38, 46-47] Recently, after extensive evaluation acute coronary syndrome and unstable ischemic heart disease has been removed as a contraindication for SonoVue®.[39] As microbubbles are frequently used for endocardial border detection and myocardial perfusion to estimate viability in patients with critical coronary perfusion, one could question whether the microbubbles were related to the reported sudden deaths. The critical coronary perfusion in these patients is more likely related to the adverse outcome. The black box has indeed been removed and contraindications for SonoVue® are limited to allergies to one of the compounds as well as to severe or suspect of severe intracardiac shunting, severe pulmonary hypertension, uncontrolled hypertension, acute respiratory distress syndrome, and during dobutamine stress echocardiography in cardiovascular instability.[38-39]

INDICATOR DILUTION METHOD AND CONTRAST-ENHANCED ULTRASOUND

More than a decade ago Mischi and coworkers developed a method for measuring cardiac transit times using dynamic contrast-enhanced echocardiography.[1] In contrast-enhanced echography, the backscattered ultrasound waves can be described not only by a linear equation which is typical for tissue, but also non-linear equations by the oscillations of the microbubbles. The backscattered ultrasound waves transmit the fundamental (linear) frequency and also sub- and higher harmonics (non-linear) (Fig. 6).[48-49] To differentiate the microbubbles in the blood stream/cardiac cavities optimally, harmonic imaging can be used to exploit the non-linear scattering properties of the microbubbles and facilitate their detection in the cardiac tissue due to an increase in signal-to-noise ratio.[38] For a reliable application of the indicator dilution theory, CEUS must comply with the above-mentioned conditions. This implies that the amount of indicator must be stable in the bloodstream and the fragile microbubbles should not be destructed during their passage in the thorax. Therefore, it is essential to minimize bubble disruption. To this end; the ultrasound scanner power has to be set at a low mechanical index (MI) indicating a low mechanical interaction with the bubbles. In order to obtain a linear relation between the concentration of bubbles in solution and the reflected signal, a much lower concentration is used than the one being used for left ventricular opacification.[2] Moreover, microbubbles at higher concentrations cause acoustic shadowing; this phenomenon occurs when the ultrasound wave is reflected by the first layers of high concentrate microbubbles, which are obscuring the other bubbles that are more distant from the transducer. Therefore, doses used for dynamic contrast-enhanced echocardiography need to be lower than the threshold where acoustic shadowing occurs. Similar to the studies with scintigraphy and DCE-MRI, regions of interest (ROI) can be drawn in the ultrasound images in the right and left side of the heart.[32, 34-35] The acoustic backscattered time intensity curves can be

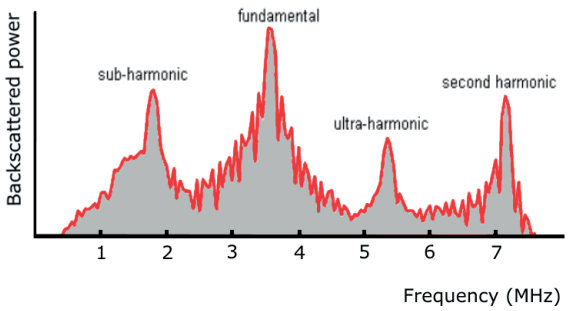

Figure 6. Frequency response of ultrasound contrast agent following excitation at the fundamental harmonic. Adapted from M. Mischi Contrast echocardiography for cardiac quantifications 2004.

estimated within the ROI. Based on the established linear relationship between acoustic intensity and contrast concentration, a time-concentration curve (IDC) can be derived. These IDCs by CEUS are prone to artefacts. The most common source is recirculation of the indicator in the down-slope of the IDC tail (Fig. 2). Furthermore, noisy sources like bad mixing, acoustic reverberation, backscatter oscillations, bubble disruption, patient movement, and blood-accelerations urges the need for a fitting model like Stewart and Hamilton.[50] The fitting model used in this thesis is the local density random walk (LDRW) model, which describes the moment of injection, diffusion, dispersion, and transportation of the indicator bolus in the blood stream.[51-53] Therefore, the LDRW model (Eq. 3) gives an interpretation of the diffusion-convection equation and describes the transport process of an indicator. The LDRW model has been adapted for acoustic IDCs giving the most accurate IDC fit and physical interpretation of the dilution process and reliable results in in-vitro volume- and transit time estimations.[1-2]

$$C(t) = \frac{m}{\mu\varphi} e^{\lambda} \sqrt{\frac{\lambda\mu}{2\pi t}} \, e^{-\frac{\lambda}{2}\left(\frac{t}{\mu}+\frac{\mu}{t}\right)} \qquad (3)$$

C(t) is the concentration change of indicator in time, which is determined by the amount (mass) of indicator injected, *m*. The distance covered by the indicator bolus is determined by μ, the mean transit time. φ is the flow of the carrier fluid or cardiac output. λ is a parameter related to the skewness of the IDC, which equals the Peclet number divided by two. The Peclet number represents the ratio between convection and diffusion in a dilution process. When the IDC is very symmetric ($\lambda \rightarrow \infty$), there will be minimal diffusion and predominantly convection of the indicator.[54] Therefore, LDRW fitting of IDCs estimates

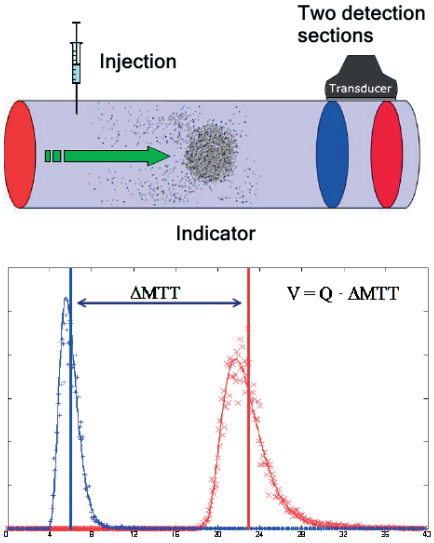

Figure 7. Measurement of indicator dilution curves at two detection sites by the ultrasound transducer. The bolus microbubbles is injected in a vessel where it is diffused and transported by the flow of the blood-stream. The passage of the bolus through the regions of interest is registered. The rough (crosses) data are registered and fitted to the local density random walk model (smooth lines) and the mean transit times are estimated (vertical blue and red line). Adapted from M. Mischi Contrast echocardiography for cardiac quantifications 2004.

the MTT of the bolus microbubbles through the ROIs in the right and left ventricles (Fig. 7) and presents the convection/diffusion ratio of the bolus microbubbles. The difference between the MTTs multiplied by flow (cardiac output) represents the volume between the detection points, the accuracy of these volumes has been validated in-vitro.[2]

SCOPE OF THIS THESIS

Dynamic contrast-enhanced echocardiography in combination with the indicator dilution theory is minimally invasive and gives the opportunity to perform measurements which up till now require intensive instrumentation and invasiveness for the patient. The purpose of this thesis is to bring dynamic contrast-enhanced imaging and UCA dilution technique into clinical practice and compare it with clinical standards.

As earlier described, thermodilution is a frequently applied method for cardiac output and central blood volume estimation in clinical practice. Therefore, in the first part of this thesis, the comparison was made between contrast-enhanced ultrasound (CEUS) and thermodilution (cold saline) estimating absolute volumes in an in-vitro model. Accordingly, first the relationship between the different UCA concentrations and the backscattered acoustic intensity had to be investigated at different temperatures. As transpulmonary thermodilution is mostly used for central blood volume estimation, the in-vitro study was repeated using CEUS and transpulmonary thermodilution. Subsequently, central blood pool volumes were measured in heart surgery patients using CEUS and transpulmonary thermodilution. Blood volume estimation requires the incorporation of the cardiac output, which could introduce errors. For this reason, transit times were used in the second part of the thesis. MRI is considered the gold standard for cardiac function evaluation. The next step was to compare pulmonary transit time (PTT) by contrast-enhanced echocardiography and dynamic contrast-enhanced MRI (DCE-MRI) with different parameters of cardiac function. Furthermore, the sensitivity of different IDC parameters using DCE-MRI was evaluated in healthy volunteers and heart failure patients. Due to the relationship between transit times and cardiac performance, we postulated in the final part of this thesis that transit time estimation by contrast-echocardiography could measure response to cardiac resynchronization therapy (CRT). In patients requiring CRT, it is well known that non-responders to CRT have further developed heart failure with subsequent deterioration of cardiac performance. Therefore, we explored if the PTT could have predictive properties to differentiate responders and non-responders.

OUTLINE OF THIS THESIS

The aim of this project was to implement and evaluate Mischi and co-workers work into clinical practice. In *Chapter 2*; as linearity is one of the prerequisites for applying the indicator dilution theory, the relationship between the backscattered acoustic intensity and contrast concentration of SonoVue® was investigated, because thermodilution is frequently used in clinical practice, acoustic intensity-contrast concentration measurements were performed at different temperatures. Furthermore, the microbubble behaviour in solution was investigated by assessing the stability of diluted SonoVue® at different temperatures, as this could influence handling of microbubbles during experiments. Secondly, in an in-vitro setup MTTs and volumes were estimated by CEUS and compared with thermodilution *(Chapter 3)*. In *Chapter 4,* using the same experimental setup the transit times and volumes by CEUS are compared with the transpulmonary thermodilution technique, a commonly used clinical method, to assess cardiac performance. Moreover, we also performed CEUS measurements in patients undergoing cardiac surgery and compared these results with transpulmonary thermodilution. Furthermore, comparisons were made between CEUS and the gold standard for cardiac performance assessment i.e. DCE-MRI. We correlated the PTTs of CEUS and DCE-MRI in *Chapter 5* and compared PTT with biomarkers for heart failure and with ventricular volumes by MRI. In *Chapter 6,* the reliability and reproducibility of PTT is assessed by eight different raters. In order to facilitate PTT analysis in clinical practice, an automatic IDC estimator is described in *Chapter 7* to develop a "press the button PTT assessment". The PTTs of the automated IDC estimator were compared with manual ROIs and fits. In the final chapters, we focus on cardiac performance and therapy in heart failure. In *Chapter 8,* the value of PTT was estimated in healthy volunteers and heart failure patients using DCE-MRI and compared with different heart failure parameters. In *Chapter 9,* the ability to measure response to heart failure therapy (i.e. cardiac resynchronization therapy) by PTT assessment using CEUS was evaluated. Moreover, PTT as predictor for response to CRT was investigated.

REFERENCES

1. Mischi M, Kalker T, Korsten HHM. Videodensitometric methods for cardiac output measurements. *EURASIP Journal on applied signal processing* 2003; **5**: 479 - 89
2. Mischi M, Kalker TA, Korsten EH. Contrast echocardiography for pulmonary blood volume quantification. *IEEE Trans Ultrason Ferroelectr Freq Control* 2004; **51**: 1137-47
3. Stewart GN. Researches on the Circulation Time and on the Influences which affect it. *J Physiol* 1897; **22**: 159-83
4. Hamilton WF, Moore JW, Kinsman JM, Spurling RG. Simultaneous determination of the pulmonary and systemic circulation times in man and of a figure related to the cardiac output. *AmJ of Physiol* 1928; **84**: 338-44
5. Zierler KL. Theoretical basis of indicator-dilution methods for measuring flow and volume. *Circ Res* 1962; **10**: 393-407
6. Newman EV, Merrell M, Genecin A, Monge C, Milnor WR, Mc KW. The dye dilution method for describing the central circulation. An analysis of factors shaping the time-concentration curves. *Circulation* 1951; **4**: 735-46
7. Grodins FS. Basic concepts in the determination of vascular volumes by indicator-dilution methods. *Circ Res* 1962; **10**: 429-46
8. Lund-Johansen P. The dye dilution method for measurement of cardiac output. *Eur Heart J* 1990; **11 Suppl I**: 6-12
9. Swan HJ, Ganz W, Forrester J, Marcus H, Diamond G, Chonette D. Catheterization of the heart in man with use of a flow-directed balloon-tipped catheter. *N Engl J Med* 1970; **283**: 447-51
10. Fegler G. Measurement of cardiac output in anaesthetized animals by a thermodilution method. *Q J Exp Physiol Cogn Med Sci* 1954; **39**: 153-64
11. Reuter DA, Huang C, Edrich T, Shernan SK, Eltzschig HK. Cardiac output monitoring using indicator-dilution techniques: basics, limits, and perspectives. *Anesth Analg* 2010; **110**: 799-811
12. Evans DC, Doraiswamy VA, Prosciak MP, et al. Complications associated with pulmonary artery catheters: a comprehensive clinical review. *Scand J Surg* 2009; **98**: 199-208
13. Connors AF, Jr., Speroff T, Dawson NV, et al. The effectiveness of right heart catheterization in the initial care of critically ill patients. SUPPORT Investigators. *JAMA* 1996; **276**: 889-97
14. Sandham JD, Hull RD, Brant RF, et al. A randomized, controlled trial of the use of pulmonary-artery catheters in high-risk surgical patients. *N Engl J Med* 2003; **348**: 5-14
15. Sakka SG, Reinhart K, Meier-Hellmann A. Comparison of pulmonary artery and arterial thermodilution cardiac output in critically ill patients. *Intensive Care Med* 1999; **25**: 843-6
16. Lewis FR, Elings VB, Hill SL, Christensen JM. The measurement of extravascular lung water by thermal-green dye indicator dilution. *Ann N Y Acad Sci* 1982; **384**: 394-410
17. Neumann P. Extravascular lung water and intrathoracic blood volume: double versus single indicator dilution technique. *Intensive Care Med* 1999; **25**: 216-9
18. Sakka SG, Ruhl CC, Pfeiffer UJ, et al. Assessment of cardiac preload and extravascular lung water by single transpulmonary thermodilution. *Intensive Care Med* 2000; **26**: 180-7
19. Isakow W, Schuster DP. Extravascular lung water measurements and hemodynamic monitoring in the critically ill: bedside alternatives to the pulmonary artery catheter. *Am J Physiol Lung Cell Mol Physiol* 2006; **291**: L1118-31

20. Godje O, Peyerl M, Seebauer T, Lamm P, Mair H, Reichart B. Central venous pressure, pulmonary capillary wedge pressure and intrathoracic blood volumes as preload indicators in cardiac surgery patients. *Eur J Cardiothorac Surg* 1998; **13**: 533-9
21. Sakka SG, Bredle DL, Reinhart K, Meier-Hellmann A. Comparison between intrathoracic blood volume and cardiac filling pressures in the early phase of hemodynamic instability of patients with sepsis or septic shock. *J Crit Care* 1999; **14**: 78-83
22. Della Rocca G, Costa GM, Coccia C, Pompei L, Di Marco P, Pietropaoli P. Preload index: pulmonary artery occlusion pressure versus intrathoracic blood volume monitoring during lung transplantation. *Anesth Analg* 2002; **95**: 835-43
23. Huber W, Umgelter A, Reindl W, et al. Volume assessment in patients with necrotizing pancreatitis: a comparison of intrathoracic blood volume index, central venous pressure, and hematocrit, and their correlation to cardiac index and extravascular lung water index. *Crit Care Med* 2008; **36**: 2348-54
24. Goepfert MS, Reuter DA, Akyol D, Lamm P, Kilger E, Goetz AE. Goal-directed fluid management reduces vasopressor and catecholamine use in cardiac surgery patients. *Intensive Care Med* 2007; **33**: 96-103
25. Lopes MR, Oliveira MA, Pereira VO, Lemos IP, Auler JO, Jr., Michard F. Goal-directed fluid management based on pulse pressure variation monitoring during high-risk surgery: a pilot randomized controlled trial. *Crit Care* 2007; **11**: R100
26. Michard F, Mountford WK, Krukas MR, Ernst FR, Fogel SL. Potential return on investment for implementation of perioperative goal-directed fluid therapy in major surgery: a nationwide database study. *Perioper Med (Lond)* 2015; **4**: 11
27. Ritter S, Rudiger A, Maggiorini M. Transpulmonary thermodilution-derived cardiac function index identifies cardiac dysfunction in acute heart failure and septic patients: an observational study. *Critical care* 2009; **13**: 1-10
28. McGaff CJ, Roveti GC, Glassman E, Milnor WR. Pulmonary blood volume in rheumatic heart disease and its alteration by isoproterenol. *Circulation* 1963; **27**: 77-84
29. Schreiner BF, Jr., Murphy GW, James DH, Yu PN. Pulmonary blood volume in patients with congestive heart failure. *Trans Assoc Am Physicians* 1966; **79**: 250-61
30. Roy SB, Bhardwaj P, Bhatia ML. Pulmonary blood volume in mitral stenosis. *Br Med J* 1965; **2**: 1466-9
31. Jones RH, Goodrich JK, Sabiston DC, Jr. Quantitative radionuclide angiocardiography in evaluation of cardiac function. *Surg Forum* 1971; **22**: 128-30
32. Jones RH, Sabiston DC, Jr., Bates BB, Morris JJ, Anderson PA, Goodrich JK. Quantitative radionuclide angiocardiography for determination of chamber to chamber cardiac transit times. *Am J Cardiol* 1972; **30**: 855-64
33. Leitl GP, Buchanan JW, Wagner HN, Jr. Monitoring cardiac function with nuclear techniques. *Am J Cardiol* 1980; **46**: 1125-32
34. Francois CJ, Shors SM, Bonow RO, Finn JP. Analysis of cardiopulmonary transit times at contrast material-enhanced MR imaging in patients with heart disease. *Radiology* 2003; **227**: 447-52
35. Shors SM, Cotts WG, Pavlovic-Surjancev B, Francois CJ, Gheorghiade M, Finn JP. Heart failure: evaluation of cardiopulmonary transit times with time-resolved MR angiography. *Radiology* 2003; **229**: 743-8
36. Gramiak R, Shah PM. Echocardiography of the aortic root. *Invest Radiol* 1968; **3**: 356-66
37. Nanda NC. History of echocardiographic contrast agents. *Clin Cardiol* 1997; **20**: I7-11

38. Senior R, Becher H, Monaghan M, et al. Contrast echocardiography: evidence-based recommendations by European Association of Echocardiography. *Eur J Echocardiogr* 2009; **10**: 194-212
39. Appis AW, Tracy MJ, Feinstein SB. Update on the safety and efficacy of commercial ultrasound contrast agents in cardiac applications. *Echo Res Pract* 2015; **2**: R55-62
40. Correas JM, Burns PN, Lai X, Qi X. Infusion versus bolus of an ultrasound contrast agent: in vivo dose-response measurements of BR1. *Invest Radiol* 2000; **35**: 72-9
41. Gorce JM, Arditi M, Schneider M. Influence of bubble size distribution on the echogenicity of ultrasound contrast agents: a study of SonoVue. *Invest Radiol* 2000; **35**: 661-71
42. Quaia E. Microbubble ultrasound contrast agents: an update. *Eur Radiol* 2007; **17**: 1995-2008
43. Unnikrishnan S, Klibanov AL. Microbubbles as ultrasound contrast agents for molecular imaging: preparation and application. *AJR Am J Roentgenol* 2012; **199**: 292-9
44. Kang ST, Yeh CK. Ultrasound microbubble contrast agents for diagnostic and therapeutic applications: current status and future design. *Chang Gung Med J* 2012; **35**: 125-39
45. Bader KB, Bouchoux G, Holland CK. Sonothrombolysis. *Adv Exp Med Biol* 2016; **880**: 339-62
46. Piscaglia F, Bolondi L. The safety of Sonovue in abdominal applications: retrospective analysis of 23188 investigations. *Ultrasound Med Biol* 2006; **32**: 1369-75
47. Katayama H, Yamaguchi K, Kozuka T, Takashima T, Seez P, Matsuura K. Adverse reactions to ionic and nonionic contrast media. A report from the Japanese Committee on the Safety of Contrast Media. *Radiology* 1990; **175**: 621-8
48. Frinking PJ, Bouakaz A, Kirkhorn J, Ten Cate FJ, de Jong N. Ultrasound contrast imaging: current and new potential methods. *Ultrasound Med Biol* 2000; **26**: 965-75
49. de Jong N, Frinking PJ, Bouakaz A, Ten Cate FJ. Detection procedures of ultrasound contrast agents. *Ultrasonics* 2000; **38**: 87-92
50. Bouakaz A, de Jong N, Cachard C, Jouini K. On the effect of lung filtering and cardiac pressure on the standard properties of ultrasound contrast agent. *Ultrasonics* 1998; **36**: 703-8
51. Sheppard CW, Savage LJ. The random walk problem in relation to the physiology of circulatory mixing. *Physical Review* 1951; **83**: 489 - 90
52. Wise ME. Tracer dilution curves in cardiology and random walk and lognormal distributions. *Acta Physiol Pharmacol Neerl* 1966; **14**: 175-204
53. Bogaard JM, Jansen JR, von Reth EA, Versprille A, Wise ME. Random walk type models for indicator-dilution studies: comparison of a local density random walk and a first passage times distribution. *Cardiovasc Res* 1986; **20**: 789-96
54. Bogaard JM, Smith SJ, Versprille A, Wise ME, Hagemeijer F. Physiological interpretation of the skewness of indicator-dilution curves; theoretical considerations and a practical application. *Basic Res Cardiol* 1984; **79**: 479-93

Chapter 2

In-vitro assessment of the stability and acoustic backscatter of different concentrations SonoVue® at different temperatures

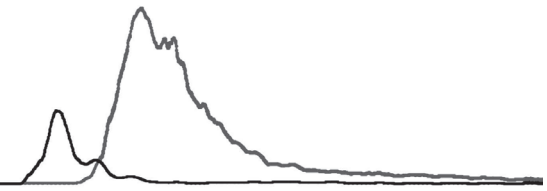

Ingeborg HF Herold
Massimo Mischi
R Arthur Bouwman
Rene JE Grouls
Erik HM Korsten

Submitted

ABSTRACT

Introduction

Ultrasound contrast agents (UCA) can be used for quantitative, diagnostic imaging based on the indicator dilution theory. However, the correct use of the indicator dilution theory with contrast-enhanced ultrasound requires to establish the relationship between UCA concentration and the backscattered acoustic intensity (AI). In this study, the AI is investigated in relation to different concentrations of SonoVue® at different temperatures and the influence of different temperatures on the stability of microbubbles is assessed.

Methods

The AI backscattered from SonoVue® was investigated imaging different concentrations at two temperatures (4 and 20 °C) with an iE33 ultrasound scanner. The stability of SonoVue® was investigated using a concentration of 5 mg/L at three temperatures (4, 20, and 37 °C).

Results

SonoVue® showed at 4 and 20 °C a linear relationship between the backscattered AI and the concentration below 1 and 2 mg/L, respectively. The stability of SonoVue® increased at lower temperatures. The backscattered AI in the stability-study was lower at 4 °C than at 20 °C, consistent with the calibration-study; however, at 37 °C the backscattered AI was lower than at 4 °C. The AI was measureable at 4 °C for at least four hours, at room temperature for two hours, and at body temperature for only 20 minutes.

Conclusion

The relationship between SonoVue® concentration and the backscattered AI was linear below 1 - 2 mg/L. Although the backscattered AI was lower at 4 °C than at 20 °C, SonoVue® at 4 °C showed the longest echogenicity in time.

INTRODUCTION

Cardiac parameter quantifications are important in the critical ill patients to measure the effectiveness of their cardiac function. Therefore, right heart catheterization, transpulmonary thermodilution techniques, and echocardiography are used to measure cardiac output, ejection fraction, and preload parameters. These parameters are used to guide fluid and inotropic therapy in patients. Mischi and co-workers developed a less invasive technique to quantify ejection fraction, pulmonary transit time, and pulmonary blood volume using contrast-enhanced echocardiography.[1-2]

Contrast-enhanced echocardiography has been used to extract acoustic intensity (AI) dilution curves by estimating the evolution of the ultrasound contrast agent (UCA) concentration within the ventricles of the heart.[2] The acoustic-intensity dilution curves were extracted by drawing regions of interest (ROI) within the cardiac chambers. The acoustic backscatter within these ROIs was estimated using commercially available software. However, the obtained indicator dilution curves can only represent the UCA-concentration evolution when the concentration has a linear relationship with the measured AI.[3] UCAs consist of microbubbles, which can pass the pulmonary circulation. The stability of the microbubble is increased by large-molecule, low-solubility gas enclosed in a shell made of e.g. phospholipids. Microbubbles are injected in the blood stream via an intravenous access. After injection, the microbubbles will warm up from room temperature to body temperature. The effect of temperature on the bubble behaviour is therefore of interest; it is of particular relevance when we perform simultaneous microbubble- and thermodilution measurements.[4]

The effect of temperature on the microbubble dynamic behaviour can be described using the modified Rayleigh-Plesset equation, which is given as:[5]

$$\rho R\ddot{R} + \frac{3}{2}\rho\dot{R}^2 = \left(\frac{2\sigma}{R_0} + P_0 - P_V\right)\cdot\left[\left(\frac{R_0}{R}\right)^{3k} - 1\right] + S_P\left(\frac{1}{R} - \frac{1}{R_0}\right) - \omega\delta_t\rho R\dot{R} - P(t), \qquad (1)$$

with ρ being the medium density, R the microbubble radius, R_0 the microbubble radius at rest condition, σ the surface tension, P_0 the ambient pressure, P_v the vapor pressure, k the polytropic exponent, S_p the shell elastic parameter, and δ_t the total damping factor. The latter includes several damping contributions: thermal damping, viscous damping, shell-friction damping, and re-radiation damping.[5-6]

The microbubble echogenicity is well described by its scattering cross-section, i.e., the ratio between scattered power and received acoustic intensity. For small oscillations, the backscatter cross-section can be derived from Eq. (1) by a first order Taylor approximation and it reads as:[6-7]

$$\Sigma(R_0, f) = \frac{4\pi R_0^2}{((f_n(R_0)/f)^2 - 1)^2 + \delta_t^2(R_0, f)}, \qquad (2)$$

with f_n being the natural frequency. According to the gas law, an increase in temperature will produce a volume expansion and, therefore, an increase in R_0,[8] resulting in a larger scattering cross-section based on Eq. (2). In addition, an increase in temperature also produces an increase in the thermal damping[7]; this will lower the resonance frequency. A decrease in surface tension and viscosity can also be expected, contributing to a further reduction in the resonance frequency. Therefore, although accurate prediction is challenging, temperature is expected to influence the microbubble dynamics by lowering the resonance frequency and increasing the scattering cross-section. As a result, an increase in the backscattered acoustic intensity can be expected, especially at lower insonating frequencies. In addition to the influence of temperature on the backscattering process, variations in the damping factors also affect the extinction cross-section and, therefore, the attenuation coefficient.[5] The global effect of temperature on contrast opacification is therefore complex and difficult to predict.

The aim of this study was to investigate experimentally the relationship between the backscattered AI at different UCA concentrations and different temperatures. Furthermore, the microbubble stability was also investigated. We hypothesized that microbubbles could increase their backscatter coefficient and become more unstable at higher temperatures, as their size increases while their surface tension decreases.

METHODS

In-vitro setups

Two custom built in-vitro setups were used for our experiments. The first setup was used for the calibration-study where different concentrations UCA were imaged at two temperatures. The second setup was built to test the stability of the microbubbles at three different temperatures.

The calibration-study

The first setup consisted of a tank, which was completely covered with ultrasound absorbing material and filled with degassed water (Fig. 1). De-airing of the water was performed by leaving it in place for 48 hours. Ice cold water has a higher solubility for gas, which increased the gas content with less bubble formation. In a small groove between the wall covering material, a TEE probe (X7-2t,Philips Healthcare, Andover, MA, USA) was submerged in the degassed water, visualizing a balloon (Ultracover, Microtek™Medical, Alpharetta, GA, USA) at a distance of 15 cm. The balloon was filled with 100 ml saline and different concentrations of SonoVue® (Bracco Imaging S.p.A., Milan, Italy), which is made of 25 mg dry powder dissolved in a sealed vial with 5 ml saline. The concentrations of SonoVue® were made using a calibrated pipette of 100-1000 µL

(Eppendorf, San Diego, CA, USA) and a beaker of 100 ml (concentrations > 0.5 mg/L) or an Erlenmeyer of 1 L (concentrations < 0.5 mg/L). The prepared concentrations were; 0, 0.05, 0.1, 0.25, 0.375, 0.5, 0.75, 1, 1.5, 2, and 3 mg/L (Fig. 1 and 2). Two temperatures were maintained; 20°C and 4°C by using ice cold saline from the refrigerator and by cooling the surrounding of the tank with ice. The temperatures were controlled by thermistors submerged in the tank. For every concentration a new balloon was used and kept in position manually. Every measurement was repeated three times to evaluate repeatability. The ultrasound scanner settings were harmonic imaging 2.7 - 5.4 MHz, frame rate 26 Hz, depth 15 cm, mechanical index (MI) 0.2, gain 65%, compression 50, echo-loop acquisition time 1 s, focus far beyond the imaging target to achieve homogeneous insonification. A low MI was adopted to minimize bubble disruption.

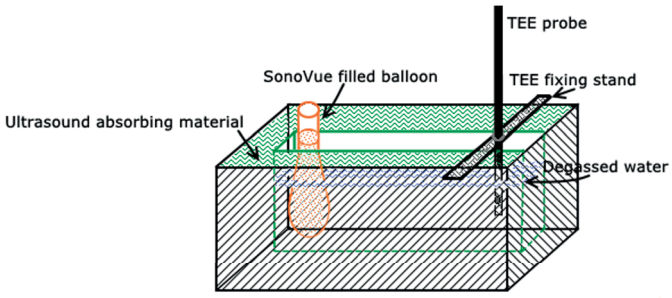

Figure 1. The plastic tank was covered with ultrasound absorbing material (rubber mats) at the walls and bottom. The tank was filled with water at 4 and 20 °C. A balloon filled with SonoVue® and saline at different concentrations was placed at one side of the groove, on the opposite side a TEE probe was positioned to image the balloon.

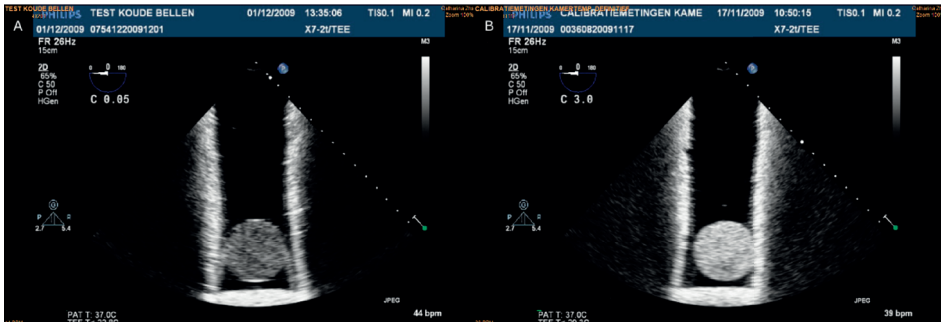

Figure 2. Screenshot **A** visualizes the balloon; SonoVue® concentration of 0.05 mg/L, temperature 4 °C. Screenshot **B** shows the balloon; SonoVue® concentration of 3 mg/L, temperature 20 °C.

The stability study

A second setup (Fig. 3 and 4) was built to test the stability of diluted SonoVue® over time. To this end, a sealed tank was connected to an afferent and efferent tube to circulate water by a membrane pump (Talamex® Marine products, Lelystad, the Netherlands). A balloon was positioned in the tank and could expand and compress driven by the pump. By use of the pump, gentle UCA mixing was obtained. The balloon was filled with 1-L Sonovue® diluted in saline at 5-mg/L concentration. The pressures within the balloon were always kept at ambient pressure. The ultrasound transducer (X7-2t) was positioned at a fixed distance to the balloon of 10 cm in the tank. The scanner iE33 (Philips Healthcare, Andover, MA, USA) generated 1-s echo loops. The settings were 2.4 – 4.8 MHz harmonic imaging, frame rate of 26 Hz, MI 0.2, depth of 17 cm, and the focus was again positioned in the far field beyond the target. Three different temperatures were maintained within the vacuum chamber; 20 ± 1 °C, 37 ± 1°C by thermo-controlled (thermistors) heaters submerged in the tank and the external water container supplying water, and 4 ± 1°C by adding ice in the container. When the setpoint of the temperature was reached, the circuit to the container was opened and warm or cold water was pumped into the vacuum chamber. The saline used for dilution of SonoVue® was kept in an incubator at 4 or 37 °C. The stability of SonoVue® was assessed every 10 minutes by imaging the balloon until no backscattered signal was visible. Before every acquisition, the SonoVue® dilution was well mixed within the balloon by manual compression and decompression of the balloon.

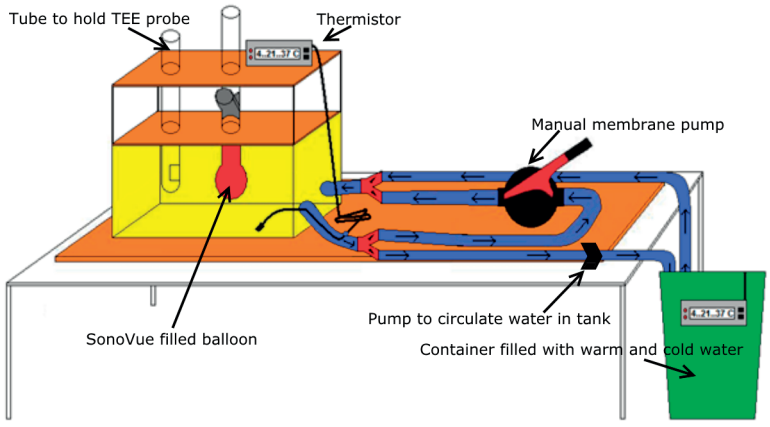

Figure 3. The sealed tank filled with water (yellow) at three different temperatures and the balloon with SonoVue®. The water in the tank could be refreshed by pumping water from a container. The manual pump was used for UCA mixing in the balloon by creating under- and over-pressure in the tank. The TEE probe was inserted via a PVC tube.

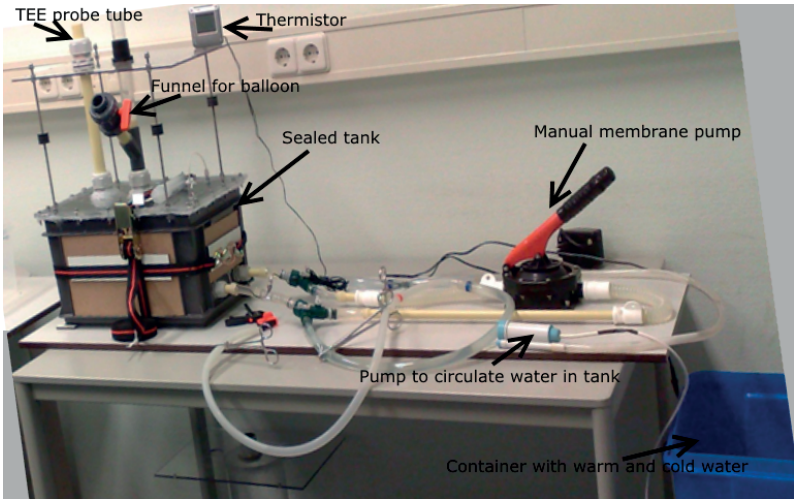

Figure 4. Picture of the model described in Figure 3.

SonoVue®

Sonovue® is made of microbubbles with a diameter ranging from 1 to 10 μm. They are suitable for intravenous injection and on average smaller than red blood cells (6 to 8 μm).[9] They are non-toxic and inert. Sonovue® consists of SF6 gas in a phospholipid monolayer.[10] This phospholipid monolayer creates a strain that opposes to Laplace pressure and stabilizes bubbles against dissolution. Sonovue® produces a significant increase in the ultrasonic energy backscatter, also at frequencies other than the insonifying frequency. This is due to the natural oscillations (contraction-expansion) of the bubbles when invested by an ultrasound pressure field, introducing several harmonics in the backscattered ultrasound waves. This behaviour can be predicted with several models of the bubble dynamics, such as the Rayleigh-Plesset equation (see Eq. (1)), which can be derived from the Navier-Stokes equation.[6, 11]

Acoustic intensity measurement

AI was estimated for both models by drawing ROIs in the balloon using Qlab 8® (Philips, Healthcare, Andover, MA, USA). The average AIs within the ROI were exported in arbitrary units (AU) as Excel files. The relationship between AI and concentration of SonoVue® was assessed by repeating each measurement (i.e. concentration) three times and by placing four ROIs within the balloon at increasing depth. Different ROIs were used to assess the impact of attenuation on the measurements (Fig. 5).

The assessment of the stability of SonoVue® was performed by obtaining a short echo loop of 1 s every 10 minutes. Three ROIs were drawn (Fig. 6) to assess the mean AI of the three ROIs. The time where attenuation disappeared was visualized in a graph as the time moment where the difference between the AI of the three ROIs was no longer significant.

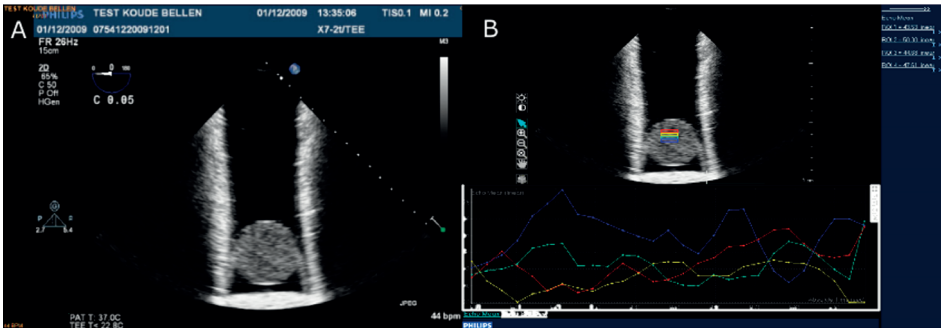

Figure 5. SonoVue® concentration of 0.05 mg/L opened as DICOM (screenshot **A**). The same DICOM of screenshot A, opened in Qlab 8® (screenshot **B**) where 4 regions of interest (ROI) were drawn. The mean acoustic intensity was recorded for 1 second in each ROI (red, yellow, green, and blue curves) and saved as Excel file.

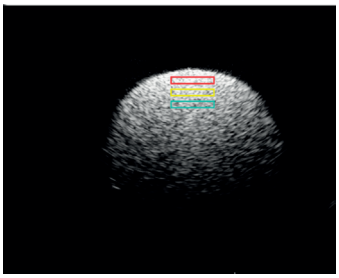

Figure 6. First recording of SonoVue® in stability study (concentration 5 mg/L) Four regions of interest were positioned in the echo-loop. The shadowing effect on the backscatterd acoustic signals due to attenuation was clearly visible.

Statistical analysis

All results are expressed as means or medians depending on the distribution of the data. The distribution of the data was tested using the Shapiro-Wilk test. The means of the repetitive measurements and the ROIs were tested for differences using the analysis of variance or the Kruskal-Wallis test depending of the distribution of the data. The relationship between the measured AI and the concentration of SonoVue® was assessed by linear regression analysis. All measurements were performed using SPSS statistics for Windows version 23.0 (IBM©, Armonk, NY, USA) except for the linear regression analysis which was performed by Excel (Microsoft Office, Redmond, WA, USA), a $p < 0.05$ was considered significant.

RESULTS

The calibration-study

The mean AI at 20°C, for all concentrations of SonoVue® was for the three repetitive measurements; 584 ± 467, 669 ± 537, and 799 ± 573 [AU], respectively. The dif-

ferences between these measurements were non-significant, $p = 0.61$. Also at 4 °C, the mean AIs of three measurements did not show a significant difference; they were equal to 550 ± 262, 441 ± 212, and 456 ± 259 [AU], $p = 0.99$.

Table 1. Acoustic intensity in each region of interest at two different temperatures

ROI number	Temp 4 °C (AU)	Temp 20 °C (AU)
1	559 ± 343	756 ± 567
2	483 ± 265	698 ± 498
3	412 ± 214	667 ± 483
4	341 ± 163	615 ± 433

ROI, region of interest; Temp, temperature; AU, arbitrary units

The AI from the ROI closest to the transducer was higher than all others, as expected due to attenuation; however, there was no significant difference between the AIs of 4 ROIs at 20 and 4 °C, $p = 0.92$, and $p = 0.20$, respectively (Table 1.) All contrast signals showed at both temperatures saturation of the AI at higher concentrations (inflection point). At 4° C, the inflection point was 1 mg/L, above which saturation is clearly recognized (Fig. 7 A, B). At 20 °C, the inflection point was 2 mg/L. Microbubbles at 4°C showed a lower mean backscatter at the saturated doses than microbubbles at 20°C. Below 1 mg/L, the AI did not differ visually between ROI 1 to 4, both at 4 and 20 °C (Fig. 7A). The AI related to the concentration showed a determination coefficient $R^2 = 0.88$ below 2 mg/L SonoVue® at 20°C and $R^2 = 0.93$ below 1.0 mg/L SonoVue® at 4 °C (Fig. 8).

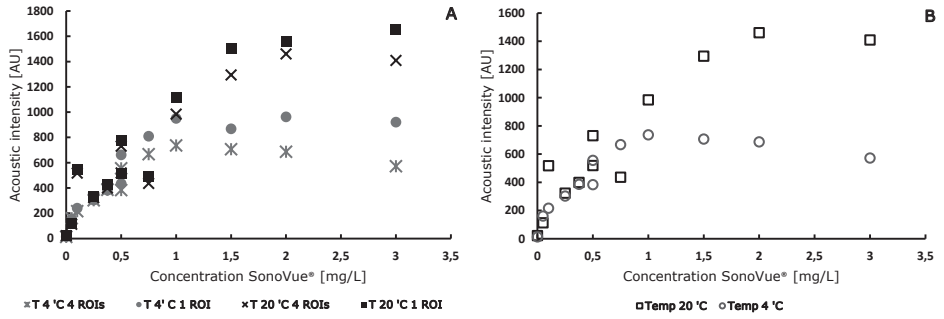

Figure 7. Acoustic intensity at 4 and 20 °C for different concentrations SonoVue®. Plot **A** shows the difference in acoustic intensity for 4 ROIs compared to 1 ROI. Plot **B** shows the mean acoustic intensity of the 4 ROIs.

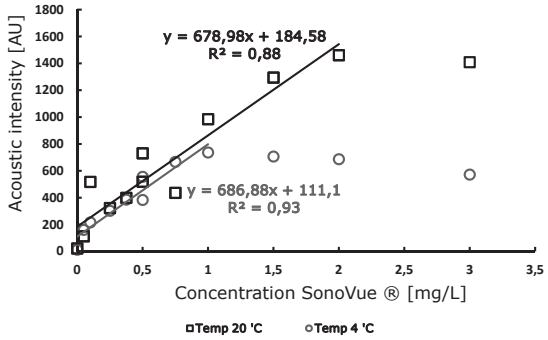

Figure 8. The linear relationship between acoustic intensity and concentration of SonoVue® at 4°C ≤ 1 mg/L (R^2 = 0.93) and at 20°C ≤ 2 mg/L (R^2 = 0.88) with the determination coefficient.

The stability-study

SonoVue® at 4°C showed an increase in AI in the first 10 minutes and maintained a steady state for one hour (Fig. 9 A and D). After one hour, an exponential decay in AI was observed, possibly caused by microbubble loss. After two hours, no attenuation was recognizable between the AIs of the different ROIs. At 20°C, a linear decay took place for 30 minutes R^2 = 0.96; after 40 minutes, saturation disappeared and an exponential decay was observed. At 37°C, an immediate decay was visualized and nearly no AI was measureable after 20 minutes. AI was overall highest closer to the transducer (ROI 1) and lowest at ROI 3, except at 37°C, which showed the highest AI at ROI 3.

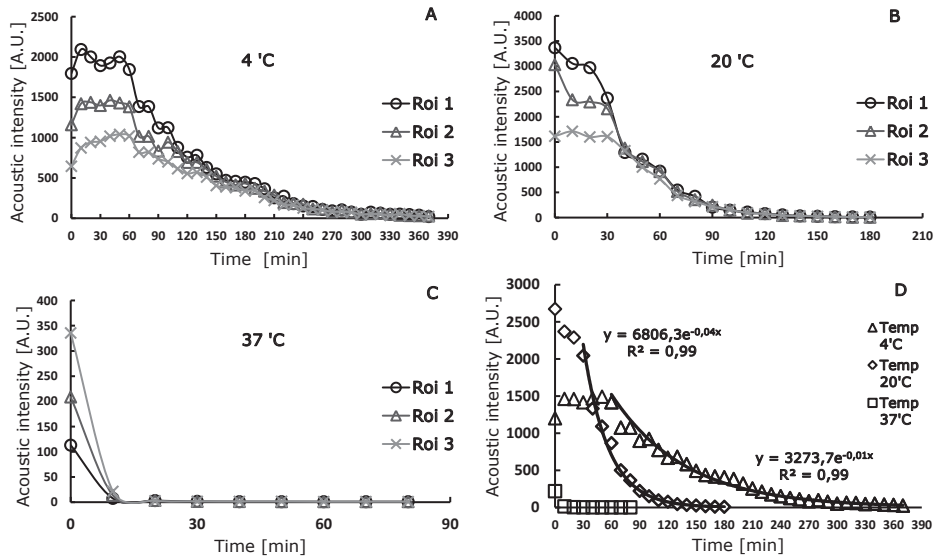

Figure 9. The stability study of SonoVue® at 4°C presented as acoustic intensity over time for three ROIs (plot **A**), 20°C (plot **B**), and 37°C (plot **C**). Plot **D** represents the mean acoustic intensity of 3 ROIs at the three temperatures.

Microbubbles at 4°C showed the longest lifetime (5 hours) and warm microbubbles showed immediate destruction in 10 min (Fig. 9D).

DISCUSSION

The establishment of the relationship between UCA concentration and AI is an important step prior to using the indicator dilution theory with CEUS. The stability of SonoVue® at different temperatures is of importance for its use in clinical practice.

The calibration-study

In this study, we found a linear relationship between concentration of SonoVue® and AI at three different temperatures. The relationship between acoustic backscatter and UCA was previously investigated by different investigators.[1, 8, 12-13] They all found a linear relationship between UCA concentrations and backscattered AI below a certain concentration. The reported linear range using a Sonos 5500 scanner and Sonovue® was up to 12.5 mg/L.[1] This inflection point is much higher compared to our results; however, the adopted contrast-specific pulse sequence was power modulation at 1.9 MHz. In our study, we used harmonic imaging at higher fundamental frequency (2.7-5.4 MHz). Importantly, in previous studies log-compressed data were often used, based e.g. on videointensity, while for quantification purposes, it is widely recognized that linearized echo data should be used.[3, 14-15]

In this study, cold microbubbles backscattered ultrasound less than warm microbubbles. The latter is in agreement with the characterization of the microbubble dynamics by the modified Rayleigh-Plesset equation, in combination with an increase in the microbubble radius due to gas expansion. The backscattered AI was higher at room temperature than at 4 °C, most probably due to an increase in the backscatter cross-section and, therefore, in the backscatter coefficient.[16-17] Furthermore, a higher inflection-point of the calibration curve was evident for the measurements at room temperature: 2 mg/L at room temperature vs. 1 mg/L at 4 °C. This seems in contradiction with expected increase in extinction cross-section with temperature. A possible explanation can relate to faster microbubble decay at room temperature, and thus fewer microbubbles being present. Moreover, the difference between the concentrations in the linear range was less pronounced with UCAs at 4°C than at room temperature, expressed by a higher discrimination coefficient (Fig. 8). We suspect that the stability of the microbubbles is larger at lower temperature, where bubble volume is decreased and the stability of the phospholipids monolayer is increased. In addition, the stability study at 37 °C showed a much lower acoustic backscatter, probably by rapid bubble rupture due to microbubble expansion and shell deterioration. This has been shown using high-speed camera images, where SonoVue®

microbubbles at blood temperature showed more excited oscillations with nonspherical expansion, fragmentation and gas expulsion.[17-18] Also the expected increase in size distribution due to gas expansion, combined with an increase in the damping factors, can bring the microbubble resonance frequency away from the adopted insonating frequencies. In agreement with our study, even if based on video intensity, the study on both Albunex and diluted FS069 (Optison®) showed a signal decrease when temperature decreased from 22 °C down to 8 °C .[8] The rate of decrease of normalized video intensity was higher at higher temperatures, indicating increased bubble instability, which confirms our findings.

Shadowing effect due to attenuation was shown above the inflection point; here the difference in AI between ROIs showed that the deeper ROIs provided less signal. Thereby, the mean AI of four ROIs was lower than the ROI closest to the transducer. This can be explained by the high concentration of microbubbles, which causes a strong backscatter of the ultrasound energy from the first layers and, therefore, a strong reduction in the energy reaching larger depths.[19] This concentration-dependent attenuation interferes with the time-intensity curves and should be avoided.[20] This effect was already recognized in the literature, where the effectiveness of contrast agents was measured by the ratio between scattering and extinction cross-sections.[21] The AIs for concentrations below the inflection point of 1 – 2 mg/L did not show significant difference between the different ROIs, proving negligible shadowing at these concentrations. These concentrations can therefore be used to generate time intensity curves that are suitable for quantitative analysis. Although several models have been proposed to interpret the dynamic behaviour of microbubbles, based e.g. on the enthalpy energy balance[22] or including additional nonlinear effects in relation to the bubble shell,[23] they all describe the same behaviour in relation to temperature. As a result, we have based our interpretation on the modified Rayleigh-Plesset equation without loss of generality.

The stability-study

The lifetime of SonoVue® at 4 °C was extremely long compared to higher temperatures. The "steady state" for one hour could be explained by attenuation at 5 mg/L, which decreased by microbubbles destruction (slowly due to the low temperature) and led to a lower concentration after one hour. At 20 °C, the backscatter was in agreement with the calibration study, which showed a higher backscatter in the first 30 minutes as compared to cold microbubbles. The decay of microbubbles was twice faster at 20 °C than at 4 °C. However, at 37 °C the microbubbles showed a low backscatter and a short lifetime of 20 minutes only. The latter is in disagreement with our prediction according to Eq. (1), where a higher backscatter was expected at 37 °C compared to room temperature. This could be ascribed to rapid bubble destruction, which has been shown in other studies.[17-18] Structural changes, bringing the microbubble off resonance and increasing the

dumping factor, can also contribute to a reduction in the backscattered energy. At these higher temperatures, SonoVue® should be injected followed by immediate visualization; however, the microbubble behaviour of SonoVue® in-vivo at these temperatures requires further evaluation.

Clinical implications

The aim of this study was to investigate the relationship between the backscattered AI from different concentrations of an UCA at different temperatures and to investigate the effect of temperature on the lifetime of the microbubbles. We found that a linear calibration can be assumed for SonoVue® concentrations below 1 - 2 mg/L for microbubbles at 4 and 20 °C. However, SonoVue® diluted in saline at 37 °C showed a rapid decay, which could affect quantification methods based on the indicator dilution theory and mass conservation law.

Limitations

The temperatures used to establish the relationship between AI and concentration of SonoVue®, were limited to 4 and 20 °C; we did not investigate 37 °C. The rapid decrease in AI at 37 °C should have been further investigated by repeated measurements. The transient effect of rapid warming up from 4 to 37 °C was not investigated. This could be of interest to evaluate the effect on the acoustic properties of cold microbubbles after injection in the human body.

CONCLUSIONS

In conclusion, we investigated the relationship between UCA concentration and backscattered AI at different temperatures. A linear relationship was found below 1 - 2 mg/L SonoVue®. SonoVue® at 4 °C showed reduced backscattering compared to 20 °C, consistent with bubble-dynamics models, and showed the longest lifetime. SonoVue® at 37°C backscattered ultrasound for 10 minutes only, and showed a low backscattered signal due to microbubble decay.

REFERENCES

1. Mischi M, Kalker T, Korsten HHM. Videodensitometric methods for cardiac output measurements. *EURASIP Journal on applied signal processing* 2003; **5**: 479 - 89
2. Jansen A, Mischi M, Bracke F, et al. Novel ultrasound contrast agent dilution method for the assessment of ventricular ejection fraction. *Eur J Echocardiogr* 2008; **9**: 489-93
3. Tang MX, Mulvana H, Gauthier T, et al. Quantitative contrast-enhanced ultrasound imaging: a review of sources of variability. *Interface Focus* 2011; **1**: 520-39
4. Herold IH, Soliman Hamad MA, van Assen HC, Bouwman RA, Korsten HH, Mischi M. Pulmonary blood volume measured by contrast enhanced ultrasound: a comparison with transpulmonary thermodilution. *Br J Anaesth* 2015; **115**: 53-60
5. Hoff L. Acoustic characterization of contrast agents for medical ultrasound imaging. *Springer Science & Business Media* 2001
6. Leighton TG. The acoustic bubble. *Academic press* 2012
7. Medwin H. Counting bubbles acoustically: a review. *Ultrasonics* 1977; **15**: 7-13
8. Mor-Avi VV, Robinson KA, Shroff SG, Lang RM. Effects of Temperature on Albunex and FS069 Echocardiographic Contrast Agents: In Vitro Investigation Using Ultrasonic Irradiation. *Echocardiography* 1997; **14**: 39-50
9. Schneider M, Arditi M, Barrau MB, et al. BR1: a new ultrasonographic contrast agent based on sulfur hexafluoride-filled microbubbles. *Invest Radiol* 1995; **30**: 451-7
10. Senior R, Becher H, Monaghan M, et al. Contrast echocardiography: evidence-based recommendations by European Association of Echocardiography. *Eur J Echocardiogr* 2009; **10**: 194-212
11. Mischi M. Echocardiography for cardiac quantifications. *PhD Thesis Eindhoven University of Technology* 2004
12. Yamada S, Komuro K, Mikami T, et al. Novel quantitative assessment of myocardial perfusion by harmonic power Doppler imaging during myocardial contrast echocardiography. *Heart* 2005; **91**: 183-8
13. Uhlendorf V. Physics of ultrasound contrast imaging: scattering in the linear range. *IEEE Trans on Ultrasonics, Ferroelectrics, and Frequency Control* 1994; **41**: 70-9
14. Peronneau P, Lassau N, Leguerney I, Roche A, Cosgrove D. Contrast ultrasonography: necessity of linear data processing for the quantification of tumor vascularization. *Ultraschall Med* 2010; **31**: 370-8
15. Rognin NG, Frinking P, Costa M, Arditi M. In-vivo perfusion quantification by contrast ultrasound: Validation of the use of linearized video data vs. raw RF data. *Ultrasonics Symposium, 2008 IUS Proceedings, IEEE* 2008: 1690 - 3
16. Gorce JM, Arditi M, Schneider M. Influence of bubble size distribution on the echogenicity of ultrasound contrast agents: a study of SonoVue. *Invest Radiol* 2000; **35**: 661-71
17. Mulvana H, Stride E, Tang M, Hajnal JV, Eckersley R. Temperature-dependent differences in the nonlinear acoustic behavior of ultrasound contrast agents revealed by high-speed imaging and bulk acoustics. *Ultrasound Med Biol* 2011; **37**: 1509-17
18. Mulvana H, Stride E, Hajnal JV, Eckersley RJ. Temperature dependent behavior of ultrasound contrast agents. *Ultrasound Med Biol* 2010; **36**: 925-34
19. Yeh CK, Yang MJ, Li PC. Contrast-specific ultrasonic flow measurements based on both input and output time intensities. *Ultrasound Med Biol* 2003; **29**: 671-8
20. Bos LJ, Piek JJ, Spaan JA. Effects of shadowing on the time-intensity curves in contrast echocardiography: a phantom study. *Ultrasound Med Biol* 1996; **22**: 217-27

21. Bouakaz A, De Jong N, Cachard C. Standard properties of ultrasound contrast agents. *Ultrasound Med Biol* 1998; **24**: 469-72
22. Gillmore FR. The growth or collapse of a spherical bubble in a viscous compressible liquid. *California Institute of Technology , Pasadena, CA* 1955
23. Marmottant P, van der Meer S, Emmer M, et al. A model for large amplitude oscillations of coated bubbles accounting for buckling and rupture. *J Acoust Soc Am* 2005; **118**: 3499-505

Chapter 3

Volume quantification by contrast-enhanced ultrasound: an in-vitro comparison with true volumes and thermodilution

Ingeborg HF Herold
Gianna Russo
Massimo Mischi
Patrick Houthuizen
Tamerlan Saidov
Marcel van het Veer
Hans C van Assen
Hendrikus HM Korsten

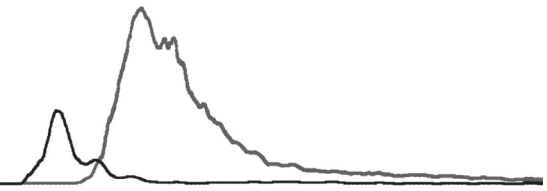

Cardiovascular Ultrasound 2013; 11: 36

ABSTRACT

Background

Contrast-enhanced ultrasound (CEUS) has recently been proposed as a minimally-invasive, alternative method for blood volume measurement. This study aims at comparing the accuracy of CEUS and the classical thermodilution techniques for volume assessment in an in-vitro setup.

Methods

The in-vitro set-up consisted of a variable network between an inflow and outflow tube and a roller pump. The inflow and outflow tubes were insonified with an ultrasound array transducer and a thermistor was placed in each tube. Indicator dilution curves were made by injecting indicator which consisted of an ultrasound-contrast-agent diluted in ice-cold saline. Both acoustic intensity- and thermo-dilution curves were used to calculate the indicator mean transit time between the inflow and outflow tube. The volumes were derived by multiplying the estimated mean transit time by the flow rate. We compared the volumes measured by CEUS with the true volumes of the variable network and those measured by thermodilution by Bland-Altman and intraclass-correlation analysis.

Results

The measurements by CEUS and thermodilution showed a very strong correlation (r_s = 0.94) with a modest volume underestimation by CEUS of –40 ± 28 ml and an overestimation of 84 ± 62 ml by thermodilution compared with the true volumes. Both CEUS and thermodilution showed a high statistically significant correlation with the true volume (r_s = 0.97 (95% CI, 0.95 - 0.98; p<0.0001) and r_s = 0.96 (95% CI, 0.94 - 0.98; p<0.0001, respectively).

Conclusions

CEUS volume estimation provides a strong correlation with both the true volumes in-vitro and volume estimation by thermodilution. It may therefore represent an interesting alternative to the standard, invasive thermodilution technique.

INTRODUCTION

Blood volume determination is a daily routine in anesthesia and intensive care practice. Most of the time, it is roughly estimated using clinical parameters such as blood pressure, heart frequency, urine output, and peripheral temperature. In sepsis, the postoperative phase and heart failure, circulating volume can be difficult to assess and in these cases classical dilution techniques are of additional value. The intrathoracic blood volume can be estimated by transthoracic thermodilution, presently one of the most widely used techniques. Its value and change in response to fluid challenge reflects the left ventricular preload and changes in preload better than more conventional measures like central venous pressure and pulmonary artery wedge pressure.[1] However, these techniques are invasive and require catheterization of the heart and/or large vessels, which can lead to complications.[2-3]

With classical dilution techniques, a known amount of indicator is injected via a central venous line into the jugular or subclavian vein and is carried through the heart and pulmonary circulation where it is mixed and diluted. Downstream, the indicator concentration-change over time is measured at a detection site to create an indicator dilution curve (IDC).[4] The IDC is used to estimate the mean transit time (MTT); this is the average time it takes for the indicator to travel from the injection site to the detection site.[5] When two detection sites are used, the product of MTT difference and flow can be used to calculate the volume in between both sites. Classical indicator-dilution techniques can be performed with different standard indicators (such as cold saline, indocyanine green or lithium) through different access sites (e.g. right or left heart-sided).[2-4, 6] The transpulmonary thermodilution technique allows measurement of cardiac output (CO) and intrathoracic blood volumes.[3, 6]

A less invasive technique may be a valuable alternative to these methods, which are hampered by their invasiveness. A promising minimally invasive alternative technique uses an ultrasound contrast agent (UCA) injected into a peripheral vein as indicator. This can be detected noninvasively by contrast-enhanced ultrasound (CEUS) imaging. Mischi and coworkers previously demonstrated that this technique can be used for estimating blood volumes.[7-9] In this study the measurement of blood volumes by means of UCA dilution with transthoracic echography (TTE) was tested and validated in-vitro. The determination coefficient between the real and the estimated volumes was larger than 0.999 in different model fits.[7] However, to date there has been no comparison with the classic thermodilution technique, which is clinically considered the gold standard for CO and blood volume measurement.

The aim of our study is to compare the CEUS with the thermodilution technique for volume quantification in an in-vitro set-up with different flows and volumes. We decided to use the transesophageal probe as this probe is often used in the perioperative setting, where large volume shifts can occur.

METHODS

In-vitro setup

The realized in-vitro setup (Fig. 1) consisted of an open circuit with a roller pump, Cobe Stoeckert multiflow bloodpump (Stoeckert Instruments, Munich, Germany), a water-filled basin, a network of tubes with a variable volume simulating the pulmonary vessels, and a pressure stabilizer. The whole setup was filled with tap water which was degassed by 24-hour rest. The temperature was maintained at 37°C with heating devices and thermostats at different positions in the set-up. The in- and outflow tubes of the network were submerged in a water-filled basin. The submerged segment of the tubes was made of a thin polyurethane layer (Ultracover®, Microtek" Medical BV, Zutphen, the Netherlands) in order to limit interference with ultrasound measurements. In the water-filled basin, a trans-esophageal (TEE) probe (X7-2 t, Philips Healthcare, MA, USA) was directly submerged in water to optimize the acoustic impedance while insonifying the submerged tubes. Two 0.014" high-fidelity pressure wires (Radiwire, St Jude Medical Inc, St. Paul, MN, USA) were inserted in these tubes. These wires measure temperature at 0 - 25 Hertz (Hz) with an accuracy of 0.05°C within a temperature range of 15 to 42°C. Distal to the centrifugal pump, cold saline and UCA were injected into the inflow tube through an injection point consisting of a single lumen central venous line (Blue flextip catheter, Arrow®, Reading, PA, USA). Between the inflow and outflow tubes, outside the basin, the circuit expanded into a network of eight tubes and converged back into a single outflow tube. This network was made of tubing which is used for cardiopulmonary bypass, matching the roller pump. The tubing (Medtronic, Minneapolis, MN, USA) of the network had a diameter of ¼" with a wall size of $^{3}/_{32}$". The afferent and efferent tubes had a diameter of ½". The length of tubing was adapted to create a physiologic range of volumes.[10-11] The network could be clamped at different positions to create different volumes. The hydrodynamic circuit was open to avoid UCA recirculation and the hydrostatic pressure of the circuit was stabilized at the output. All tubes were isolated with polyethylene covers (Climaflex®, NMC, Eynatten, Belgium) to prevent temperature loss to the surroundings.

Ultrasound system and settings

A commercially available scanner (iE33, Philips Healthcare, Andover, MA, USA) was used to obtain cross-sectional B-mode images of the inflow and outflow tubes. Harmonic imaging at 2.7 - 5.4 MHz was used in order to increase the signal-to-noise ratio (SNR) for low UCA concentration together with a low mechanical index (MI) of 0.2 to reduce bubble disruption. Frame rate was set at 27 Hz, the same time-gain and lateral-gain compensation were employed over all measurements, compression was set at 50 dB, general gain at 60%, and image depth was 8 cm with the focus being at the level of both tubes.

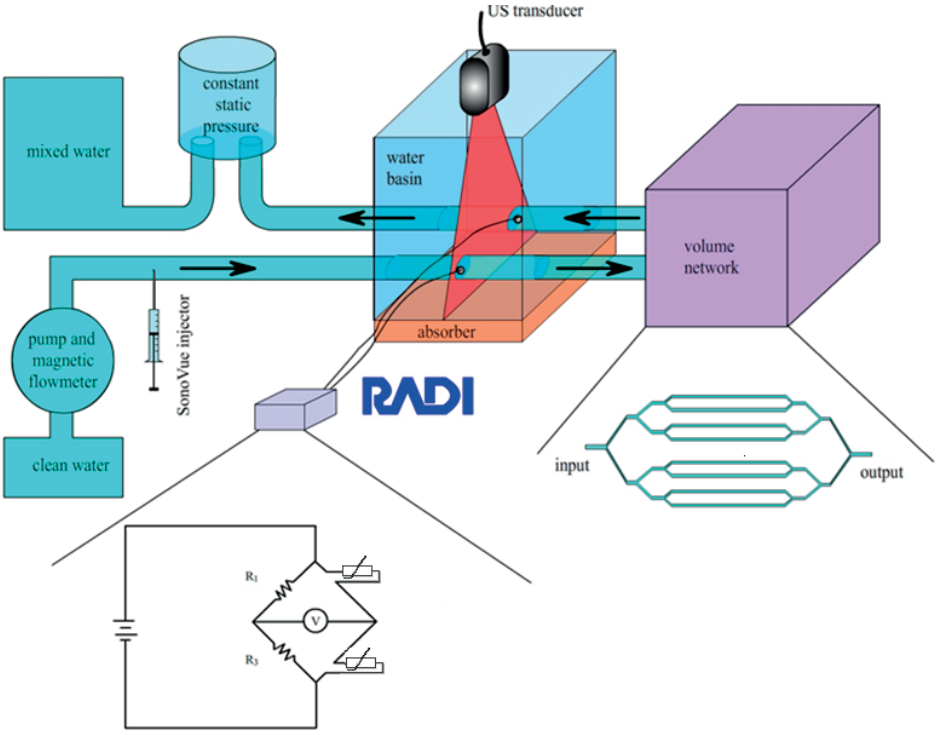

Figure 1. The in-vitro set-up in a schematic overview. The variable network can be clamped at different points to create different volumes.

Calibration

For direct application of the indicator dilution theory, a linear relationship between UCA concentration and detected acoustic intensity is necessary.[8] Therefore, we measured the different acoustic intensities of different doses of UCA (SonoVue®, Bracco SpA, Geneva, Italy) diluted in saline at room temperature and at 4°C. This calibration was performed according to the protocol described by Mischi and coworkers.[7] It had a twofold objective: finding the range of UCA concentrations that show a linear relationship with the measured acoustic intensity, and investigating the effect of temperature on the UCA behavior. The relationship between SonoVue®-concentration and measured acoustic intensity was linear below 1.5 mg/L (Fig. 2) at room temperature and 1 mg/L at 4°C. Above these concentrations shadowing was seen.

Thermodilution measurement

Thermodilution measurements were performed using the pressure wires as described above. These pressure wires have temperature sensing tips that were positioned in the polyurethane tubes and were intercepted by the ultrasound beam for contrast quantifica-

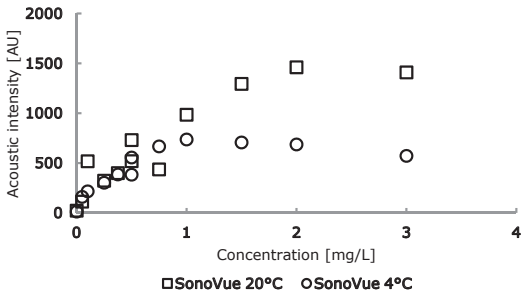

Figure 2. Acoustic intensity calibration curves of SonoVue® at room temperature and at a temperature <4°C. Acoustic intensity is presented on the Y-axis at different temperatures and at different concentrations of SonoVue®. At room temperature (square) there is attenuation above 1.5 mg/L; at a temperature <4°C (circle) attenuation occurs at a concentration between 1 mg/L and 1.5 mg/L. A linear relationship between concentration and acoustic intensity is seen below 1 to 1.5 mg/L at both temperatures.

tion. The temperature sensors of both pressure wires were connected to a Wheatstone bridge adjusted to halfbridge configuration in order to output measured IDCs from both sensors. The electrical circuit further comprised a feedback amplifier (INA 118, Burr-Brown Corporation, Tucson, AZ, USA), a power supply (Delta Elektronica, Zierikzee, the Netherlands), and a data acquisition board (NI USB-6341, National Instruments, Austin, TX, USA). The bridge was balanced by manual adjustment of the value of an embedded potentiometer. The output signal was amplified in such a way that the full range of the analog-to-digital converter of the data acquisition card (0-10 V) was exploited. High frequency noise suppression was achieved by placing an additional capacitance in parallel with the input impedance of the amplifier. All devices were shielded and grounded to minimize ambient disturbances. The thermodilution curves were acquired with LabVIEW (National Instruments, Austin, TX, USA) and processed in MATLAB® 2009b (The Mathworks, Natick, MA, USA). The full system was calibrated by mapping the measured voltage as a function of temperature in a water-filled basin measured by a digital thermometer (Keithley 871, Keithley Instruments, Cleveland, OH, USA). The calibration showed a linear relationship with a slope of 0.65 V/°C and r^2 = 0.999. These results confirmed the system linearity for temperatures in a range 24°C - 40°C.

Ultrasound contrast measurement

Different flows were generated by adjusting the rounds per minute (rpm) of the centrifugal pump. Six flows were used for the measurements that varied between 1 and 4 liters per minute in increments of 0.5 liter per minute. Flow was measured using a flow sensor (Flow controller ARS 260, Biotech, Vilshofen, Germany), at the end of the circuit. By clamping different bifurcations of the variable network, four different volumes were gener-

ated, namely 890 milliliter (ml), 718 ml, 530 ml, and 356 ml (Fig. 1). These volumes have been chosen to cover a range that is slightly broader than the pulmonary blood volumes reported in patients, which range from 271 ml/m^2 (~500 ml) to 421 ml/m^2 (~800 ml) in heart failure patients.[10-11] Every measurement was repeated three times, at six flows and four volumes. With every measurement a bolus of 0.2 ml SonoVue® diluted in 20 ml cold saline (4°C) was injected. The change in acoustic intensity on B-mode ultrasound was stored in an uncompressed format for subsequent analysis with commercially available software (QLAB 8, Philips Healthcare, Andover, MA, USA). This software allows drawing of multiple regions of interest (ROIs) to obtain acoustic IDCs. Two ROIs were drawn within the thin polyurethane layer of the inflow and outflow tube in the water-filled basin. The IDCs were processed and fitted by the local density random walk (LDRW) model using MATLAB® 2009b.[12] The LDRW model was employed since it provides both the best least square error fit to the IDC and a physical description of the dilution process. The MTT of the contrast bolus between the injection and the detection sites was directly derived from the parameters of the fitted model.[7] Volumes were then calculated as the product between the measured flow and the difference in MTT between the two curves.

The MTT can be derived using two different methods. First, the MTT of each IDC can be estimated as the first order statistical moment of the fitted model, using the double fit method (Fig. 3). Second, the indicator dilution system can also be interpreted as a linear system; therefore, the impulse response approach can be employed.[7-8] The impulse

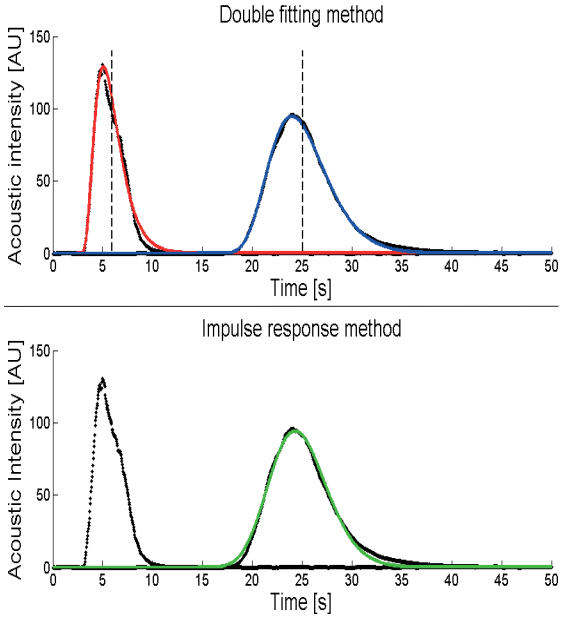

Figure 3. Indicator dilution curves (IDCs) fitted by LDRW double fit method and impulse response method. These IDCs were constructed from post-processing imaging analysis at the level of inflow and outflow tubes at a flow of 2 L/min and true volume of 718 mL. The dotted black line is the IDC at the level of the inflow tube and outflow tube. In the upper picture, the red and blue lines depict the IDCs by the double fit method according to the LDRW model of the inflow and outflow tube. The vertical dashed lines represent the MTTs of each curve. In the bottom picture, the green line depicts the IDC according to the LDRW model impulse response method.

response of the system between the two indicator detection sites was estimated by means of a parametric deconvolution technique, using the system input and output signals represented by the measured IDCs.[8] The estimated impulse response is represented by the LDRW model, which allows blood volume assessments (Fig. 3). The advantage of using a deconvolution technique over a double IDC fitting consists of the independency of the resulting impulse response from the injection function.[7]

Statistics

All data were reported as mean values ± standard deviation (SD) or as median ± interquartile range (IQR) depending on the distribution of the variables of three consecutive measurements. The first goal was to investigate the agreement between measured volumes by both techniques and the true setup volumes. Statistical significance was considered as a two-sided $p<0.05$. Bland-Altman analysis was used to determine the agreement between measured volumes and the true volumes.[13] The effect of the different flows on the volume measurement was also investigated and reported in dedicated plots. Reproducibility was assessed by the intraclass-correlation coefficient (ICC). ICC consists of a basic calculation as repeated-measures analysis of variance (ANOVA) and the intraobserver reliability (ICC (1,1)). ICC assesses the agreement of quantitative variables on its reliability and consistency.[14-15] The second goal was to analyze the correlation between the CEUS volumes and thermodilution volumes, assuming thermodilution as the gold standard. Correlation coefficients were assessed using the Pearson correlation coefficient R or the Spearman cor- relation coefficient r_s depending on normal distribution or non-normal distribution of variables, respectively. Statistical analysis was performed using GraphPad Prism version 5.03 (GraphPad Software, San Diego, CA, USA) except for the intraclass-correlation, which was analyzed by Unistat® Statistical Package for Windows™ version 6.0 (Unistat House, London, England). Statistical analysis was performed by using all data (n=72 measurements) to exclude a bias.

RESULTS

Measurements

A total of 79 measurements were performed. Seven measurements could not be used for analysis as a result of failed acquisition on the ultrasound equipment (n=5) or due to technical failure of the Wheatstone bridge (n=2). All remaining 72 measurements were used for analysis. The CEUS derived median volume of these, using the LDRW model double fit method was 590 (394 – 764) ml. For the impulse response method, the volume was 574 (382 –725) ml. The median volumes estimated with the thermodilution

technique double fit method and impulse response method were 722 (489 – 944) ml and 693 (459 – 886) ml, respectively.

Reproducibility

Repeated-measures ANOVA demonstrated no significant variance between the measures for both CEUS and thermodilution-derived volumes. Intraclass-correlation between three repetitive measurements was ICC = 0.99 (95% confidence interval (CI), 0.98 – 1.00) for the CEUS derived volumes and ICC = 0.97 (95% CI, 0.94 – 0.98) for the thermodilution calculated volumes, using the double fit method. The intraclass-correlation for the measured volumes using the impulse response method was ICC = 0.98 (95% CI, 0.96 – 0.99) for CEUS and ICC = 0.98 (95% CI, 0.97 – 0.99) for thermodilution.

Effect of flow and volume on the measurements

With the setup completely open (largest volume, 890 ml), the CEUS-derived volumes, averaged over all flows, were underestimated by –74 ml, for a true volume of 718 ml the underestimation was –43 mL, for 530 ml it was –30 ml, and for 356 ml it was –13 ml. Using thermodilution on the other hand, a general overestimation was seen. For 890 ml the average overestimation was +122 ml, for 718 ml it was +88 ml, for 530 ml it was + 64 ml, and for 356 ml it was + 63 ml. All the volumes were measured by the LDRW double fit method. In both CEUS and thermodilution, the deviations with respect to the true volumes were larger at larger volumes (Fig. 4).

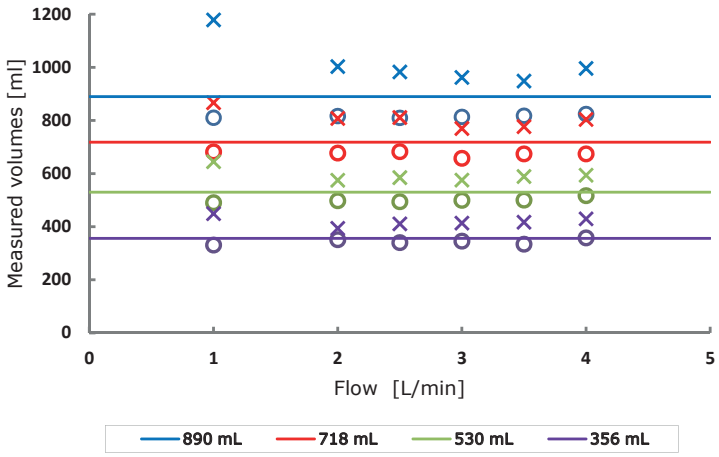

Figure 4. Volume measurements using contrast enhanced ultrasound (bullets) or thermodilution (crosses) at different flow rates and volumes. The different volume settings (true volumes) are indicated in the legend and expressed in the graph as solid lines. Each volume measurement is the average of three repetitions.

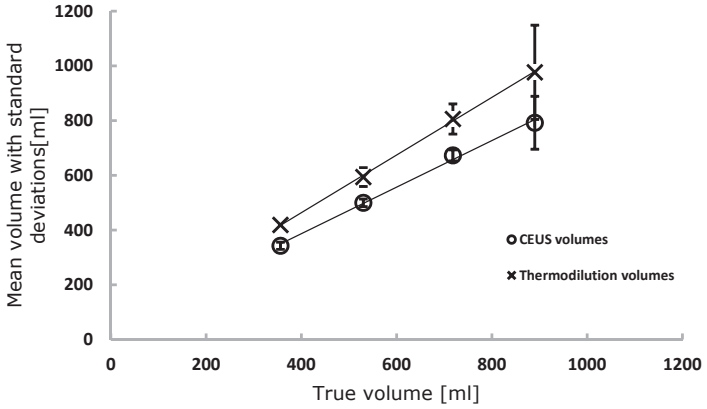

Figure 5. Correlation with standard deviation is shown between the mean volumes measured by contrast-enhanced ultrasound or thermodilution and true volumes. For volume measurements the LDRW double fit method was used. Linear regression analysis revealed following trend: Mean CEUS volume = 0.85 true volume + 47 (r^2 = 0.996). Mean thermodilution volume = 1.05 true volume + 42 (r^2 = 0.999).

Correlation between the measured volumes and true volumes

The correlation between the 72 volumes measured with CEUS and the true volumes showed r_s = 0.97 (95% CI, 0.95 – 0.98; p<0.0001) using the LDRW double fit method and r_s = 0.97 (95% CI, 0.95 – 0.98; p<0.0001), using the LDRW impulse response method. The correlation for the 72 measured volumes using the thermodilution technique showed r_s = 0.96 (95% CI, 0.94 – 0.98; p<0.0001) using the LDRW double fit method. When the LDRW impulse response method was used for the thermodilution measured volumes r_s = 0.97 (95% CI, 0.95 – 0.98; p<0.0001). Figure 5 shows the linear regression analysis for volumes measured with CEUS and the LDRW double fit method. All measured volumes correlated significantly with the true volumes. Bland-Altman analysis (Fig. 6) demonstrated a bias between CEUS and true volumes of –40 ± 28 ml using the LDRW double fit method and –53 ± 41 ml using the LDRW impulse response method. The bias of the thermodilution volumes compared to the true volumes was 84 ± 62 ml and 55 ± 40 ml, for the double fit and impulse method respectively (Fig. 7).

Correlation between volumes estimated with CEUS and the thermodilution technique

The correlation between CEUS and thermodilution technique showed r_s = 0.94 (95% CI, 0.90 – 0.96; p<0.0001), using the LDRW double fit method and r_s = 0.97 (95% CI, 0.95 – 0.98; p<0.0001), using the impulse response method. The Bland-Altman analysis showed a bias of –124 ± 74 ml using the LDRW model double fit method, where thermodilution estimated volumes were on average larger than CEUS volumes. For the LDRW model impulse response method the bias was –108 ± 67 ml.

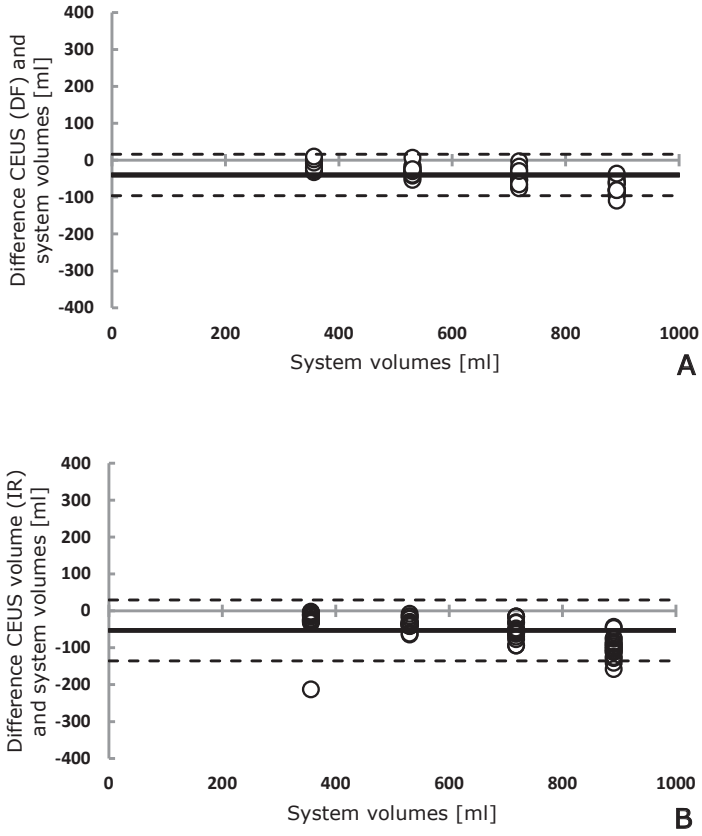

Figure 6. Bland-Altman plots showing the agreement between measured volumes by contrast enhanced ultrasound and true volume of the setup. The volumes measured with contrast-enhanced ultrasound are displayed in left and right panel, using the LDRW double fit (DF) method and LDRW impulse response (IR) method, respectively. The bold line indicates the mean difference between CEUS measured and true volumes (bias), the dashed lines indicate two times the standard deviation.

DISCUSSION

In the present study, comparing volume measurement by CEUS with thermodilution in a controlled in-vitro set-up, we have demonstrated that there is a good correlation between volumes measured by CEUS and by thermodilution (r_s = 0.94 with the LDRW double fit method). Using the Bland-Altman analysis, there was a good level of agreement (bias –108 ± 67 ml with the LDRW double fit method) between both methods with only a modest underestimation of the true volume by CEUS (bias –40 ± 28 ml with the LDRW double fit method). Interestingly, compared to the gold standard of thermodilution, CEUS demonstrated to provide a more accurate measure of a known volume in this in-vitro

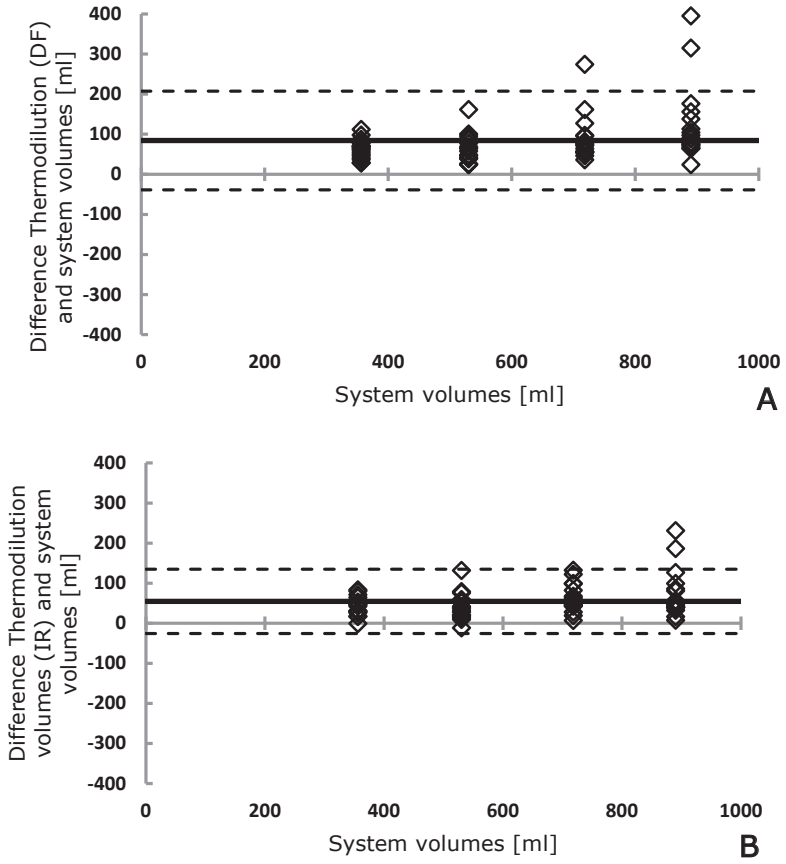

Figure 7. Bland-Altman plots showing the agreement between measured volumes by thermodilution technique and true volumes of the setup. The volumes measured with thermodilution technique are indicated in left and right panel, using the LDRW double fit (DF) method and the LDRW impulse response (IR) method, respectively. The bold line indicates the mean difference between CEUS measured and true volumes (bias), the dashed lines indicate two times the standard deviation.

setup with a bias of only –40 ± 28 ml compared to 84 ± 62 ml for the thermodilution method.

In general, the thermodilution technique overestimated all volumes (Fig. 4). The overestimation of the thermodilution volumes can be explained, in the first place, by loss of heat to the surroundings due to conduction across the tube wall. Heat loss is more marked at low flows and large volumes (Fig. 4) due to longer contact-time and larger surface area, respectively. In order to minimize this effect, we isolated the whole setup and the temperature was kept stable in a narrow range around 37°C. Despite this, the volume overestimation was consistently present even at small volumes (356 ml) and high flows (4 liters per minute), when heat loss is expected to be minimal.

In our study, we used a TEE matrix probe, as this is a more realistic setup to perform volume measurements by CEUS during open heart surgery and the perioperative phase. In general, the proposed methods are also feasible by TTE, as shown in studies by Mischi.[7-8] In comparison to TTE, TEE is closer to the heart with minimal ultrasound attenuation in between. Whether the results with a TEE or TTE probe are interchangeable needs to be investigated in future research.

As no calibration is available for the adopted TEE probe in literature, we calibrated the probe by determining the relationship between the SonoVue® concentration and measured acoustic intensity. The calibration was performed at two different temperatures, namely ambient room temperature (20°C) and the typical temperature used for cold thermodilution (4°C). To this purpose, we diluted SonoVue® in saline at 4°C to obtain sufficient signal-to-noise ratio for the thermodilution IDC and because this temperature is routinely used for clinical thermodilution measurements. We found UCA bubbles to be stable longer at lower temperatures, however at the cost of a reduced echogenicity (Fig. 2).[16] This is in line with the reported decrease in bubble stability at higher temperatures.[17-18] At higher temperature the UCA bubbles expand 5% by gas expansion and show increased acoustic backscatter.[19] Our calibration showed no attenuation below 1.0 mg/L at 4°C. Higher doses will produce a non-stationary (concentration dependent) shadow effect that will influence the IDC quantification, possibly affecting the MTT. We calculated our diluting volume for SonoVue® as the total volume in the circuit, which was over 1 liter. Nevertheless at the lowest volume of the tube network (356 ml) and highest flow (4 L/min) we registered some attenuation in the IDC, probably due to a low effective diluting volume of less than 1 L. In spite of this, the MTT reproducibility at these settings was high with an intraclass-correlation of ICC = 0.99 and an average difference with the true volumes of +2 ml for CEUS and for thermodilution +74 ml (Fig. 4). Therefore, the influence of attenuation on the MTT assessment seems negligible.

The IDCs are fitted using dedicated models that can possibly influence volume measurement thus leading to over- and/or underestimation. With this respect, the LDRW model seems superior as the fitting is based on both the ascending and descending slopes of the IDC which makes it less sensitive to noise. Still, this may lead to underestimation of the IDC tail compared to more common models like mono-exponential and power-law model.[5] In a study of Ugander and coworkers magnetic resonance imaging was evaluated as a method for estimating pulmonary blood volume.[20] An in-vitro validation of pulmonary blood volume measurements was carried out, showing a mean difference between the measured volumes and true volumes of 10 ± 2% for the peak-to-peak method and 4 ± 3% for the center of gravity method.[20] The center of gravity and peak-to-peak methods do not use model fitting for the MTT estimation, and they are more sensitive to low signal-to-noise ratios and contrast recirculation. Moreover, they do not provide a physical interpretation of the investigated convective diffusion process, as

provided by the LDRW model.[21] The LDRW model provides better fits of skewed IDCs, which are present at high flows and small volumes.[5] Our mean difference for CEUS and the true volumes was –6.5 ± 2.8% using the LDRW double fit method and –8.5 ± 2.9% using LDRW impulse response method. A volume underestimation of –3.3 ± 2.3% was also found by different models and settings in another in-vitro study for volume quantification with magnetic resonance imaging.[22] In particular, a slightly lower accuracy and volume underestimation by the impulse response method was reported; however, this was not confirmed by intra-thoracic blood volume measurements in the volunteers. The advantage of the impulse response method consists of making the measurement robust to recirculation and variations in the injection function. Moreover, the identification of the full transpulmonary dilution impulse response brings additional information, possibly adding diagnostic value to the analysis.[22]

Another finding to be discussed relates to the volume underestimation by CEUS. This is likely to be explained with the bubble transport kinetics. It has been reported that bubbles, especially for laminar flow (Reynolds < 2000), show a velocity profile that differs from that of the carrier fluid, leading to a shorter MTT. In particular, while the carrier fluid shows a typical parabolic flow profile, bubbles are reported to travel with a "flatter" profile, whose average velocity over the tube cross section is higher than that of the carrier fluid.[23-24] Additional explanations, to be verified in future studies, might relate to the concentration profile of bubbles across the tube.

In-vivo studies have another carrier fluid, blood, which could influence the indicator dilution curve. As blood is a more viscous carrier fluid than water, the Reynolds number will decrease. As a result, the diffusion coefficient is expected to be lower. The diffusion coefficient influences the parameter λ of the LDRW model, which equals the Peclet number divided by 2. The Peclet number represents the ratio between diffusion and convection time. An increase in viscosity produces therefore an increase in λ, whereas μ, which is representative of the MTT, is not affected.[25]

Our study may provide a good alternative for volume measurement in the perioperative setting and in critical care. The safety of SonoVue® has been investigated in different settings. In a large retrospective study on assessment of adverse events in 28 Italian Centers, serious adverse events were found in 0.0086%.[26-27] SonoVue® microbubbles are composed of SF6 gas with a phospholipid monolayer shell. The elimination of the SF6 gas via the lung is reported to be, even in patients with obstructive pulmonary disease and pulmonary fibrosis, in the same range as in healthy volunteers with a 80-90% clearance within 11 minutes.[26] The phospholipid monolayer is metabolized in the liver. These monolayers are commonly used in the formulation and manufacturing of liposomes, a drug delivery system that is approved by the United States Food and Drug Administration (FDA) and considered biologically safe.[28] Even in blunt abdominal trauma patients, the use of SonoVue® was proven to be safe.[29] Only in patients with a recent

cardiac infarction or heart failure class III and IV, the European Medicines Agency (EMA) took precautions and these conditions are contraindicated for use of SonoVue®.

Limitations of our study relate to the thermodilution technique. Even with extended isolation of the setup, volumes were overestimated using thermodilution. The pressure wires are normally used in coronary arteries to measure flow with thermodilution. These wires are very thin and ideal in our in-vitro setup but not used for larger blood volume measurement. Thus, this correlation cannot be extrapolated in-vivo. Further research will be needed to compare CEUS and evaluate the margin of error with clinically used thermodilution methods for volume measurement, such as PiCCO® (Pulsion Medical Systems, Munich, Germany), and to estimate its value as a minimally-invasive and bedside-applicable technique in the ICU and operating room.[3, 30]

CONCLUSIONS

CEUS seems a promising, minimally-invasive technique to measure volumes. Our in-vitro measurements showed a good correlation and level of agreement between CEUS volumes and the true volumes. We found a general overestimation of the measured volumes by the thermodilution technique and a general underestimation by CEUS, the latter being more evident for larger volumes and lower flows. This study suggests the use of CEUS to be superior to thermodilution and a good equivalent to the gold standard. We believe that this novel, minimally-invasive and non-nuclear method for measuring blood volume can be an asset in clinical research and practice. However, it is mandatory to validate this novel technique with frequently used techniques in daily, clinical practice.

REFERENCES

1. Pinsky MR, Payen D. Functional hemodynamic monitoring. *Crit Care* 2005; **9**: 566-72
2. Swan HJ, Ganz W, Forrester J, Marcus H, Diamond G, Chonette D. Catheterization of the heart in man with use of a flow-directed balloon-tipped catheter. *N Engl J Med* 1970; **283**: 447-51
3. Sakka SG, Ruhl CC, Pfeiffer UJ, et al. Assessment of cardiac preload and extravascular lung water by single transpulmonary thermodilution. *Intensive Care Med* 2000; **26**: 180-7
4. Reuter DA, Huang C, Edrich T, Shernan SK, Eltzschig HK. Cardiac output monitoring using indicator-dilution techniques: basics, limits, and perspectives. *Anesth Analg* 2010; **110**: 799-811
5. Brands J, Vink H, Van Teeffelen JW. Comparison of four mathematical models to analyze indicator-dilution curves in the coronary circulation. *Med Biol Eng Comput* 2011; **49**: 1471-9
6. Maddison B, Wolff C, Findlay G, Radermacher P, Hinds C, Pearse RM. Comparison of three methods of extravascular lung water volume measurement in patients after cardiac surgery. *Crit Care* 2009; **13**: R107
7. Mischi M, Kalker TA, Korsten EH. Contrast echocardiography for pulmonary blood volume quantification. *IEEE Trans Ultrason Ferroelectr Freq Control* 2004; **51**: 1137-47
8. Mischi M, Jansen AH, Korsten HH. Identification of cardiovascular dilution systems by contrast ultrasound. *Ultrasound Med Biol* 2007; **33**: 439-51
9. Korsten HH, Mischi M, Grouls RJ, Jansen A, van Dantzig JM, Peels K. Quantification in echocardiography. *Semin Cardiothorac Vasc Anesth* 2006; **10**: 57-62
10. Schreiner BF, Jr., Murphy GW, James DH, Yu PN. Pulmonary blood volume in patients with congestive heart failure. *Trans Assoc Am Physicians* 1966; **79**: 250-61
11. McGaff CJ, Roveti GC, Glassman E, Milnor WR. Pulmonary blood volume in rheumatic heart disease and its alteration by isoproterenol. *Circulation* 1963; **27**: 77-84
12. Wise ME. Tracer dilution curves in cardiology and random walk and lognormal distributions. *Acta Physiol Pharmacol Neerl* 1966; **14**: 175-204
13. Bland JM, Altman DG. Statistical methods for assessing agreement between two methods of clinical measurement. *Lancet* 1986; **1**: 307-10
14. Shrout PE, Fleiss JL. Intraclass correlations: uses in assessing rater reliability. *Psychol Bull* 1979; **86**: 420-8
15. Weir JP. Quantifying test-retest reliability using the intraclass correlation coefficient and the SEM. *J Strength Cond Res* 2005; **19**: 231-40
16. Herold I, Kuenen IM, Mischi IM, Korsten H. Blood volume and ejection fraction measurements using CEUS.
17. Mulvana H, Stride E, Hajnal JV, Eckersley RJ. Temperature dependent behavior of ultrasound contrast agents. *Ultrasound Med Biol* 2010; **36**: 925-34
18. Goddi A, Novario R, Tanzi F, Di Liberto R, Nucci P. In vitro analysis of ultrasound second generation contrast agent diluted in saline solution. *Radiol Med* 2004; **107**: 569-79
19. Vos R. Single microbubble imaging. *Erasmus MC Rotterdam* 2010: 131-45
20. Ugander M, Kanski M, Engblom H, et al. Pulmonary blood volume variation decreases after myocardial infarction in pigs: a quantitative and noninvasive MR imaging measure of heart failure. *Radiology* 2010; **256**: 415-23
21. Mischi M, den Boer JA, Korsten HH. On the physical and stochastic representation of an indicator dilution curve as a gamma variate. *Physiol Meas* 2008; **29**: 281-94

22. Mischi M, van den Bosch HC, den Boer JA, et al. Intra-thoracic blood volume measurement by contrast magnetic resonance imaging. *Magn Reson Med* 2009; **61**: 344-53
23. Keller MW, Segal SS, Kaul S, Duling B. The behavior of sonicated albumin microbubbles within the microcirculation: a basis for their use during myocardial contrast echocardiography. *Circ Res* 1989; **65**: 458-67
24. Tangelder GJ, Slaaf DW, Muijtjens AM, Arts T, oude Egbrink MG, Reneman RS. Velocity profiles of blood platelets and red blood cells flowing in arterioles of the rabbit mesentery. *Circ Res* 1986; **59**: 505-14
25. Mischi M, Kalker AA, Korsten HH. Cardiac image segmentation for contrast agent videodensitometry. *IEEE Trans Biomed Eng* 2005; **52**: 277-86
26. Morel DR, Schwieger I, Hohn L, et al. Human pharmacokinetics and safety evaluation of SonoVue, a new contrast agent for ultrasound imaging. *Invest Radiol* 2000; **35**: 80-5
27. Piscaglia F, Bolondi L. The safety of Sonovue in abdominal applications: retrospective analysis of 23188 investigations. *Ultrasound Med Biol* 2006; **32**: 1369-75
28. Kang ST, Yeh CK. Ultrasound microbubble contrast agents for diagnostic and therapeutic applications: current status and future design. *Chang Gung Med J* 2012; **35**: 125-39
29. Cagini L, Gravante S, Malaspina CM, et al. Contrast enhanced ultrasound (CEUS) in blunt abdominal trauma. *Crit Ultrasound J* 2013; **5 Suppl 1**: S9
30. Linton RA, Band DM, Haire KM. A new method of measuring cardiac output in man using lithium dilution. *Br J Anaesth* 1993; **71**: 262-6

Chapter 4

Pulmonary blood volume measured by contrast enhanced ultrasound: a comparison with transpulmonary thermodilution

Ingeborg HF Herold
Mohamed A Soliman Hamad
Hans C van Assen
R Arthur Bouwman
Erik H M Korsten
Massimo Mischi

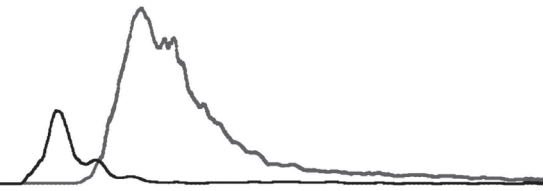

British Journal of Anaesthesia 2015; 115(1): 53-60

ABSTRACT

Background

Blood volume quantification is essential for haemodynamic evaluation guiding fluid management in anaesthesia and intensive care practice. Ultrasound contrast agent (UCA)-dilution measured by contrast-enhanced ultrasound (CEUS) can provide the UCA mean transit time (MTT) between the right and left heart, enabling the assessment of the intrathoracic blood volume ($ITBV^{UCA}$). The purpose of the present study was to investigate the agreement between UCA-dilution using CEUS and transpulmonary thermodilution (TPTD) in-vitro and in-vivo.

Methods

In an in-vitro setup, with variable flows and volumes, we injected a double indicator, ice-cold saline with SonoVue®, and performed volume measurements using transesophageal echo and thermodilution by PiCCO®. In a pilot study, we assigned 17 patients undergoing elective cardiac surgery for pulmonary blood volume (PBV) measurement using TPTD by PiCCO® and ITBV by UCA-dilution. Correlation coefficients and Bland-Altman analysis were performed for all volume measurements.

Results

In-vitro, 73 experimental MTT's were obtained using PiCCO® and UCA-dilution. The volumes by PiCCO® and UCA-dilution correlated with true volumes; $r_s = 0.96$ (95% CI, 0.93 – 0.97; $p<0.0001$) and $r_s = 0.97$ (95% CI, 0.95 – 0.98; $p<0.0001$), respectively. The bias of PBV by PiCCO® and $ITBV^{UCA}$ were -380 ml and -42 ml, respectively. In 16 patients, 86 measurements were performed. The correlation between PBV by PiCCO® and $ITBV^{UCA}$ was $r_s = 0.69$ (95% CI 0.55 – 0.79; $p<0.0001$). Bland-Altman analysis revealed a bias of -323 ml.

Conclusions

ITBV assessment with CEUS seems a promising technique for blood volume measurement, which is minimally-invasive and bedside applicable.

INTRODUCTION

Blood volume quantification is an essential part of haemodynamic evaluation to guide fluid management in anaesthesia and intensive care practice. While cardiac filling pressures, like central venous pressure and pulmonary artery occlusion pressure, are frequently used to estimate preload, volumetric preload parameters obtained with transpulmonary thermodilution (TPTD) proved to be superior to this end.[1-3] With TPTD, arterial thermodilution curves are obtained after injection of a bolus of cold saline in a central vein, providing intrathoracic blood volume (ITBV) and global end-diastolic volume (GEDV).[4] Both parameters significantly relate to changes in stroke volume and cardiac index in various clinical settings.[1-3 5-7] However, TPTD requires insertion of catheters and installation of a device, which is time consuming and not always feasible during anaesthesia.

Recently, contrast-enhanced ultrasound (CEUS) has been proposed as a minimally-invasive, alternative method for blood volume measurement. With CEUS, transpulmonary indicator dilution curves are obtained with a small amount of ultrasound contrast agent (UCA) injected in a peripheral vein. In a previous experimental study, we demonstrated that volume estimation with CEUS in in-vitro conditions was accurate and showed excellent agreement with volume estimation by thermodilution.[8-11] Moreover, we demonstrated the clinical feasibility of pulmonary blood volume (PBV) measurements with CEUS in patients.[8-9] However, comparison of CEUS with TPTD is currently lacking. In this study, we therefore aimed to investigate the agreement between volumes obtained by UCA-dilution and TPTD in an in-vitro setup as well as in a pilot study in patients.

METHODS

In-vitro setup

The agreement of volumes derived from TPTD and UCA-dilution was tested in an in-vitro setup as previously described.[10] The setup consisted of a network of tubes - mimicking the pulmonary vessels - connected to a roller pump (Cobe Stoeckert multiflow bloodpump, Stoeckert Instruments, Munich, Germany) (Fig. 1). Degassed water was used as transport medium and the in- and out-flow tubes were submerged in a water-filled basin at 37 °C. A transesophageal (TEE) probe X7-2t (Philips Healthcare, Andover, MA, USA) was also submerged in the water-filled basin to optimize the acoustic impedance while insonifying the tubes. In the outflow tube a 5 F thermistor-tipped catheter, PV2015 (Pulsion Medical Systems, Munich, Germany) was positioned at the point where the ultrasound beam intercepted the inflow and outflow tubes. With each measurement, a syringe with 20 ml of 4 °C saline and 0.2 ml SonoVue® (Bracco Imaging SpA, Milan, Italy) was injected into the inflow tube through an injection point consisting of a single lumen central venous

line (Blue flextip catheter, Arrow®, Reading, PA, USA) and an injectate temperature sensor PV4046 (Pulsion Medical Systems, Munich, Germany). This SonoVue® dose ensures a linear relationship between concentration and measured acoustic intensity, which is essential for application of the indicator dilution theory.[10]

The injectate temperature sensor and the PiCCO® catheter were connected via an interface cable to the PiCCO® plus monitor (Pulsion Medical Systems, Munich, Germany), which was connected to a computer. Data were accessible with PiCCO®-Win software (Pulsion Medical Systems, Munich, Germany). After a thermodilution measurement, the software provided time, cardiac output (CO), GEDV, $ITBV^{TH}$, extravascular lung water (EVLW), mean transit time (MTT), and down-slope time (DSt).

The volume of the network between the ultrasound interception points was varied to create different system-volumes, namely 890 ml, 718 ml, 530 ml, and 356 ml. All tubes were isolated with polyethylene covers (Climaflex®, NMC, Eynatten, Belgium) preventing heat loss and the hydrodynamic circuit was open to avoid indicator recirculation. The flow generated by the roller pump was varied between 1 and 4 litres min^{-1} in increments of 0.5 litre min^{-1} and controlled by a flow sensor (Flow controller ARS 260, Biotech, Vilshofen, Germany) positioned at the end of the circuit.

The TEE probe made cross-sectional B-mode images of the inflow and outflow tubes (Fig. 2). The ultrasound scanner (iE33, Philips Healthcare, Andover, MA, USA) used harmonic imaging, 2.7 - 5.4 MHz, to increase the signal-to-noise ratio (SNR) for UCA, with a low mechanical index (MI) of 0.2 to reduce microbubble destruction. The other settings were dynamic range of 50 dB, general gain at 60%, frame rate of 27 Hz, and image depth of 8 cm. The B-mode images were stored in an uncompressed format and two regions of interest (ROIs) were drawn in each cross-sectional tube image using commercially available software (QLAB 8, Philips Healthcare, Andover, MA, USA) (Fig. 2A). The passage of SonoVue® along the tubes was registered and acoustic indicator dilution curves (IDCs) were extracted from the ROIs. These acoustic IDCs were fitted by the local density random walk (LDRW) model using MATLAB® 2009b (The Mathworks, Natick, MA, USA) as this model provides the best least square error fit to the IDC and a physical description of the dilution process.[12] The MTT of UCA between the inflow and outflow tubes was directly derived from the parameters of the fitted acoustic IDCs.[8] Volumes ($ITBV^{UCA}$) were calculated as the product of the flow measured by the ARS 260-flow controller and the difference in MTT between the two curves.

Thermodilution acquired volumes were calculated using CO, MTT, and DSt according to the PiCCO® algorithm. The estimated CO and MTT of the thermal indicator are multiplied to determine the thermal distribution volume between the injection site and the thermistor: intrathoracic thermal volume (ITTV).[4, 13] Thermal distribution of cold saline is within the vessel and in the surrounding tissue; therefore, ITTV comprises of $ITBV^{TH}$ and EVLW. The DSt estimated between 85% and 45% of the peak temperature represents the

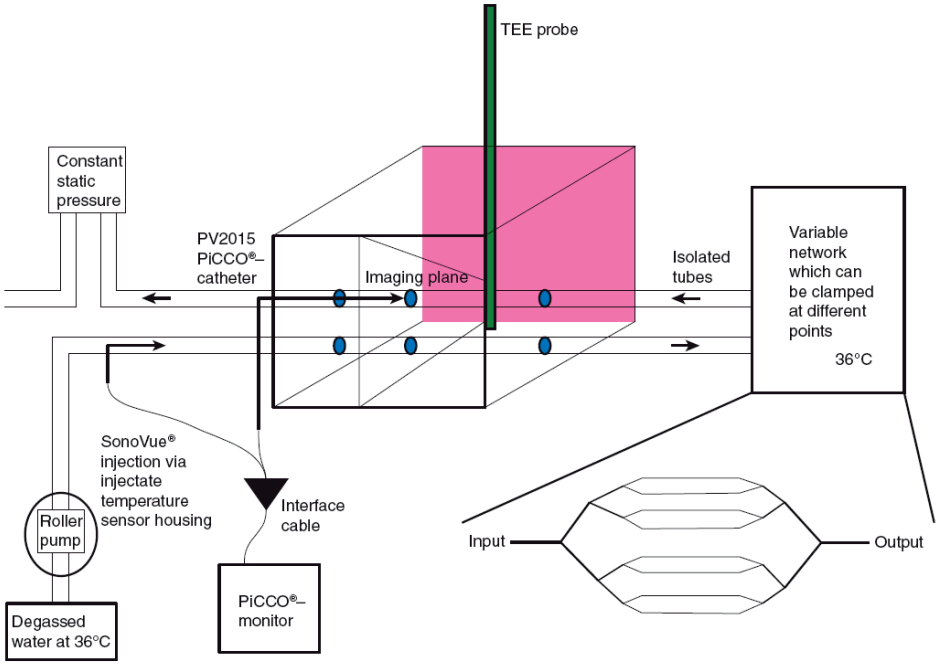

Figure 1. Schematic overview of the in-vitro setup.

time constant of the largest mixing compartment. More precisely, it is the time required by the indicator to pass the largest mixing volume in a cascade of volumes at constant flow. Thus, in clinical applications, DSt represents the time needed to pass the pulmonary circulation and can be used to estimate the pulmonary thermal volume (PTV).[4, 13] PTV consists of the intravascular PBV and the EVLW.

In the in-vitro setup we investigated the agreement between $ITBV^{UCA}$ and ITTV, as we expect the ITTV to correlate the $ITBV^{UCA}$ minus the volume between the injection point and the point where the ultrasound beam intercepts the inflow tube; this was 159 ml. We also investigated the agreement between $ITBV^{UCA}$ and PBV by TPTD, as the PBV is consistent with the intravascular part between the right ventricle and left atrium in patients. The UCA SonoVue® consists of microbubbles which stay intravascular and does not extravasate outside the vessels like cold saline.

Patients

Patients were participating in a follow up study that examined the effect of cardiac resynchronization therapy in cardiac surgery patients with impaired LVEF on ITBV.[14] This study was approved by the Institutional Review board of the Catharina hospital Eindhoven (ISRCTN90330260). Patients scheduled for elective coronary artery bypass grafting surgery were included after written informed consent was obtained. Patients were aged

18 years and above, had an ejection fraction ≤ 35%, sinus rhythm, QRS duration over 130 milliseconds and left bundle branch block pattern. Patients with preoperative atrial fibrillation, a myocardial infarction within the past three months, a history of gastric or oesophageal disease and allergy to sulphur-hexafluoride were excluded.

Measurement protocol

After induction of anaesthesia, all patients received an 8.5 F central venous catheter (DM- 12853, Arrow®, Reading, PA, USA) in the right jugular vein. The medial lumen was connected to the injectate temperature sensor (PV4046, Pulsion Medical Systems, Munich, Germany). The Pulsiocath 5 F termistor-tipped catheter, PV2015L20A (Pulsion Medical Systems, Munich, Germany), was placed in the femoral artery. Both the injectate sensor and Pulsiocath were connected to the PiCCO$_2$® monitor (Pulsion Medical Systems, Munich, Germany). For UCA-dilution, a TEE probe X7-2t, connected to an iE33 ultrasound scanner (both, Philips Healthcare, Andover, MA, USA) was placed in the esophagus.

Measurements were performed during the operation except during cardiopulmonary bypass time. At least three measurements were done before and after cardiopulmonary bypass. Each measurement consisted of a simultaneous ultrasound registration and TPTD by injecting a double indicator: 20 ml ice-cold saline with 0.2 ml SonoVue®. Injection of the indicator through the injectate temperature sensor automatically started the TPTD measurement on the PiCCO$_2$® monitor. Thermodilution data were stored on a personal computer connected to the monitor using PiCCO®-Win software. The MTT, DSt, CO, and ITTV were registered. GEDV is the end-diastolic volume of the four heart chambers and is given as the difference between ITTV and PTV. The ITBVTH is calculated according to the simplified equation: 1.25 • GEDV, which is used in the PiCCO® software.[15] The EVLW is calculated by subtracting the ITBVTH from the ITTV. Finally, PBV is calculated by subtracting the EVLW from the PTV.

The ultrasound settings were harmonic imaging at 2.7-5.4 MHz, frame rate of 27 Hz, MI 0.2, and linear post-processing. The digital loops were recorded in a standard four chamber view with a maximum loop-time of 180 seconds to acquire the right atrium (RA) and left atrium (LA) UCA indicator dilution curves (UCA-IDCs). The acoustic intensity evolution over time of the UCA-IDCs was measured by drawing ROIs in the RA and LA, using Qlab 8 software for acoustic quantification (Fig. 2B). These IDCs were fitted by the LDRW model (Fig. 2D) as mentioned in the in-vitro section. The difference in MTT (ΔMTT) between LA and RA was derived by model fitting and subtraction, and the ITBV^{UCA} was calculated by multiplying ΔMTT by the CO assessed by thermodilution, measured simultaneously by PiCCO®.

As described above, the agreement between the ITBV^{UCA} and the PBV was assessed, as the PBV is the closest to the anatomical volume assessed by ITBV^{UCA} in patients.

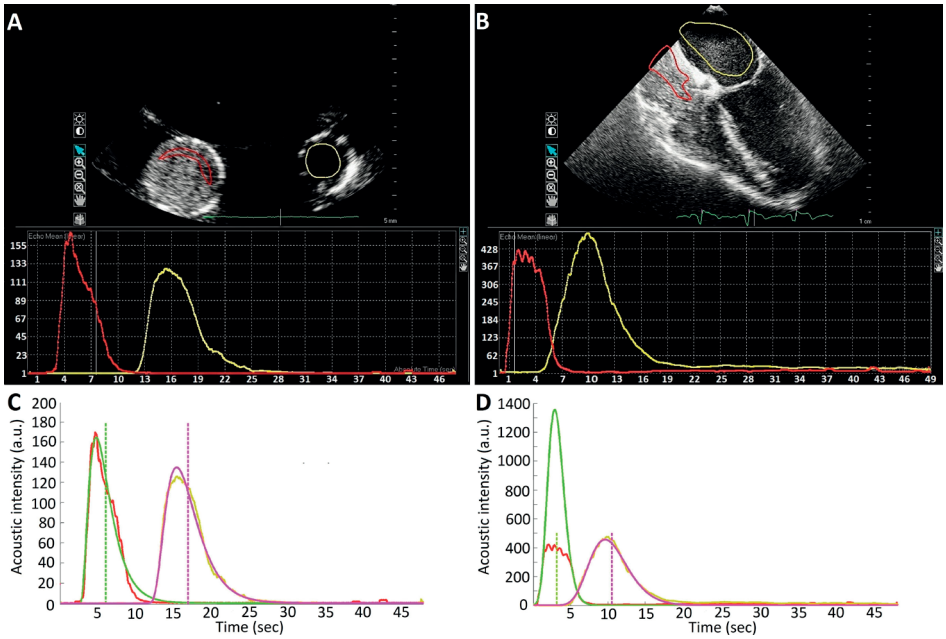

Figure 2. (A.) Cross-sectional B-mode images of the inflow and outflow tubes obtained by an iE33 ultrasound scanner in the water-filled basin at pump flow of 2 litre min^{-1} and a true volume of 530 ml. Two regions of interest are drawn in the inflow and outflow tube. At the bottom of the figure, the acoustic dilution curves are presented. They represent the acoustic intensity over time in the selected region of interest. (B.) Four chamber view with harmonic imaging; ice-cold SonoVue® is injected via a central venous line and passage through the four heart chambers is acquired with an iE33 TEE-probe. Two regions of interest are drawn in the right atrium and left atrium resulting in acoustic intensity over time signals, which are presented at the bottom of the figure. (C and D.) The acoustic intensity dilution curves (A-IDC) of the above-presented B-mode images, both fitted by the LDRW model. The red and yellow lines are the measured A-IDCs, corresponding to panel A and B. The green and pink curves are the fitted IDCs of the inflow tube and right atrium, and outflow tube and left atrium, the green and pink dotted vertical lines express the MTT of each IDC.

Statistical analysis

GraphPad Prism version 5.03 (GraphPad Software, San Diego, CA, USA) statistical software was used for all statistical analysis. In both the in-vitro and in-vivo datasets, the distribution of the volume-data was assessed using the D'Agostino-Pearson normality test. All normally distributed parameters are expressed as mean ± SD and differences were calculated using Student's unpaired *t*-tests. Non-parametric data are expressed as median (25^{th}, 75^{th} percentiles) and assessed for differences using the Mann-Whitney U-tests. For all tests, a p value < 0.05 was considered as significant. The relation between ITTV, PBV, $ITBV^{UCA}$ in-vitro and true volumes was analyzed by linear regression. The level of agreement between ITTV, PBV, $ITBV^{UCA}$ and true volumes of the in-vitro setup was determined with Bland-Altman analysis.[16] In patients, PBV and $ITBV^{UCA}$ were compared by regression analysis. Bland-Altman analysis was used to analyze the agreement between PBV and

ITBV^{UCA} and was corrected for repeated measures using MedCalc Statistical Software version 14.8.1 (MedCalc Software bvba, Ostend, Belgium).[17]

RESULTS

In-vitro comparison of TPTD versus UCA-dilution

A total of 73 simultaneous UCA-dilution and TPTD measurements were performed at different volumes and flows. Both ITTV and PBV showed good correlation with the true volumes, r_s = 0.96 (95% CI, 0.93 – 0.97; p<0.0001) for ITTV, and r_s = 0.96 (95% CI, 0.93 – 0.97; p<0.0001) for PBV. ITBV^{UCA} showed excellent correlation with the true volumes with a correlation coefficient r_s = 0.97 (95% CI, 0.95 – 0.98; p<0.0001) (Fig. 3A).

Bland-Altman analysis of the TPTD volumes and true volumes revealed a bias of 499 ml (limits of agreement 176 ml to 821 ml) for ITTV and -380 ml (limits of agreement of -88 ml to -672 ml) for the PBV. ITBV^{UCA} Bland-Altman analysis yielded a bias of -42 ml (limits of agreement of -103 ml to 18 ml) (Fig. 3B). When comparing the measured volumes by UCA-IDC and PBV by TPTD, the bias was -338 ml (limits of agreements of -90 ml to

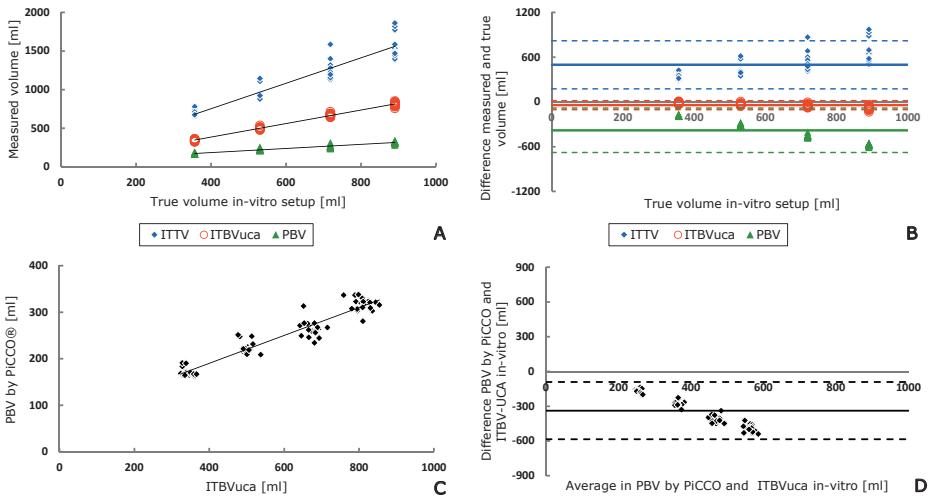

Figure 3. (A.) Correlation between ITTV (blue diamonds) and PBV (green triangles) by PiCCO® as well as ITBV^{UCA} (red circles) with the true volumes in the in-vitro setup. Solid lines are lines of regression. (B.) Bland-Altman plot of the ITBV^{UCA} (red circles) and the true volume in the in-vitro setup and of both ITTV (blue diamonds) and PBV (green triangles) by PiCCO® with respect to the true volume; solid lines present mean differences (bias); dotted lines represent limits of agreement [bias (1.96 SD)]. (C.) Correlation between PBV by PiCCO® and ITBV^{UCA}, in-vitro. Solid line is a line of regression. (D.) Bland-Altman plot of PBV by PiCCO® and ITBV^{UCA}; solid line is the mean difference (bias); dotted lines are limits of agreement [bias (1.96 SD)].

-585 ml). In detail, Bland-Altman analysis showed that TPTD largely overestimated the true volumes at higher volumes. This trend between bias and volume was not observed for UCA derived volumes (Fig. 3B and D).

In-vivo comparison of PBV by TPTD and ITBV by UCA-dilution

Patient characteristics and the demographic data are presented in Table 1. 17 patients were enrolled; one patient was excluded because of inadequate TPTD data acquisition. In each patient, at least 2 simultaneous loops were performed with echocardiography and TPTD, before and after cardiopulmonary bypass.

A total of 86 measurements were performed. The median PBV was 356 ml (IQR 306 - 418 ml) and the median $ITBV^{UCA}$ was 685 ml (IQR 567 - 771ml). The correlation between the PBV and the $ITBV^{UCA}$ was $r_s = 0.69$ (95% CI, 0.55 - 0.79; $p<0.0001$). Bland-Altman analysis for repeated measures revealed a bias of -323 ml with limits of agreement ranging from -69 ml to -578 ml (Fig. 4).[17]

Table 1. Patient characteristics and preoperative data.

Male/female (n)	16/1
Age (yr)	66 (47-80)
Weight (kg)	81 (14)
Height (cm)	172 (9)
ASA classification	3
Hypertension, n (%)	6 (35)
LVEF (%)	32 (7)
Diabetes mellitus, n (%)	4 (24)
COPD, n (%)	3 (18)
Hypercholesterolaemia, n (%)	11 (65)
QRS duration (ms)	127 (30)

Data are presented as number (n), mean (SD), and percentages. ASA, American Society of Anaesthesiologists classification system; LVEF, left ventricular ejection fraction; COPD, Chronic Obstructive Pulmonary Disease

DISCUSSION

The present study investigated the agreement between ITBV measured by UCA-dilution and ITTV as well as PBV, measured by TPTD, both in an in-vitro setup and in patients. In the in-vitro setup, $ITBV^{UCA}$ showed an excellent agreement over the whole range of true volumes and flows of the setup, while a considerable bias was noted in the thermodilution derived volumes especially at the lower flows and higher volumes.

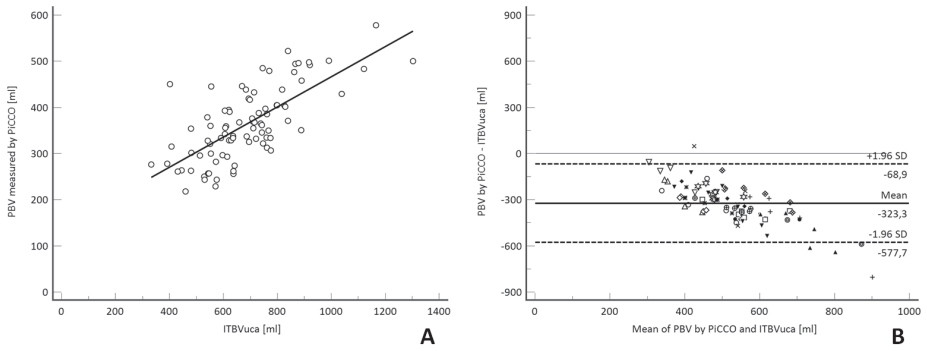

Figure 4. (A.) Correlation between the PBV by PiCCO® and $ITBV^{UCA}$ by UCA-dilution in patients. Solid line is the line of regression. (B.) Bland-Altman plot for repeated measures of the PBV measured by TPTD and $ITBV^{UCA}$ in patients; Solid line is the mean difference (bias); dotted lines are limits of agreement [bias (1.96 SD)].

In patients, a good correlation was found between the $ITBV^{UCA}$ and PBV by TPTD. However, a large bias was found, with $ITBV^{UCA}$ being nearly twice as large as PBV by thermodilution. Here, $ITBV^{UCA}$ is defined as the intravascular volume between the right atrium and left atrium; we therefore expect to find a bias corresponding to the average right ventricular volume. The results from the in-vitro setup are in line with previous observations, where UCA-dilution was used next to thermodilution using thermistor equipped high fidelity pressure wires.[10] Also in this study, a small bias was found between the UCA-dilution acquired volumes and the true volumes.[8, 10] Correspondingly, a large bias was also found for ITTV acquired volumes with an overestimation especially at higher volumes.[10] Likewise, Mischi and coworkers found a high correlation between the UCA-dilution volumes and the true volumes in another in-vitro setup with a continuous flow pump.[8] The ITTV estimated volumes, in this study, were corrected for the volume between the injection point and the interception of the ultrasound beam at the inflow tube, which is not an explanation for the overestimation. As in the previous study, the overestimation of the volumes can be explained by loss of indicator (heat) to the surroundings.[10] In a corresponding study in patients, where intrathoracic compartments were measured by ultrasound dilution in an extracorporeal arteriovenous loop and PiCCO®, the GEDV by PiCCO® overestimated the corresponding ultrasound dilution acquired total end-diastolic volumes.[18]

On the other hand, the PBV by thermodilution underestimated the true volume; this can partly be explained by the algorithm. Single TPTD used Newman's "slope-volume method" to estimate the PTV.[19] However, Newman's model assumes instantaneous mixing in a single compartment, which is not a realistic assumption in the pulmonary circulation and in the adopted in-vitro setup; in fact, precise anatomic boundaries probably cannot be assigned.[20] As MTT measurements by thermodilution depend on flow and on diffusion

of heat through two compartments, measurement errors may occur easier; cold saline is an indicator that diffuses both in the intravascular and extravascular compartments. Therefore, especially for low CO and high EVLW, significant errors in the measurement of MTT and thus EVLW may occur.[21]

In addition, the volumes measured with UCA-dilution correspond to volumes previously reported in literature. Using dye dilution technique during right and left heart catheterization Roy and co-authors noted that the pulmonary circulation was on average 211 ml m^{-2}.[22] The same study showed that in patients with mitral valve insufficiency, pulmonary volumes closely matched the clinical signs of pulmonary congestion ranging from exertional dyspnoea (mildly elevated PBV i.e. 266 ml m^{-2}) to nocturnal dyspnoea (severely elevated PBV i.e. 478 ml m^{-2}).[22] These ranges of PBV are in agreement with other studies with rheumatic heart disease and congestive heart failure and studies with radionuclide imaging.[23-26] Interestingly, the volumes by UCA-dilution (average $ITBV^{UCA}$ –indexed of 355 ml m^{-2}) seem more in this range with respect to this patient category with decreased EF and widened QRS-duration. To the best of our knowledge, PBV by PiCCO® has never been evaluated. The mismatch of the PBV by TPTD and those of other studies may challenge the PBV measurements derived from PiCCO®.

As discussed previously, in in-vitro conditions we observed for the TPTD volume estimations an inverse relation between volume and bias suggesting that PBV measurements underestimate especially at larger volumes. Interestingly, in patients, we found a similar inverse relation between volume and bias, which seems to confirm that the limitations of TPTD may also apply in the in-vivo measurements. However, whether blood volume estimations with UCA-dilution provide more reliable results in patients needs to be addressed in future studies.

This study has some limitations. The volumes in the in-vitro setup where not completely matched, as PiCCO® uses a single catheter technique with an algorithm to calculate the intrathoracic compartment using the DSt. We tried to minimize the bias for PiCCO® by applying a correction, but the difference was too large and the bias was not constant. In our pilot study, the patient number is low and our patient population had a low EF with widened QRS duration. The UCA-dilution used the LA and RA for measuring the $ITBV^{UCA}$ because of shadowing as a result of the intra-atrial septum over the right ventricle; this yields a difference comparing this volume to the actual PBV between the LA and pulmonary artery.

Future studies should be aimed at validating $ITBV^{UCA}$ in patients with preserved LV EF and compare the results with heart failure patients. Also, future analyses should include assessment of trending accuracy, as relative changes are often clinically more important than absolute values. Second, in radiology, a strong correlation was found between pulmonary transit time by cardiac magnetic resonance imaging (CMR) and different heart failure parameters like: LV diastolic function, N-terminal pro-B-type natriuretic peptide,

LV volumes and, inversely, with LV EF.[27-28] Validating this relationship with UCA-dilution would be of interest to confirm the value of our technique with echocardiography. Third, PiCCO®'s DSt, underestimates the volumes both in-vitro and in-vivo; these volumes should be evaluated using double catheter techniques with an indicator, which is more bound to the intravascular compartment, like dye dilution. Finally, automatic MTT derivation from any ROI in the cavity and reliability tests should be obtained to make it clinically accessible.

In conclusion, we investigated the agreement between ITBV measurements using PiCCO® and UCA-dilution technique. UCA-dilution had the lowest bias in-vitro. Although in patients, the observed differences in PBV between the two methods were relatively large, the UCA-dilution estimated volumes are more in line with the reported normal range of the PBV measured by dye-dilution or radionuclide imaging in literature. This novel minimally-invasive technique using echocardiography and UCAs deserves further investigation as it could provide an additional clinical tool for estimation of cardiac preload and LV function at the bedside.

REFERENCES

1. Sakka SG, Bredle DL, Reinhart K, Meier-Hellmann A. Comparison between intrathoracic blood volume and cardiac filling pressures in the early phase of hemodynamic instability of patients with sepsis or septic shock. *J Crit Care* 1999; **14**: 78-83
2. Della Rocca G, Costa GM, Coccia C, Pompei L, Di Marco P, Pietropaoli P. Preload index: pulmonary artery occlusion pressure versus intrathoracic blood volume monitoring during lung transplantation. *Anesth Analg* 2002; **95**: 835-43
3. Huber W, Umgelter A, Reindl W, et al. Volume assessment in patients with necrotizing pancreatitis: a comparison of intrathoracic blood volume index, central venous pressure, and hematocrit, and their correlation to cardiac index and extravascular lung water index. *Crit Care Med* 2008; **36**: 2348-54
4. Sakka SG, Ruhl CC, Pfeiffer UJ, et al. Assessment of cardiac preload and extravascular lung water by single transpulmonary thermodilution. *Intensive Care Med* 2000; **26**: 180-7
5. Goedje O, Seebauer T, Peyerl M, Pfeiffer UJ, Reichart B. Hemodynamic monitoring by double-indicator dilution technique in patients after orthotopic heart transplantation. *Chest* 2000; **118**: 775-81
6. Muller L, Louart G, Bengler C, et al. The intrathoracic blood volume index as an indicator of fluid responsiveness in critically ill patients with acute circulatory failure: a comparison with central venous pressure. *Anesth Analg* 2008; **107**: 607-13
7. Bindels AJ, van der Hoeven JG, Graafland AD, de Koning J, Meinders AE. Relationships between volume and pressure measurements and stroke volume in critically ill patients. *Crit Care* 2000; **4**: 193-9
8. Mischi M, Kalker TA, Korsten EH. Contrast echocardiography for pulmonary blood volume quantification. *IEEE Trans Ultrason Ferroelectr Freq Control* 2004; **51**: 1137-47
9. Mischi M, Jansen AH, Korsten HH. Identification of cardiovascular dilution systems by contrast ultrasound. *Ultrasound Med Biol* 2007; **33**: 439-51
10. Herold IH, Russo G, Mischi M, et al. Volume quantification by contrast-enhanced ultrasound: an in-vitro comparison with true volumes and thermodilution. *Cardiovasc Ultrasound* 2013; **11**: 36
11. Korsten HH, Mischi M, Grouls RJ, Jansen A, van Dantzig JM, Peels K. Quantification in echocardiography. *Semin Cardiothorac Vasc Anesth* 2006; **10**: 57-62
12. Wise ME. Tracer dilution curves in cardiology and random walk and lognormal distributions. *Acta Physiol Pharmacol Neerl* 1966; **14**: 175-204
13. Neumann P. Extravascular lung water and intrathoracic blood volume: double versus single indicator dilution technique. *Intensive Care Med* 1999; **25**: 216-9
14. Soliman Hamad MA, van Gelder BM, Bracke FA, van Zundert AA, van Straten AH. Acute hemodynamic effects of cardiac resynchronization therapy in patients with poor left ventricular function during cardiac surgery. *J Card Surg* 2009; **24**: 585-90
15. Reuter DA, Felbinger TW, Moerstedt K, et al. Intrathoracic blood volume index measured by thermodilution for preload monitoring after cardiac surgery. *J Cardiothorac Vasc Anesth* 2002; **16**: 191-5
16. Bland JM, Altman DG. Statistical methods for assessing agreement between two methods of clinical measurement. *Lancet* 1986; **1**: 307-10
17. Bland JM, Altman DG. Agreement between methods of measurement with multiple observations per individual. *J Biopharm Stat* 2007; **17**: 571-82

18. Galstyan G, Bychinin M, Alexanyan M, Gorodetsky V. Comparison of cardiac output and blood volumes in intrathoracic compartments measured by ultrasound dilution and transpulmonary thermodilution methods. *Intensive Care Med* 2010; **36**: 2140-4
19. Newman EV, Merrell M, Genecin A, Monge C, Milnor WR, Mc KW. The dye dilution method for describing the central circulation. An analysis of factors shaping the time-concentration curves. *Circulation* 1951; **4**: 735-46
20. Grodins FS. Basic concepts in the determination of vascular volumes by indicator-dilution methods. *Circ Res* 1962; **10**: 429-46
21. Isakow W, Schuster DP. Extravascular lung water measurements and hemodynamic monitoring in the critically ill: bedside alternatives to the pulmonary artery catheter. *Am J Physiol Lung Cell Mol Physiol* 2006; **291**: L1118-31
22. Roy SB, Bhardwaj P, Bhatia ML. Pulmonary blood volume in mitral stenosis. *Br Med J* 1965; **2**: 1466-9
23. McGaff CJ, Roveti GC, Glassman E, Milnor WR. Pulmonary blood volume in rheumatic heart disease and its alteration by isoproterenol. *Circulation* 1963; **27**: 77-84
24. Schreiner BF, Jr., Murphy GW, James DH, Yu PN. Pulmonary blood volume in patients with congestive heart failure. *Trans Assoc Am Physicians* 1966; **79**: 250-61
25. Jones RH, Sabiston DC, Jr., Bates BB, Morris JJ, Anderson PA, Goodrich JK. Quantitative radionuclide angiocardiography for determination of chamber to chamber cardiac transit times. *Am J Cardiol* 1972; **30**: 855-64
26. Slutsky R, Higgins C, Bhargava V, et al. Pulmonary blood volume: correlation of equilibrium radionuclide and dye-dilution estimates. *Invest Radiol* 1982; **17**: 233-40
27. Cao JJ, Wang Y, McLaughlin J, et al. Left ventricular filling pressure assessment using left atrial transit time by cardiac magnetic resonance imaging. *Circ Cardiovasc Imaging* 2011; **4**: 130-8
28. Shors SM, Cotts WG, Pavlovic-Surjancev B, Francois CJ, Gheorghiade M, Finn JP. Heart failure: evaluation of cardiopulmonary transit times with time-resolved MR angiography. *Radiology* 2003; **229**: 743-8

Chapter 5

Pulmonary transit time measurement by contrast-enhanced ultrasound in left ventricular dyssynchrony

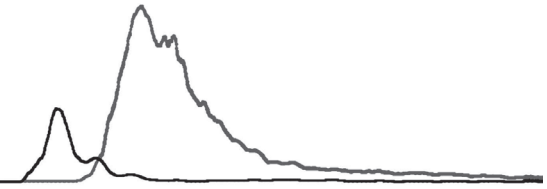

Ingeborg HF Herold
Salvatore Saporito
Massimo Mischi
Hans C van Assen
R Arthur Bouwman
Anouk GW de Lepper
Harrie CM van den Bosch
Hendrikus HM Korsten
Patrick Houthuizen

Echo Res Pract 2016; 3: 35-43

ABSTRACT

Background

Pulmonary transit time (PTT) is an indirect measure of preload and left ventricular function, which can be estimated using the indicator dilution theory by contrast-enhanced ultrasound (CEUS). In this study, we first assessed the accuracy of PTT-CEUS by comparing it with dynamic contrast-enhanced magnetic resonance imaging (DCE-MRI). Secondly, we tested the hypothesis that PTT-CEUS correlates with the severity of heart failure, assessed by MRI and N-terminal pro-B-type natriuretic peptide (NT-proBNP).

Methods and Results

Twenty patients referred to our hospital for cardiac resynchronization therapy (CRT) were enrolled. DCE-MRI, CEUS, and NT-proBNP measurements were performed within an hour. Mean transit time (MTT) was obtained by estimating the time evolution of indicator concentration within regions of interest drawn in the right and left ventricles in video loops of DCE-MRI and CEUS. PTT was estimated as the difference of the left and right ventricular MTT. Normalized PTT (nPTT) was obtained by multiplication of PTT with the heart rate. Mean PTT-CEUS was 10.5 ± 2.4 s and PTT-DCE-MRI was 10.4 ± 2.0 s (p=0.88). The correlations of PTT and nPTT by CEUS and DCE-MRI were strong; r = 0.75 (p=0.0001) and r = 0.76 (p=0.0001), respectively. Bland–Altman analysis revealed a bias of 0.1 s for PTT. nPTT-CEUS correlated moderately with left ventricle volumes. The correlations for PTT-CEUS and nPTT-CEUS were moderate to strong with NT-proBNP; r = 0.54 (p=0.022) and r = 0.68 (p=0.002), respectively.

Conclusions

PTT/nPTT-CEUS showed strong agreement with that by DCE-MRI. Given the good correlation with NT-proBNP level, PTT/nPTT-CEUS may provide a novel, clinically feasible measure to quantify the severity of heart failure.

INTRODUCTION

Intrathoracic transit time of blood flow can be used to estimate preload, blood volumes, and global ventricular function.[1] More than five decades ago, it was demonstrated that the invasively measured pulmonary blood volume was related to the severity of heart failure as expressed by the New York Heart Association (NYHA) classification.[2] Also, the relationship between the intrathoracic circulation time derived from dynamic contrast-enhanced magnetic resonance imaging (DCE-MRI) and different heart failure parameters has been confirmed.[3,4]

Pulmonary transit time (PTT), which is a component of intrathoracic transit time, might be suitable to quantify the severity of congestive heart failure, a disease characterized by increased circulation times and elevated filling pressures.[3-5] Nowadays, there is an increasing interest to assess PTT less invasively by applying the indicator dilution theory to contrast-enhanced ultrasound (CEUS).[5-7] Experimental research has validated the relationship between PTT measurement by CEUS and the extent of heart failure.[8] The reliability of transit time measurements and volume estimations with CEUS is accurate and reproducible, whereas the traditional thermodilution measurements tended to overestimation, probably because of extravascular indicator loss.[7,9] The promising results of PTT measurements by CEUS make it a potential clinical tool, easy to apply at the bedside.[5,10]

In this study, we investigated the agreement between the PTT measured by CEUS and DCE-MRI in a cohort of heart failure patients referred for cardiac resynchronization therapy (CRT). We hypothesized that PTT is a parameter related to the severity of congestive heart failure and therefore correlates with MRI parameters of left ventricular dysfunction, echocardiographic estimates, and N-terminal pro-B-type natriuretic peptide (NT-proBNP).

METHODS

Study population

The patient population consisted of 20 patients referred to the Catharina Hospital in Eindhoven (the Netherlands) for implantation of a CRT device. According to the hospital protocol, all patients underwent extensive evaluation before resynchronization that included echocardiography, electrocardiography, and measurement of NT-proBNP level. The majority of patients were in heart failure (New York Heart Association (NYHA) functional classes II–IV) with left ventricular systolic failure (ejection fraction ≤35%) and electrical dyssynchrony (QRS duration >120 ms). Patients were eligible for inclusion if they were in sinus rhythm and had no contraindications for ultrasound contrast agents (UCAs) or gadolinium (i.e., acute coronary syndrome or acute heart failure within the past

3 months, any mechanical or biological valve prosthesis, atrial septal defect, right to left shunt, severe pulmonary hypertension, uncontrolled arterial hypertension, known allergy to sulfur hexafluoride, end- stage renal or hepatic disease, pregnancy) as well as general contraindications to DCE-MRI. The Institutional Review Board of the Catharina Hospital, Eindhoven, approved the study (NCT01735838), and written informed consent was obtained from all subjects.

PTT estimation

Mean transit times (MTTs) of the indicator, UCA in echocardiography (Fig. 1) and gadolinium in DCE-MRI were obtained using the indicator dilution theory.[6,11] Briefly, the transcardiac passage after an injection of a bolus indicator was registered by the ultrasound or MRI scanner. From the acquired video clips, indicator dilution curves (IDCs) were generated by measuring the time evolution of, respectively, acoustic intensity (echocardiography) or MR signal from regions of interest (ROIs) drawn within the right and left ventricle (Fig. 1). As for both indicators, the applied dose ensured linearity between concentration and reflected intensity, IDCs reliably represent contrast concentration changes.[6,11] For the echo loops, ROI tracing was performed using commercially available software (Qlab 8.1 Advanced Quantification Software, Philips Healthcare). For the MRI signal within the ROIs, custom-made software was used in MATLAB 2014b (The Mathworks, Natick, MA, USA).[11] The IDCs were then fitted according to the local density random walk (LDRW) model using MATLAB 2014b. This model gives a physical description of the indicator transport through the circulation as a convective dispersion process.[12-14] MTTs of both right and left ventricles were subsequently derived from the fitted IDCs. The difference between the MTT in the left and right ventricles represented the PTT. As the PTT can be influenced by the heart rate, it was normalized to heart rate (nPTT) by multiplication with the number of heart beats per second. The heart rate was estimated by the R-R interval of the pulsed Doppler aortic flow and phase-contrast angiography for echocardiography and MRI, respectively. The nPTT expresses the number of stroke volumes needed to pass the pulmonary vascular bed.[15]

DCE-MRI

Cardiac magnetic resonance (CMR) imaging was performed on a clinical whole-body 1.5-T Achieva Intera scanner (Philips Healthcare) with acquisition of two-chamber, four-chamber, and short-axis steady-state free precession cine loops. Patients were positioned in the supine position. Phase-contrast angiography for estimation of the cardiac output and the R-R intervals, a retrospective gated fast field echo sequence with a 20° flip angle, and a repetition time (TR) of 5 ms across the aorta was used. Cardiac output and forward stroke volume were estimated off-line using quantitative software (CAAS, Pie Medical Imaging, Maastricht, the Netherlands). DCE-MRI was used to estimate the

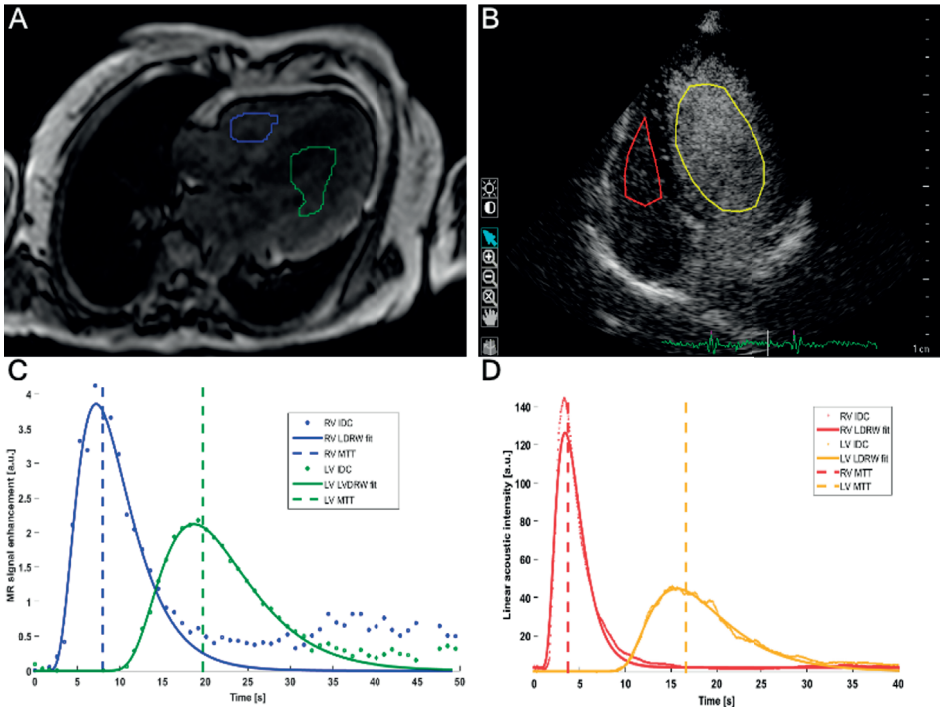

Figure 1. Overview of a DCE-MRI (A) and CEUS (B) in one patient. A bolus of gadolinium (A) and UCA, SonoVue® 10 µL/mL (B), passed through the right and left ventricles (RV and LV). ROIs are drawn in the right (blue ROI (A) and red ROI (B)) and left ventricle (green ROI (A) and yellow ROI (B)), and signal or acoustic IDCs are estimated within the ROIs, expressed in panels C and D. The raw IDC (dotted lines) are fitted to the LDRW model (straight lines), and MTT (dashed vertical lines) of the contrast bolus in both ventricles is estimated. The difference in MTT is referred to as the pulmonary transit time. AU, arbitrary units.

MTTs in the left and right ventricles. The DCE-MRI scan used a T1-weighted scan, after intravenous administration of a single bolus of 0.1 mmol gadolinium diluted in 5 ml saline (Prohance, gadoteridol, Bracco Imaging S.p.A., Milan, Italy) by a Spectris MR injector (Medrad, Indianola, PA, USA) programmed at the rate of 5 ml s^{-1} and followed by a saline flush of 15 ml. A dynamic single-shot single-slice spoiled turbo field echo was used; sequence parameters were flip angle of 7°, TR of 5.7 ms, and echo time (TE) of 2.7 ms. A saturation prepulse with a delay of 200 ms was used to obtain T1 weighting. Under these circumstances, a linear relationship between gadolinium and MR signal was obtained.[11] The sequence was prospectively triggered by the R-peak on the vectorcardiogram to acquire one image per cardiac cycle in mid-diastole and to minimize motion artifacts. These measurements were performed during end-expiratory breath hold. Parallel imaging using sensitivity encoding (SENSE) with a factor of 2 was used in combination with a half-scan technique to reduce the shot duration to approximately 170 ms. The typical voxel size was 1.7 × 1.7 × 10 mm^3. Commercially

available postprocessing software (ViewForum, Philips Healthcare) was used to measure left ventricular volumes and ejection fraction by combining all short-axis tracings at end-systole and end-diastole according to the Simpson's rule algorithm.

CEUS and Doppler echocardiography

Two-dimensional and Doppler transthoracic echocardiography (TTE) were performed within 1 h after the MRI using an iE33 ultrasound scanner equipped with a S5-1 transducer (Philips Healthcare) with the patient in the left lateral recumbent position. Two-dimensional echocardiography included Doppler outflow signals of the mitral valve, right and left ventricles, and aortic valve as well as contrast-enhanced apical four-chamber and two-chamber views. Tissue Doppler recordings were made of the ventricular septal wall. Interventricular mechanical delay (IVMD) as a measure of interventricular dyssynchrony (threshold 40 ms) was defined as the time difference between the onset of QRS and the onset of right ventricular and left ventricular ejection, respectively.[16] Intraventricular dyssynchrony was evaluated by determining the time difference between peak septal and peak posterior wall excursion on midventricular short-axis M-mode recordings (septal-to-posterior wall motion delay (SPWMD); threshold 130 ms).[17]

PTT was estimated after intravenous administration of UCA, SonoVue® (Bracco Imaging S.p.A., Milan, Italy) consisting of microbubbles with a SF6 gas enclosed in a phospholipid monolayer shell. All dynamic contrast-enhanced TTE imaging was performed by an experienced imaging-cardiologist (PH) recording four-chamber apical views using harmonic imaging selecting a four-chamber apical view without breath-hold.[18] Three different bolus injections of 10 ml saline with gradual increasing SonoVue concentrations (2.5 µL ml^{-1} (low dose), 5 µL ml^{-1} (half dose), and 10 µl ml^{-1} (full dose)) were used by diluting 1 ml SonoVue in saline (1:400, 1:200, and 1:100). This historical hospital protocol was adopted in a dose-finding study; however, the interdose difference is minimal and highly repeatable.[18] The protocol has not been changed as it enables us to use the minimal total amount of SonoVue®. These low doses provided an approximately linear relationship between the UCA concentration and the measured acoustic intensity, which is a prerequisite for application of the indicator dilution theory.[6,9]

N-terminal pro-B-type natriuretic peptide sampling

NT-proBNP sampling was performed in all patients to exclude other pathologies for exertional dyspnea and to evaluate the severity of heart failure in relationship to CRT.[19,20]

Statistical analysis

Statistical analysis was performed in IBM SPSS Statistics for Windows version 22.0 (IBM). Continuous variables were assessed for normality with the Shapiro–Wilk test and presented as mean with SD or median with range. Dichotomous data are presented as numbers

and percentages. Differences between normal distributed parameters were calculated using Student's *t*-test or one-way analysis of variance. Differences between nonparametric parameters were assessed with Mann–Whitney U-tests or Kruskal–Wallis tests. The level of agreement between PTT and nPTT by CEUS and DCE-MRI was assessed by correlation and Bland–Altman analysis using MedCalc Statistical Software version 14.8.1 (MedCalc Software bvba, Ostend, Belgium).[21] The relationship between PTT and nPTT by CEUS and DCE-MRI and several echocardiographic and laboratory heart failure parameters was evaluated by Pearson's *r* or Spearman's rho correlation depending on the distribution of the data. Interpretation of the strength of the correlation is performed by the differentiation by Evans.[22] For all analyses, a *p* value less than 0.02 was considered statistically significant, due to the small sample size, to prevent a type I error.

RESULTS

Patient characteristics and demographic data are given in Table 1. Twenty-three patients were enrolled in the study. In two patients, MRI analysis was not possible because of a violation of the acquisition protocol, and in one patient, the CEUS images were accidentally lost from the digital archive. The mean PTT-MRI was 10.4 ± 2.0 s. Of all 60 SonoVue® injections (three injections per patient), in two (3.3%), it was not possible to fit the LDRW model to the acoustic IDC. In the remaining 58 PTT-CEUS measurements, the mean PTT-CEUS was 10.2 ± 2.1 s, 10.4 ± 2.7 s, and 10.6 ± 2.3 s (p=0.86) for full, half, and low dose, respectively. The mean PTT-CEUS of all doses was 10.5 ± 2.4 s and was not different compared with PTT-MRI (p=0.88). The correlation between both techniques was r = 0.75 (95% confidence interval (CI) 0.46–0.90; p=0.0001). For the normalized values, nPTTs were comparable (11.3 ± 2.5 vs 11.2 ± 3.0 for nPTT-CEUS and nPTT-MRI, respectively; p=0.93), and correlation between nPTT from CEUS and MRI was r = 0.76 (95% CI: 0.49–0.90; p=0.0001) (Fig. 2). Bland–Altman analysis showed a bias of 0.1 s with limits of agreement of −3 to 3.2 s and a bias of 0.1 with limits of agreement of −3.9 to 3.7 for PTT and nPTT, respectively (Fig. 3).

PTT as a measure for cardiac function

Correlations between PTT measurements and other heart failure parameters are given in Table 2. Spearman's rank correlation coefficient between NT-proBNP was strong for nPTT by CEUS and MRI, whereas was moderate for the PTT by CEUS (Fig. 4 and Table 2).

The left ventricular end-diastolic volume index measured by MRI moderately correlated with nPTT by CEUS and MRI. The left ventricular end-systolic volume index by MRI correlated significantly with the nPTT by both techniques. Stroke volume measurement by MRI showed no correlation with the PTT or nPTT measurement. However, the forward stroke

Table 1. Demographics of the subjects (n = 20).

Age (yr)	67 ± 10
Male/Female (n)	10/10
BMI (kg/m^2)	28.9 ± 6.2
BSA	1.9 ± 0.2
QRS (ms)	160 ± 18
LBBB (n)	18/20
Non-LBBB (n)	2/20
NYHA Functional classes (n)	
I	4/20
II	6/20
III	10/20
IV	0
Mitral valve insufficiency (n)	19/20
Mild	14
Moderate	3
Severe	2
Cardiovascular medication	
ACEi (n)	15/20
AR blockers (n)	4/20
Beta Blocker (n)	19/20
Aldosteron inhibitor(n)	6/20
Diuretic (n)	11/20
Echocardiographic parameters	
LVEDV index (ml/m^2)	120±41
LVESV index (ml/m^2)	82±38
EF (%)	35±11
IVWD (ms)	48±31
SPWMD (ms)	294±117
MRI parameters	
LVEDV index (ml/m^2)	137±42
LVESV index (ml/m^2)	97±42
EF (%)	32±13
fSV (ml)	68±13
Laboratory parameter	
NT-proBNP (pmol/L)*	188±216

Results are presented as mean ± SD or as absolute numbers. ACE, angiotensin-converting enzyme inhibitor; AR, angiotensin-II receptor antagonist; BMI, body mass index; BSA, body surface area according to the Dubois & Dubois equation; EF, ejection fraction; fSV, forward stroke volume; IVMD, interventricular mechanical delay; LBBB, left bundle branch block; LVEDV, left ventricular end-diastolic volume; LVESV, left ventricular end-systolic volume; NT-proBNP, N-terminal pro-B-type natriuretic peptide; NYHA, New York Heart Association Classification; SPWMD, septal-to- posterior wall motion delay; asterisk indicates 18 patients

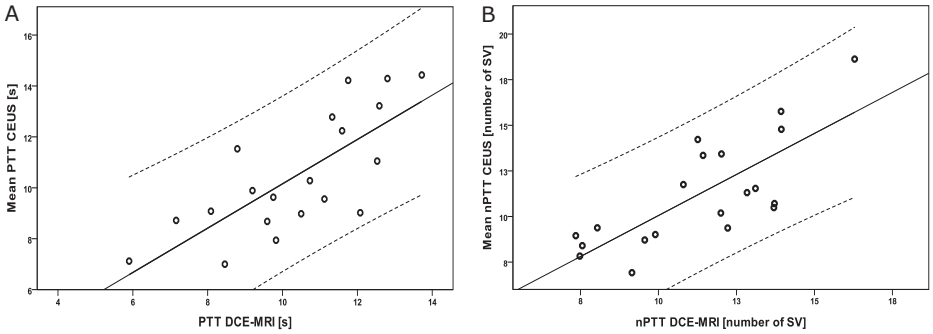

Figure 2. The correlation between PTT-MRI and mean PTT-CEUS of three measurements by CEUS (A). Correlation between both techniques for nPTT (B). The dotted lines indicate the 95% CIs.

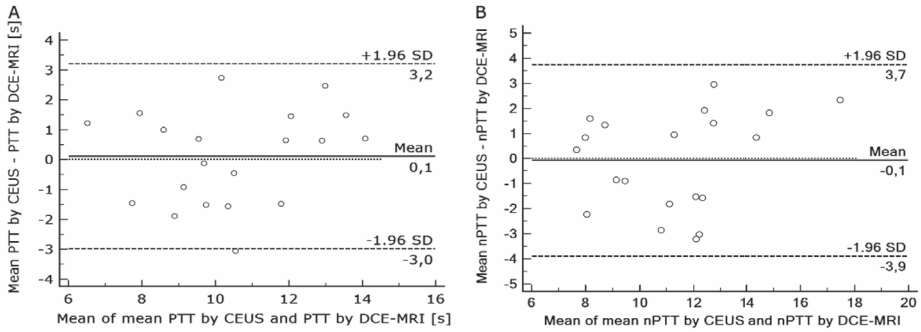

Figure 3. Bland–Altman analysis of PTT-CEUS and PTT-MRI (A). Solid line is the mean difference (bias); dashed lines are the limits of agreement (1.96 SD.). Bland–Altman analysis of nPTT-CEUS and nPTT-MRI (B).

volume using phase-contrast MR angiography showed a trend correlation in 19 patients with nPTT by both techniques. Ejection fraction measured by MRI correlated strongly with nPTT-CEUS and PTT/nPTT-MRI.

PTT/nPTT-CEUS in relation to echocardiographic parameters

Our patient population consisted mainly of left ventricular systolic heart failure patients. The left atrial size was mean 38 ± 12 ml m^{-2}. The left atrial size correlated significantly with PTT and nPTT by CEUS (Table 3). Parameters of left ventricular filling pressures showed a median mitral valve *E/A* ratio of 0.89 (IQR 0.66–1.30) in 19 patients and a median tissue Doppler *E/e'* ratio at the septal mitral valve annulus of 13.5 (IQR 11.0–17.7) in 18 patients. Both markers correlated significantly with nPTT-CEUS (Table 3). Right ventricular function according to tricuspid annular plane systolic elevation was measured in 19 patients as 17.9 ± 5.1 mm; this value did not correlate with PTT/nPTT-CEUS. In only eight patients, tricuspid regurgitation was obtainable with a maximum tricuspid regurgitation velocity of 246 ± 32 cm s^{-1} (Table 3).

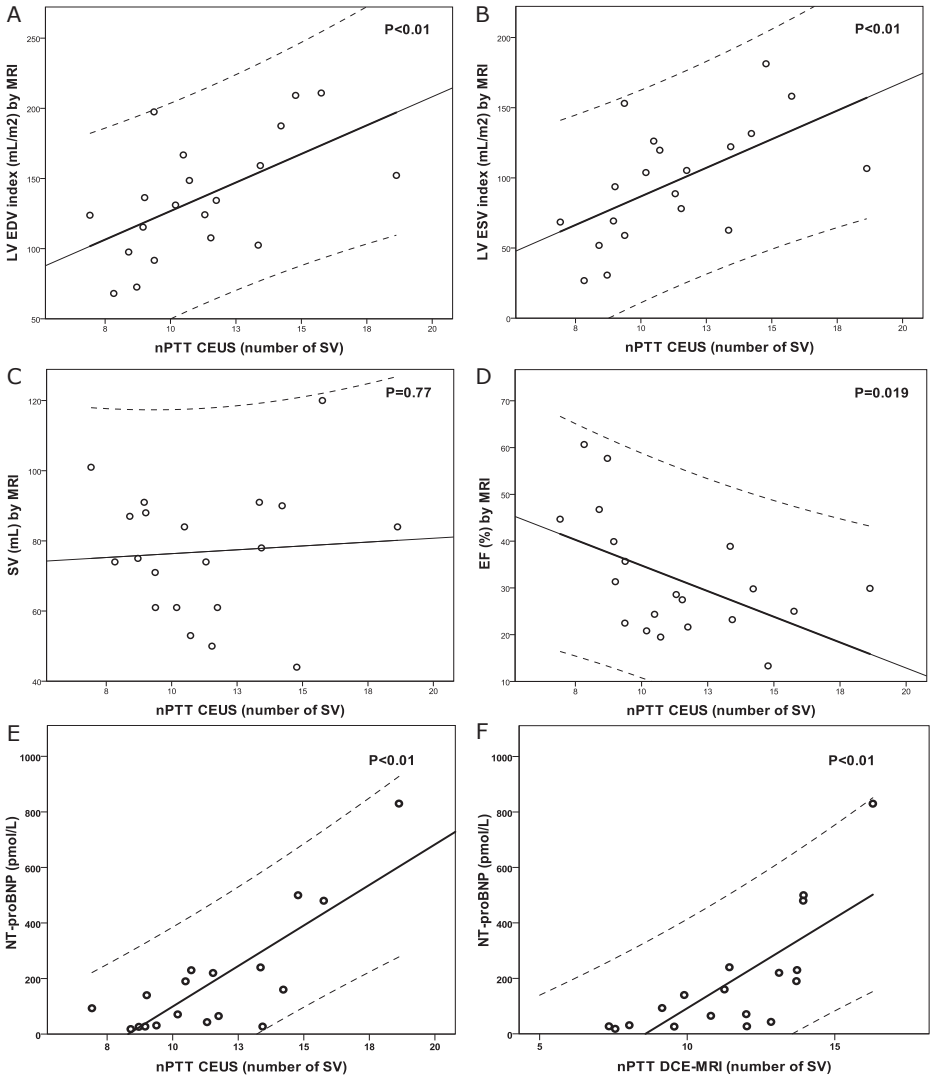

Figure 4. Correlations of nPTT by CEUS and left ventricular end-diastolic volume (LVEDV) index (A), left ventricular end-systolic volume (LVESV) index (B), stroke volume (SV) nonsignificant (C), ejection fraction (EF) (D), and NT-proBNP (E), and correlation of nPTT by DCE-MRI with NT-proBNP (F). Dotted lines represent 95% CI for the predicted values.

Table 2. Correlation of PTT/nPTT with volumes measured by MRI and NT-proBNP.

	PTT_{CEUS}	$nPTT_{CEUS}$	$PTT_{DCE\text{-}MRI}$	$nPTT_{DCE\text{-}MRI}$
LVEDVmri (ml/m^2)	0.46 p=0.043	0.58 p=0.008	0.45 p=0.047	0.65 p=0.002
LVESVmri (ml/m^2)	0.45 p=0.048	0.58 p=0.007	0.50 p=0.026	0.70 p=0.001
SVmri (ml)	0.12 p=0.625	0.07 p=0.766	-0.16 p=0.504	-0.15 p=0.531
fSVmri (ml)	-0.06 p=0.797	-0.34 p=0.157	-0.07 p=0.779	-0.44 p=0.058
EFmri (%)	-0.44 p=0.053	-0.52 p=0.019	-0.61 p=0.004	-0.71 p<0.001
NT-proBNP (pmol/L)	0.54* p=0.022	0.68* p=0.002	0.64* p=0.004	0.79* p<0.001

Correlation expressed as Pearson's r of pulmonary transit time (PTT) measurements by contrast-enhanced ultrasound (CEUS) and dynamic contrast-enhanced MRI (DCE-MRI) with left ventricular end-diastolic volume (LVEDV), left ventricular end-systolic volume (LVESV), stroke volume (SV), forward stroke volume (fSV) measured by phase-contrast MR angiography in 19 patients, ejection fraction (EF), and NT-proBNP (18 measurements). Asterisk indicates Spearman's ρ.

Table 3. Correlation of PTT/nPTT with different echocardiographic parameters that could influence PTT.

Left ventricular parameters	PTT_{CEUS}	$nPTT_{CEUS}$
MR gradient	0.21 p=0.376	0.44 p=0.051
LA size (ml/m^2)	0.50 p=0.025	0.50 p=0.025
MV *E/A* n=19	0.55* p=0.014	0.69* p=0.001
TDI *E/e'* n=18	0.46* p=0.054	0.69* p=0.002
Right ventricular parameters		
TAPSE (mm) n=19	-0.32 p=0.181	-0.08 p=0.743
TR max velocity (cm/s) n=8	0.69 p=0.057	0.47 p=0.242

Correlation expressed as Pearson's r of mitral regurgitation (MR), left atrium (LA), early and late diastolic Doppler flow ratio across the mitral valve (MV *E/A*), tissue Doppler imaging *E/e'* (TDI *E/e'*), tricuspid annular plane systolic elevation (TAPSE), and tricuspid regurgitation (TR). Asterisk indicates Spearman's ρ.

DISCUSSION

This study demonstrates that assessment of PTTs with CEUS is feasible in heart failure patients. Our measurements proved independent of the dose of UCA, and the observed dropout rate was minimal. In combination with the good agreement with MRI, these results indicate that CEUS may serve as a reliable method for bedside measurement of PTTs. Moreover, the observed relation between PTTs, left ventricular ejection fraction, and NT-proBNP suggests that PTTs may be used as an independent parameter for heart failure. In our patient group with systolic heart failure, we found accompanying elevated filling pressures by Doppler measurement and increased left atrial volumes, both correlating with PTT/nPTT-CEUS. However, a relationship with right ventricular function was not found in this small patient group.

Previous work indicated the feasibility of transit time assessment using CEUS in-vitro and also in patients.[7,9] Several authors suggested a relationship between PTT and different systolic and diastolic heart failure parameters obtained with MRI.[3,4] They found a significant prolongation in cardiopulmonary transit time in heart failure patients.[3,4] Moreover, Brittain and coworkers have recently demonstrated in a pilot study the relation of CEUS-derived transit times with heart failure parameters.[5] Our present results are in line with these previous observations and add to this current knowledge that obtaining PTTs using CEUS is also feasible and valid in patients with severe heart failure requiring resynchronization therapy.

Based on our experience with thermodilution-obtained transit times, we expected to find a bias between PTT/nPTT by CEUS and MRI. Thermodilution in comparison with CEUS is known to overestimate transit times most likely due to extravasation.[7,9] UCAs are true intravascular indicators, producing more accurate estimates of blood pool volumes. As gadolinium is not bound to proteins and is known to extravasate, a difference between PTT-CEUS and PTT-MRI was expected. However, Bland–Altman analysis showed minimal difference and extravasation in the first pass was not substantiated (Fig. 3). This suggests that PTT measurement by MRI or CEUS in patients with larger PTTs is feasible. The relatively wide limits of agreement, possibly due to the differences in timing or positioning during PTT measurement, may pose a limitation for the use of PTT in clinical practice and warrants further exploration in future studies.

We compared the PTT/nPTT-CEUS with the MRI ventricular volumes as echocardiographic volumes are known for inaccuracies due to image plane positioning errors and foreshortening of the left ventricle (LV).[23,24]

The transit times derived from CEUS correlating with the ventricular volumes and NT-proBNP seemed to become stronger after normalization of the heart rate. This phenomenon is confirmed by other studies.[4,5,15,25] The correction for the heart rate is important, as a larger PTT can be due to a lower heart rate or smaller stroke volume. This has been shown in a study on healthy athletes whose pulmonary blood volumes and PTTs were increased to meet the increased aerobic capacity. However, after correction for the heart rate, nPTTs were in the same range as non-trained healthy subjects.[26]

Furthermore, the relationship between PTT/nPTT by CEUS or MRI and stroke volume was not substantiated. In our patient group, the explanation for the absence of this relationship could be a high number of patients with mitral regurgitation (Table 1). Choi and coworkers found an inverse relationship between interventricular transit time by CEUS and cardiac output (which consists of heart rate and stroke volume) measured by right heart catheterization.[10] Probably, our study was underpowered to observe a significant effect in comparison with the study of Choi and coworkers. This observation is supported by a positive trend between the forward stroke volume by phase-contrast MR angiography and nPTT-CEUS (Table 2).

NT-proBNP is indicative for volume and pressure overload in congestive heart failure.[19] Therefore, the correlation of NT-proBNP with PTT/nPTT by MRI and CEUS may indicate that PTT/nPTT could serve as a possible new noninvasive parameter for detecting hemodynamic derangements in these patients. Besides this correlation, we found a correlation with the left ventricular end-systolic volumes by MRI. Previous studies showed that not only end-systolic volume but also NT-proBNP changes are significantly higher in CRT responders than in nonresponders.[27,28] Whether PTT/nPTT-CEUS change agrees to CRT responders and nonresponders remains a topic for future research.

PTT estimate is a supplement to the echocardiographic parameters as this parameter is less dependent on image quality. PTT is a highly reliable, repeatable, and reproducible parameter and obtainable during a standard contrast-enhanced echocardiography at the cost of a longer recording time.[18] It is minimally invasive and bedside applicable, even in outpatients. It could be analogous to invasive cardiopulmonary estimates with a discriminative character for cardiopulmonary dysfunction. PTT above a certain threshold could implicate cardiopulmonary pump dysfunction.[5,29] Earlier studies have shown that PTT can have prognostic capabilities even to predict mortality.[29]

Limitations

In general, the limits of agreement between PTT/nPTT-CEUS and PTT/nPTT-MRI were nearly 30% of the bias. The intertechnique difference in positioning, breathing, and timing could cause some changes in pulmonary blood volume, intrathoracic pressure, and cardiac output. Furthermore, effects due to cardiac displacement by respiration on the IDC within the ROI may influence the accuracy of the measurement. Alternatively, PTT/nPTT-CEUS is very easy to perform, minimally invasive, and bedside applicable; these advantages may counterweight possible imperfections.

In this study, all patients had sinus rhythm. PTT of patients with atrial fibrillation cannot be normalized for heart rate, which is shown (Table 2) to better reflect cardiopulmonary function. As in our study, the correlation between PTT-CEUS (nonnormalized) and NT-proBNP is still moderate; the relationship between PTT-CEUS and cardiopulmonary function in patients with atrial fibrillation could be of interest and warrants assessment in future studies.

This study covered a small study population limited to patients referred to the hospital with dyspnea due to dyssynchrony and systolic heart failure. Although our patient population consisted of low ejection fractions with a large standard deviation, the discrimination of the PTT is diminished by the lack of normal ejection fractions. However, given the encouraging results of this pilot study larger studies including patients with different spectra of ejection fractions are desirable.

We used different doses of SonoVue and compared them to one dose of gadolinium. The use of the average PTT could favor the analysis by decreasing variation. However, the variability among the data has been shown to be low.[18]

CONCLUSIONS

The measurement of PTT/nPTT-CEUS is an easy-to-perform and feasible procedure; it shows a strong agreement with PTT/nPTT-MRI. PTT/nPTT-CEUS also had moderate to strong correlation with Doppler and MRI parameters for heart failure. The strong relationship with NT-proBNP suggests that PTT/nPTT-CEUS, which is bedside applicable and minimally invasive, may provide a novel and clinically feasible measure of cardiac performance and heart failure.

REFERENCES

1. Sakka SG, Reuter DA & Perel A The transpulmonary thermodilution technique. *Journal of Clinical Monitoring and Computing* 2012; **26**: 347–353
2. Roy SB, Bhardwaj P & Bhatia ML Pulmonary blood volume in mitral stenosis. *BMJ* 1965; **2**: 1466–1469
3. Shors SM, Cotts WG, Pavlovic-Surjancev B, Francois CJ, Gheorghiade M & Finn JP Heart failure: evaluation of cardiopulmonary transit times with time-resolved MR angiography. *Radiology* 2003; **229**:743–748
4. Cao JJ, Wang Y, McLaughlin J, Haag E, Rhee P, Passick M, Toole R, Cheng J, Berke AD, Lachman J, et al. Left ventricular filling pressure assessment using left atrial transit time by cardiac magnetic resonance imaging. *Circulation: Cardiovascular Imaging* 2011; **4**: 130–138
5. Brittain EL, Doss LN, Saliba L, Irani W, Byrd BF & Monahan K Feasibility and diagnostic potential of pulmonary transit time measurement by contrast echocardiography: a pilot study. Echocardiography 2015; **32**: 1564–1571
6. Mischi M, Kalker TA & Korsten EH Contrast echocardiography for pulmonary blood volume quantification. *IEEE Transactions on Ultrasonics, Ferroelectrics, and Frequency Control* 2004; **51:** 1137–1147
7. Herold IH, Soliman Hamad MA, van Assen HC, Bouwman RA, Korsten HH & Mischi M Pulmonary blood volume measured by contrast enhanced ultrasound: a comparison with transpulmonary thermodilution. *Br J Anaesth* 2015; **115**: 53–60
8. Streitberger A, Modler P & Haggstrom J Increased normalized pulmonary transit times and pulmonary blood volumes in cardiomyopathic cats with or without congestive heart failure. *Journal of Veterinary Cardiology* 2015; **17**: 25–33
9. Herold IH, Russo G, Mischi M, Houthuizen P, Saidov T, van het Veer M, van Assen HC & Korsten HH Volume quantification by contrast-enhanced ultrasound: an in-vitro comparison with true volumes and thermodilution. *Cardiovasc Ultrasound* 2013; **11:** 36
10. Choi BG, Sanai R, Yang B, Young HA, Mazhari R, Reiner JS & Lewis JF Estimation of cardiac output and pulmonary vascular resistance by contrast echocardiography transit time measurement: a prospective pilot study. *Cardiovascular Ultrasound* 2014; **12**: 44
11. Mischi M, van den Bosch HC, den Boer JA, Verwoerd J, Grouls RJ, Peels CH & Korsten HH Intra-thoracic blood volume measurement by contrast magnetic resonance imaging. *Magnetic Resonance in Medicine* 2009; **61:** 344–353
12. Sheppard CW & Savage LJ The random walk problem in relation to the physiology of circulatory mixing. *Physical Review* 1951; **83**: 489–490
13. Wise ME Tracer dilution curves in cardiology and random walk and lognormal distributions. *Acta Physiologica et Pharmacologica Neerlandica* 1966; **14**: 175–204
14. Mischi M, Kalker T & Korsten HHM Videodensitometric methods for cardiac output measurements. *EURASIP Journal on Applied Signal Processing* 2003; **5**: 479–489
15. Lord P, Eriksson A, Haggstrom J, Jarvinen AK, Kvart C, Hansson K, Maripuu E & Makela O Increased pulmonary transit times in asymptomatic dogs with mitral regurgitation. *Journal of Veterinary Internal Medicine* 2003; **17**: 824–829
16. Bax JJ, Ansalone G, Breithardt OA, Derumeaux G, Leclercq C, Schalij MJ, Sogaard P, St John Sutton M & Nihoyannopoulos P Echocardiographic evaluation of cardiac resynchronization therapy: ready for routine clinical use? A critical appraisal. *Journal of the American College of Cardiology* 2004; **44**: 1–9

17. Pitzalis MV, Iacoviello M, Romito R, Massari F, Rizzon B, Luzzi G, Guida P, Andriani A, Mastropasqua F & Rizzon P Cardiac resynchronization therapy tailored by echocardiographic evaluation of ventricular asynchrony. *Journal of the American College of Cardiology* 2002; **40**: 1615–1622
18. Herold IH, Saporito S, Bouwman RA, Houthuizen P, van Assen HC, Mischi M & Korsten HH Reliability, repeatability, and reproducibility of pulmonary transit time assessment by contrast enhanced echocardiography. *Cardiovascular Ultrasound* 2016; **14**: 1
19. Taub PR, Gabbai-Saldate P & Maisel A Biomarkers of heart failure. Congestive Heart Failure 2010; **16**: S19–S24
20. Fruhwald FM, Fahrleitner-Pammer A, Berger R, Leyva F, Freemantle N, Erdmann E, Gras D, Kappenberger L, Tavazzi L, Daubert JC, et al. Early and sustained effects of cardiac resynchronization therapy on N-terminal pro-B-type natriuretic peptide in patients with moderate to severe heart failure and cardiac dyssynchrony. *European Heart Journal* 2007; **28**: 1592–1597
21. Bland JM & Altman DG Statistical methods for assessing agreement between two methods of clinical measurement. *Lancet* 1986; **1**: 307–310
22. Evans JD Straightforward Statistics for the Behavioral Sciences. 1996 Pacific Grove, CA, USA: *Brooks/Cole Publishing Company*.
23. Malm S, Frigstad S, Sagberg E, Larsson H & Skjaerpe T Accurate and reproducible measurement of left ventricular volume and ejection fraction by contrast echocardiography: a comparison with magnetic resonance imaging. *Journal of the American College of Cardiology* 2004; **44**: 1030–1035
24. Sapin PM, Schroeder KM, Gopal AS, Smith MD & King DL Three-dimensional echocardiography: limitations of apical biplane imaging for measurement of left ventricular volume. *Journal of the American Society of Echocardiography* 1995; **8**: 576–584
25. Streitberger A, Hocke V & Modler P Measurement of pulmonary transit time in healthy cats by use of ultrasound contrast media "Sonovue(R)": feasibility, reproducibility, and values in 42 cats. *Journal of Veterinary Cardiology* 2013; **15**: 181–187
26. Falch DK & Stromme SB Pulmonary blood volume and interventricular circulation time in physically trained and untrained subjects. European Journal of Applied Physiology and Occupational Physiology 1979; **40**: 211–218
27. Hoogslag GE, Hoke U, Thijssen J, Auger D, Marsan NA, Wolterbeek R, Holman ER, Schalij MJ, Bax JJ, Verwey HF, et al. Clinical, echocardiographic, and neurohormonal response to cardiac resynchronization therapy: are they interchangeable? *Pacing and Clinical Electrophysiology* 2013; **36**: 1391–1401
28. Magne J, Dubois M, Champagne J, Dumesnil JG, Pibarot P, Philippon F, O'Hara G & Senechal M Usefulness of NT-pro BNP monitoring to identify echocardiographic responders following cardiac resynchronization therapy. *Cardiovascular Ultrasound* 2009; **7**: 39
29. Swift AJ, Telfer A, Rajaram S, Condliffe R, Marshall H, Capener D, Hurdman J, Elliot C, Kiely DG & Wild JM Dynamic contrast-enhanced magnetic resonance imaging in patients with pulmonary arterial hypertension. *Pulmonary Circulation* 2014; **4**: 61–70

Chapter 6

Reliability, repeatability, and reproducibility of pulmonary transit time assessment by contrast enhanced echocardiography

Ingeborg HF Herold
Salvatore Saporito
R. Arthur Bouwman
Patrick Houthuizen
Hans C van Assen
Massimo Mischi
Hendrikus HM Korsten

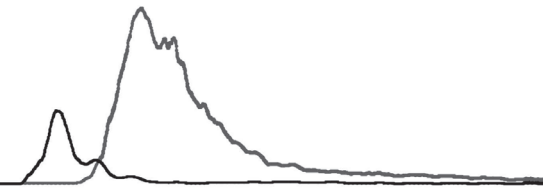

Cardiovascular Ultrasound 2016; 14: 1

ABSTRACT

Background

The aim of this study is to investigate the inter and intra-rater reliability, repeatability, and reproducibility of pulmonary transit time (PTT) measurement in patients using contrast enhanced ultrasound (CEUS), as an indirect measure of preload and left ventricular function.

Methods

Mean transit times (MTT) were measured by drawing a region of interest (ROI) in right and left cardiac ventricle in the CEUS loops. Acoustic intensity dilution curves were obtained from the ROIs. MTTs were calculated by applying model-based fitting on the dilution curves. PTT was calculated as the difference of the MTTs. Eight raters with different levels of experience measured the PTT (time moment 1) and repeated the measurement within a week (time moment 2). Reliability and agreement were assessed using intra-class correlations (ICC) and Bland-Altman analysis. Repeatability was tested by estimating the variance of means (ANOVA) of three injections in each patient at different doses. Reproducibility was tested by the ICC of the two time moments.

Results

Fifteen patients with heart failure were included. The mean PTT was 11.8 ± 3.1 s at time moment 1 and 11.7 ± 2.9 s at time moment 2. The inter-rater reliability for PTT was excellent (ICC = 0.94). The intra-rater reliability per rater was between 0.81- 0.99. Bland-Altman analysis revealed a bias of 0.10 s within the rater groups. Reproducibility for PTT showed an ICC = 0.94 between the two time moments. ANOVA showed no significant difference between the means of the three different doses F = 0.048 (p = 0.95). The mean and standard deviation for PTT estimates at three different doses was 11.6 ± 3.3 s.

Conclusions

PTT estimation using CEUS shows a high inter- and intra-rater reliability, repeatability at three different doses, and reproducibility by ROI drawing. This makes the minimally invasive PTT measurement using contrast echocardiography ready for clinical evaluation in patients with heart failure and for preload estimation.

INTRODUCTION

Pulmonary blood volume quantification by transpulmonary dilution analysis is an essential part of the hemodynamic evaluation to guide fluid management in anesthesia and intensive care practice. Recently, contrast-enhanced ultrasound (CEUS) has been proposed as a minimally-invasive, alternative method for pulmonary transit time (PTT) estimation.[1–3] This technique uses transthoracic echocardiography (TTE) to visualize the transcardiac passage of an ultrasound contrast-agent (UCA) bolus injected in a peripheral vein. Indicator dilution curves (IDCs) are then derived from the acoustic backscatter of the UCA bolus in the four heart chambers. The mean transit time (MTT) of these acoustic IDCs can be estimated by different methods. The most frequently used methods in clinical practice are based on assessment of the "peaks" of the IDCs or "frame counting" of the appearance of the first bubbles in the heart chambers.[3–5] We estimate the MTT by model fitting using the local density random walk (LDRW) model, which takes into account the Brownian motion of the bolus contrast in the blood stream through the pulmonary vessels and heart chambers.[1, 2, 6, 7] In previous studies, we demonstrated that volume estimation by CEUS, resulting from the multiplication of the flow by the PTT (i.e. the difference between the MTTs of the left atrium and the right ventricle (RV)), showed excellent agreement with the actual volumes, both in-vitro and in-vivo.[2,6] Moreover, it showed even better accuracy than transpulmonary thermodilution volume estimation.[1,8] However, the reliability of PTTs derived with CEUS and the LDRW in-vivo has not been established.

Therefore, in this study we investigated the reliability and reproducibility of the assessment of PTT with CEUS using the LDRW model, in patients referred for cardiac resynchronization therapy. We also investigated the effect of different UCA doses on the PTT measurement. In addition, to evaluate the complexity of the PTT assessment by means of CEUS-recording analysis, PTT was also estimated by non-physicians. If also non-physicians can obtain reliable measurements, this would imply a fast learning curve, favoring the method adoption in clinical practice. Therefore, our second objective was to evaluate the reliability and agreement between PTT measurements obtained by physicians and non-physicians.

METHODS

Patients

As per local hospital protocol, all patients referred for cardiac resynchronization therapy underwent extensive echocardiographic evaluation including contrast enhanced ejection fraction measurements. This patient population scheduled for contrast-enhanced TTE to assess ejection fraction and eligibility were included for this observational study. In

general, these were patients with symptomatic heart failure, a decreased ejection fraction, and QRS- widening by more than 120 ms. Patients were excluded in case of atrial fibrillation, an acute coronary syndrome within the past three months, a known allergy to sulphurhexafluoride, or a poor acoustic window (impossibility to visualize an apical 4-chamber view). The Institutional Review Board of the Catharina Hospital Eindhoven approved the study, and written informed consent for use of echocardiography data for scientific purposes was obtained from all subjects.

Measurement protocol

Patients referred for a left ventricle (LV) dyssynchrony evaluation received a standard of care CEUS echocardiography according to our hospital protocol (Fig. 1). In all patients, an 18-gauge catheter was inserted in a peripheral vein of the fore-arm and the patient was positioned in left lateral position. The UCA was administered according to our hospital CEUS protocol. All contrast-enhanced TTE imaging was performed by an experienced imaging-cardiologist (PH) using an iE33 ultrasound scanner equipped with a S5-1 transducer (Philips Healthcare, Andover, MA, USA). Four chamber apical views were obtained using harmonic imaging at 1.3–2.6 MHz, a low mechanical index (MI) of 0.19 to reduce microbubble destruction, a frame rate of 23 Hz, and a dynamic range of 50 dB with linear post- processing.

SonoVue® (Bracco SpA, Milan, Italy) consisting of microbubbles with a SF6 gas enclosed in a phospholipids monolayer shell was used as UCA. These microbubbles, with an average size of 3 to 9 μm, pass the pulmonary circulation and can be visualized in both RV and LV.[9]

After a peripheral bolus injection, the passage of microbubbles through the right and left heart was visualized from a four chamber apical view without breath-hold by selecting the proper probe angle, to minimize movement artifacts. We diluted 1 ml SonoVue® in saline (1:400, 1:200, and 1:100) and injected a bolus of 10 ml of the solution. Three different CEUS loops were recorded in consistent consecutive order. The injections were performed in a reproducible way as a manual instantaneous bolus and each dose was administered as soon as the recirculating microbubbles disappeared from the left ventricle. These are doses lower than those used for left ventricular opacification,[10] but give good opacification of the ventricles while providing an approximately linear relationship between the UCA concentration and the measured acoustic intensity; the latter is a prerequisite for application of the indicator dilution theory.[1, 2]

Reliability was tested by eight raters: four physicians who were all experienced with echocardiography but with different levels of experience with measuring MTT (one rater was experienced (IH), one rater had some experience (HK), and two had experience in endocardial border tracing (PH, JD)), and four technicians from the Eindhoven University of Technology of whom three were inexperienced with echocardiography and MTT

(HA, GW, AG) and one was an expert in the field (MM). All raters received a detailed guide for drawing ROIs in both RV and LV at the two time moments. Each rater received the same fifteen anonymized ultrasound apical four chamber view loops following the injection of a SonoVue® in saline bolus at a dilution of 1:200 (Fig. 1). The raters were instructed to draw regions of interest (ROIs) independently within the endocardial borders of the RV and LV throughout the cardiac cycle; no specified ROI surface was predefined. ROI position was fixed over all the frames. Movement of borders or valve structures within the ROI will create artifacts in the IDC. Therefore, the instructions emphasized that the ROIs should be kept within the endocardial border during the entire cardiac cycle. To this end, the freeform splines ROIs were drawn using QLab 8 software (Philips, Healthcare, Andover, MA, USA). The acoustic intensity over time in the ROIs was expressed as an IDC.

To test the reproducibility of the measurement itself, the raters repeated the drawings in the same dataset within a week interval; these time points are referred to as time moment 1 and 2. The raters were blinded for their previous results and to the measurement outcome; also the order of the patients in the dataset was changed between time

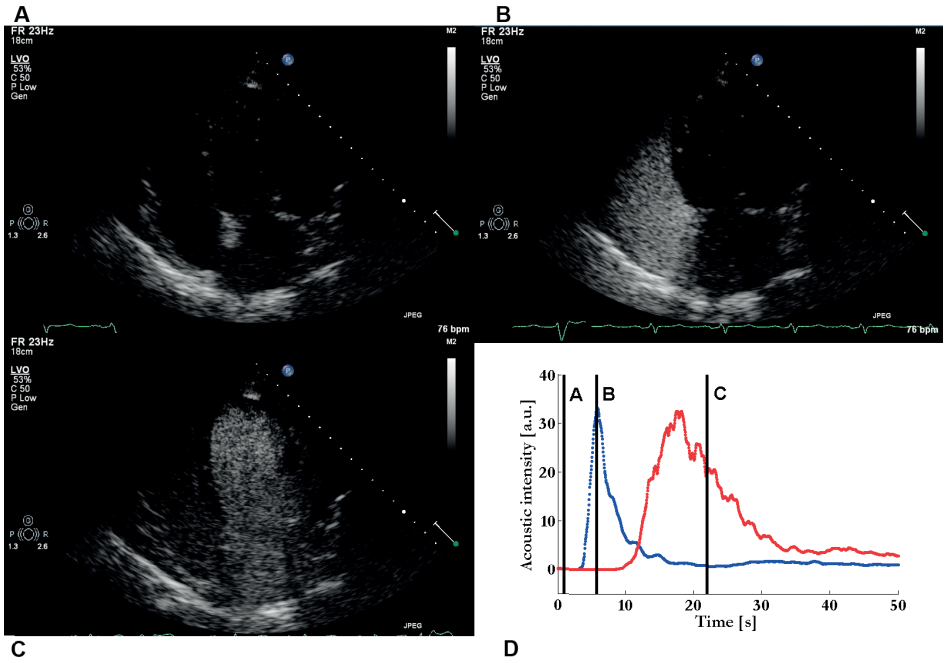

Figure 1. The passage of a bolus of SonoVue® through the right atrium and ventricle (panel B) and left atrium and ventricle (panel C). ROIs are drawn in the right and left ventricle. The acoustic intensities according to panel A, B, and C are expressed in panel D. The acoustic dilution curves of the right (blue indicator dilution curve (IDC)) and left ventricle (red IDC) are fitted according to the local density random walk model and the mean transit times (vertical black lines) are then calculated

moment 1 and 2. The extracted data were saved as Excel files and were afterwards analyzed using a custom software to fit the local density random walk (LDRW) model to the measured IDCs; the method was implemented in MATLAB® 2009b (The Mathworks, Natick, MA, USA).[11]

The interdose repeatability was tested by one rater (IH) who drew ROIs in all three different echo loops at the three different doses for the fifteen patients. Thereby, ROI size was measured and the difference in MTT in the fifteen cine loops at three different doses. The IDCs were fitted by the LDRW model by an independent researcher (GW). The fitting was performed automatically as described by Mischi and coworkers.[11] The analysis of the acoustic IDC provides parameters related to the convection and dispersion of the injected SonoVue® bolus including the MTT.[2, 12] The difference in MTT (ΔMTT) between LV and RV, presenting the PTT, was derived by subtraction.[7]

Statistical analysis

The analysis and rendering of this observational study are in line with the guideline for reporting reliability and agreement studies (GRRAS).[13] The intra-class correlation for random effects models based on repeated-measures ANOVA was used to evaluate intra-rater and inter-rater reliability.[14] These were analyzed for the different time moments 1 and 2 and the different classes: physicians versus technicians. The level of agreement between the PTT measured by physicians and technicians was determined with Bland-Altman analysis to estimate the feasibility of CEUS using MedCalc Statistical Software version 14.8.1 (MedCalc Software bvba, Ostend, Belgium).[15] The distributions of the MTTs of both ventricles and the PTTs were tested by the Shapiro-Wilk test. The MTTs and PTTs are presented as mean and standard deviation (for normal distributions) or median and interquartile ranges (for non-normal distributions). Coefficients of variation were measured for the PTT and computed among the rater groups. The repeatability of the three different doses and different loops was tested using univariate ANOVA analysis. The ROI size was tested for its distribution as described above for PTT. Statistical analyses were performed using IBM SPSS statistics for Windows version 22.0 (IBM©, Armonk, NY, USA).

RESULTS

Fifteen patients (12 men and 3 women) were enrolled in the study. Mean age was 67 ± 7 years with an ejection fraction of 31 ± 11 % (Table 1). The transit times at any time moment had a normal distribution according to the Shapiro-Wilk test. The mean MTT of the RV was 8.5 ± 3.1 s and 8.7 ± 3.1 s at time moment 1 and 2, respectively. For the LV, these values were 20.4 ± 5.6 s and 20.3 ± 5.5 s, respectively. The mean PTT was 11.8 ± 3.1 s at time moment 1 and 11.7 ± 2.9 s at time moment 2.

Table 1. Demographic characteristics

	Mean ± SD (n = 15)	Min – max (n = 15)
Gender (n male/women)	12/3	
Age (yr)	67 ± 7	58 - 78
Weight (kg)	81 ± 15	51 - 109
Height (cm)	176 ± 9	158 - 188
BMI	26 ± 4	19 - 37
BSA	2.0 ± 0.2	1.5 – 2.3
NYHA classification n (%)		
Class II	7 (47)	
Class III	5 (33)	
Class IV	3 (20)	
Echocardiography		
LVEF (%)	31 ± 11	17 – 53
RV dysfunction		
TAPSE < 16 mm (n)	4/15	
Pulmonary hypertension		
TR velocity > 2.8 m/s (n)	2/15	
Electrocardiogram		
Heart rate	72 ± 17	50 – 110
QRS duration (ms)	151 ± 27	118 – 194
IVMD (ms) in 13 patients	42 ± 14	20 – 60
SPWMD (ms) in 11 patients	152 ± 70	10 – 240
Comorbidities n (%)		
Hypertension	5 (33)	
Congestive heart failure	11 (73)	
Coronary artery disease	14 (93)	
COPD	6 (40)	
Diabetes mellitus	3 (20)	
Medication n (%)		
Beta-blocker	12 (80)	
ACE inhibitors	11 (73)	
AT II blockers	2 (13)	
Loop diuretics	12 (80)	
K-sparing agents	6 (40)	
Statins	14 (93)	
Laboratory		
Creatinine (µmol/L)	105 ± 28	31 - 160
NT-proBNP (pmol/L)	162 ± 111	36 - 440

SD, standard deviation; BMI, body mass index; BSA, body surface area; NYHA, New York Heart Association; LVEF, left ventricular ejection fraction; RV, right ventricle; TAPSE, tricuspid annular plane systolic excursion; TR, tricuspid regurgitation; IVMD, interventricular mechanical delay; SPWMD, septal to posterior wall motion delay; COPD, chronic obstructive pulmonary disease; ACE, angiotensin-converting enzyme; AT II, angiotensine-II-receptor antagonist; K-sparing, potassium sparing; NT-proBNP, N-terminal pro-B-type natriuretic peptide

The MTT assessments made at the two different time moments per rater showed a high reliability with intraclass correlation coefficient (ICC) for the PTT equal to 0.94 (95 % CI, 0.90–0.97). For the MTTs of the RV and LV, the ICC was 0.98 (95 % CI, 0.97–0.99) and 0.99 (95 % CI, 0.98–0.99), respectively (Table 2 and Fig. 2). In Figure 2, the peak of the IDCs of the different ROIs, drawn by the raters, is visualized and its effect on the MTT of the LV evidenced. In this figure, it is shown that the difference in LV MTT is very low among the raters. The coefficient of variation was lowest for the LV (1.21 %) and highest for the PTT (3.30 %) (Table 2). Reproducibility for the measurements between the two time moments performed by all raters demonstrated an ICC of 0.99 (95 % CI, 0.98–0.99), 0.99 (95 % CI, 0.98–0.99), and 0.94 (95 % CI, 0.92–0.94) for the RV MTT, LV MTT, and PTT, respectively (Table 3). Reproducibility between the two time moments for the PTT per rater showed an ICC between 0.81 and 0.99. The ICC was 0.99 for all technicians; for the physicians it varied between 0.81 and 0.99 (Table 4). Bland-Altman analysis revealed a mean difference of 0.10 (±0.54) s between the physicians and technicians. The 95 % limits of agreement ranged from – 0.95 s to 1.16 s (Fig. 3).

ANOVA analysis of the three repeated injections showed a mean PTT of 11.4 ± 3.4 s, 11.6 ± 3.4 s, and 11.8 ± 3.2 s at 1:100, 1:200, and 1:400 dilutions of SonoVue® in saline, respectively. The variability amongst the means was F 0.048, which was not significant (p=0.95). The measure of effect for the SonoVue® dose on the PTT accounted for 2 %, η^2 0.02. The means and standard deviations of the different PTTs per patient per

Table 2. Inter-rater reliability of the mean transit times measured in the right and left ventricle and of the pulmonary transit time of the two time moments between the eight raters. The coefficient of variation is expressed as a percentage

	ICC (95% CI)	Coefficient of variation (± SD) %
Right ventricle mean transit time	0.98 (0.97 – 0.99)	2.61 (3.00)
Left ventricle mean transit time	0.99 (0.98 – 0.99)	1.21 (1.18)
Pulmonary transit time	0.94 (0.90 – 0.97)	3.30 (3.35)

ICC, intra-class correlation coefficient; CI, confidence interval; SD, standard deviation

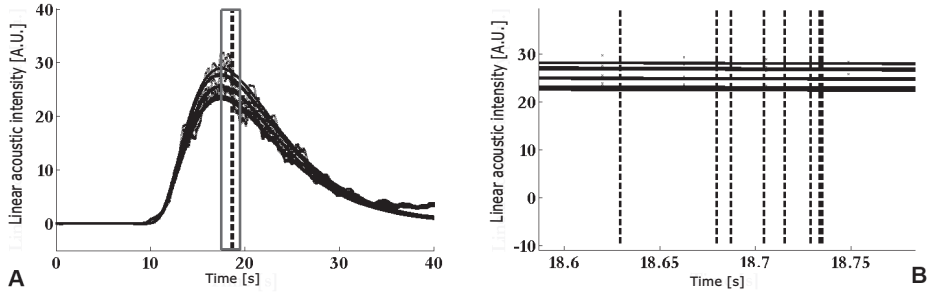

Figure 2. The fitted curves by eight raters of one patient's left ventricle indicator dilution curve (IDC) (panel A). The difference in mean transit times of these fitted IDCs among the eight raters in one patient (panel B)

Table 3. Intra-rater reliability of the mean transit times measured in the right and left ventricle and of the pulmonary transit time by all the raters between the two time moments

	ICC (95% CI)
Right ventricle mean transit time	0.99 (0.98 – 0.99)
Left ventricle mean transit time	0.99 (0.98 – 0.99)
Pulmonary transit time	0.94 (0.92 – 0.96)

ICC, intra-class correlation coefficient; CI, confidence interval

Table 4. Intra-rater reliability per rater for the pulmonary transit time (PTT). Raters 1,2,3, and 8 are physicians and raters 4,5,6, and 7 are technicians. The mean PTTs of the fifteen patients are expressed with their standard deviation at time moment 1 and 2, measured by each rater

	ICC (95% CI)	Mean PTT t1 (± SD)	Mean PTT t2 (± SD)
Rater 1	0.91 (0.76 – 0.97)	11.86 (3.14)	12.13 (3.14)
Rater 2	0.99 (0.99 – 1.00)	11.77 (3.00)	11.69 (2.99)
Rater 3	0.92 (0.79 – 0.97)	11.82 (3.08)	11.49 (3.22)
Rater 4	0.99 (0.99 – 1.00)	11.64 (2.89)	11.70 (2.96)
Rater 5	0.99 (0.98 – 1.00)	11.84 (3.09)	11.82 (2.99)
Rater 6	0.99 (0.99 – 1.00)	11.76 (3.12)	11.71 (3.03)
Rater 7	0.99 (0.98 – 1.00)	11.65 (2.95)	11.60 (2.93)
Rater 8	0.81 (0.54 – 0.93)	12.17 (4.15)	11.60 (2.96)

ICC, intra-class correlation coefficient; CI, confidence interval; SD, standard deviation; t1, time moment 1; t2, time moment 2

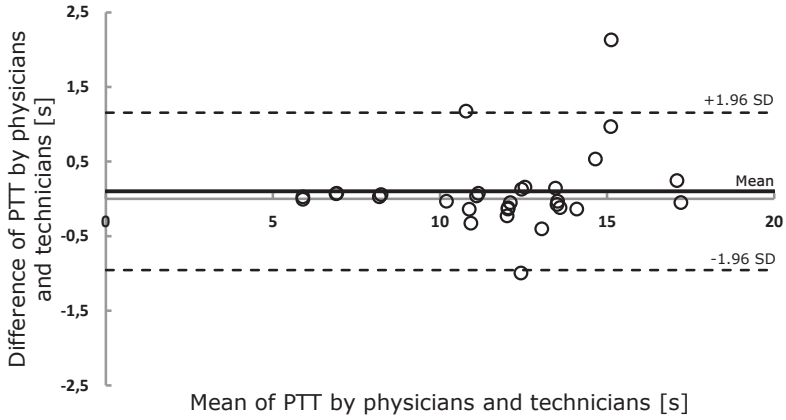

Figure 3. Bland-Altman analysis. The X-axis represents the mean of the average pulmonary transit time (PTT) in the two time moments measured by physicians and technicians. The Y-axis represents the difference of the average PTTs in the two time moments between the physicians and technicians. The solid line is the mean difference (bias); dotted lines are limits of agreement [bias ± (1.96 SD)]

dose are shown in Fig. 4. The mean PTT and standard deviation for the three different doses was 11.6 ± 3.3 s. The coefficient of variation was 5.3 ± 4.4 %. The ROI sizes were normally distributed and the mean ROI size for the RV was 12 ± 3 mm^2 and for the LV 25 ± 6 mm^2. The coefficient of variation of the ROI size based on the three different doses was for the RV 11.3 ± 4.5 % and 9.0 ± 5.3 % for the LV.

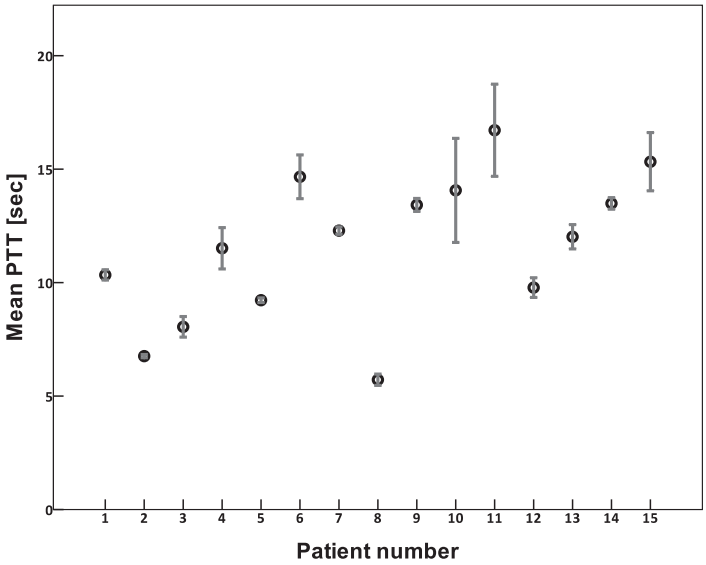

Figure 4. Means of pulmonary transit times in seconds for each patient based on three different SonoVue® concentrations, expressed as bullets and standard deviations as error bars

DISCUSSION

This study demonstrated that measurement of PTT derived from IDCs of an UCA bolus injected in a peripheral vein is feasible and highly reliable. The inter- and intra-rater correlations are high, and a very low bias between physicians and technicians was observed. Therefore, the drawing of the ROI in the CEUS recordings is not only reproducible, but also operator independent for measurement of the PTT. According to the high coefficient of variation of the ROI size, the size does not influence the PTT measurement. This makes measurement of the PTT feasible. We also showed that PTT measurement is repeatable, at three different doses in the linear range between concentration and acoustic intensity. The dose did not show any effect on the PTT measurement. The results are in accordance with the volumes measured in an in-vitro model.[1] In this previous study, the volumes were calculated by multiplying the flow through the circuit by the difference in MTT between an inflow and outflow tube.[1] A high ICC of 0.99 (95 % CI, 0.98–1.00)

was measured for the three repetitions of an UCA bolus at the same flow and volume of the circuit.

We previously showed that transthoracic and transesophageal CEUS can be used to estimate transit times and pulmonary blood volumes in patients.[2, 8] The values of the PTTs derived with CEUS are in line with cardiopulmonary transit times measured by low-dose contrast-enhanced time-resolved magnetic resonance (MR) angiography, where the magnetic resonance imaging (MRI) signal is measured in the pulmonary artery and ascending aorta.[16] In a patient population similar to ours, with reduced LV function, Shors and coworkers reported cardiopulmonary transit times of 11.2 ± 4.0 s in patients with a left ventricular ejection fraction (LVEF) between 21 and 30 % and 9.0 ± 1.7 s for a LVEF between 31 % and 40 %.[16] Our patient population had a mean LVEF of 31 % and the average PTT was 11.8 ± 3.0 s. However, in our cohort two patients had moderate pulmonary hypertension and four patients had moderate right ventricle dysfunction (Table 1), both lead to a prolonged cardiopulmonary circulation times as expressed by PTT.[3] Although in the study of Shors and coworkers, the ROIs were drawn at different regions in the heart and vessels, the transit times are in line with each other. In this study, three-dimensional gradient-echo fast low-angle shots imaging was performed through the pulmonary artery and aorta during inspiration breath-holding.[16] This is different from our study, where the measurements were performed without breath-hold. The advantage of ultrasound is that the temporal resolution of ultrasound is much higher (frame rate 23 Hz) than that of MRI (typically 1 Hz, electrocardiographically triggered on the R-peak depending on the heart rate).[16]

The reliability of our study is in agreement with a recently-published report on the PTT measured in cats using CEUS.[17] The time elapsed to pass the pulmonary circulation by a bolus of SonoVue® was derived by appearance time recording in both the pulmonary artery and left atrium. Veterinarians with different levels of experience evaluated the contrast-enhanced short axis echocardiography loops. Similarly as in our study, no influence of the observers' experience on PTT measurements was found (median inter-observer variability of 6.8 %).[17] They concluded that this procedure is simple and robust, and does not need to be limited to experienced operators in echocardiography.[17] Notably, our data suggest the measurement variability to be even lower by the high ICCs (Table 2). This can be explained by the way the individual pulmonary artery or chamber MTTs were estimated. In this study, PTT was estimated by the appearance of contrast behind the pulmonic valve and in the left atrium. Appearance of contrast started or stopped a timer.[17] A similar way to estimate PTT was used by Choi and coworkers.[4] In this study, investigating transit time as an estimate for cardiac output between the RV and LV, the transit time was 3.2 ± 1.2 s in patients with a mean LVEF of 50 ± 16 %.[4] The transit time was calculated by identification of the first bubble appearance, full opacification, and peak opacification of both ventricles in 27 patients.[4] Incorporating a model like the

LDRW, in the MTT assessment, makes it less subjective to human errors. The model-free parameters do not take into account the underlying kinetics of the UCA bolus in the blood stream, like the Brownian motion described by the LDRW model.[12, 18] Though the transit time estimated by two observers at two time moments showed a high intra-observer correlation (1 month interval) of 0.92, the inter-observer correlation was lower (0.79).[4] This can be explained by the analyses of the UCA passage, by the timing of the first bubble appearance to full opacification of the ventricles; this problem could be solved by using LDRW model fitting, as shown in our results with a higher inter-rater reliability. In the feasibility study of the PTT measurement, an ICC of 0.94 was found in nine patients and two observers using frame counting.[3] This emphasizes the simplicity of this procedure, which by using a model-based method may become more accurate.

The total dosage of SonoVue® used to perform the complete examination according to the protocol was 0.875 mg, which is less than the recommended dose by Bracco. We did not encounter any side effects of SonoVue®. Blood pressure, electrocardiogram, and heart rate were monitored during the examination, and the intravenous access was left in place for 30 min. The chance of side effects has been shown to be low; in a large study with 23,188 abdominal CEUS procedures the overall reporting rate of serious adverse events was 0.0086 %.[19] The chance of any serious allergic reactions has been shown to have a very low incidence (estimated to be 1:10 000).[10]

We used for the analyses three injections of SonoVue® at a total amount of 0.875 mg SonoVue®. Thus, we kept all our doses in the linear range between concentration of SonoVue® and acoustic intensity measured by the ultrasound scanner, avoiding attenuation and shadowing effects.[1, 2] It has been shown that, provided that no shadowing occurs, the effect of the ultrasound scanner settings on the errors in linearization of the video data exported in DICOM files are kept to a minimum when the dynamic range is exceeding approximately 45 dB.[20] Then a wide range of gain values can be used with excellent agreement with those derived from raw radiofrequency data.[20] The percent of error on the MTT measurements, derived from patients with colorectal liver metastasis, at 50 dB and a gain value of 50 dB was 2.8 ± 3.1 %.[21] At lower dynamic range settings, these error percentages were higher.[21]

Study Limitation

Although promising, some limitations should be considered in the interpretation of our results. Sensitivity of the PTT measurement was not addressed in this study. However, several authors reported over a range of cardiac function good correlation with the measured PTT by CEUS. A cut-off point of approximately 4.5 s distinguished normals from patients with diminished function.[3, 4] In our population, with diminished ejection fractions (± 30 % and dyssynchrony), PTT was 11.2 s. A good differentiation can be ap-

preciated between the different ventricular functions based on PTT-measurements, which is also reported in MRI studies as described above.[16, 22]

It is known that intra-cardiac shunts due to for example atrial septum defect or ventricular septum defect will influence the IDC.[23] These shunt characteristics are well known in transpulmonary thermodilution where a thermistor is positioned in the femoral artery. In case of a left-to-right shunt in patients with a ventricular septum defect the tail of the IDC will show an extra humb as the indicator will be recycled from the left to the right atrium.[23] In a right-to-left shunt the IDC will show a biphasic humb at the ascending part of the IDC, meaning an earlier increase and decrease of the curve followed by the actual peak of a normal passage of the indicator.[23, 24] In our patients no atrial or ventricular septum defects were present. However, given the high prevalence of patent foramen ovale (PFO) of 35 % in the general population, we cannot exclude the presence of a PFO in a part of our patients.[25] Still, a PFO would probably not influence the results as only a minority of PFO's will demonstrate a spontaneous right-to-left shunt and all patients were spontaneous breathing without respiratory distress, which means no right-to-left shunts would be expected. Indeed, most PFO's only exhibit shunting during Valsalva manoeuvre. However, knowing that CEUS is contraindicated in patients with intra-cardiac shunts and the indicator should only pass the detection point once, the effect of an intra-cardiac shunt on the MTT of the left ventricle could be of interest for future studies.[10, 26]

Our study population consisted of patients with a dilated LV and low ejection fraction; this could benefit the feasibility of ROI drawing in the LV. A larger LV with diminished contractions could facilitate ROI drawing, reducing interference with the septal and lateral walls. Indeed a higher coefficient of variation of the MTT of the much smaller, good contracting RV 2.61 % versus 1.21 % for the LV is supported by the higher coefficient of variation of the ROI size of the RV. Nevertheless, the ICC of 0.98 for the RV is comparable with the LV ICC (Table 2). This observation suggests that contribution of ventricular size to the variability of MTT measurement is limited and implies that MTT measurement in the normal LV is as reliable.

The difference in reliability between the physicians and non-physicians could not be explained as we did not include other performance parameters in the present study, such as time to complete measurements per ROI, per patient, for the whole set of patients, and the two time moments. The explanation for this difference needs to be investigated.

Although, an ICC larger than 0.8 is still almost perfect according to Landis and Koch (1977), the intra-rater reliability per rater showed some variation with ICCs ranging from 0.81 to 0.99 (Table 4).[27] This variation can be explained by a deviating MTT measurement at one of the time moments, which can probably be overcome by a higher number of repetitions to increase the precision.[28] In analogy to cardiac output measurements using intermittent bolus thermodilution, three repeated injections could be necessary to estimate transit times with a high precision. However, for cardiac out- put estimations,

the use of four indicator injections improved the precision to 5 % compared to the 'true' value.[28] The number of repeated injections required to ensure a high precision for MTT estimation needs to be explored.

In this study, we did not investigate the effect of different ultrasonographers on the estimation of the PTT. However, we showed in an earlier study using transesophageal echocardiography that the MTT measurement is easy to perform; a good and stable view on the chamber or vessel under investigation during the whole cardiac cycle is necessary.[8] It is of importance to keep in- and expirations in a normal and regular pattern, otherwise artifacts may occur due to the displacement of the heart in the imaging window.

The development of automated algorithms for ROI definition and MTT estimation could enhance clinical feasibility of this novel CEUS tool.[29] This could create the opportunity to simplify PTT calculation at the bedside.

The relationship between the PTT and cardiac function has been investigated mainly by MRI and radionuclides.[16, 30] The relationship to different echocardiographic parameters has recently been investigated and seems promising, further investigations are necessary to evaluate its diagnostic characteristics.[3]

CONCLUSIONS

PTT assessment by drawing ROIs in CEUS recordings is a reliable technique with a high inter- and intra-rater reliability and reproducibility. Each measurement also showed a high repeatability between three different echo loops at three different doses. Differences in ROI size hardly affect the MTT per ROI. This makes this novel bedside applicable technique for measuring the PTT reliable to be performed by experienced and inexperienced operators, having an ultrasound scanner and an UCA with intravenous access. This motivates for further investigation of its clinical application in order to replace invasive measurements requiring catheterization.

REFERENCES

1. Herold IH, Russo G, Mischi M, Houthuizen P, Saidov T, van het Veer M, et al. Volume quantification by contrast-enhanced ultrasound: an in-vitro comparison with true volumes and thermodilution. *Cardiovasc Ultrasound*. 2013; **11**: 36
2. Mischi M, Kalker TA, Korsten EH. Contrast echocardiography for pulmonary blood volume quantification. *IEEE Trans Ultrason Ferroelectr Freq Control*. 2004; **51**: 1137–47
3. Brittain EL, Doss LN, Saliba L, Irani W, Byrd 3rd BF, Monahan K. Feasibility and diagnostic potential of pulmonary transit time measurement by contrast echocardiography: a pilot study. *Echocardiography*. 2015; **32**: 1564–71
4. Choi BG, Sanai R, Yang B, Young HA, Mazhari R, Reiner JS, et al. Estimation of cardiac output and pulmonary vascular resistance by contrast echocardiography transit time measurement: a prospective pilot study. *Cardiovasc Ultrasound*. 2014; **12**: 44
5. Ugander M, Kanski M, Engblom H, Gotberg M, Olivecrona GK, Erlinge D, et al. Pulmonary blood volume variation decreases after myocardial infarction in pigs: a quantitative and noninvasive MR imaging measure of heart failure. *Radiology*. 2010; **256**: 415–23
6. Korsten HH, Mischi M, Grouls RJ, Jansen A, van Dantzig JM, Peels K. Quantification in echocardiography. *Semin Cardiothorac Vasc Anesth*. 2006; **10**: 57–62
7. Mischi M, Jansen AH, Korsten HH. Identification of cardiovascular dilution systems by contrast ultrasound. *Ultrasound Med Biol*. 2007; **33**: 439–51
8. Herold IH, Soliman Hamad MA, van Assen HC, Bouwman RA, Korsten HH, Mischi M. Pulmonary blood volume measured by contrast enhanced ultrasound: a comparison with transpulmonary thermodilution. *Br J Anaesth*. 2015; **115**: 53–60
9. Gorce JM, Arditi M, Schneider M. Influence of bubble size distribution on the echogenicity of ultrasound contrast agents: a study of SonoVue. *Invest Radiol*. 2000; **35**: 661–71
10. Senior R, Becher H, Monaghan M, Agati L, Zamorano J, Vanoverschelde JL, et al. Contrast echocardiography: evidence-based recommendations by European Association of Echocardiography. *Eur J Echocardiogr*. 2009; **10**: 194–212
11. Mischi M, Kalker T, Korsten HHM. Videodensitometric methods for cardiac output measurements. *EURASIP J Appl Signal Processing*. 2003; **5**: 479–89
12. Sheppard CW, Savage LJ. The random walk problem in relation to the physiology of circulatory mixing. *Phys Rev*. 1951; **83**: 489–90
13. Kottner J, Audige L, Brorson S, Donner A, Gajewski BJ, Hrobjartsson A, et al. Guidelines for Reporting Reliability and Agreement Studies (GRRAS) were proposed. *J Clin Epidemiol*. 2011; **64**: 96–106
14. Shrout PE, Fleiss JL. Intraclass correlations: uses in assessing rater reliability. *Psychol Bull*. 1979; **86**: 420–8
15. Bland JM, Altman DG. Statistical methods for assessing agreement between two methods of clinical measurement. *Lancet*. 1986; **1**: 307–10
16. Shors SM, Cotts WG, Pavlovic-Surjancev B, Francois CJ, Gheorghiade M, Finn JP. Heart failure: evaluation of cardiopulmonary transit times with time- resolved MR angiography. *Radiology*. 2003; **229**: 743–8
17. Streitberger A, Hocke V, Modler P. Measurement of pulmonary transit time in healthy cats by use of ultrasound contrast media "Sonovue(R)": feasibility, reproducibility, and values in 42 cats. *J Vet Cardiol*. 2013; **15**: 181–7

18. Wise ME. Tracer dilution curves in cardiology and random walk and lognormal distributions. *Acta Physiol Pharmacol Neerl*. 1966; **14**: 175–204
19. Piscaglia F, Bolondi L. The safety of Sonovue in abdominal applications: retrospective analysis of 23188 investigations. *Ultrasound Med Biol*. 2006; **32**: 1369–75
20. Rognin NG, Frinking P, Costa M, Arditi M. In-vivo perfusion quantification by contrast ultrasound: Validation of the use of linearized video data vs. raw RF data. *Ultrasonics Symposium, 2008 IUS Proceedings*, IEEE 2008:1690-3
21. Gauthier TP, Averkiou MA, Leen EL. Perfusion quantification using dynamic contrast-enhanced ultrasound: the impact of dynamic range and gain on time-intensity curves. *Ultrasonics*. 2011; **51**: 102–6
22. Cao JJ, Wang Y, McLaughlin J, Haag E, Rhee P, Passick M, et al. Left ventricular filling pressure assessment using left atrial transit time by cardiac magnetic resonance imaging. *Circ Cardiovasc Imaging*. 2011; **4**: 130–8
23. Giraud R, Siegenthaler N, Park C, Beutler S, Bendjelid K. Transpulmonary thermodilution curves for detection of shunt. *Intensive Care Med*. 2010; **36**: 1083–6
24. Michard F, Alaya S, Medkour F. Monitoring right-to-left intracardiac shunt in acute respiratory distress syndrome. *Crit Care Med*. 2004; **32**: 308–9
25. Meier B, Lock JE. Contemporary management of patent foramen ovale. *Circulation*. 2003; **107**: 5–9
26. Zierler KL. Theoretical basis of indicator-dilution methods for measuring flow and volume. *Circ Res*. 1962; **10**: 393–407
27. Landis JR, Koch GG. The measurement of observer agreement for categorical data. *Biometrics*. 1977; **33**: 159–74
28. Nilsson LB, Nilsson JC, Skovgaard LT, Berthelsen PG. Thermodilution cardiac output–are three injections enough? Acta Anaesthesiol Scand. 2004; **48**: 1322–7
29. Saporito S, Herold IH, Houthuizen P, van den Bosch HC, Korsten HH, van Assen HC, et al. Automatic indicator dilution curve extraction in dynamic-contrast enhanced imaging using spectral clustering. *Phys Med Biol*. 2015; **60**: 5225–40
30. Jones RH, Sabiston Jr DC, Bates BB, Morris JJ, Anderson PA, Goodrich JK. Quantitative radionuclide angiocardiography for determination of chamber to chamber cardiac transit times. *Am J Cardiol*. 1972; **30**: 855–64

Chapter 7

Automatic indicator dilution curve extraction in dynamic-contrast enhanced imaging using spectral clustering

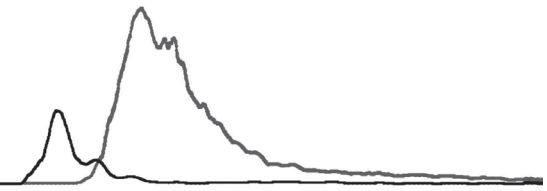

Salvatore Saporito
Ingeborg HF Herold
Patrick Houthuizen
Harrie CM van den Bosch
Hendrikus HM Korsten
Hans C van Assen
Massimo Mischi

Phys Med Biol 2015; 60: 5225-40

ABSTRACT

Indicator dilution theory provides a framework for the measurement of several cardiovascular parameters. Recently, dynamic imaging and contrast agents have been proposed to apply the method in a minimally invasive way. However, the use of contrast-enhanced sequences requires the definition of regions of interest (ROIs) in the dynamic image series; a time-consuming and operator dependent task, commonly performed manually. In this work, we propose a method for the automatic extraction of indicator dilution curves, exploiting the time domain correlation between pixels belonging to the same region. Individual time intensity curves were projected into a low dimensional subspace using principal component analysis; subsequently, clustering was performed to identify the different ROIs. The method was assessed on clinically available DCE-MRI and DCE-US recordings, comparing the derived IDCs with those obtained manually. The tracer kinetic parameters derived on real images were in agreement with those obtained from manual annotation. The presented method is a clinically useful preprocessing step prior to further ROI-based cardiac quantifications.

INTRODUCTION

Indicator dilution theory allows the measurement of different cardiovascular and hemodynamic parameters of clinical interest.[1] The method consists of the injection of a bolus containing a known amount of a suitable tracer into a peripheral or central vein. Subsequent measurement of the indicator concentration over time in different anatomical locations results in indicator dilution curves (IDCs). Model-based[2] fitting of the measured IDCs permits the derivation of parameters of interest, such as cardiac output[3-4], pulmonary blood volume (PBV)[5], ejection fraction[6], and extravascular lung water.[7-8] Specifically, the volume between two sampling sites can be determined by multiplying the difference in mean transit time (MTT) of the two IDCs by the flow rate between the two sites, as stated by the central volume theorem.[9] Purely intravascular indicators allow the measurement of absolute blood volumes, while indicators crossing capillary membranes will provide volume estimates considering also the extracellular space. Recently, quantification of blood volumes has received increasing clinical attention as a promising tool to assess congestion in chronic heart failure (HF) patients.[10-11] The development of objective and minimally invasive techniques for the assessment of pulmonary congestion has huge potential for optimizing the diagnosis, prognostic stratification, and management of HF patients.

Different indicators have been proposed, such as cold saline[12], dyes[13] or lithium[14], which are commonly used in intensive care units and in operating rooms. However, the use of these indicators requires central vessel catheterization, which is costly, invasive, and can lead to complications for the patient.[15]

Ultrasound[16-20], X-ray computed tomography[21], and magnetic resonance imaging (MRI) contrast agents[22-24] have been proposed as indicators for cardiovascular quantifications.[25] These indicators allow the application of indicator dilution methods in a minimally invasive way, as the measurement of the IDCs in the blood pool (e.g. the cardiac chambers) can be performed from the outside of the body.[26]

The application of the method using dynamic imaging techniques requires the definition of regions of interest (ROIs) in the dynamic image series. ROIs are typically defined in the cardiac chambers. This is usually performed manually, limiting the reproducibility and repeatability of the measurement as inter-observer and intra-observer variability are introduced. Moreover, the manual definition of ROIs is a time demanding procedure and it may be challenging also for trained operators, especially at low SNR conditions. Automatic definition of the ROIs would improve the reliability of the derived parameters[27] and is therefore desirable. Requirements for the ideal ROIs are to cover the largest uniformly mixed area possible without including other tissues in order to improve the statistics and SNR of the derived curves, since the IDCs are obtained by averaging the signal within the ROI.

A prerequisite for the application of indicator dilution theory using imaging as sensing technique is a known, strictly-monotonic relationship between contrast agent concentration and signal intensity. This can be evaluated experimentally through calibration procedures.

The problem of defining ROIs may be addressed as a segmentation task. However, the use of contrast-specific imaging protocols may result in poor enhancement of anatomical features used by traditional segmentation algorithms.[28] Furthermore, traditional medical image segmentation methodologies often require prior knowledge, for instance shape models[29-30], or user interaction as in graph cut approaches.[31]

Several studies have shown the applicability of clustering techniques in dynamic imaging by grouping pixels according to their temporal behaviour.[32] Some authors proposed to perform clustering directly in the time domain, using the intensity of a pixel in each frame as a feature.[33-34] However, this approach is computationally demanding and of limited applicability when the spatio-temporal resolution increases, resulting in a high dimensionality of the feature spaces.[35] Dimensionality reduction techniques can then be useful.[36-38]

K-means has been proposed[39] as a clustering technique, but this choice could be inappropriate when clusters differ considerably in size, like the different heart chambers. Some used nonlinear dimensionality reduction[40-41]; however, the benefit of introducing additional parameters to the method has not been clearly motivated. Few studies have reported similar approaches, combining clustering and linear dimensionality reduction techniques.[42-44] Most of them presented results on a single image modality.

In this work, we present a general automatic ROI identification method based on statistical rather than on anatomical criteria. The method assumes the presence of large regions composed of correlated individual pixel intensity curves. Dynamic contrast-enhanced four chamber view recordings of the heart were measured using ultrasound and MRI scanners. The method consists of a separated, image modality-dependent, preprocessing step consisting in spatio-temporal smoothing, background subtraction and respiratory artifacts exclusion; subsequently principal component analysis (PCA) and clustering based on Gaussian mixture models is applied, independently of the considered image modality. The latter dimensionality reduction and clustering steps are repeated two times in order to separate the left from the right heart first, and to separate the atria from the ventricles later. Morphological post-processing and connected component analysis are used to exclude small undesired regions. Finally, IDCs were derived from the resulting ROIs in the different cardiac chambers; model-based fitting of the obtained IDCs allowed the extraction of cardiovascular parameters. The accuracy is assessed by comparing IDCs from automatically derived ROIs with their manually derived counterparts in 15 DCE-US and 18 DCE-MRI recordings.

METHODS

In this paper, we focused our analysis on the estimation of the MTTs from the right ventricle (RV) and left ventricle (LV) IDCs, as well as their difference, the pulmonary transit time (PTT).[45] The latter allows the estimation of the intra-thoracic fluid volume, when the cardiac output is known.

Several models have been used in the literature for IDC interpretation; in this work the local density random walk (LDRW) kinetic model introduced by was adopted to fit the obtained IDCs.[46] The model is a solution of the diffusion equation and it is thus strongly related to the underlying indicator dispersion physics.[47]

The expression for the model is given as:

$$C(\hat{t}) = \alpha \sqrt{\frac{K}{2\pi\hat{t}}}\, e^{\frac{-K(\hat{t}-\mu)^2}{2\hat{t}}}$$

where κ is a shape parameter, μ is the MTT of the indicator, α is the area under the curve, and $\hat{t} = t - t_0$ is the time that has passed since the theoretical injection time t_0. The fitting procedure was implemented by an iterative Levenberg–Marquardt non-linear least squares regression.[48-49]

Image acquisition

DCE-MRI

A 1.5 T Intera MRI scanner (Philips Healthcare, Andover, MA, USA) equipped with a cardiac coil array was used. Each subject underwent a cardiac triggered, maximum breath-hold scanning procedure. The acquisition was delayed with respect to the R-peak on the ECG of the patient for acquiring images in late diastolic phase, where the influence of cardiac motion was expected to be minimal. Two-dimensional images with a slice thickness of 10 mm were acquired. A turbo field echo sequence was used with a flip angle of 7 ◦, TR=2.9 ms, TE=1.7 ms, and a readout bandwidth of 234 Hz/pixel. In order to obtain T1 contrast, a saturation pre-pulse was applied 200 ms before the acquisition of the central line in k-space. SENSE parallel acquisition and half-scan strategies were used to reduce the total imaging time. The acquired field of view was 224 × 224 pixels, with reconstructed pixel size of 1.65 mm × 1.65 mm. Bolus injections of 0.1 mmol and 0.3 mmol of contrast agent (Dotarem; Guerbet, Aulnay-sous-Bois, France) diluted in 20 ml of saline solution were performed using an automated injector at a rate of 5 ml/s (Spectris MR; Medrad Indianola, PA, USA). Under these conditions, a linear relationship between the signal enhancement and contrast agent concentration was observed.[22] The recording was concluded after the acquisition of 120 images.

DCE-US

Dynamic constrast-enhanced (DCE-US) ultrasound recordings were acquired using an iE33 ultrasound scanner in combination with an S5-1 (Philips Healthcare, Andover, MA, USA) trans-thoracic probe to obtain B-mode images. Harmonic imaging with a transmission frequency of 2.7 MHz was used; while the mechanical index was lower than 0.2 in order to avoid contrast agent disruption. Acquisition depth was adjusted to achieve complete visualization of both atria and ventricles, with a typical pixel size of 0.39 mm × 0.39 mm and acquired image size of 800 × 600 pixels. The dynamic range was set to 50 dB and gain was adjusted to avoid saturation. Bolus injections of 0.025 ml of SonoVue® (Bracco Research SA, Geneva, Switzerland) diluted in a 10 ml saline solution were performed manually. Under these conditions, linearity of the acoustic intensity with respect to UCA concentration was expected.[50-51] The frame rate was typically 23 Hz; the first 75 s only of the recording were considered for the subsequent analysis.

Image analysis

All the following algorithms were implemented in MATLAB 2014a (The MathWorks, Inc., Natick, Massachusetts, USA) on an Intel Core i5 3.4 GHz workstation with 8 GB RAM using a 64 bit workstation.

DCE-MRI image preprocessing

Each of the N_{FR} frames within the recording was smoothed by convolution with a square, isotropic Gaussian kernel (σ = 7.4 mm) of 14 mm. Contrast enhancement was obtained by subtraction of the background from each frame E[x, y, t]= I[x, y, t]– B[x, y] if I[x, y, t] – B[x, y]> 0, E[x, y, t] = 0 otherwise. B[x, y] was estimated by averaging over time the frames corresponding to the first 5 seconds of the recording, thus considering frames in which the position of the heart was constant and the contrast agent was absent. In order to identify the areas of contrast agent passage, each pixel-wise time intensity curve E[x, y, t], t = 0 . . . N_{FR} was smoothed by a finite impulse response low-pass filter with cutoff frequency of 0.2 Hz, giving $\tilde{E}$[x, y, t]. Subsequently, an enhancement map A[x, y] was derived as A[x, y] = max {$\tilde{E}$[x, y, t]} – min {$\tilde{E}$[x, y, t]}. Automated thresholding of A[x, y] using the automated Otsu method[52] resulted in separation A between a foreground component and background component. In order to discriminate between enhancement due to the presence of contrast agent and grayscale changes due to through-plane and/or breathing motion, the sum of absolute differences (SAD) between consecutive frames was considered:

$$\mathbf{SAD}[t] = \sum_{x=1}^{N_X} \sum_{y=1}^{N_y} |\mathbf{I}[x, y, t] - \mathbf{I}[x, y, t-1]|$$

The SAD was thresholded using SAD_{TH} given by its mean value plus one standard deviation. Frames exceeding that threshold occurring after 45 seconds from the injec-

tion (physiological limit for contrast agent first passage) were considered corrupted by motion. In order to exclude those regions from subsequent processing, a motion map M was derived:

$$M[x, y] = \sum_{\substack{t^*: \\ SAD[t^*]>SAD_{TH} \\ t^*>45s}} |\mathbf{I}[x, y, t] - \mathbf{I}[x, y, t-1]|$$

Segmentation of M[x, y] by means of Otsu automatic thresholding resulted in a binary mask $\mathbb{M}$. The two binary masks were combined to derive a final contrast induced enhancement map by means of logical operations $\mathbb{F}[x, y]= \mathbb{A}[x, y]$ AND NOT $(\mathbb{M}[x, y])$. $\mathbb{F}$ was used to select pixels considered for further processing.

DCE-US image preprocessing

Log-compressed video-intensity grey values of the single frames composing the recordings were linearized according to Gauthier and coworkers.[53] Each frame was smoothed by convolution with a square and isotropic Gaussian kernel (σ = 2.7 mm) of 12.2 × 12.2 mm. Afterwards, images were down-sampled by a factor 4 in each dimension. The background B[x, y] was estimated with the same approach as described for DCE-MRI images, now using the first 1.2 s of each recording. Enhancement maps A[x, y] were thresholded to obtain $\mathbb{A}$ using the same approach as for DCE-MRI. Preprocessing steps in order to exclude intensity enhancements due to motion artifacts were considered unnecessary for DCE-US.

Dimensionality reduction

After subtracting the mean value from each frame composing the recording, the selected IDCs were rearranged as a matrix D[t, i] of N_{FR} rows and N_{PIX} columns, with each row having zero mean. A covariance matrix C was estimated as $C= \frac{1}{N_{PIX}} DD^T$. Eigenvalue decomposition was performed, $C = U\Lambda U^T$, where U is a matrix whose columns are eigenvectors for C and principal components of D, and Λ is a diagonal matrix whose elements λ_i are eigenvalues for C, describing the relative fraction of variance explained by the corresponding eigenvectors. The original data were projected into a low-dimensional subspace by using the first $N_{RED}< N_{FR}$ columns, $U_{N_{RED}}$, of U corresponding to the largest eigenvalues λ_i in absolute value.

Let $R = U^T_{U_{RED}}D$ be the low dimensional representation of the original data. N_{RED} was set automatically to preserve 95% of the explained variance, such that

$$\frac{\sum_{i=1}^{n} \lambda_i}{\sum_{i=1}^{N_{FR}} \lambda_i} < 0{,}95 \;\forall\; n < N_{RED}$$

Clustering

Clustering was applied in the low dimensional subspace where each original pixel IDC was described by the projected $r_p \in \mathbb{R}^{N_{RED}}$, $p = 1 \ldots N_{PIX}$. A Gaussian mixture model (GMM) was used. The probability density function fitted to the r_p distribution was:

$$p(r_p;\phi_i,\mu,\Sigma) = \sum_{i=i}^{k} \phi_i N(\mu_i, \Sigma_i)$$

where ϕ_i are the weights for each of the $j = 1 \ldots K$ components of the mixture and μ_i, Σ_i are the mean value and variance of the corresponding N component of the mixture of normal distributions, respectively. Maximum likelihood estimates $\hat{\phi}$, $\hat{\mu}$, $\hat{\Sigma}$ of the mixture parameters were obtained iteratively using an expectation-maximization approach.[54] Individual pixels r_p were assigned to a cluster L_i based on maximum a posteriori probability criteria $i = \text{argmax}_i p_i$, where $p_i = N(r_p; \hat{\mu}_i, \hat{\Sigma}_i)$. Pixels with posterior probability lower than 0.05 in all the estimated components were interpreted as outliers and rejected from subsequent clusters. The procedure was repeated 10 times with different initial values for the mixture parameters to avoid local minima to affect the parameter estimation. The dimensionality reduction and clustering procedure was executed two times, in both cases the number of mixtures was set to 2. During the second execution, the same clustering procedure was automatically applied to all the ROIs identified from the first clustering. The number of the clusters was chosen based on prior knowledge about the anatomy of the heart; the first clustering was performed in order to separate the left and the right side of the heart, the second to discriminate between atria and ventricles.

Post-processing of the ROIs

Based on our assumption of contiguity of the desired ROIs, corresponding clusters were divided into connected regions. Morphological erosion with a spherical kernel was applied to exclude small regions misidentified in previous steps and to smooth the region contours. Based on the assumption of minimum area necessary for subsequent IDC quantifications, ROIs smaller than a certain threshold were rejected. In this work, region size thresholds of 200 pixels and 100 pixels were used for DCE-US and DCE-MRI, respectively. The four largest ROIs were considered. From each ROI, an IDC was obtained averaging the image intensity in the ROI over space yielding S(t). The signal intensity S(t) was converted into contrast agent concentration by $\tilde{C}(t) = \frac{S(t)-S_0}{S_0}$ for the DCE-MRI, and by $\tilde{C}(t) = S(t) - S_0$ for the DCE-US, where S_0 was the baseline obtained averaging the signal intensity before the passage of the contrast agent.

Validation

Patient data

All the patient data were collected at the Catharina hospital (Eindhoven, the Netherlands) from a DCE-US and DCE-MRI study approved by the local Medical Ethical Committee. Informed written consent was obtained from all patients. All images were exported in DICOM format. 15 DCE-US and 18 DCE-MRI recordings acquired from HF patients were considered.

Due to the absence of a ground truth for the ROIs in patients, the method was evaluated against manually defined ROIs. The endpoint of the analysis was the estimation of LV and RV MTTs, as well as the PTT. For the DCE-US loops four users were asked to draw ROIs in the RV and in the LV using Q-LAB 8 (Philips Healthcare). For the DCE-MRI loops two users were asked to draw ROIs in the RV and LV. Subsequently, the LDRW model was fitted to the obtained IDCs. For the DCE-US, the inter-observer variation over a parameter θ was quantified as $e\theta = \sigma\theta / \mu\theta$, where $\mu\theta$ and $\sigma\theta$ were the average and standard deviation of the estimates of θ from the different users. For the DCE-MRI, the inter-observer variation was defined as the ratio between the difference and average of the estimates from the two different users, respectively. The difference on parameter estimates θAUTO derived from the fitting of the automatically extracted IDCs was evaluated with respect to the average obtained by manual annotation $\mu\theta$.

RESULTS

Sample frames from DCE-MRI and DCE-US recordings are shown in Figure 1. The total computational costs of the complete method were in the order of 60 s when the method was applied on DCE-MRI sequences, and less than 180 s when considering DCE-US recordings.

DCE-MRI

The steps implemented for MRI preprocessing are shown for one case in Figure 2.

An example of clustering results, automatically derived ROI and corresponding IDC for a DCE-MRI recording is shown in Figure 3. In two cases, the method produced unrealistic ROIs, resulting in IDCs with low (<0.6) determination coefficient, R^2, of the fit. These two cases were excluded from the statistical analysis. In two cases, the manually selected ROIs resulted in artifact-corrupted IDCs from all the users, resulting in non realistic parameter values. Those cases were excluded from the inter-observer variability analysis.

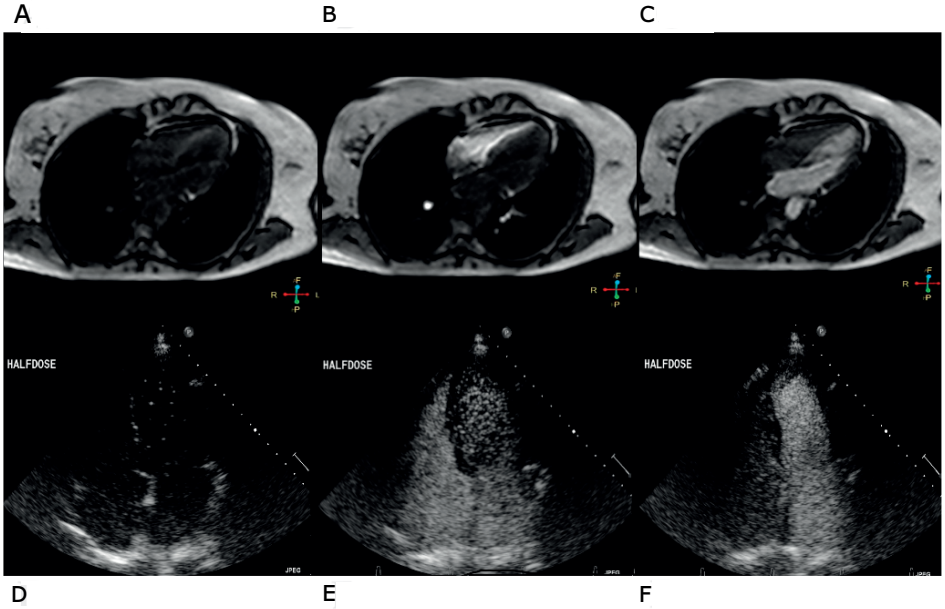

Figure 1. Top row left to right: sample frame from a DCE-MRI recording at baseline (A), during passage of the contrast agent in right heart (B), and during passage of the contrast agent in left heart (C); bottom row left to right (D-F): same for DCE-US.

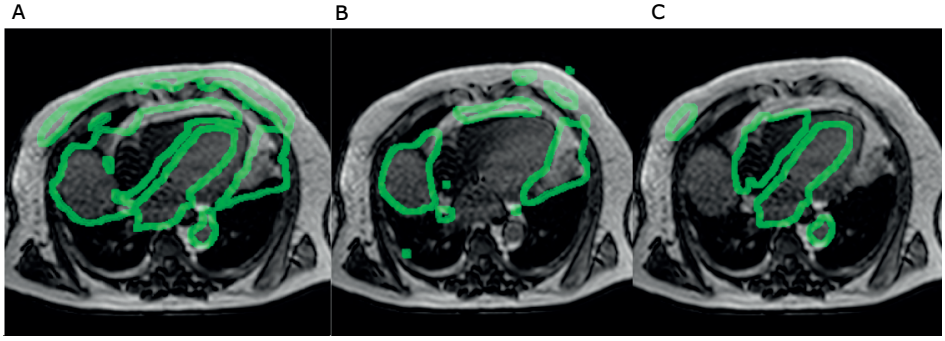

Figure 2. Left to right: (A) a sample frame from a DCE-MRI with overlaid enhanced regions; (B) same frame with overlaid motion corrupted regions; (C) same frame with regions selected for successive clustering. Small undesired regions in (C) were clustered using the proposed method and later excluded during the automatic post-processing phase based on their size.

The average coefficient R^2 was 0.96 ± 0.05, and 0.97 ± 0.03 for the manually derived LV and RV IDCs, respectively, while it was 0.96 ± 0.07, and 0.96 ± 0.04 for the automatically derived LV and RV IDCs, respectively.

The average MTT difference between manual and automatically derived IDCs was 0.62 ± 0.82 s, and 0.37 ± 0.87 s for the LV and RV MTT, respectively. The average

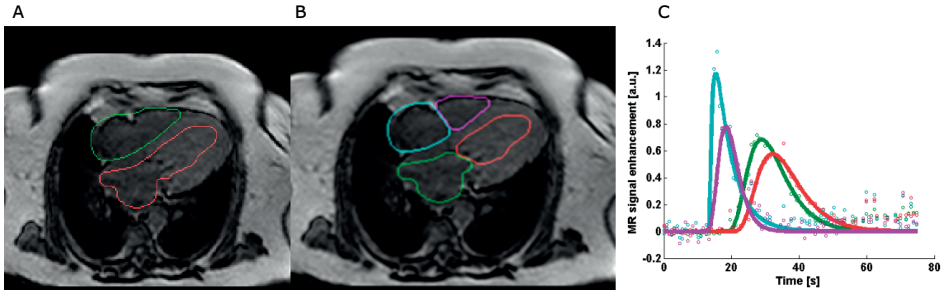

Figure 3. Left to right: (A) Result of the first clustering of the enhanced regions; (B) results of the second clustering of the enhanced regions; (C) corresponding indicator dilution curves after the second clustering.

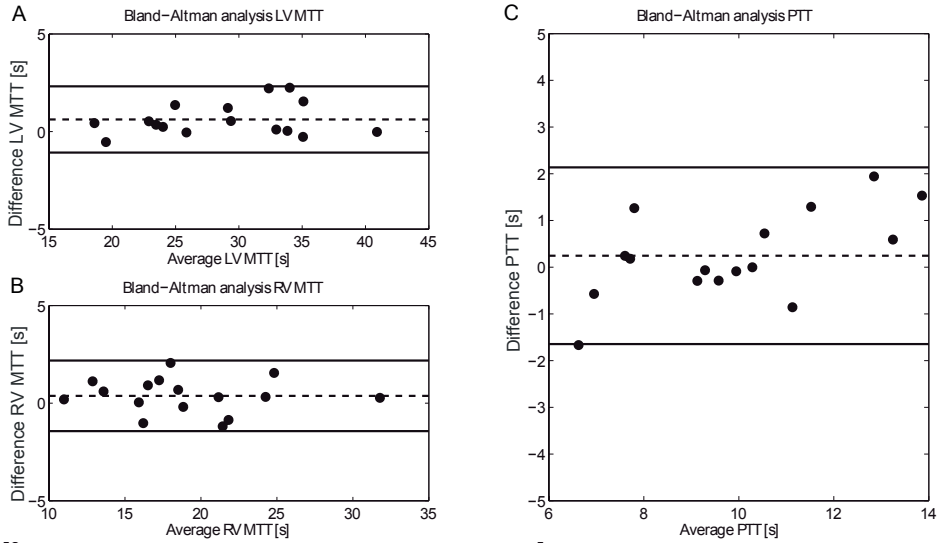

Figure 4. Left top: (A) Bland-Altman plot for left ventricle (LV) mean transit time (MTT) estimates by DCE-MRI; bottom (B) Bland-Altman for right ventricle MTT estimates by DCE-MRI; right: (C) Bland-Altman for pulmonary transit time (PTT) estimates by DCE-MRI.

PTT difference was 0.25 ± 0.92 s. When comparing the error to the average of the two, the difference was 2.1 ± 2.7 %, and 2.2 ± 4.8 % for the LV and RV MTT, respectively, while it was 3.1 ± 7.4 % for the PTT.

The inter-observer variability was 0.8 ± 1.0 %, 0.4 ± 0.4 %, and 2.0 ± 2.1 % for LV MTT, RV MTT, and PTT, respectively. Accuracy of the individual measurements is shown with a Bland-Altman plot in Figure 4.[55]

The SNR was 25.1 ± 18.7 dB, and 20.1 ± 10.7 dB for LV IDCs derived from manual ROIs and automatic ones respectively, while it was 22.1 ± 14.5 dB, and 24.0 ± 17.8 dB for RV IDCs.

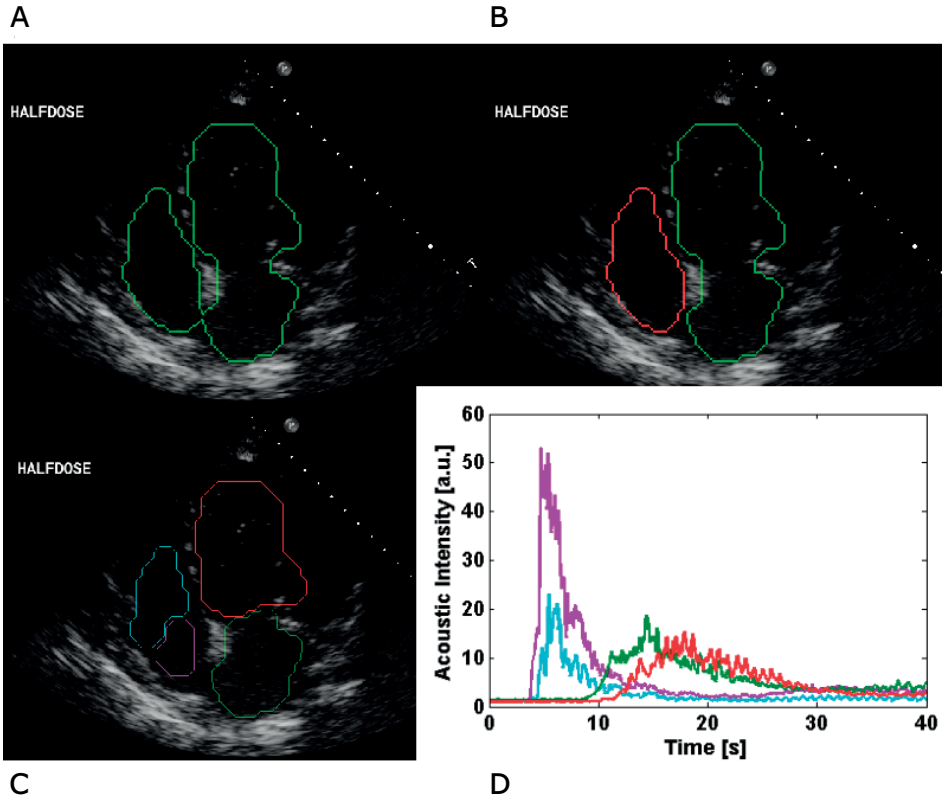

Figure 5. Left top: (A) enhanced regions; top right: (B) results of the first clustering; bottom left: (C) results of the second clustering; bottom right: (D) indicator dilution curves corresponding to the regions of interest.

DCE-US

An example of automatically derived ROIs and corresponding ventricular IDCs is shown in Figure 5, together with the clustering results. In two cases, the method produced ROIs not corresponding to any anatomical location by visual inspection; these cases were excluded from the statistical analysis. The absolute difference in LV MTT, RV MTT, and PTT estimates by manual and automatic segmentation was –0.03 ± 0.30 s, –0.19 ± 0.34 s, and 0.16 ± 0.39 s, respectively. The relative differences for the same parameters were –0.2 ± 1.6%, –2.6 ± 3.5%, and –1.3 ± 3.5%. On the same data, the inter-observer variability was 0.6 ± 0.6%, 2.2 ± 2.2%, and 1.8 ± 0.9%. Differences in the individual measurements are illustrated by a Bland-Altman plot in Figure 6. The intra-observer differences were 0.1 ± 0.8%, –0.1 ± 2.0%, and 0.3 ± 2.1%, respectively. The average R^2 for the fits of the LV IDC for manual and automatic ROIs were 0.97 ± 0.04 and 0.97 ± 0.03, respectively. The average R^2 for the fits of the manually defined RV IDC was 0.97 ± 0.03, while it was 0.96 ± 0.04 for the automatically derived IDCs.

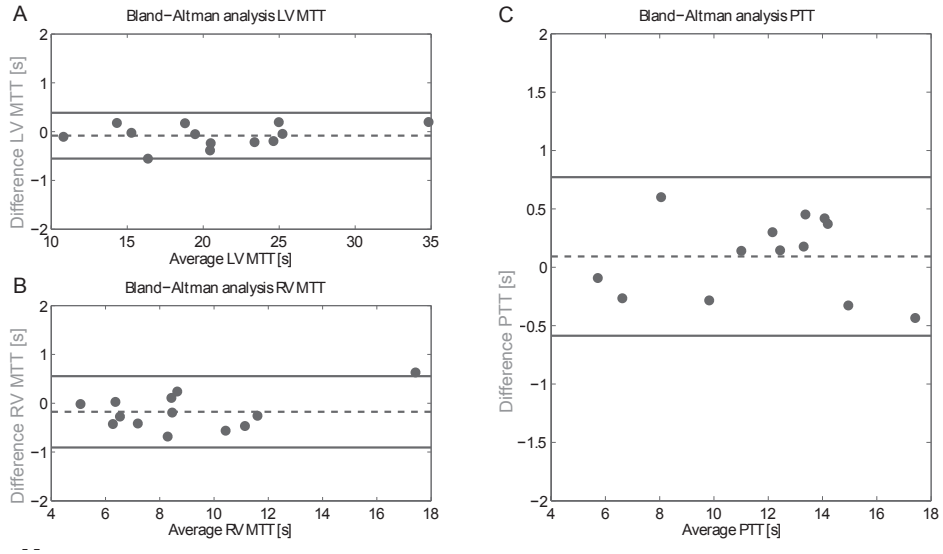

Figure 6. Left top: (A) Bland-Altman plot for left ventricle (LV) mean transit time (MTT) estimates by DCE-US; left bottom: (B) Bland-Altman for right ventricle (RV) MTT estimates by DCE-US; right: (C) Bland-Altman plot for pulmonary transit times (PTT) estimates by DCE-US.

The manually derived PTTs from both DCE-US and DCE-MRI are compared with the automatically derived ones in Figure 7.

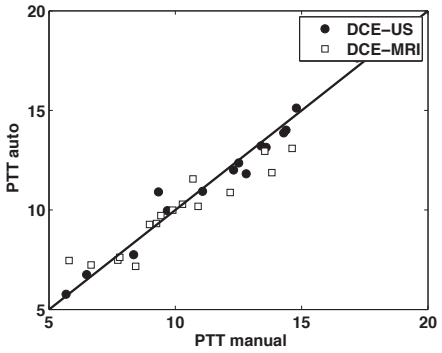

Figure 7. Comparison between automatically and manually determined pulmonary transit times (PTT).

DISCUSSION

Despite their invasiveness, indicator dilution techniques represent the gold standard approach to measure PBV and CO in clinical settings. The use of DCE-MRI and DCE-US in combination with appropriate contrast agents may reduce the invasiveness of the

method promoting a larger clinical adoption. The definition of ROIs is a crucial step in the application of the method, which can be time consuming and lead to suboptimal ROI positioning, hampering the clinical applicability of the method.

The results on in-vivo data suggest that the proposed method is able to identify ROIs in clinically available DCE-MRI and DCE-US recordings; derived IDC parameters are in agreement with those obtained manually.

When the flow in the system, i.e. the CO, is known, the PTT derived from dynamic imaging can be used to derive intra-thoracic fluid volume estimates minimally-invasively. The differences between the blood volume estimates obtained by purely intravascular indicators as the UCA, and multi-compartmental volume estimates by gadolinium-based contrast agents, which extravasate may provide additional insight on pulmonary congestion status and will be part of a future dedicated study. As similar SNR levels are achieved by manually and automatically derived ROIs, the automatic method is preferable as it results in time savings and improved reproducibility of the derived parameters. Advantage of the proposed method is its applicability in different image modalities.

We did not assess the limitations in terms of SNR for real images. On a limited number of cases, the method failed to define correct ROIs, mainly due to motion artifacts violating the method assumptions. However, those cases could be easily identified; therefore they can hardly reduce the clinical applicability of the method, as a final review of the results by an expert clinician should always be available.

Possible directions for future work are the evaluation and comparison of different clustering techniques. Nonlinear dimensionality reduction techniques can also be further evaluated in order to identify their effect in relation to the choice of the clustering method.

CONCLUSION

We proposed a method based on spectral clustering for the identification of blood pools in cardiac dynamic contrast-enhanced imaging. A modality-dependent preprocessing was followed by dimensionality reduction of the IDCs; clustering was subsequently applied to identify the different blood pools. We validated the method in comparison with manual ROI delineation on clinically available images. The derived indicator kinetic parameters were in agreement with those obtained manually. Therefore, the proposed method is a clinically useful and practical preprocessing step prior to further IDC quantification.

REFERENCES

1. Zierler K. Indicator dilution methods for measuring blood flow, volume, and other properties of biological systems: a brief history and memoir. *Ann Biomed Eng* 2000; **28**: 836-48
2. Harabis V, Kolar R, Mezl M, Jirik R. Comparison and evaluation of indicator dilution models for bolus of ultrasound contrast agents. *Physiol Meas* 2013; **34**: 151-62
3. Ganz W, Donoso R, Marcus HS, Forrester JS, Swan HJ. A new technique for measurement of cardiac output by thermodilution in man. *Am J Cardiol* 1971; **27**: 392-6
4. Hamilton WF, Moore JW, Kinsman JM, Spurling RG. Studies on the circulation. *American Journal of Physiology* 1932; **99**: 534-51
5. Dock DS, Kraus WL, Mc GL, Hyland JW, Haynes FW, Dexter L. The pulmonary blood volume in man. *J Clin Invest* 1961; **40**: 317-28
6. Holt JP. Estimation of the residual volume of the ventricle of the dog's heart by two indicator dilution technics. *Circ Res* 1956; **4**: 187-95
7. Goresky CA, Cronin RF, Wangel BE. Indicator dilution measurements of extravascular water in the lungs. *J Clin Invest* 1969; **48**: 487-501
8. Sakka SG, Ruhl CC, Pfeiffer UJ, et al. Assessment of cardiac preload and extravascular lung water by single transpulmonary thermodilution. *Intensive Care Med* 2000; **26**: 180-7
9. Grodins FS. Basic concepts in the determination of vascular volumes by indicator-dilution methods. *Circ Res* 1962; **10**: 429-46
10. Katz SD. Blood volume assessment in the diagnosis and treatment of chronic heart failure. *Am J Med Sci* 2007; **334**: 47-52
11. Picano E, Gargani L, Gheorghiade M. Why, when, and how to assess pulmonary congestion in heart failure: pathophysiological, clinical, and methodological implications. *Heart Fail Rev* 2010; **15**: 63-72
12. Forrester JS, Ganz W, Diamond G, McHugh T, Chonette DW, Swan HJ. Thermodilution cardiac output determination with a single flow-directed catheter. *Am Heart J* 1972; **83**: 306-11
13. Imai T, Takahashi K, Fukura H, Morishita Y. Measurement of cardiac output by pulse dye densitometry using indocyanine green: a comparison with the thermodilution method. *Anesthesiology* 1997; **87**: 816-22
14. Kurita T, Morita K, Kato S, et al. Lithium dilution cardiac output measurements using a peripheral injection site comparison with central injection technique and thermodilution. *J Clin Monit Comput* 1999; **15**: 279-85
15. Polanczyk CA, Rohde LE, Goldman L, et al. Right heart catheterization and cardiac complications in patients undergoing noncardiac surgery: an observational study. *JAMA* 2001; **286**: 309-14
16. Wei K, Jayaweera AR, Firoozan S, Linka A, Skyba DM, Kaul S. Quantification of myocardial blood flow with ultrasound-induced destruction of microbubbles administered as a constant venous infusion. *Circulation* 1998; **97**: 473-83
17. Feinstein SB. The powerful microbubble: from bench to bedside, from intravascular indicator to therapeutic delivery system, and beyond. *Am J Physiol Heart Circ Physiol* 2004; **287**: H450-7
18. Mischi M, Kalker TA, Korsten EH. Contrast echocardiography for pulmonary blood volume quantification. *IEEE Trans Ultrason Ferroelectr Freq Control* 2004; **51**: 1137-47
19. Wei K. Contrast echocardiography: applications and limitations. *Cardiol Rev* 2012; **20**: 25-32
20. Brittain EL, Doss LN, Saliba L, Irani W, Byrd BF, Monahan K. Feasibility and Diagnostic Potential of Pulmonary Transit Time Measurement by Contrast Echocardiography: A Pilot Study. *Echocardiography* 2015; **32**: 1564-71

21. Mahnken AH, Klotz E, Hennemuth A, et al. Measurement of cardiac output from a test-bolus injection in multislice computed tomography. *Eur Radiol* 2003; **13**: 2498-504
22. Mischi M, van den Bosch HC, den Boer JA, et al. Intra-thoracic blood volume measurement by contrast magnetic resonance imaging. *Magn Reson Med* 2009; **61**: 344-53
23. Oechsner M, Muhlhausler M, Ritter CO, et al. Quantitative contrast-enhanced perfusion measurements of the human lung using the prebolus approach. *J Magn Reson Imaging* 2009; **30**: 104-11
24. Pannek K, Fidler F, Kartausch R, Jakob PM, Hiller KH. Contrast agent derived determination of the total circulating blood volume using magnetic resonance. *MAGMA* 2012; **25**: 215-22
25. Mischi M, Jansen AH, Kalker AA, Korsten HH. Identification of ultrasound contrast agent dilution systems for ejection fraction measurements. *IEEE Trans Ultrason Ferroelectr Freq Control* 2005; **52**: 410-20
26. Herold IH, Soliman Hamad MA, van Assen HC, Bouwman RA, Korsten HH, Mischi M. Pulmonary blood volume measured by contrast enhanced ultrasound: a comparison with transpulmonary thermodilution. *Br J Anaesth* 2015; **115**: 53-60
27. Heye T, Merkle EM, Reiner CS, et al. Reproducibility of dynamic contrast-enhanced MR imaging. Part II. Comparison of intra- and interobserver variability with manual region of interest placement versus semiautomatic lesion segmentation and histogram analysis. *Radiology* 2013; **266**: 812-21
28. Phillips PJ. Contrast pulse sequences (CPS): imaging nonlinear microbubbles. *Ultrasonics symposium 2001* 2001: 1739-45
29. Bosch JG, Mitchell SC, Lelieveldt BP, et al. Automatic segmentation of echocardiographic sequences by active appearance motion models. *IEEE Trans Med Imaging* 2002; **21**: 1374-83
30. van Assen HC, Danilouchkine MG, Frangi AF, et al. SPASM: a 3D-ASM for segmentation of sparse and arbitrarily oriented cardiac MRI data. *Med Image Anal* 2006; **10**: 286-303
31. Chen W, Giger ML, Bick U. A fuzzy c-means (FCM)-based approach for computerized segmentation of breast lesions in dynamic contrast-enhanced MR images. *Acad Radiol* 2006; **13**: 63-72
32. Goutte C, Toft P, Rostrup E, Nielsen F, Hansen LK. On clustering fMRI time series. *Neuroimage* 1999; **9**: 298-310
33. Lucht RE, Knopp MV, Brix G. Classification of signal-time curves from dynamic MR mammography by neural networks. *Magn Reson Imaging* 2001; **19**: 51-7
34. Twellmann T, Meyer-Baese A, Lange O, Foo S, Nattkemper TW. Model-Free Visualization of Suspicious Lesions in Breast MRI Based on Supervised and Unsupervised Learning. *Eng Appl Artif Intell* 2008; **21**: 129-40
35. Beyer K, Goldstein J, Ramakrishnan R, Shaft U. When is nearest neighbor meaningful? *In Database Theory ICDT99* 1999; Springer Berlin Heidelberg: 217-35
36. Cootes TD, Taylor CJ, Cooper DH, Graham J. Active shape models- their training and application. *Computer vision and image understanding* 1995; **61**: 38-59
37. Viswanath S, Bloch BN, Genega E, et al. A comprehensive segmentation, registration, and cancer detection scheme on 3 Tesla in vivo prostate DCE-MRI. *Med Image Comput Comput Assist Interv* 2008; **11**: 662-9
38. Moradi M, Wachinger C, Fedorov A, et al. MRI Confirmed prostate tissue classification with laplacian Eigenmaps of ultrasound RF spectra. *Machine Learning in Medical Imaging* 2012; Springer Berlin Heidelberg: 19-26
39. Wong KP, Feng D, Meikle SR, Fulham MJ. Segmentation of dynamic PET images using cluster analysis. *IEEE Transactions on Nuclear Science* 2002; **49**: 200-7

40. Jamieson AR, Giger ML, Drukker K, Li H, Yuan Y, Bhooshan N. Exploring nonlinear feature space dimension reduction and data representation in breast Cadx with Laplacian eigenmaps and t-SNE. *Med Phys* 2010; **37**: 339-51
41. Mouysset S, Zbib H, Stute S, et al. Segmentation of dynamic PET images with kinetic spectral clustering. *Phys Med Biol* 2013; **58**: 6931-44
42. Frouin F, Duteil S, Lesage D, Carlier PG, Herment A, Leroy-Willig A. An automated image-processing strategy to analyze dynamic arterial spin labeling perfusion studies. Application to human skeletal muscle under stress. *Magn Reson Imaging* 2006; **24**: 941-51
43. Peng SL, Chuang CC, Chuang KS, et al. Spatialtemporal clustering analysis in functional magnetic resonance imaging. *Physics in medicine and biology* 2009; **54**: 7301-14
44. Glaer S, Roschner S, Preim B. Adapted spectral clustering for evaluation and classification of DCE-MRI breast tumors. *Bildverarbeitung fur die Medizin* 2014; Springer Berlin Heidelberg: 198-203
45. Boronyak S, Monahan K, Brittain E, Merryman D. An Inflection Point Method for Determination of Pulmonary Transit Time from Contrast Echocardiography. *IEEE Trans Biomed Eng* 2015; **62**: 1853-61
46. Sheppard CW, Savage LJ. The random walk problem in relation to the physiology of circulatory mixing. *Physical Review* 1951; **83**: 489 - 90
47. Norwich KH, Zelin S. The dispersion of indicator in the cardio-pulmonary system. *Bull Math Biophys* 1970; **32**: 25-43
48. Levenberg K. A method for the solution of certain problems in least squares. *Quarterly of applied mathemethics* 1944; **2**: 164-8
49. Mischi M, Kalker T, Korsten HHM. Videodensitometric methods for cardiac output measurements. *EURASIP Journal on applied signal processing* 2003; **5**: 479 - 89
50. Rognin NG, Frinking P, Costa M, Arditi M. In-vivo perfusion quantification by contrast ultrasound: Validation of the use of linearized video data vs. raw RF data. *Ultrasonics Symposium, 2008 IUS Proceedings, IEEE* 2008: 1690 - 3
51. Lampaskis M, Averkiou M. Investigation of the relationship of nonlinear backscattered ultrasound intensity with microbubble concentration at low MI. *Ultrasound Med Biol* 2010; **36**: 306-12
52. Otsu N. A threshold selection method from gray-level histograms. *Automatica* 1975; **11**: 23-7
53. Gauthier TP, Averkiou MA, Leen EL. Perfusion quantification using dynamic contrast-enhanced ultrasound: the impact of dynamic range and gain on time-intensity curves. *Ultrasonics* 2011; **51**: 102-6
54. Dempster AP, Laird NM, Rubin DB. Maximum likelihood from incomplete data via the EM algorithm. *Journal of the Royal Statistical Society* 1977; Series B (Methodological): 1-38
55. Bland JM, Altman DG. Statistical methods for assessing agreement between two methods of clinical measurement. *Lancet* 1986; **1**: 307-10

Chapter 8

Model-based characterization of the transpulmonary circulation by dynamic contrast-enhanced magnetic resonance imaging in heart failure and healthy volunteers

Salvatore Saporito
Ingeborg HF Herold
Patrick Houthuizen
Harrie CM van Den Bosch
Jacques A Den Boer
Erik HM Korsten
Hans C van Assen
Massimo Mischi

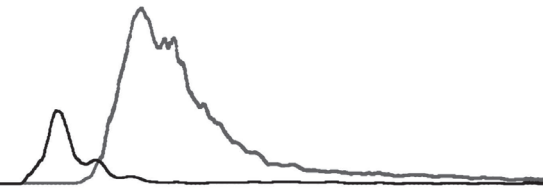

Invest Radiol 2016; Jul1: Epub ahead

ABSTRACT

Objectives

Novel quantitative measures of transpulmonary circulation status may allow the improvement of heart failure (HF) patient management. In this work, we propose a method for the assessment of the transpulmonary circulation using measurements from indicator time intensity curves, derived from dynamic contrast-enhanced magnetic resonance imaging (DCE-MRI) series. The derived indicator dilution parameters in healthy volunteers (HVs) and HF patients were compared, and repeatability was assessed. Furthermore, we compared the parameters derived using the proposed method with standard measures of cardiovascular function, such as left ventricular (LV) volumes and ejection fraction.

Materials and Methods

In total, 19 HVs and 33 HF patients underwent a DCE-MRI scan on a 1.5 T MRI scanner using a T1-weighted spoiled gradient echo sequence. Image loops with 1 heartbeat temporal resolution were acquired in 4-chamber view during ventricular late diastole, after the injection of a 0.1-mmol gadoteriol bolus. In a subset of subjects (8 HFs, 2 HVs), a second injection of a 0.3-mmol gadoteriol bolus was performed with the same imaging settings. The study was approved by the local institutional review board. Indicator dilution curves were derived, averaging the MR signal within regions of interest in the right and left ventricle; parametric deconvolution was performed between the right and LV indicator dilution curves to identify the impulse response of the transpulmonary dilution system. The local density random walk model was used to parametrize the impulse response; pulmonary transit time (PTT) was defined as the mean transit time of the indicator. λ, related to the Péclet number (ratio between convection and diffusion) for the dilution process, was also estimated.

Results

PTT was significantly prolonged in HF patients (8.70 ± 1.87 seconds vs 6.68 ± 1.89 seconds in HV, $p<0.005$) and even stronger when normalized to subject heart rate (normalized PTT, 9.90 ± 2.16 vs 7.11 ± 2.17 in HV, dimensionless, $p<0.001$). λ was significantly smaller in HF patients (8.59 ± 4.24 in HF vs 12.50 ± 17.09 in HV, dimensionless, $p<0.005$), indicating a longer tail for the impulse response. PTT correlated well with established cardiovascular parameters (LV end-diastolic volume index, $r = 0.61$, $p<0.0001$; LV ejection fraction, $r = -0.64$, $p<0.0001$). The measurement of indicator dilution parameters was repeatable (correlation between estimates based on the 2 repetitions for PTT: $r = 0.94$, $p<0.001$, difference between 2 repetitions 0.01 ± 0.60 second, for λ: $r = 0.74$, $p<0.01$, difference 0.69 ± 4.39).

Conclusions

Characterization of the transpulmonary circulation by DCE-MRI is feasible in HF patients and HVs. Significant differences are observed between indicator dilution parameters measured in HVs and HF patients; preliminary results suggest good repeatability for the proposed parameters.

INTRODUCTION

The assessment of thoracic fluid volumes is crucial for the diagnosis, management, and stratification and follow-up of heart failure (HF) patients. Existing methods measure surrogates of the actual thoracic fluid volume; inaccurate assessment may lead to inappropriate therapy with adverse consequences. There is therefore an urgent clinical need for quantitative and highly specific measurement techniques for this purpose.[1,2]

Most hospitalizations of patients with HF are due to acute hemodynamic congestion.[3] Several studies illustrate that the signs and symptoms anticipating acute episodes of cardiac decompensation[1] occur days or weeks after the actual start of hemodynamic congestion.[4–6] Previous research has shown that the congestive disorder consists mainly in fluid redistribution rather than accumulation.[4,7,8] Congestion can be assessed by semi-quantitative scores based on clinical signs such as dyspnea, edema, rales, and jugular venous distension.[9,10] However, these scores offer limited clinical value because of the low reproducibility, specificity, and sensitivity.[11]

Elevated left ventricular (LV) filling pressure leads to back pressure to the pulmonary circulation and consequent elevation in pulmonary capillary wedge pressure (PCWP). Due to the compliance of the pulmonary vasculature, elevated pressure in the pulmonary circulation is reflected in increased pulmonary fluid volume. Moreover, HF patients often present enlarged extravascular lung water (EVLW) volumes with pulmonary edema[12] caused by increased capillary pressure. However, direct assessment of PCWP would require right heart catheterization[13]; PCWP is therefore unsuitable for screening.[14] Moreover, pressures in the circulation are influenced by a set of regulatory mechanisms operating on different time scales[15]; therefore, abnormal volumes may be present regardless of normal PCWP values.[2]

It is well known that low cardiac output (CO) and large blood lung volume result in prolongation of circulation times,[16–18] which can be assessed by indicator dilution techniques. In these techniques, a detectable indicator is injected into the circulation; by sampling the indicator concentration during its passage, indicator dilution curves (IDC) can be derived. Kinetic analysis of the derived IDCs allows absolute volume measurement. The absolute volume between 2 detection sites can be obtained by multiplying the difference in mean transit time (MTT) of the indicator with the flow rate of the dilution system (which in the case of pulmonary volume equals the CO)[19]; depending on the access of the indicator to the extravascular extracellular space, the obtained estimates will be purely blood volumes or volumes also including the interstitial fluids, when intravascular or extravascular indicators are used, respectively.

Dynamic contrast-enhanced magnetic resonance imaging (DCE-MRI) allows minimally invasive measurement of IDCs, with the advantage of simultaneous sampling in the different heart chambers. DCE-MRI has been validated in-vitro for volume measurement.[20,21]

Small boluses of contrast agent are used[22] to ensure a linear relationship between contrast concentration and image intensity, a requirement from indicator dilution theory.

In this work, we consider the local density random walk (LDRW) kinetic model for describing the transpulmonary indicator dilution; the model can be derived by solving the drift-diffusion equation for a soluble indicator in a mono-compartmental tube.[23] We propose quantifying the influence of multi-compartmental kinetics on this purely intravascular model. If the indicator is diluted in a 2-compartment system, such as pulmonary blood volume and EVLW, then the skewness or asymmetry of the IDCs may be a measure of the relative contribution to the indicator transport of convection and diffusion, which is influenced by the exchange between the 2 compartments.[24]

We investigated the characteristics of transpulmonary circulation assessed by DCE-MRI. The dilution process in transpulmonary circulation is modeled as a linear system characterized by its impulse response, which can be derived by parametric deconvolution. We compared the indicator dilution parameters between healthy volunteers (HVs) and HF patients. The derived bolus kinetic parameters were compared with standard measures of cardiac function.

METHODS

Population

We included HF patients who underwent a MRI examination as a part of routine clinical assessment at Catharina Hospital Eindhoven (Eindhoven, the Netherlands). Patients showed symptoms of HF and decreased LV ejection fraction (LVEF) assessed by echocardiography; end-stage kidney or hepatic disease constituted an exclusion criterion for this study. Healthy volunteers without a known history of cardiac pathologies or general contraindications for MRI served as controls.

The results in this article are based on a subanalysis of the data collected within 2 different clinical studies approved by the institutional review board of the Catharina Hospital Eindhoven. One of the studies recruited HF patients referred for cardiac resynchronization therapy device implantation, the other recruited HVs. Informed consent was obtained from all the HF patients and from all HVs.

Magnetic Resonance Imaging

Magnetic resonance imaging scans were performed at Catharina Hospital Eindhoven on a clinical whole-body Philips 1.5 T scanner (Intera or Ingenia) in combination with a 5-element phased array cardiac coil (Philips Healthcare, Best, the Netherlands).

The protocol included the acquisition of retrospectively vectorcardiographic-triggered cine steady-state free precession loops of multiple short-axis, 2-chamber, and 4-chamber

views. The short-axis cine loops had a voxel size of 1.35 x 1.35 x 10 mm^3; the temporal resolution was in the order of 25 ms. Typical sequence parameters were TR/TE/flip angle of 3.4 ms/1.7 ms/70 degrees with a readout bandwidth of 723 Hz/pixel and SENSE parallel imaging with acceleration factor 2; typically, 35 to 40 phases were acquired during the cardiac cycle in short-axis, during breath-holds of the approximate duration of 12 seconds; typical acquired matrix size was in the order of 208 x 202 for the short-axis images.

Semi-automated segmentation of the left ventricle (LV) endocardium in cine MRI data was performed using CAAS MRV 3.4 (Pie Medical Imaging BV, Maastricht, the Netherlands). Left ventricular end-diastolic volumes (LVEDVs), LV end-systolic volumes (LVESVs), and ejection fraction were derived from the sum of the volumes in the short-axis images, with a correction for longitudinal motion applied based on long-axis images. LEDV and LVESV were indexed (LVEDVI, LVESVI) to body surface area estimated using the Du Bois formula.[25]

Cardiac output was calculated by integrating the flow across the aortic arch during the cardiac cycle from phase-contrast MRI (PC-MRI) data using CAAS FLOW 1.2 (Pie Medical Imaging). For the acquisition of PC-MRI images, a retrospective gated fast field echo sequence with a 20-degree flip angle and a typical TR/TE of 4.3 ms/2.7 ms was used; velocity encoding was 150 cm/s for a typical acquisition matrix size of 144 x 142; acquisition of 20 cardiac phases was performed during a breath-hold of approximate duration of 12 seconds using SENSE acceleration (factor 2).

DCE-MRI

Each subject underwent a cardiac triggered, maximum end-expiratory breath-hold scanning procedure; acquisition was manually started after patients were coached for the breathing and breath-hold maneuvers by the MR operator. The acquisition was delayed with respect to the R-peak on the patient's vectorcardiographic for acquiring images in late diastolic phase, where the influence of cardiac motion was expected to be minimal. Four-chamber view images with a slice thickness of 10 mm were acquired. A turbo field echo sequence was used with a flip angle of 7 degrees, TR = 2.9 ms, TE = 1.7 ms, and a readout bandwidth of 234 Hz/pixel. To obtain T1 contrast, a saturation prepulse was applied 200 ms before the acquisition of the central line in k-space. SENSE parallel acquisition (factor 2) and half-scan strategies were used to reduce the total imaging time of 27 profiles to 175 ms, with linear profile ordering. The matrix size was 104 x 106 after zero-filling and SENSE reconstruction, resulting in reconstructed image size of 224 x 224 pixels with pixel size of 1.65 x 1.65 mm^2. Bolus injections of 0.1 mmol gadoteriol (Dotarem; Guerbet, Aulnay-sous-Bois, France) diluted in 5 ml of saline solution were performed using an automated injector at a rate of 5 ml/s (Spectris MR; Medrad, Indianola, PA) in each subject left upper arm, followed by saline flush of 15

ml. The adopted dose was between 1% and 3% of the recommended dose for perfusion studies (0.1 mmol/kg). Under these conditions, a linear relationship between the signal enhancement and contrast agent concentration was observed.[20] A minimum number of 45 images (i.e. 45 heartbeats) were acquired; the acquisition of 45 heartbeats in breath-hold was challenging in HF patients; however, all the subjects could hold their breath for at least 20 heartbeats, sufficient to observe the first passage of the contrast agent bolus in the LV and RV.

In a subset of 8 HF patients and 2 HVs, a second bolus injection was performed around 10 minutes later using 0.3 mmol of Dotarem diluted in 5 ml saline, followed by the same 15-ml saline flush.

In the post-processing phase, manual region of interest (ROI) tracing in the right ventricle (RV) and LV was performed on the acquired image to extract IDCs using custom software written in MATLAB 2014a (The MathWorks, Natick, MA).

Dilution System Identification

The transpulmonary circulation was characterized using an impulse response approach.[26]

In particular, the dilution model used was the LDRW model,[16] which is defined as:

$$h(t) = a \sqrt{\frac{\lambda\mu}{2\pi t}}\, e^{-\frac{\lambda}{2}\left(\frac{t}{\mu}+\frac{\mu}{t}\right)}$$

where h(t) is the identified impulse response, μ is the MTT, λ is a measure of skewness proportional to the Péclet number,[24] with higher values indicating more symmetric curve, and a is a normalizing factor.

The peak of h(t) is reached for t = Tp, with

$$T_p = \frac{\mu}{2\lambda}\left(\sqrt{1+4\lambda^2}-1\right)$$

It can be shown that Tp = μ if $\lambda \to \infty$, which corresponds to a negligible contribution of diffusion with respect to convection in the dilution process. The downslope (DST) of the indicator dilution model is given by $\lim_{t\to\infty} \log\frac{dh}{dt}$ and is equal to

$$DST = -\frac{\mu}{2\lambda}$$

for the LDRW model. Dilution system parameters were derived by parametric unconstrained least squares iterative deconvolution using the Nelder-Mead Simplex Method.[27] Quality of the estimated impulse response was quantified by the determination coefficient R^2, given by the squared correlation coefficient between the data and the model fit. Pulmonary transit time (PTT) was defined as the MTT of the identified dilution system. Normalized PTT (nPTT) was defined as the product of PTT and the corresponding heart rate. Physiologically, the nPTT corresponds to the mean number of stroke volumes neces-

sary for the indicator to pass through the pulmonary circulation. We also calculated the left to right heart time-to-peak (ΔTTP) given by the difference in time-to-peak of the RV and LV IDCs.

Statistical Methods

The probability distribution of each presented variable was tested for normality distribution using a 1-sample Shapiro-Wilk test. Normally distributed features are presented by their mean and standard deviation; non-normally distributed variables are described by their median and interquartile range. If the hypothesis of normal distribution was accepted, comparison between the measures of patients and HV was performed using an unpaired Student's t-test assuming unequal class variance. If the normality hypothesis of the distribution was rejected, a Mann-Whitney U test was used to compare the measure between HF patients and healthy subjects. For both statistical tests, a p value smaller than 0.05 was considered significant. Univariate correlation was described by means of Pearson correlation coefficient. Intraclass correlation coefficient (ICC) was used to quantify the repeatability of the estimated transpulmonary circulation parameters between the 2 injections.

RESULTS

Clinical characteristics of the populations are shown in Table 1. A total of 33 HF patients and 19 HVs were considered in this study. Cine MRI and PC-MRI loops were not available for 5 HVs.

One subject was excluded because of poor image quality, 1 patient was excluded due to poor SNR resulting in poor impulse response fit, and one was excluded due to repeated electrocardiographic triggering failure during contrast agent first passage. In the remaining (30 HFs, 19 HVs), the average coefficient of determination R^2 was 0.95 ± 0.05 for HF patients and 0.93 ± 0.10 for HVs; for the repeated dose, it was 0.99 ± 0.01. An example of a DCE-MRI image with traced ROIs is shown in Figure 1, together with the corresponding IDCs.

Comparison between HF and HV

Example DCE-MRI LV and RV IDCs from an HV and from an HF patient are shown in Figure 2, together with an example of the identified transpulmonary dilution system.

PTT was longer (p<0.005) in HF patients (8.70 ± 1.87 seconds) than in HVs (6.68 ± 1.89 seconds); nPTT was larger (p<0.001) in HF patients (9.90 ± 2.16, dimensionless) than in controls (7.11 ± 2.17, dimensionless). Distribution of the PTTs and nPTTs for both groups are shown in Figure 3. λ was significantly smaller (p<0.005) for HF patients

Table 1. Clinical characteristics of the populations

	Healthy volunteers (n=19)	Heart failure patients (n=33)
Age	28 (18)	67(18)
Male/Female	17/2	19/14
BMI	23.05 (6.70)	27.13 (6.70)
BSA	1.87 ± 0.23	1.95 ± 0.23
NYHA classes (I / II / III / IV)	-	4 / 12 / 17 / 0
LVEDVI (ml/m^2)	68.04 ± 12.17	135.48 ± 38.46
LVESVI (ml/m^2)	28.04 ± 8.03	96.85 ± 47.64
LVEF (%)	59.90 ± 7.06	31.09 ± 11.37
HR (bpm)	68.95 ± 13.72	64.4 ± 13.3
CO (L/min)	5.4 (1.2)	4.0 (0.8)

Data are shown as mean ± standard deviation or median (inter-quartile range). HV, healthy volunteer; HF, heart failure; BMI, body mass index; BSA, body surface area; NYHA, New York Heart Association classification; LVEDVI, left ventricular end-diastolic volume index; LVESVI, left ventricular end-systolic volume index; HR, heart rate; LVEF, left ventricular ejection fraction; CO, cardiac output.

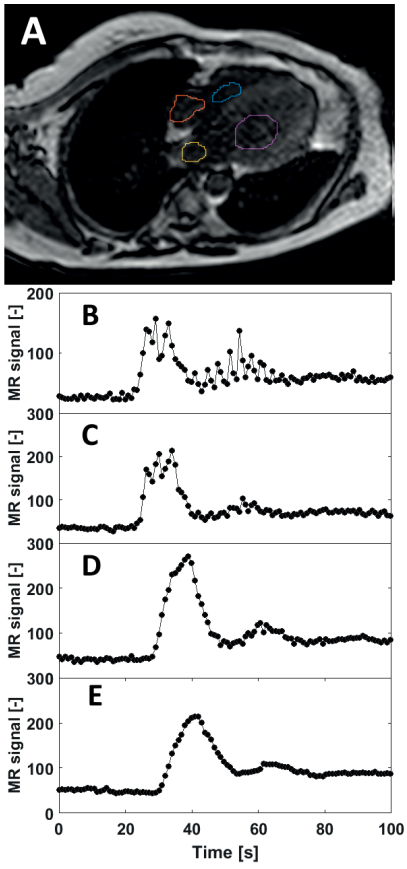

Figure 1. Example frame from DCE-MRI recording and corresponding indicator dilution curves (IDCs). From top to bottom: A, example frame from DCE-MRI 4-chamber view before contrast agent passage with overlaid region of interest (ROI) in the 4 heart chambers; B–E, IDCs obtained by averaging the MR signal intensity in the ROIs for right atrium (B), right ventricle (C), left atrium (D), and left ventricle (E).

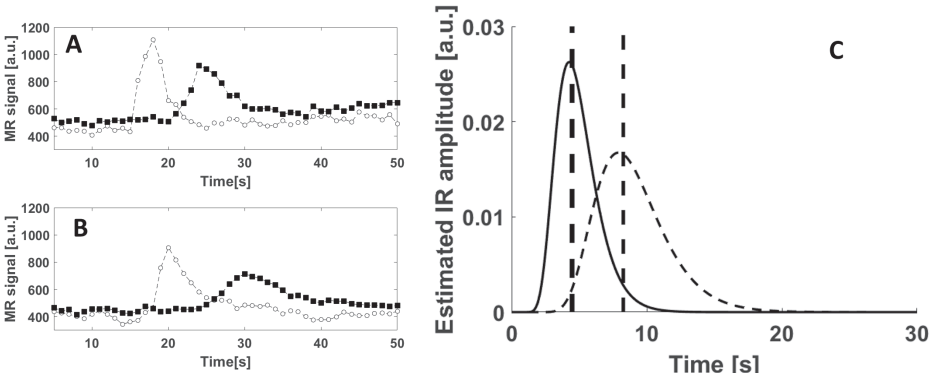

Figure 2. Example of indicator dilution curves (IDCs) and transpulmonary impulse response. From top to bottom: comparison of right ventricular (white circles) and left ventricle (black squares) IDCs from a healthy volunteer (HV) (A) and from a heart failure (HF) patient (B); corresponding transpulmonary impulse responses (C) obtained by parametric deconvolution for a HV (continuous line) and a HF patient (dashed line), respectively.

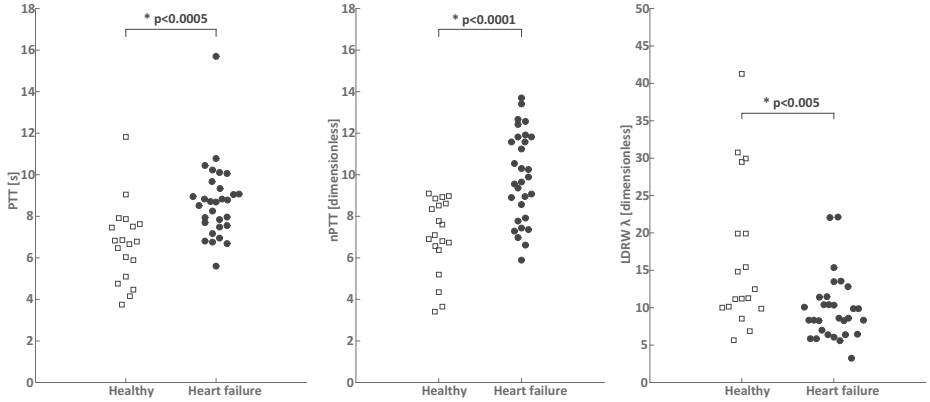

Figure 3. Distribution of indicator dilution parameters in the 2 groups. From left to right: distribution of pulmonary transit time (PTT), normalized PTT (nPTT), and λ from local density random walk (LDRW) model. *Mann-Whitney U test.

(8.59 ± 4.24, dimensionless) than for HVs (12.50 ± 17.09, dimensionless), reflecting a more asymmetrical transpulmonary impulse response in patients. The distribution of λ is also shown in Figure 3.

Repeatability of the PTT measurement was good (r = 0.94, p<0.001), with an average difference between the 2 repeated measurements of 0.01 ± 0.60 second with an ICC of 0.97 (0.89–0.99); the PTT differences between the 2 injections were not significant (p>0.2). Normalized PTT repeatability was good as well (r = 0.71, p<0.05, difference –0.10 ± 1.57). λ obtained from the 2 injections within the 1 subject were also correlating well (r = 0.74; p<0.01; difference 0.69 ± 4.39; ICC = 0.76; CI, 0.10–0.94). A comparison between the 2 repeated injections is shown in Figure 4.

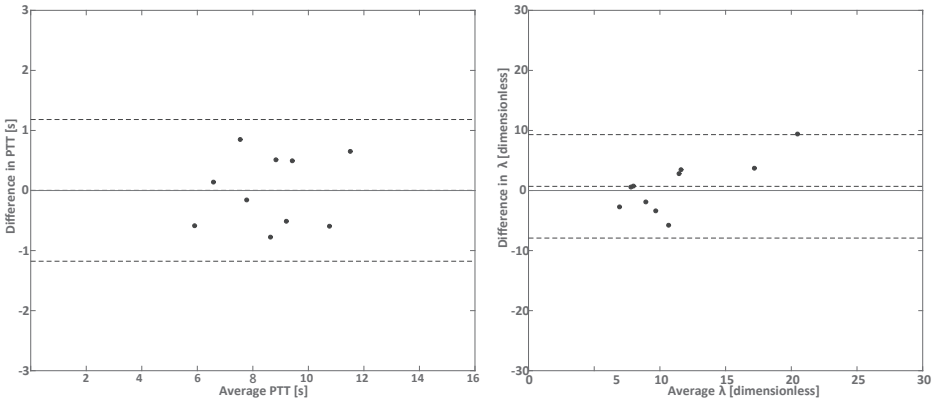

Figure 4. Test-retest reproducibility for transpulmonary dilution parameters. From left to right: (A) pulmonary transit time (PTT) obtained from 2 bolus injection 0.1 mmol (first) and 0.3 mmol (second) of gadoteriol; (B) same for λ from local density random walk model.

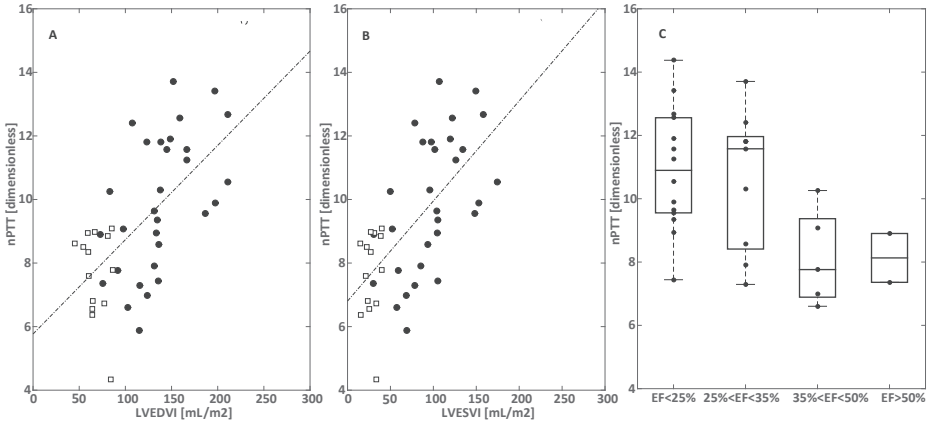

Figure 5. Comparison of normalized pulmonary transit time (nPTT) with standard measures from cardiovascular magnetic resonance. From left to right: (A), nPTT plotted against left ventricular end-diastolic volume index (LVEDVI) for healthy volunteers (white squares, n = 14) heart failure patients (black circles, n = 30); (B) nPTT against left ventricular end-systolic volume index (LVESVI); (C) distribution of nPTT with respect to left ventricular ejection fraction (LVEF).

Comparison with standard cardiac function measures

Correlation between PTT, nPTT, and λ with standard measures of cardiovascular function (LV indexed volumes, LVEF, and CO) are reported in Table 2. Normalized PTT correlated positively (r = 0.61, p<0.0001) with LVEDVI and negatively with LVEF (r = –0.64, p < 0.0001). The distribution of nPTT with respect to LVEDVI, to LVESVI, and to LVEF is shown in Figure 5.

Table 2. Correlation with standard cardiovascular measures

	PTT		nPTT		λ	
	Pearson *r*	*p*-value	Pearson *r*	*p*-value	Pearson *r*	*p*-value
LVEDVI	0.48	<0.001	0.61	<0.0001	0.30	0.06
LVESVI	0.51	<0.005	0.65	<0.0001	-0.24	0.11
LVEF	-0.52	<0.005	-0.64	<0.0001	-0.27	0.07
SV	-0.28	<0.05	-0.58	<0.001	0.31	<0.05
CO	-0.53	<0.0001	-0.34	<0.01	0.27	0.06

Comparison of indicator dilution transpulmonary measures to standard cardiovascular measures derived from cine MRI and phase-contrast MRI data. PTT, pulmonary transit time; nPTT, normalized pulmonary transit time; LVEDVI, left ventricular end-diastolic volume index; LVESVI, left ventricular end-systolic volume index; LVEF, left ventricular ejection fraction; SV, stroke volume; CO, cardiac output.

Comparison with time-to-peak measures

Time-to-peak was 6.43 ± 2.42 seconds for HV, whereas it was 8.90 ± 3.37 seconds in HF ($p<0.001$). PTT and ΔTTP were correlated both in HF ($r = 0.51$, $p<0.005$) and in HV ($r = 0.91$, $p<0.001$). Differences between ΔTTP and PTT were not significant in HV (–0.01 ± 1.23 seconds, $p=0.62$), but they were statistically significant in HF (–0.35 ± 2.27 seconds, $p=0.04$).

DISCUSSION

In the present study, we proposed a method for the characterization of the transpulmonary circulation by DCE-MRI. Indicator dilution curves were derived after an intravenous bolus injection of MRI contrast agent; subsequent model-based identification of the impulse response allowed the estimation of contrast agent kinetic parameters.

Feasibility and contrast agent usage

Imaging was feasible in HF patients and HVs, only 2 subjects were excluded for poor image quality and one for a triggering failure during the first passage of the contrast agent. The adopted contrast agent dose was relatively small compared with those considered potentially harmful in patients with impaired renal function[28]; the adopted 0.1 mmol dose is between 1% and 3% of the typically recommended dose for perfusion studies (0.1 mmol/kg).

Comparison of HF patients versus healthy subjects, reproducibility, and repeatability

When comparing healthy subjects and HF patients, PTT was significantly prolonged in the HF group; nPTT was also prolonged. We also observed a significantly smaller

λ in patients, indicating a more skewed transpulmonary dilution impulse response. The considerable overlap shown between PTT in HF and HV is reduced by normalizing the PTT by subject heart rate; this was necessary to compare healthy subjects with different aerobic capacity, which may result in large PTT values also in healthy subjects.[29,30] The remaining overlap between HV and HF can be ascribed to the relatively broad spectrum of HF patients included in the study; a number of patients had relatively good cardiovascular function, quantified here by ejection fraction; the shortest nPTTs were measured in these patients. A clear cutoff value for detecting HF could not be identified based on the nPTT and λ presented in this study; however, the proposed method can be used to derive adjunctive parameters of cardiopulmonary function, which can be estimated easily and practically during a standard magnetic resonance imaging examination on a commercial scanner.

The reproducibility of PTT with respect to inter-observer and intra-observer variability introduced by ROI drawing procedure has been shown to be good in previous studies.[31,32] The presented preliminary results also showed a good test-retest repeatability for PTT in a subset of the available patients. To the best of our knowledge, no previous studies assessed the reproducibility of PTT by DCE-MRI. We also observed a significant correlation between λs obtained from 2 injections; however, the relatively large variations between the 2 estimates suggest that further studies are necessary to clarify the effect of contrast agent doses on this parameter.

Comparison with difference in time-to-peak approach

When comparing the PTT with the ΔTTP difference, we found no statistically significant differences in healthy subjects; the differences were significant in HF patients, where the change in shape of the IDCs resulted in a larger difference between ΔTTP derived by frame counting and the first statistical moment of the identified indicator dilution impulse response. This is in line with the analytical expression associating ΔTTP and PTT derived from the LDRW model expression, and with findings from Giuntini and coworkers[33] relating the difference between ΔTTP and PTT to the downslope of the LV enhancement curves. An analytical relationship between TTP and MTT of the LDRW has been provided in the methods section; the relationship confirms that the differences between ΔTTP and PTT increase for small values of λ (which were found in patients in this study).

Quantitative comparison with PTT values reported in the literature

The presented PTT values in controls are in line with the differences in time-to-peak found between RV and LV reported by Skrok and coworkers,[34] and with those reported by Lakoma and coworkers[35] and Shors and coworkers[36] (6.8 ± 1.4 seconds, 7.2 ± 1.2 seconds, respectively), even though they considered time differences between the pulmonary artery and ascending aorta. Our PTT estimates in controls are slightly

larger than those reported by Swift and coworkers[37] and Cao and workers[38] (4.5 ± 1.7 seconds and 5.7 ± 0.9 seconds, respectively); however, the latter values were considered with respect to the left atrium; therefore, they did not take into account the passage to the LV, which may account for the difference. Further larger studies would be necessary to establish consensus values for transit times in the different blood pools. Comparison with other studies is not straightforward as many authors referred the transit times to the absolute injection time,[16,39] whereas we focused on relative transit time between RV and LV.

Comparison of the method with the literature

The adopted MR sequence and small dose of contrast agent ensures the linearity of the contrast agent/MR signal relationship, a prerequisite for indicator dilution parameter estimate.[20]

Approaches based only on contrast agent arrival time do not take into account statistical aspects of the contrast agent transport kinetic: they neglect the multipath trajectory of the indicator transport[40] introducing a bias toward the shortest path; by relying on a threshold for defining the indicator arrival, and on only 1 point on the time-enhancement curve, they are more susceptible to noise in the image acquisition. The proposed model-based approach is not limited by the imaging sampling rate (1 sample per heartbeat in DCE-MRI), which bounds the accuracy of the PTT estimation when measured as frame difference in peak enhancement between the different heart chambers, as in many previous studies.[34,36,41,42] To refine the estimation using frame counting techniques, interpolation methods would be necessary; however, those methods would require making assumptions, which would be impractical to verify in in-vivo conditions. Studies in the literature have focused on the analysis of the left atrial enhancement curve alone,[39] neglecting the dilution of the indicator occurring in the circulatory tree between the injection site and the RV. Our approach makes use of a physical indicator dispersion model and takes into account the dilution of the indicator between injection and sampling site, making it more robust with respect to variations in the injection procedure and to recirculation.

A further advantage in our proposed approach, the estimation of the transpulmonary dilution skewness, here quantified by λ, may provide additional insight about pulmonary capillary membrane status.[24] At present, no minimally invasive techniques are available for the quantitative assessment of extravascular fluids in the transpulmonary circulation for HF.

Quantifications based on the downslope of the LV IDCs are used in clinical practice at present time. In particular, as shown by Sakka and coworkers,[43] the downslope of the LV thermodilution curve (an extravascular indicator such as gadolinium) can be used to provide absolute EVLW volume estimates, when population-based calibration values against a criterion standard are provided. The approach proposed by Sakka and

coworkers is currently applied in commercial devices. Requiring right heart catheterization, this method introduces potential risks for the patient and is therefore unsuitable for diagnostic screening. The parameter λ presented in this study aims at providing a measure of diffusion (reflecting an altered capillary membrane status or increased EVLW) occurring in the pulmonary circulation, which is more robust to variations in the injection procedure and in the dilution occurring between the injection site and the right heart, neglected by the analysis of the downslope time of the LV enhancement curve. Single indicator thermodilution is the current criterion standard for EVLW; the parameter λ of the LDRW model considered in this work is analytically related to the downslope time used in that approach.

Multi-compartment pharmacokinetic modeling has been used for the interpretation of DCE-MRI measurements[44,45]; however, assumptions are often made regarding the time scale of the changes in indicator concentration in the different physiological compartments, for example, the use of the adiabatic approximation.[46] Such assumptions greatly simplify the models for contrast agent kinetics and permit deriving closed-form solutions in the time domain[46,47]; however, limited data are available regarding the dynamics of DCE-MRI contrast agent extravasation from the pulmonary circulation. In this work, we quantified the relative contribution of diffusion and convection in the transpulmonary dilution process, assessed by the parameter λ in the LDRW model[23,24]; increased diffusion between an intravascular and an extravascular compartment, such as pulmonary blood volume and EVLW, would reflect in an increased skewness for the dilution system, due to indicator exchange between the compartments.[24]

Dynamic contrast-enhanced ultrasound (DCE-US) has been proposed as a minimally invasive alternative for pulmonary blood volume estimation[48,49]; however, ultrasound-based estimates have limited accuracy in CO estimation.[50] Furthermore, the relationship between indicator concentration and signal enhancement depends on acquisition settings[51] and shows high inter-subject variability in in-vivo conditions. Nevertheless, repeatability of PTT/nPTT measurements from DCE-US was shown to be good.[32]

PTT as congestion measure

PTT, often defined as the difference in MTT between the right and left heart, is a good measure of preload[52] and LV filling pressure.[39] PTT was measured in congestive HF patients and correlated with alternative indirect measures.[38] However, limited data were available in the literature regarding bolus kinetic parameters in healthy subjects. PTT correlated significantly with LVEDVI and LVESVI in this study. The relationship shown between left atrial arrival time and filling pressures[39] suggests that a noninvasive filling pressure estimation may be possible based on circulation times only, without the need for catheterization, therefore improving patient safety. An additional advantage of PTT is that

it is directly related to volume status,[19] which is subject to slower regulatory mechanisms with respect to blood pressure.

Future work

Further studies are necessary to quantify the sensitivity of indicator dilution parameters to surgical interventions or acute fluid displacements. Moreover, DCE-MRI based measures could be compared with noninvasive measures such as thoracic impedance, which can only measure relative changes in thoracic fluid status,[2] for a possible combined use as an absolute calibration system. The comparison between bolus kinetic parameters obtained by extravascular and purely intravascular contrast agents may allow absolute quantitative EVLW estimation.

The prognostic value of the proposed method should be assessed in conditions resulting in altered cardiopulmonary hemodynamic conditions, such as pulmonary artery hypertension, where transit times have been shown to be predictors of mortality.[37] The clinical value of the technique should also be tested to assess changes in pulmonary blood volumes after pulmonary endarterectomy[42] or valve surgery.[53,54]

Limitations

The main limitation of the study was the lack of a criterion standard measurement technique for thoracic fluid volumes against which the estimated DCE-MRI indicator dilution parameters could be compared. The considered sample was relatively small, and the groups were not age and sex matched; we did not assess the influence of RV performance on transpulmonary parameters. The main limitations of this MRI-based technique are cost and availability; however, with a focus on intravascular kinetics, DCE-US may allow PTT assessment at the bedside.[44] Furthermore, MRI cannot be used for patients with certain implanted cardiac devices, and in the case of atrial fibrillation, the quality of images may be degraded due to the irregularity of the heartbeat. Patients with kidney failure were excluded from this study as MRI contrast media can be particularly harmful for patients with severe renal disease.

CONCLUSIONS

Characterization of the pulmonary circulation by DCE-MRI measurements is feasible in HF patients and healthy subjects. We observed significant differences in indicator dilution parameters between HVs and HF patients. Pulmonary transit time measurement is shown to be practical and repeatable, and it may constitute a valuable alternative for the assessment of pulmonary congestion. Further research is necessary to fully assess the clinical value of this measurement technique.

REFERENCES

1. Picano E, Gargani L, Gheorghiade M. Why, when, and how to assess pulmonary congestion in heart failure: pathophysiological, clinical, and methodological implications. *Heart Fail Rev*. 2010; **15**: 63–72
2. Katz SD. Blood volume assessment in the diagnosis and treatment of chronic heart failure. *Am J Med Sci*. 2007; **334**: 47–52
3. Gheorghiade M, Vaduganathan M, Fonarow GC, et al. Rehospitalization for heart failure: problems and perspectives. *J Am Coll Cardiol*. 2013; **61**: 391–403
4. Cotter G, Metra M, Milo-Cotter O, et al. Fluid overload in acute heart failure re-distribution and other mechanisms beyond fluid accumulation. *Eur J Heart Fail*. 2008; **10**: 165–169
5. Adamson PB, Magalski A, Braunschweig F, et al. Ongoing right ventricular hemodynamics in heart failure: clinical value of measurements derived from an implantable monitoring system. *J Am Coll Cardiol*. 2003; **41**: 565–571
6. Chaudhry SI, Wang Y, Concato J, et al. Patterns of weight change preceding hospitalization for heart failure. *Circulation*. 2007; **116**: 1549–1554
7. Dunlay SM, Gheorghiade M, Reid KJ, et al. Critical elements of clinical follow-up after hospital discharge for heart failure: insights from the EVEREST trial. *Eur J Heart Fail*. 2010; **12**: 367–374
8. Blair JE, Khan S, Konstam MA, et al. Weight changes after hospitalization for worsening heart failure and subsequent re-hospitalization and mortality in the EVEREST trial. *Eur Heart J*. 2009; **30**: 1666–1673
9. Gheorghiade M, Follath F, Ponikowski P, et al. Assessing and grading congestion in acute heart failure: a scientific statement from the acute heart failure committee of the heart failure association of the European society of cardiology and endorsed by the European society of intensive care medicine. *Eur J Heart Fail*. 2010; **12**: 423–433
10. Ambrosy AP, Pang PS, Khan S, et al. Clinical course and predictive value of congestion during hospitalization in patients admitted for worsening signs and symptoms of heart failure with reduced ejection fraction: findings from the EVEREST trial. *Eur Heart J*. 2013; **34**: 835–843
11. Stevenson LW, Perloff JK. The limited reliability of physical signs for estimating hemodynamics in chronic heart failure. *JAMA*. 1989; **261**: 884–888
12. Lange N, Schuster D. The measurement of lung water. *Crit Care*. 1999; **3**: R19–R24
13. Drazner MH, Hellkamp AS, Leier CV, et al. Value of clinician assessment of hemodynamics in advanced heart failure: the ESCAPE trial. *Circ Heart Fail*. 2008; **1**: 170–177
14. Polanczyk CA, Rohde LE, Goldman L, et al. Right heart catheterization and cardiac complications in patients undergoing noncardiac surgery: an observational study. *JAMA*. 2001; **286**: 309–314
15. Lanfranchi PA, Somers VK. Arterial baroreflex function and cardiovascular variability: interactions and implications. *Am J Physiol Regul Integr Comp Physiol*. 2002; **283**: R815–R826
16. Francois CJ, Shors SM, Bonow RO, et al. Analysis of cardiopulmonary transit times at contrast material-enhanced MR imaging in patients with heart disease. *Radiology*. 2003; **227**: 447–452
17. Selzer A, Dunlap RW, Wray HW, et al. A critical appraisal of the circulation time test. *Arch Intern Med*. 1968; **122**: 491–495
18. Jones RH, Sabiston DC, Bates BB, et al. Quantitative radionuclide angiocardiography for determination of chamber to chamber cardiac transit times. *Am J Cardiol*. 1972; **30**: 855–864
19. Meier P, Zierler KL. On the theory of the indicator-dilution method for measurement of blood flow and volume. *J Appl Physiol*. 1954; **6**: 731–744

20. Mischi M, van den Bosch HCM, den Boer JA, et al. Intra-thoracic blood volume measurement by contrast magnetic resonance imaging. *Magn Reson Med*. 2009; **61**: 344–353
21. Ugander M, Kanski M, Engblom H, et al. Pulmonary blood volume variation decreases after myocardial infarction in pigs: a quantitative and noninvasive MR imaging measure of heart failure. *Radiology*. 2010; **256**: 415–423
22. Nacif MS, Arai AA, Lima JA, et al. Gadolinium-enhanced cardiovascular magnetic resonance: administered dose in relationship to united states food and drug administration (FDA) guidelines. *J Cardiovasc Magn Reson*. 2012; **14**: 18
23. Bogaard JM, Jansen JR, von Reth EA, et al. Random walk type models for indicator-dilution studies: comparison of a local density random walk and a first passage times distribution. *Cardiovasc Res*. 1986; **20**: 789–796
24. Bogaard JM, Smith SJ, Versprille A, et al. Physiological interpretation of the skewness of indicator-dilution curves; theoretical considerations and a practical application. *Basic Res Cardiol*. 1984; **79**: 479–493
25. Du Bois D, Du Bois EF. A formula to estimate the approximate surface area if height and weight be known. 1916. *Nutrition*. 1989; **5**: 303–311
26. Mischi M, Jansen AH, Korsten HH. Identification of cardiovascular dilution systems by contrast ultrasound. *Ultrasound Med Biol*. 2007; **33**: 439–451
27. Nelder JA, Mead R. A simplex method for function minimization. *Comput J*. 1964; **7**: 308–313
28. Thomsen HS. ESUR guideline: gadolinium-based contrast media and nephrogenic systemic fibrosis. *Eur Radiol*. 2007; **17**: 2692–2696
29. Eriksson A, Hansson K, Häggström J, et al. Pulmonary blood volume in mitral regurgitation in Cavalier King Charles Spaniels. *J Vet Intern Med*. 2010; **24**:1393–1399
30. Hopkins SR, Belzberg AS, Wiggs BR, et al. Pulmonary transit time and diffusion limitation during heavy exercise in athletes. *Respir Physiol*. 1996; **103**: 67–73
31. Saporito S, Herold IH, Houthuizen P, et al. Automatic indicator dilution curve extraction in dynamic-contrast enhanced imaging using spectral clustering. *Phys Med Biol*. 2015; **60**: 5225–5240
32. Herold IH, Saporito S, Bouwman RA, et al. Reliability, repeatability, and reproducibility of pulmonary transit time assessment by contrast enhanced echocardiography. *Cardiovasc Ultrasound*. 2016; **14**: 1–9
33. Giuntini C, Lewis ML, Luis AS, et al. A study of the pulmonary blood volume in man by quantitative radiocardiography. *J Clin Invest*. 1963; **42**: 1589–1605
34. Skrok J, Shehata ML, Mathai S, et al. Pulmonary arterial hypertension: MR imaging-derived first-pass bolus kinetic parameters are biomarkers for pulmonary hemodynamics, cardiac function, and ventricular remodeling. *Radiology*. 2012; **63**: 678–687
35. Lakoma A, Tuite D, Sheehan J, et al. Measurement of pulmonary circulation parameters using time-resolved MR angiography in patients after Ross procedure. *AJR Am J Roentgenol*. 2010; **194**: 912–919
36. Shors SM, Cotts WG, Pavlovic-Surjancev B, et al. Heart failure: evaluation of cardiopulmonary transit times with time-resolved MR angiography. *Radiology*. 2003; **229**: 743–748
37. Swift AJ, Telfer A, Rajaram S, et al. Dynamic contrast-enhanced magnetic resonance imaging in patients with pulmonary arterial hypertension. *Pulm Circ*. 2014; **4**: 61–70
38. Cao JJ, Wang Y, McLaughlin J, et al. Prolonged pulmonary transit time by cardiac MRI is a marker of hemodynamic derangement in patients with congestive heart failure. *J Cardiovasc Magn Reson*. 2010; **12**(Suppl 1): 96

39. Cao JJ, Wang Y, McLaughlin J, et al. Left ventricular filling pressure assessment using left atrial transit time by cardiac magnetic resonance imaging. *Circ Cardiovasc Imaging*. 2011; **4**: 130–138
40. Mischi M, Den Boer JA, Korsten HH. On the physical and stochastic representation of an indicator dilution curve as a gamma variate. *Physiol Meas*. 2008; **29**: 281–294
41. Jörgensen K, Müller MF, Nel J, et al. Reduced intrathoracic blood volume and left and right ventricular dimensions in patients with severe emphysema: an MRI study. *Chest*. 2007; **131**: 1050–1057
42. Schoenfeld C, Cebotari S, Hinrichs J, et al. MR imaging-derived regional pulmonary parenchymal perfusion and cardiac function for monitoring patients with chronic thromboembolic pulmonary hypertension before and after pulmonary endarterectomy. *Radiology*. 2015; **28**: 150765
43. Sakka SG, Rühl CC, Pfeiffer UJ, et al. Assessment of cardiac preload and extra-vascular lung water by single transpulmonary thermodilution. *Intensive Care Med*. 2000; **26**: 180–187
44. Tofts PS, Brix G, Buckley DL, et al. Estimating kinetic parameters from dynamic contrast-enhanced T(1)-weighted MRI of a diffusable tracer: standardized quantities and symbols. *J Magn Reson Imaging*. 1999; **10**: 223–232
45. Sourbron SP, Buckley DL. On the scope and interpretation of the Tofts models for DCE-MRI. *Magn Reson Med*. 2011; **66**: 735–745
46. St Lawrence KS, Lee TY. An adiabatic approximation to the tissue homogeneity model. *J Cereb Blood Flow Metab*. 1998; **18**: 1365–1377
47. Turco S, Janssen AJ, Lavini C, et al. Time-efficient estimation of the magnetic resonance dispersion model parameters for quantitative assessment of angiogenesis. *Biomed Signal Process Control*. 2016; **26**: 23–33
48. Mischi M, Kalker TA, Korsten EH. Contrast echocardiography for pulmonary blood volume quantification. *IEEE Trans Ultrason Ferroelectr Freq Control*. 2004; **51**: 1137–1147
49. Brittain EL, Doss LN, Saliba L, et al. Feasibility and diagnostic potential of pul- monary transit time measurement by contrast echocardiography: a pilot study. *Echocardiography*. 2015; **32**: 1564–1571
50. Lee VS, Spritzer CE, Carroll BA, et al. Flow quantification using fast cine phase-contrast MR imaging, conventional cine phase-contrast MR imaging, and Doppler sonography: in vitro and in vivo validation. *Am J Roentgenol*. 1997; **169**: 1125–1131
51. Gauthier TP, Averkiou MA, Leen EL. Perfusion quantification using dynamic contrast-enhanced ultrasound: the impact of dynamic range and gain on time-intensity curves. *Ultrasonics*. 2011; **51**: 102–106
52. Fredholm A, Kanski M, Maret-Ouda J, et al. The pulmonary blood volume measured by cardiovascular magnetic resonance imaging relation to cardiac pumping and anthropometric measures. *J Cardiovasc Magn Reson*. 2014; **16** (Suppl 1):261
53. Slutsky RA, Bhargava V, Higgins CB. Pulmonary circulation time: comparison of mean, median, peak, and onset (appearance) values using indocyanine green and first-transit radionuclide techniques. *Am Heart J*. 1983; **106**: 41–45
54. Yamada T, Sakamoto T, Hatano R, et al. Pulmonary hemodynamics following reconstructive mitral valve surgery. *Jpn J Surg*. 1973; **3**: 163–172

Chapter 9

Pulmonary transit time predicts response to cardiac resynchronization therapy

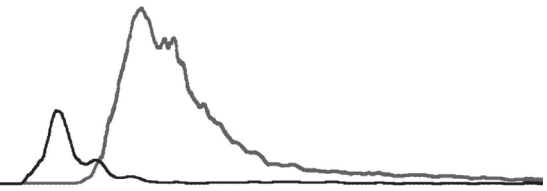

Ingeborg HF Herold
Salvatore Saporito
R Arthur Bouwman
Hans C van Assen
Anouk GW de Lepper
Erik HM Korsten
Patrick Houthuizen
Massimo Mischi

Submitted

ABSTRACT

Aims

Prediction and assessment of response to cardiac resynchronization therapy (CRT) is still a clinical challenge. This study evaluated the dynamic parameter pulmonary transit time (PTT) by contrast-enhanced echocardiography to predict and assess the response to CRT.

Methods and Results

Sixty-seven patients, referred for CRT, underwent baseline and 3-months follow-up contrast-enhanced echocardiography. Time intensity curves were extracted by drawing regions of interest (ROI) in the left and right ventricle in dynamic contrast-enhanced echo loops. PTT was estimated by the difference in mean transit time of the time intensity curves. Response was defined by different criteria based on a clinical parameter (Minnesota Living With Heart Failure score) and an echocardiographic parameter (left ventricular end-systolic volume (LVESV) decrease of 15%). A significant decrease in PTT was seen in the responder groups for both criteria. In the non-responder group defined by LVESV, PTT did not change. However, PTT decreased in the non-responder group defined by MLWHF score. PTT as predictor of response showed a significantly larger baseline PTT for non-responders than responders according to LVESV-change. PTT cut-off value for response was 12.5 s with a sensitivity and specificity of both 67%.

Conclusion

Prediction and assessment of response to CRT was feasible by PTT estimation using contrast-enhanced echocardiography, which is minimally invasive and bedside applicable. Future studies are needed to assess its value during CRT-device implantation.

INTRODUCTION

Cardiac resynchronization therapy (CRT) effectively improves cardiac function in 60-70% of the patients with systolic heart failure with prolonged QRS duration.[1] However, prediction and assessment of successful response to CRT remains a clinical challenge.[2] The standard to define positive response is a decrease of the left ventricle end-systolic volume (LVESV) by more than 15%. Alternative cut-off points, such as an increase in left ventricle ejection fraction (LVEF) or decrease of N-terminal of the prohormone brain natriuretic peptide (NT-proBNP) level, are also employed.[3-5] Clinical response is often classified by a decrease in New York Heart Association (NYHA) classification and/or improvement of the quality of life score (QoL) (e.g. Minnesota Living With Heart Failure (MLWHF) score).[3] In about 25% of the patients a clinical response is observed without a response on echocardiography, which may possibly relate to a placebo effect of CRT therapy.[3, 6] Moreover, CRT response is more likely in case of non-ischemic cardiomyopathy, prolonged QRS duration, smaller end-diastolic volumes (LVEDV) on echocardiography, and the ability to walk more than 225 m in the 6MWT.[6-10] The last two parameters probably reflect severity of the disease, where improvement of cardiac function or remodeling is no longer feasible in patients with very dilated ventricles and/or poor exercise capacity. However, a good predictor for response or no-response to date is not available.

Previous evidence shows that pulmonary transit time (PTT) and normalized PTT (nPTT) correlate with cardiopulmonary function.[11-12] PTT significantly correlates with left ventricular systolic and diastolic function assessed by contrast-enhanced echocardiography and by dynamic contrast-enhanced magnetic resonance imaging (DCE-MRI).[11-14] Interestingly, a direct relationship between PTT/nPTT and NT-proBNP in a group of heart failure patients has been demonstrated,[15] and a cut-off value for normal and non-normal cardiopulmonary circulation has been appreciated.[11]

In this study, we hypothesized that PTT/nPTT will change after CRT implantation in relation to clinical and volumetric-echocardiographic measures. We aimed to demonstrate in patients undergoing CRT that PTT/nPTT is a sensitive and easy-to-assess parameter to accurately predict clinical and echocardiographic response.

METHODS

The institutional review board of the Catharina Hospital approved this observational study, which was conducted from January 2012 to April 2014 (registered as niet-WMO 15-34). All patients who underwent baseline echocardiography in the work-up for CRT implantation in our hospital were included. Typically, patients were in systolic heart

failure (LVEF < 35%) with signs of electrical dyssynchrony on the electrocardiogram (QRS>120 ms). All patients provided written informed consent for the use of their data.

Transthoracic echocardiography

For the assessment of the eligibility of CRT implantation, patients underwent transthoracic echocardiography according to the standard of care to assess ventricular function and mechanical dyssynchrony. During transthoracic echocardiography, a complete two-dimensional, color, pulsed and continuous wave Doppler examination was obtained. Contrast-enhanced LVESV and LVEDV were estimated using the biplane method of discs. Inter-ventricular mechanical delay (IVMD) was estimated by time-difference between onset of QRS and onset of right ventricular (RV) and left ventricular (LV) ejection with an IVMD > 40 ms considered as abnormal.[16] The septal to posterior wall motion delay (SPWMD) was estimated from Tissue Doppler Imaging M-mode recordings as the time difference between peak septal and peak posterior wall excursion on midventricular short axis views, SPWMD >130 ms was regarded abnormal.[17] If no contraindications for ultrasound contrast agents (UCAs) such as allergies for sulphur hexafluoride were present, contrast-enhanced echocardiography was performed in all patients to estimate ventricular volumes before and three months after implantation of the biventricular pacemaker.[18]

Estimation of the pulmonary transit time

PTT was estimated from transthoracic contrast-enhanced echocardiograms according to our hospital protocol using SonoVue® (Bracco Imaging S.p.A., Milan, Italy) in three incremental doses (10 ml of 1:400 (low dose), 1:200 (half dose), 1: 100 (full dose) SonoVue® in saline).[19] The UCA was administered through an 18 Fr peripheral intravenous access positioned in the forearm. With the patient in the left lateral recumbent position, a four chamber apical view was obtained using an iE33 ultrasound scanner with a S5-1 ultrasound probe (Philips Healthcare, Andover, MA, USA) to visualize the passage of the UCA (Fig.1). Patients were allowed to breathe freely, and instructed to avoid deep breaths or coughs to prevent movement artifacts interfering with endocardial tracing. The echo cine loops were assessed in QLab®8 (Philips Healthcare), by manually drawing regions of interest (ROIs) within the endocardial borders during the cardiac cycle in the RV and LV. The acoustic intensity changes over time within the ROIs were calculated by QLab®, yielding intensity dilution curves (IDCs). Subsequently, all acoustic IDCs were fitted by the local density random walk (LDRW) model using customized software in Matlab®2015a (MatWorks, Natick, MA, USA).[20] The model fits were performed automatically. Inaccurate fits as assessed by visual inspection were fitted semi-automatically, with an operator manually selecting the time interval of the IDC to fit, excluding large breathing motion artifacts and recirculation overlapping the first passage of the UCA bolus. From the fitted curves the mean transit times (MTTs) of the SonoVue®

bolus in the RV and LV were estimated. The PTT was calculated as the difference between these MTTs. Normalization of the PTT (nPTT) was performed by dividing the PTT by the R-R interval in the aorta or multiplying the PTT with the heart rate estimated via the ECG. Steps throughout the whole process are illustrated in Fig. 1.

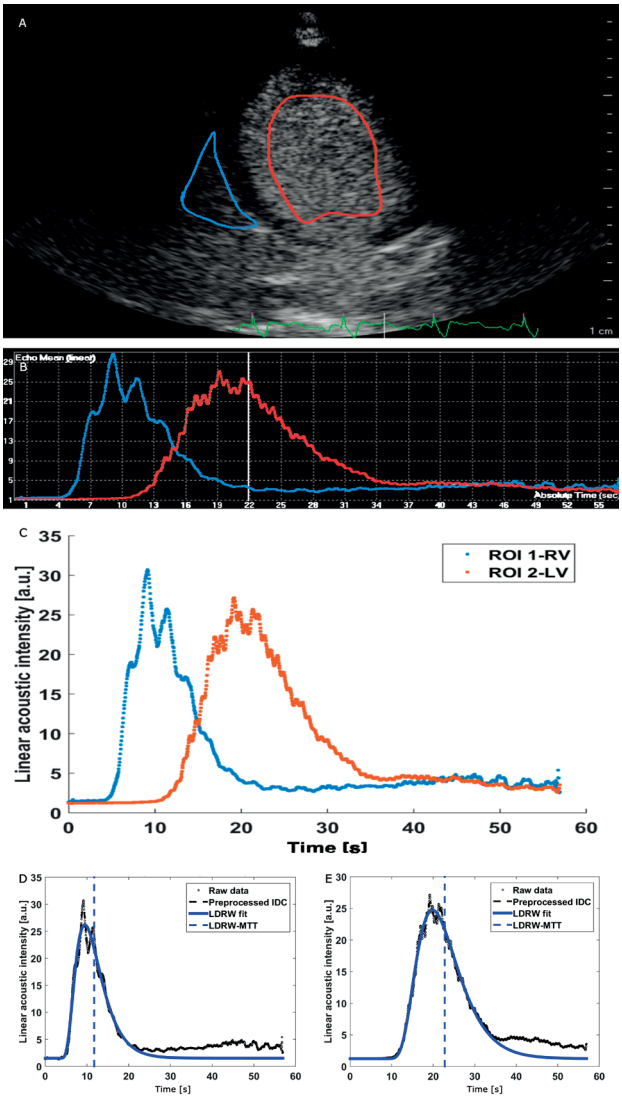

Figure 1. Ultrasound contrast agent bolus passing through right and left ventricle (panel A) in a transthoracic four chamber view; within the ventricles regions of interest (ROI) are drawn. Blue ROI and curves in panels A,B, and C are right ventricle, red ROI and curves are left ventricle. The acoustic intensity curves within the ROI are estimated using Qlab® (panel B). The curves are imported in Matlab® (panel C) and fitted by the local density random walk model (panels D and E). The mean transit times (LDRW-MTT) of the right ventricle (panel D) and left ventricle (panel E) are obtained from the model after fitting.

Evaluation of clinical response to CRT

Patients' physical improvements were evaluated by the physician by estimating the NYHA functional class. Clinical response to CRT is defined as ≥ 1 point decrease in NYHA class.[21] Additionally, patients completed a QoL questionnaire (MLWHF score) before and three months after implantation of the CRT device. The MLWHF score is sensitive to response to therapy for heart failure.[22-23] The cut-off point for clinical response according to the MLWHF score was a decrease of 13 points.[24]

Evaluation of echocardiographic and biomarker response to CRT

Reverse remodeling was assessed by contrast-enhanced echocardiography and defined as a decrease of LVESV by 15% three months after CRT device implantation. Furthermore, biomarker response was evaluated by NT-proBNP.

Statistical analysis

Distribution of the data was assessed using the Shapiro-Wilk test. Normally distributed data are expressed as mean and standard deviation and non-normally distributed data are expressed as median and interquartile ranges. The PTT/nPTTs were assessed in all patients and divided into two groups, namely responders and non-responders defined by an LVESV reduction and MLWHF score decrease. Baseline characteristics were compared for statistical significance using Student's t-test or the Mann-Whitney U test, as appropriate. At baseline and 3 months after CRT, PTT/nPTTs were analyzed using a paired t-test or Wilcoxon rank test to assess the effects of CRT. The ability to predict response according to a decrease in LVESV by baseline PTT/nPTT was tested by a t-test or Mann-Whitney U test. Subgroup analysis was performed by using the ANOVA or Kruskal-Wallis test to predict response by PTT/nPTT in patients with improvement of QoL (MLWHF score) and LVESV decrease; multiple comparisons adjusted *p*-values are presented. Sensitivity and specificity for prediction of CRT responders were determined for various cut-off values of PTT using receiver-operating characteristic (ROC) curves. Sensitivity of the test for response was assessed in relation to decrease of the LVESV by 15%. Analysis was performed using SPSS version 23 (IBM©, Armonk, NY, USA); a *p*-value <0.05 was considered significant.

RESULTS

A total of seventy-one patients who received contrast-enhanced echocardiography both at baseline and at 3-months after CRT were analyzed (Table 1). Four patients were excluded because the acoustic IDCs could not be obtained (n=2) or fitted by the LDRW model (n=2). From the 402 IDCs of all available doses, 6 low dose curves (1.5%), 4 half

Table 1. Demographic characteristics

	Mean ± SD (n=67)
Gender (male/female)	43/24
Age	70.5 ± 8.0
BMI (kg/m^2)	27.1 ± 5.2
NYHA classification	2.6 ± 0.6
Comorbidities n (%)	
Hypertension	27 (40)
Diabetes mellitus	18 (27)
COPD	7 (10)
iCMP	34 (51)
Medication n (%)	
Beta blocker	56 (84)
ACE inhibitors	49 (73)
ATII blockers	13 (19)
Loopdiuretics	40 (60)
Aldosteron antagonists	23 (34)
Laboratory	
Glomerular filtration rate (ml/min)	52 ± 11
NT-proBNP (pmol/l) (n=54)	185.0 (105.3 – 322.5)
Electrocardiogram	
Rhythm SR/PMR or nodal/AF	51/13/3
QRS duration	163 ± 24
LBBB/Non LBBB	47/20
Echocardiogram	
Ejection fraction (%)	27.8 ± 8.4
LVEDV (ml)	229 ± 69
LVESV (ml)	167 ± 61
IVMD (ms)	48 ± 25
SPWMD (ms)	193 ± 135
LA volume (ml)	87 ± 38
TAPSE (cm)	1.5 ± 0.5
MR severity (%)	
None	23 (34)
Mild	24 (36)
Moderate	22 (16)
Severe	9 (13)

BMI, body mass index; NYHA, New York Heart Association classification; COPD, chronic obstructive pulmonary disease; iCMP, ischemic cardiomyopathy; NT-proBNP, N-terminal pro-B-type natriuretic peptide; LBBB, left bundle branch block; LVEDV, left ventricle end-diastolic volume; LVESV, left ventricle end-systolic volume; IVMD, interventricular mechanical delay; SPWMD, septal to posterior wall mechanical delay; LA, left atrium; TAPSE, tricuspid annular systolic elevation; MR, mitral regurgitation

dose curves (1.0%), and 10 full dose curves (2.5%) showed a poor LDRW model fit (R^2< 0.85) and were therefore excluded from the analysis. The majority of the model-fits (68%) were performed completely automatically. The median PTTs at baseline and at 3-months follow-up were 11.8 (10.1-14.3) s and 11.0 (9.3-13.0) s, *p*=0.03, respectively. The nPTT was 13.7 (10.9-15.7) at baseline and 12.0 (10.0-13.6) after 3-months, *p*=0.01. The difference between the three doses was not significant for PTT and nPTT at baseline (*p*=0.95 and *p*=0.96, respectively) and at 3-months follow-up (*p*=0.62 and *p*=0.66, respectively). CRT significantly improved LV volumes, EF, NT-proBNP, NYHA, and MLWHF score (Table 2).

Table 2. Parameter changes due to CRT

Variable (n)	Responders/Non-responders (%)	Baseline	3 Months	*p*-value
PTT (s) (67)		11.8 (10.1 – 14.3)	11.0 (9.3 – 13.0)	0.033
nPTT (67)		13.7 (10.9 – 15.7)	12.0 (10.0 – 13.6)	0.006
NYHA class (64)		3.0 (2 – 3)	2.0 (1.25 – 2)	<0.0005
MLWHF score (56)	36/20 (64%)	45.0 (24.5 – 58)	25.0 (11 – 38)	0.001
NT-proBNP (pmol/l) (50)		185.0 (105.3 – 322.5)	115 (43.0 – 232.5)	0.02
LVEDV (ml)* (67)		228.9 ± 69.1	196.0 ± 69.3	<0.0005
LVESV (ml)* (67)	43/24 (64%)	167.5 ± 61.3	128.7 ± 66.0	<0.0005
LVEF (%)* (67)		27.9 ± 8.3	37.0 ± 10.9	<0.0005

PTT, pulmonary transit time; nPTT, normalized PTT; the rest of the abbreviations are explained in Table 1. All data are expressed as median and inter-quartile ranges. $p < 0.05$ is significant. Asterisk indicates mean ± standard deviation and paired-samples t-test.

Response to CRT

All patients who responded to CRT, independently of the definition of response, showed a significant decrease in PTT/nPTT after 3 months (Fig. 2 and Table 3). In non-responders, based on LVESV, PTT/nPTT remained unchanged (Fig. 2 and Table 4). In non-responders based on the MLWHF score, nPTT remained unchanged; however, PTT decreased significantly (Table 4).

Furthermore, 64% of the patients demonstrated a clinical response to CRT. With respect to reverse remodeling, 64% of patients responded to CRT with a decrease in LVESV (Table 2).

Prediction of response to CRT

Based on reverse remodeling measured by echocardiography, we found a significant difference in baseline PTT (not nPTT) of responders and non-responders (11.4 (9.5 – 13.2) s and 13.5 (11.4 – 14.6) s, respectively, *p*=0.02 (Fig. 3). However, the baseline

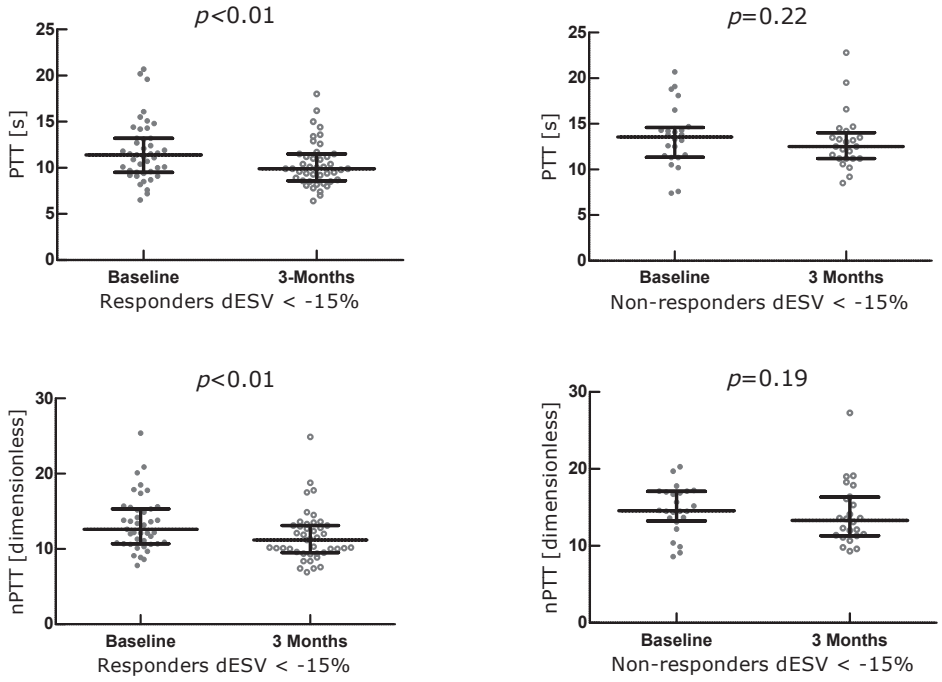

Figure 2. Change in PTT and nPTT after cardiac resynchronization therapy. Closed circles represent PTT/nPTTs at baseline of each patient and open circles represent the PTT/nPTTs after three months divided by responding and non-responding patients. Bars represent medians and inter-quartile ranges. Two-tailed *p*-value < 0.05 is significant.

Table 3. PTT and nPTT of responders based on different criteria

PTT/nPTT and criterion for response (n)	Baseline	3 months	*p*-value
PTT (s) - MLWHF score decrease 13 points (36)	11.8 (10.0 – 14.6)	10.8 (9.5 – 13.0)	0.011
PTT (s) - Decrease LVESV of 15% (43)	11.4 (9.5 – 12.2)	9.9 (8.6 – 11.5)	0.00028
nPTT - MLWHF score decrease 13 points (36)	14.0 (10.8 – 16.9)	11.4 (9.4 – 13.6)	0.003
nPTT - Decrease LVESV of 15% (43)	12.6 (10.7 – 15.3)	11.2 (9.5 – 13.1)	0.002

Abbreviations are explained in Table 1. All data are expressed as median and inter-quartile ranges. p < 0.05 is significant.

Table 4. PTT and nPTT of non-responders based on different criteria

PTT/nPTT and criterion for response (n)	Baseline	3 months	*p*-value
PTT (s) - MLWHF score decrease 13 points (20)	11.7 (10.1 – 14.2)	10.7 (9.2 – 13.0)	0.026
PTT (s) - Decrease LVESV of 15% (24)	13.6 (11.4 – 14.6)	12.5 (11.2 – 14.0)	0.224
nPTT - MLWHF score decrease 13 points (20)	13.8 (11.0 – 16.7)	12.4 (10.4 – 15.1)	0.211
nPTT - Decrease LVESV of 15% (24)	14.6 (13.2 – 17.1)	13.3 (11.3 – 16.3)	0.189

Abbreviations are explained in Table 1. All data are expressed as median and inter-quartile ranges. p < 0.05 is significant.

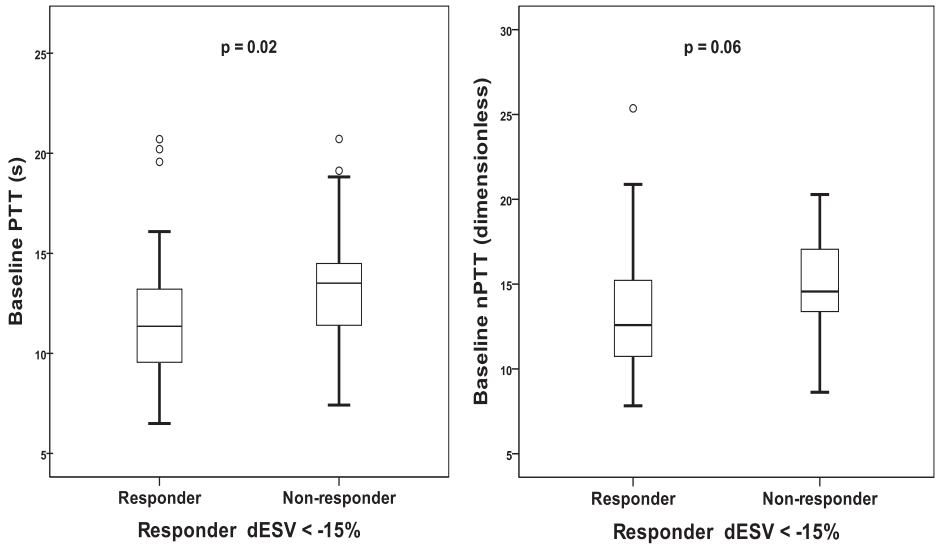

Figure 3. Difference in baseline PTT (left panel) and nPTT (right panel) between responders and non-responders defined by change in end-systolic volume (dLVESV). Box is inter-quartile range, horizontal line is median and whiskers are 95% confidence intervals. Two-tailed *p*-value < 0.05 is significant.

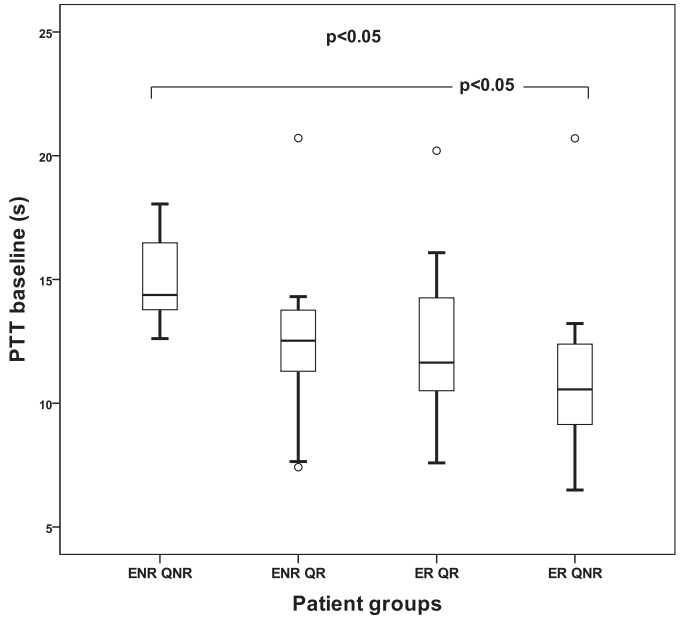

Figure 4. Subgroup analysis of pulmonary transit time (PTT) at baseline in comparison to response according to left ventricular end-systolic volume increase by more than 15% (Echo +/-) and/or quality of life improvement by decrease of 13 points of the Minnesota Living With Heart Failure Questionnaire (QoI +/-). ENR QNR Echo - QoI - (n=6), ENR QR Echo - QoI + (n=13), ER QR Echo + QoI + (n=23), ER QNR Echo + QoI - (n=14). Overall is Kruskal-Wallis, hooked lines is Mann-Whitney U test. *p*-values are corrected for multiple comparisons.

PTT/nPTT defined by MLWHF score were not significantly different for responders and non-responders.

In the subgroup analysis, the differences in baseline PTT between the four patient categories of combinations of clinical and echocardiographic response were significant, p=0.02 (Fig. 4). The non-responding patients based on both MLWHF score and LVESV had the longest baseline PTT, which was significantly different from the other categories. This difference was not significant in baseline nPTT, p = 0.06.

ROC analysis using the echocardiographic response criterion (ΔLVESV), demonstrated an area under the curve (AUC) of 0.67 (95% confidence interval (CI) 0.54 – 0.80), p=0.02, with cut-off value at 12.5 s for PTT (sensitivity and specificity both 67%) (Fig. 5).

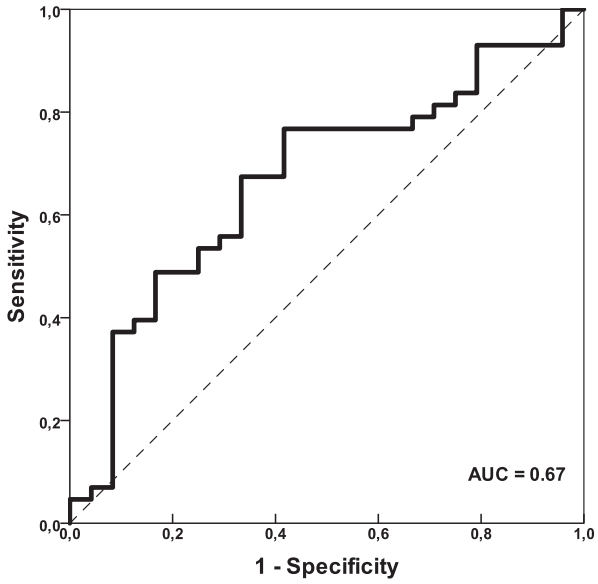

Figure 5. Receiver operating curve analysis response according to left ventricular end-systolic volume decrease of more than 15%. AUC = area under the curve.

DISCUSSION

Primary results

The presented study investigated whether PTT/nPTT assessed with contrast-enhanced echocardiography can be used in the evaluation and prediction of response to CRT. The results show that PTT/nPTT significantly decreases 3 months after CRT implantation, indicating an improvement in global cardiac performance (Table 2). In the responding patients, we found a reduction in PTT/nPTT (Fig. 2). This reduction was irrespective of the response criterion used (Table 2). This suggests that improvement of cardiopulmonary

pump function by synchronizing ventricular contraction is directly measureable by a decrease in PTT/nPTT. In addition, our data indicate that PTT (not nPTT) could predict response to CRT; patients with longer baseline PTTs were less likely to respond to CRT based on LVESV (Fig. 3). Moreover, in the subgroup analysis the largest PTTs (not nPTTs) were clinical and echographic non-responders (Fig. 4).

Decrease in PTT/nPTT due to CRT

Advanced heart failure based on dyssynchrony coincides with decreased EF, LV dilation, increased LV filling pressures, and possibly increased left atrial volumes. PTT measures the efficiency of the blood circulation by the cardiopulmonary pump. Studies on PTT using DCE-MRI showed a strong correlation with LV volumes and LV filling pressures.[12-14] Studies using contrast-enhanced echocardiography consistently supported these findings with correlations between PTT/nPTT and LVESV, LVEDV, EF, and NT-proBNP.[11, 15] Therefore, LV dilation due to remodeling with subsequent mitral regurgitation and atrial dilation will lead to an increase in PTT/nPTT. Responders to CRT show reverse remodeling with a decrease in ventricular volumes and improved cardiac performance, implicating improvement in PTT/nPTT, which was confirmed in this study.

PTT as a predictor of response to CRT

PTT of non-responders was significantly larger than the PTT of responders to CRT. It was already mentioned that the clinical and echographic non-responders had the longest baseline PTT; this could be of interest for explaining the previously described 25% placebo effect.[3, 6] The prolonged PTTs are in line with previously described pathophysiological changes; indicating irreversible remodeling and a severely dysfunctional cardiopulmonary pump function.[9] This is consistent with observations that severe LV dilation or severely decreased functional capacity measured by 6-MWT jeopardizes resynchronization.[10] Furthermore, PTT differentiates between patients with normal and non-normal cardiopulmonary function.[11] Moreover, prolonged PTTs from DCE-MRI in patients with pulmonary hypertension predicted adverse outcomes caused by enlarged right-sided cardiac volumes and low cardiac output.[25] Our data showed a significantly larger PTT in non-responders with a cut-off value of 12.5 s. The estimated cut-off value to predict response to CRT had a relatively low sensitivity and specificity. This could be explained by the fact that transit time is estimated between the RV and LV; therefore, RV function and pulmonary hypertension may have influenced the PTT. Indeed our mean left atrium volume was enlarged (87 ± 38 ml) and the RV function decreased (Table 1). In comparison to other studies with different criteria for response, e.g., dP/dt and aorta velocity time index, our sensitivity and specificity are in agreement.[26-27] Obviously, PTT/nPTT cannot be used to discriminate the origin of cardiac dyssynchrony (ischemic or non-ischemic); however, it could be of value in the selection of CRT patients, either alone

or in conjunction with other (objective) parameters of cardiac function.[28-29] Given the fact that CRT is a frequently applied treatment for patients with dyssynchronous systolic heart failure with high cost and mediocre success rate of 70%[30], it is of importance to define a set of parameters able to predict response in this patient category with complex pathophysiologic changes.

Potential clinical implications

This study showed that PTT/nPTT-measurements by contrast-enhanced echocardiography are highly repeatable, and independent of UCA dose, given the linear relationship between acoustic reflected backscatter and SonoVue® concentration for all doses used in this protocol. This finding among 67 patients corroborates earlier results in two smaller groups,[15, 19] which one partly overlaps with the group in this study.[19]

Up till now, there has been less attention for direct hemodynamic response to CRT, except in the study of acute improvement of dP/dt, which is a predictor of long-term outcome to CRT.[31] This study showed that baseline PTT seems to be a possible predictor for response to CRT. Additionally, the relationship between improvement in cardiac performance by CRT and its effect on PTT/nPTT was shown. Additionally, baseline PTT seems to be a possible predictor for response to CRT. Both results could be of value during CRT device implantation. Therefore, pre-implant PTT may give the cardiologist insight on whether response is to be expected, while during implantation response can be estimated by assessing the PTT. PTT can easily be obtained at the bedside, the additional value in the CRT population needs to be evaluated in future research. This technique may reduce costs if non-responders can be better identified from responders a priori.

Limitations

The clinical routine of this observational study changed in the two years of execution; not all patients answered the MLWHF questionnaires. Many different criteria for response are commonly used, but the agreement between them is poor. We used those which are frequently applied in literature to describe clinical and volumetric change to CRT.[2] We did not use the NYHA class as clinical criterion for response, as this score is highly subjective to interpretation by the physician. We did not perform the 6-MWT test regularly, which according to literature gives a stronger parameter for clinical response.[7]

The moment for evaluation of definite response is most often defined at 6 months; we assessed our patients at 3 months, this may have caused a possible underestimation of the number of responders. The reason why nPTT did not have predictive value remains an open question and needs further evaluation, especially considering that nPTT correlated better with LV volumes than PTT.[15]

CONCLUSION

This study showed that PTT/nPTT measured by contrast-enhanced echocardiography provides a good estimate of global cardiac performance. In patients with LV dyssynchrony and heart failure treated with CRT: PTT/nPTT could differentiate responders from non-responders. Moreover, the PTT before CRT-implantation was significantly prolonged in non-responders; a PTT above 12.5 s could predict in 67% for non-response. PTT may be of value for physicians evaluating heart failure treatment and for predicting response to CRT.

REFERENCES

1. Cleland JG, Daubert JC, Erdmann E, et al. The effect of cardiac resynchronization on morbidity and mortality in heart failure. *N Engl J Med* 2005; **352**: 1539-49
2. Fornwalt BK, Sprague WW, BeDell P, et al. Agreement is poor among current criteria used to define response to cardiac resynchronization therapy. *Circulation* 2010; **121**: 1985-91
3. Bleeker GB, Bax JJ, Fung JW, et al. Clinical versus echocardiographic parameters to assess response to cardiac resynchronization therapy. *Am J Cardiol* 2006; **97**: 260-3
4. Bax JJ, Bleeker GB, Marwick TH, et al. Left ventricular dyssynchrony predicts response and prognosis after cardiac resynchronization therapy. *J Am Coll Cardiol* 2004; **44**: 1834-40
5. Hoogslag GE, Hoke U, Thijssen J, et al. Clinical, echocardiographic, and neurohormonal response to cardiac resynchronization therapy: are they interchangeable? *Pacing Clin Electrophysiol* 2013; **36**: 1391-401
6. Auger D, van Bommel RJ, Bertini M, et al. Prevalence and characteristics of patients with clinical improvement but not significant left ventricular reverse remodeling after cardiac resynchronization therapy. *Am Heart J* 2010; **160**: 737-43
7. Diaz-Infante E, Mont L, Leal J, et al. Predictors of lack of response to resynchronization therapy. *Am J Cardiol* 2005; **95**: 1436-40
8. Reuter S, Garrigue S, Barold SS, et al. Comparison of characteristics in responders versus nonresponders with biventricular pacing for drug-resistant congestive heart failure. *Am J Cardiol* 2002; **89**: 346-50
9. Castel MA, Mendez F, Tamborero D, et al. Six-minute walking test predicts long-term cardiac death in patients who received cardiac resynchronization therapy. *Europace* 2009; **11**: 338-42
10. Shanks M, Delgado V, Ng AC, et al. Clinical and echocardiographic predictors of nonresponse to cardiac resynchronization therapy. *Am Heart J* 2011; **161**: 552-7
11. Brittain EL, Doss LN, Saliba L, Irani W, Byrd BF, Monahan K. Feasibility and Diagnostic Potential of Pulmonary Transit Time Measurement by Contrast Echocardiography: A Pilot Study. *Echocardiography* 2015; **32**: 1564-71
12. Cao JJ, Wang Y, McLaughlin J, et al. Left ventricular filling pressure assessment using left atrial transit time by cardiac magnetic resonance imaging. *Circ Cardiovasc Imaging* 2011; **4**: 130-8
13. Francois CJ, Shors SM, Bonow RO, Finn JP. Analysis of cardiopulmonary transit times at contrast material-enhanced MR imaging in patients with heart disease. *Radiology* 2003; **227**: 447-52
14. Shors SM, Cotts WG, Pavlovic-Surjancev B, et al. Non-invasive cardiac evaluation in heart failure patients using magnetic resonance imaging: a feasibility study. *Heart Fail Rev* 2005; **10**: 265-73
15. Herold IH, Saporito S, Mischi M, et al. Pulmonary transit time measurement by contrast-enhanced ultrasound in left ventricular dyssynchrony. *Echo Res Pract* 2016; **3**: 35-43
16. Bax JJ, Ansalone G, Breithardt OA, et al. Echocardiographic evaluation of cardiac resynchronization therapy: ready for routine clinical use? A critical appraisal. *J Am Coll Cardiol* 2004; **44**: 1-9
17. Pitzalis MV, Iacoviello M, Romito R, et al. Cardiac resynchronization therapy tailored by echocardiographic evaluation of ventricular asynchrony. *J Am Coll Cardiol* 2002; **40**: 1615-22
18. Senior R, Becher H, Monaghan M, et al. Contrast echocardiography: evidence-based recommendations by European Association of Echocardiography. *Eur J Echocardiogr* 2009; **10**: 194-212
19. Herold IH, Saporito S, Bouwman RA, et al. Reliability, repeatability, and reproducibility of pulmonary transit time assessment by contrast enhanced echocardiography. *Cardiovasc Ultrasound* 2016; **14**: 1

20. Mischi M, Kalker T, Korsten HHM. Videodensitometric methods for cardiac output measurements. *EURASIP Journal on applied signal processing* 2003; **5**: 479 - 89
21. Pires LA, Abraham WT, Young JB, Johnson KM. Clinical predictors and timing of New York Heart Association class improvement with cardiac resynchronization therapy in patients with advanced chronic heart failure: results from the Multicenter InSync Randomized Clinical Evaluation (MIRACLE) and Multicenter InSync ICD Randomized Clinical Evaluation (MIRACLE-ICD) trials. *Am Heart J* 2006; **151**: 837-43
22. Morcillo C, Aguado O, Delas J, Rosell F. [Utility of the Minnesota Living With Heart Failure Questionnaire for assessing quality of life in heart failure patients]. *Rev Esp Cardiol* 2007; **60**: 1093-6
23. van Bommel RJ, Marsan NA, Koppen H, et al. Effect of cardiac resynchronization therapy on cerebral blood flow. *Am J Cardiol* 2010; **106**: 73-7
24. Upadhyay GA, Choudhry NK, Auricchio A, Ruskin J, Singh JP. Cardiac resynchronization in patients with atrial fibrillation: a meta-analysis of prospective cohort studies. *J Am Coll Cardiol* 2008; **52**: 1239-46
25. Swift AJ, Telfer A, Rajaram S, et al. Dynamic contrast-enhanced magnetic resonance imaging in patients with pulmonary arterial hypertension. *Pulm Circ* 2014; **4**: 61-70
26. Kato H, Shimano M, Sumi T, et al. Acute improvement of left ventricular relaxation as a predictor of volume reduction after cardiac resynchronization therapy: a pilot study assessing the value of left ventricular hemodynamic parameter. *Pacing Clin Electrophysiol* 2014; **37**: 1544-52
27. Bonakdar HR, Jorat MV, Fazelifar AF, et al. Prediction of response to cardiac resynchronization therapy using simple electrocardiographic and echocardiographic tools. *Europace* 2009; **11**: 1330-7
28. Marsan NA, Westenberg JJ, Ypenburg C, et al. Magnetic resonance imaging and response to cardiac resynchronization therapy: relative merits of left ventricular dyssynchrony and scar tissue. *Eur Heart J* 2009; **30**: 2360-7
29. Ypenburg C, van Bommel RJ, Delgado V, et al. Optimal left ventricular lead position predicts reverse remodeling and survival after cardiac resynchronization therapy. *J Am Coll Cardiol* 2008; **52**: 1402-9
30. Bax JJ, Gorcsan J, 3rd. Echocardiography and noninvasive imaging in cardiac resynchronization therapy: results of the PROSPECT (Predictors of Response to Cardiac Resynchronization Therapy) study in perspective. *J Am Coll Cardiol* 2009; **53**: 1933-43
31. Tournoux FB, Alabiad C, Fan D, et al. Echocardiographic measures of acute haemodynamic response after cardiac resynchronization therapy predict long-term clinical outcome. *Eur Heart J* 2007; **28**: 1143-8

Chapter 10

Discussion and future perspectives

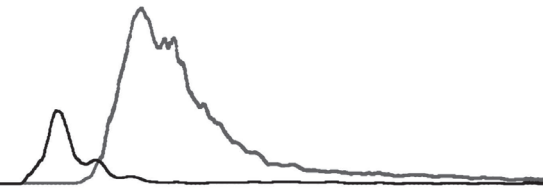

Global cardiac performance is mainly assessed, in anaesthesia and intensive care, by arterial and central vein catheterization. In the outpatient clinic, cardiac performance can be evaluated by a comprehensive echocardiography. However, quantitative parameters in echocardiography can be difficult to obtain.

This thesis proposes a novel method for measuring pulmonary transit time (PTT) and pulmonary blood volumes as parameter for cardiac performance. This method is based on the indicator dilution theory and performed using a minimally-invasive approach based on contrast-enhanced echocardiography. Therefore, this proposed technique can be adopted at the bedside in the outpatient clinic as well as in the critically ill patient or in patients at the operating room, using a transthoracic or transesophageal ultrasound probe. For this purpose, a small bolus of ultrasound contrast agent (UCA) is injected in a peripheral vein. The transport of the bolus through the right and left heart chambers can be visualized using echocardiography. Indicator dilution curves (IDC) are obtained from four-chamber images by measuring acoustic intensity change over time within regions of interest (ROI) drawn in the cardiac chambers. Specific modelling of the IDC provides mean transit times (MTT) of the right and left ventricle. The difference in MTT of the left and right ventricle determines the PTT. The purpose of this thesis is to bring dynamic contrast-enhanced imaging and UCA dilution technique into clinical practice and compare it with clinical standards.

PART ONE- IN-VITRO VALIDATION OF CONTRAST-ENHANCED TRANSIT TIME ESTIMATION

In part one of this thesis, we focused on the validation of the mean transit time (MTT) measurement using CEUS and the standard clinical method thermodilution in an in-vitro setup.[1]

Chapter 2

A prerequisite to apply the indicator dilution theory is a linear relationship between the acoustic backscattered intensity and the ultrasound contrast agent concentration, therefore calibration studies were performed at different temperatures. The calibration study showed for SonoVue® microbubbles that the stability and lifetime increased at lower temperatures. At higher temperatures more bubbles are disrupted and destroyed leading to decreased microbubble concentrations. This could be the explanation for the shift in threshold for attenuation; at lower temperature the concentration for shadowing was lower than at higher temperature. This is probably caused by the lower amount of microbubbles in dilution at higher temperatures, and therefore less saturation and shadowing.

Chapter 3

Simultaneous injection of cold saline and UCA was feasible within the linear ranges of the backscattered acoustic intensity and concentration. Furthermore, previous reports showed that contrast-enhanced ultrasound (CEUS) could be used for estimation of MTTs.[2] In this study, different volumes were quantified. We were especially interested in the difference in volumes estimated by CEUS and thermodilution, as this could result from the different kinetics of the employed indicators. In the in-vitro setup for thermodilution, we used two RADI wires, which were positioned with their thermistors exactly at the point where the ultrasound beam intercepted the in- and out-flow tube of the model. Under these controlled circumstances, we have found a strong correlation between the volumes measured by CEUS and by thermodilution (r_s = 0.94); however Bland-Altman analysis revealed a bias of –108 ± 67 ml. In comparison with the true volumes of the in-vitro model, the bias of thermodilution-volumes compared to true volumes were nearly twice as large as the bias for CEUS-volumes compared to true volumes (84 ± 62 ml and -40 ± 28 ml respectively). The volumes estimated by thermodilution were all overestimated in comparison with the true in-vitro volumes, especially at low flows and high volumes. The overestimations could be explained by heat loss through the tube walls (vessel) into the surrounding. The CEUS-volumes showed an underestimation at the larger true volumes. The reason might result from the concentration distribution of microbubbles across the tube, possibly showing the trend to concentration in the centre. Therefore, the microbubbles would have an average velocity over the tube cross section that is higher than that of the carrier fluid.[3-4]

Limitations

Limitations of this study are more related to thermodilution and less to CEUS. The thermodilution transit times and volumes were more overestimated than the underestimation by CEUS in comparison to the true volumes of the in-vitro setup. This could be explained by temperature loss to the environment despite extensive isolation of the in-vitro setup. Furthermore, the used thermistors in the RADI wires are normally not used for large volume estimations in patients, therefore inaccuracies could occur. However, repeatability of the volume measurements was high. Therefore, we continued evaluating the relationship between MTTs by thermodilution and CEUS with transpulmonary thermodilution equipment (PiCCO®, Pulsion Medical SE, Feldkirchen, Germany), which is frequently applied in patients. The use of two indicators simultaneously could affect each other's behaviour. The effect of temperature on the microbubbles showed at cold temperatures stabilization of the microbubbles with lower acoustic intensities, however during warming up of the microbubbles in the circulation, reflectivity will increase but also the threshold for disruption. The effect of warming up in the circulation and its effect on the indicator dilution curve needs further evaluation.

PART TWO- IN-VIVO VALIDATION OF CONTRAST-ENHANCED TRANSIT TIME ESTIMATION

Chapter 4

This part of the thesis focused on the comparison of the volumes estimated by CEUS using transesophageal echocardiography and by transpulmonary thermodilution by PiCCO®, in-vitro and in patients. The thermistor used in the in-vitro set-up was a PiCCO® catheter instead of the two RADI wires as in the previous study. The thermodilution estimated volumes (intrathoracic total volume (ITTV)) were in agreement with the findings of the first in-vitro study; thermodilution-volumes were larger than the CEUS-volumes and the true volumes of the in-vitro circuit.

The algorithm by PiCCO® estimates the pulmonary total volume (PTV) by the exponential downslope time of the thermodilution IDC. The PBV is a fraction of the largest mixing volume i.e. PTV.[5] The correlation for the PBV estimated by PiCCO® in-vitro with the true volumes was strong r_s = 0.96 (95% CI, 0.93 - 0.97; P<0.0001) with a bias (underestimation) especially at higher volumes. Also the CEUS obtained volumes correlated strongly r_s = 0.97 (95% CI, 0.95 - 0.98; P<0.0001) with the true volumes of the in-vitro setup. Bland Altman analysis showed a marked slope comparing PBV measured by thermodilution and the volumes by CEUS in-vitro. This in-vitro observation was used to interpret the results of the in-vivo study, because in patients the comparison was made between the PBV measured by CEUS and PiCCO®.

In seventeen patients, the median PBV by PiCCO® was 356 ml and the median intrathoracic blood volume between the right and left atrium estimated by CEUS was 685 ml. The correlation between the volumes was moderate, r_s = 0.69 (95% CI, 0.55 - 0.79; P<0.0001). The PiCCO® PBVs were much smaller than the CEUS-volumes. This is in agreement with the findings of the in-vitro study. Moreover, the CEUS-volumes were more in line with the previous reported PBVs measured by dye dilution, using right and left heart catheterization or in studies with radionuclides.[6-8] The study population included patients undergoing coronary artery bypass surgery and they all had decreased ejection fraction (EF) and widened QRS duration. Also, our measured volumes by CEUS were in agreement with the PBVs in a similar patient category.[9-10] We concluded that the volumes measured by CEUS are more in line with the PBVs reported in literature, and the transpulmonary thermodilution measured PBVs did not agree with the CEUS volumes, which deserves further investigation.

Limitations

The comparison with thermodilution revealed that cold saline was not the ideal indicator to validate CEUS with thermodilution. Ideally, we should have used a true intravascular indicator like indocyanine green. However, this implied a more invasive technique by

right and left heart catheterization in our patients. Transpulmonary thermodilution is a method which is still invasive but less laborious than the formerly used techniques. The PBV-estimate derived by single catheter-transpulmonary thermodilution is not frequently used in clinical practice; this value is calculated by an algorithm in the PiCCO® system (*Chapter 1*). It has been shown that the PiCCO® estimated volumes correlate poorly with the true intrathoracic blood volumes, which is in line with our findings.[11] However, we measured the transit time between the right and left atrium; therefore the PBV by CEUS included the mean right ventricle volume, hence, the volumes measured by CEUS were anatomically larger than the true PBV. Ideally, we should measure the transit time difference between the pulmonary artery and the left atrium. However, due to shadowing of the intra-atrial septum on the right ventricle in the four-chamber view and the small volume of the pulmonary artery, ROIs were drawn in the right atrium.

Chapter 5

In this study, we compared the PTT estimated by CEUS using transthoracic echocardiography (TTE) with the PTT measured by DCE-MRI. Recently, DCE-MRI has been used to measure the PTT and PBV.[10, 12-14] In twenty patients, we compared the PTTs measured between the right and left ventricle, using CEUS and DCE-MRI. We also evaluated the correlation between PTTs and heart failure parameters such as left ventricular end-systolic volume (LVESV), left ventricular end-diastolic volume (LVEDV), ejection fraction (EF), and N-terminal Pro-B-type Natriuretic Peptide (NT-proBNP). The results showed a strong correlation between PTT by CEUS and DCE-MRI (r=0.75 (95% CI, 0.46 - 0.90; P = 0.0001)). PTT by CEUS and DCE-MRI showed a moderate to strong correlation with the left ventricle volumes and EF. This correlation between left ventricular volumes and PTT was also found in earlier studies using DCE-MRI.[13] The strength of the correlation increased by normalization for heart rate by multiplying the PTT by heart rate, representing the number of stroke volumes needed to pass the pulmonary circulation. This can be explained by the link between heart rate and cardiovascular hemodynamics.[15] The novelty of this study was the strong correlation between PTT by CEUS/DCE-MRI and NT-proBNP. The relationship between PTT and different systolic and diastolic heart failure parameters using MRI was also confirmed in literature.[10, 13, 16] Brittain and coworkers found significant correlations between PTT and cardiopulmonary dysfunction, they differentiated right ventricular failure, pulmonary arterial hypertension, left ventricular diastolic heart failure, and left ventricular systolic heart failure. Parameters of the different parts of the cardiopulmonary conduit have shown significant correlations with PTT using CEUS and DCE-MRI.[13, 16-17] The PTTs by CEUS in our heart failure population were in line with the PTTs found in different categories of EF assessed by contrast-enhanced echocardiography.[13, 16] The measured relationship between PTT and NT-proBNP confirmed the correlation between PTT and heart failure. Brittain and coworkers described a cut-off point for PTT[16] above

which cardiopulmonary pump dysfunction could be present. However, the underlying mechanism e.g. valvular disease, right ventricle dysfunction, pulmonary arterial hypertension, and left ventricle diastolic or systolic dysfunction cannot be identified.

Limitations

We evaluated the value of PTT in a small group of patients with heart failure due to left ventricular dyssynchrony. This is a specific category of heart failure patients. We did not evaluate different types of heart failure such as right ventricle and diastolic heart failure, and we did not appreciate different categories of EFs (as described in *Chapter 8*). More diversity in EF would enable better investigation of the discrimination properties of PTT by contrast-enhanced echocardiography. According to our hospital protocol, we used three different doses of UCA and compared them with one dose of gadolinium. The average of three doses could decrease variation. However, subsequent analysis revealed that the contribution of different contrast doses to variation in transit times was limited. On the other hand, PTT by DCE-MRI showed better correlation with ventricular volumes and NT-proBNP than CEUS. This can be explained by the freehand acquisition of the IDCs of CEUS making them more susceptible to moving artefacts and thus decreased fits, therefore, the signal-to-noise ratio of DCE-MRI is higher.

PART THREE- RELIABILITY, REPEATABILITY, AND REPRODUCIBILITY OF MANUAL AND AUTOMATIC PTT ASSESSMENT

Chapter 6

In this study, we tested the reliability, repeatability, and reproducibility of PTT assessment by drawing ROIs in contrast-enhanced four-chamber echo loops. The study was performed in a patient population referred for CRT. By hospital protocol, all patients received a contrast-enhanced TTE. We tested the reliability in fifteen four-chamber echo loops of patients who received three injections with increasing dose. One of the three doses was assessed by eight raters for each patient at two time moments with one week interval. The inter-rater reliability of the eight raters was high (intraclass correlation ICC = 0.98) and also the intra-rater reproducibility of the PTT measurement between the two time moments was high (ICC = 0.98). Repeatability of the PTT measurement was assessed by the analysis of variance between the three injections, which showed no significant difference ($p = 0.95$). Our results were in agreement with former PTT studies using CEUS in-vitro,[18] in animals,[19] and in patients.[20] In these studies, a small variance was found for the assessment of the PTT in the echo loop as well as between different sonographers, indicating the PTT measurement to be reliable, repeatable, and reproducible.[16, 20]

Chapter 7

Drawing ROIs and fitting the curves was still laborious, hence, automatic transit time estimation was an essential step in the development of PTT-estimation. Therefore, we evaluated a method for the automatic extraction of IDCs, exploiting the time domain correlation between pixels belonging to the same region. Individual time intensity curves were projected into a low dimensional subspace using principal component analysis; subsequently, clustering was performed to identify the different ROIs. However, a comparison of different clustering techniques still needs to be done for blood pool description, to increase the method applicability in more noisy CEUS loops. This method for the automatic extraction of IDCs was assessed on clinically available DCE-MRI and CEUS recordings, comparing the derived IDCs with those obtained manually. The difference between the manual and automatic obtained MTTs and PTTs on the CEUS and DCE-MRI recordings was minimal. The inter-observer variability for CEUS between the four observers was between 0.6, 2.2, and 1.8% for the LV MTT, RV MTT, and PTT, respectively. Furthermore, the inter-observer variability for DCE-MRI between four observers was 0.8, 0.4, and 2.0% for the LV-MTT, RV-MTT, and PTT, respectively. These findings are in line with reliability findings in *Chapter 6*. In conclusion, this method for automated transit time estimation could be a good alternative to facilitate transit time assessment in clinical practice.

Limitations

The reliability studies only examined the process of ROI drawing. Obtaining contrast-enhanced four-chamber views by different sonographers was not investigated. In future studies, the difference in PTT could be evaluated between different sonographers. However, in the study by Choi et al. the variance of the PTT measurement between two sonographers was not significant.[20] In contrast to earlier reports, we used the local density random (LDRW) model for analysis of the IDC. This approach provided a more accurate interpretation of the physical behaviour of a contrast bolus in the blood stream.[21] In those earlier reports, MTTs were evaluated by frame counting, bubble appearance, or by evaluating the peak to peak difference of the IDC.[12, 16, 20, 22] However, these methods do not take into account the influence of noise on the IDC, which is fitted by the LDRW model.

PART FOUR- PTT ASSESSMENT IN THE EVALUATION OF CARDIAC PERFORMANCE

Chapter 8

In this study, we compared the indicator dilution parameters assessed by model-based trans-pulmonary impulse response modelling using DCE-MRI in healthy volunteers and HF patients. The LDRW model was used to describe the transpulmonary dilution system. The PTT was compared with standard measures of cardiac function. PTT/nPTT was significantly longer in heart failure patients than in healthy volunteers, which was confirmed by the relationship between nPTT and different categories of EFs. Furthermore, the left ventricular volumes correlated well with PTT/nPTT in agreement with *Chapter 5* and reports in literature.[13, 16]

There was a significant difference between the patients and healthy volunteers in the λ of the IDC; λ was smaller, reflecting more asymmetrical transpulmonary dilution in patients than in healthy volunteers. λ is proportional to the ratio between convection and diffusion in a dilution system, these variations can therefore be explained by the fact that the cardiac output in patients is much lower than in healthy volunteers, which means less convection and more diffusion in patients compared to healthy volunteers. The repeatability of λ from two injections was significant, but there was still a large variation. Theoretically, we could postulate that in the compromised cardiopulmonary circulation, λ could be a measure of pulmonary oedema. For future studies, the repeatability of λ and the relationship between λ and the extension of pulmonary oedema measured by e.g. NT-proBNP could be of interest.

Limitations

The considered population was small and the groups were not matched in number. We did not correlate the effect of λ and EF, which could be of interest to evaluate the effect of higher cardiac outputs on the value of λ. We had some patients with right ventricular dysfunction in our CEUS population; it would be of interest to evaluate the right ventricular function in relation to the symmetry of the IDC. Moreover, we found some typical asymmetrical IDCs in the right ventricle in our CEUS population; it could be of interest to evaluate these curves in relation to the right ventricular function.

Chapter 9

In this observational study, we evaluated whether PTT and nPTT could assess and predict response to cardiac resynchronization therapy (CRT). Response to CRT can be defined by different criteria; one of the most frequently used is a decrease in LVESV of 15% by reverse remodelling. Clinical response is based on an improvement of the quality of life

by a decrease of 13 points in the Minnesota Living With Heart Failure questionnaire (MLWHF questionnaire).

We evaluated 67 patients with LVEF < 35% and QRS-duration > 120 ms, before and 3 months after CRT implantation. The responders all showed, independently from the criteria described above, a decrease in PTT/nPTT in response to CRT. With respect to LVESV change, the non-responders did not show a difference in PTT/nPTT after CRT, which supports no change in cardiac performance. However, in the non-responder group based on MLWHF score PTT (not nPTT) decreased. All baseline PTT/nPTTs were prolonged in agreement with decreased left ventricular function supporting earlier publications.[13,16] These observations are consistent with earlier findings where PTT/nPTT correlated well with cardiac volumes and NT-proBNP (*Chapter 5)*.

Additionally, we found a difference in baseline PTT in the responder and non-responder group, where the non-responders based on LVESV change showed a significant longer PTT. This difference was not found for nPTT. In addition to these findings, a cut-off point for PTT predicting response to CRT could be discriminated, above which response was not expected. In the subgroup analysis, the PTTs were significantly longer in clinically- and echographically-non-responders based on quality of life and LVESV change. Our results can be explained by reported observations where patients with poor clinical performance or severe LV dilation showed lower response to CRT.[23] Thereby, PTT cut-off points have been described for estimation of compromised global cardiac performance and as predictor for outcome in patients with pulmonary hypertension.[16-17]

Limitations

This observational study had some drawbacks due to changes in clinical routine; the criteria for response used were not applied in all patients. Therefore, the number of patients per group varied. We evaluated our moment of response after 3 months, whether PTT/nPTT can assess response directly after CRT device implantation, needs further investigation. nPTT did not show predictive properties which is remarkable since a strong correlation with volumetric parameters was found and needs further consideration. Whether clinical and echographic non-responders/responders can be differentiated by PTT remains a topic for further investigation.

FUTURE DIRECTIONS

The echocardiographic evaluation of left ventricle systolic function, diastolic function, and valve functioning remains challenging in atrial fibrillation due to variable cardiac cycle length and absence of atrial kick. Even though the PTT cannot be normalized in patients with atrial fibrillation, our data show a moderate correlation between PTT-CEUS and NT-

proBNP. Differentiation of cardiopulmonary pump dysfunction could be assessed by PTT as it measures the global blood stream through the heart. Therefore, it could be of interest to evaluate the PTT in relation to specific cardiopulmonary pathologies such as, e.g. valvular disease, right ventricular dysfunction, and pulmonary hypertension. Treatment of different pathologies could be evaluated together with the effect on PTT. Additionally, it could be interesting to assess the effect of cardioversion of atrial fibrillation on PTT. Moreover, the PTT could perhaps discriminate patients who remain in sinus rhythm or who will relapse in atrial fibrillation. Paroxysmal atrial fibrillation has a higher incidence with atrial dilation and PTT is correlated to atrial size. Therefore, it could be of interest to evaluate PTT in relation to paroxysmal atrial fibrillation.

Future studies could focus on cardiopulmonary pump failure in different categories of patients such as systolic heart failure, diastolic heart failure, and right ventricle dysfunction in agreement with the study of Brittain et al.[16] Re-evaluation of the threshold of PTT above which cardiopulmonary pump dysfunction was expected should be performed. Additionally, the effect of treatment on PTT should be evaluated in CRT patients and in other cardiopulmonary pump treatments, e.g., inotropics, assist devices etc. Thereby, the observation that the pre-CRT PTT discriminated responders to non-responders could further be investigated with respect to other treatments. Also the evaluation of the PTT set against $ScvO_2$ could be of interest to explore in a population of ICU care patients with cardiopulmonary dysfunction. Moreover, PTT/nPTT could be an interesting parameter to obtain in routine evaluation of cardiac function, either by ultrasound or by MRI. In case of an abnormal PTT, further investigation to the origin of the dysfunction would be advised.

Thereby, the λ parameter of the IDC could be investigated. Validation could be performed in measuring pulmonary oedema in patients. The effect of the symmetry of the IDC i.e. the effect of right ventricular function on λ could be of further interest, since the right ventricular function is difficult to quantify and λ may prove to be a suitable parameter for the right ventricular function.

PTT/nPTT was acquired using Qlab® and Matlab®, this approach is time consuming. The development of automatic endocardial delineation with ROI description and transit time estimation is a first step to a fully automatic PTT estimation. Ideally, this should be implemented in the ultrasound scanner. Such a development should be validated with manual estimations.

Cost evaluation should be performed in using CEUS for the proposed application. For an accurate measurement, the ideal number of injections should be evaluated. We used up to three injections and the results were very consistent.[24] The dose used was very low, thus the amount present in the vial is too much. Perhaps new packages should be marketed for the proposed measurements. Also the type of microbubble should be evaluated. We used SonoVue®, which was the only registered microbubble in Europe when we started this research and therefore did not evaluate other microbubbles.

In conclusion PTT measurement using CEUS is shown to be reliable, repeatable, and reproducible. PTT correlated well with the PTT by DCE-MRI and both PTTs correlated well with volumetric parameters for heart failure and NT-proBNP. With regard to the effect of CRT on the PTT, PTT/nPTT has decreased significantly in responders after CRT. Moreover, PTT assessment before CRT discriminated responders from non-responders in this study. We believe that the proposed methods in this thesis can be an asset for cardiologists, intensivists, and also cardio-anaesthesiologists. PTT measurement by CEUS is applicable in a wide range of patients, easy to perform at the bedside and readily obtainable.

REFERENCES

1. Pinsky MR, Payen D. Functional hemodynamic monitoring. *Crit Care* 2005; **9**: 566-72
2. Mischi M, Kalker TA, Korsten EH. Contrast echocardiography for pulmonary blood volume quantification. *IEEE Trans Ultrason Ferroelectr Freq Control* 2004; **51**: 1137-47
3. Keller MW, Segal SS, Kaul S, Duling B. The behavior of sonicated albumin microbubbles within the microcirculation: a basis for their use during myocardial contrast echocardiography. *Circ Res* 1989; **65**: 458-67
4. Tangelder GJ, Slaaf DW, Muijtjens AM, Arts T, oude Egbrink MG, Reneman RS. Velocity profiles of blood platelets and red blood cells flowing in arterioles of the rabbit mesentery. *Circ Res* 1986; **59**: 505-14
5. Sakka SG, Reuter DA, Perel A. The transpulmonary thermodilution technique. *J Clin Monit Comput* 2012; **26**: 347-53
6. Roy SB, Bhardwaj P, Bhatia ML. Pulmonary blood volume in mitral stenosis. *Br Med J* 1965; **2**: 1466-9
7. Schreiner BF, Jr., Murphy GW, James DH, Yu PN. Pulmonary blood volume in patients with congestive heart failure. *Trans Assoc Am Physicians* 1966; **79**: 250-61
8. Jones RH, Sabiston DC, Jr., Bates BB, Morris JJ, Anderson PA, Goodrich JK. Quantitative radionuclide angiocardiography for determination of chamber to chamber cardiac transit times. *Am J Cardiol* 1972; **30**: 855-64
9. McGaff CJ, Roveti GC, Glassman E, Milnor WR. Pulmonary blood volume in rheumatic heart disease and its alteration by isoproterenol. *Circulation* 1963; **27**: 77-84
10. Shors SM, Cotts WG, Pavlovic-Surjancev B, Francois CJ, Gheorghiade M, Finn JP. Heart failure: evaluation of cardiopulmonary transit times with time-resolved MR angiography. *Radiology* 2003; **229**: 743-8
11. Galstyan G, Bychinin M, Alexanyan M, Gorodetsky V. Comparison of cardiac output and blood volumes in intrathoracic compartments measured by ultrasound dilution and transpulmonary thermodilution methods. *Intensive Care Med* 2010; **36**: 2140-4
12. Ugander M, Kanski M, Engblom H, et al. Pulmonary blood volume variation decreases after myocardial infarction in pigs: a quantitative and noninvasive MR imaging measure of heart failure. *Radiology* 2010; **256**: 415-23
13. Cao JJ, Wang Y, McLaughlin J, et al. Left ventricular filling pressure assessment using left atrial transit time by cardiac magnetic resonance imaging. *Circ Cardiovasc Imaging* 2011; **4**: 130-8
14. Mischi M, van den Bosch HC, den Boer JA, et al. Intra-thoracic blood volume measurement by contrast magnetic resonance imaging. *Magn Reson Med* 2009; **61**: 344-53
15. Falch DK, Stromme SB. Pulmonary blood volume and interventricular circulation time in physically trained and untrained subjects. *Eur J Appl Physiol Occup Physiol* 1979; **40**: 211-8
16. Brittain EL, Doss LN, Saliba L, Irani W, Byrd BF, Monahan K. Feasibility and Diagnostic Potential of Pulmonary Transit Time Measurement by Contrast Echocardiography: A Pilot Study. *Echocardiography* 2015; **32**: 1564-71
17. Swift AJ, Telfer A, Rajaram S, et al. Dynamic contrast-enhanced magnetic resonance imaging in patients with pulmonary arterial hypertension. *Pulm Circ* 2014; **4**: 61-70
18. Herold IH, Russo G, Mischi M, et al. Volume quantification by contrast-enhanced ultrasound: an in-vitro comparison with true volumes and thermodilution. *Cardiovasc Ultrasound* 2013; **11**: 36

19. Streitberger A, Hocke V, Modler P. Measurement of pulmonary transit time in healthy cats by use of ultrasound contrast media "Sonovue(R)": feasibility, reproducibility, and values in 42 cats. *J Vet Cardiol* 2013; **15**: 181-7
20. Choi BG, Sanai R, Yang B, et al. Estimation of cardiac output and pulmonary vascular resistance by contrast echocardiography transit time measurement: a prospective pilot study. *Cardiovasc Ultrasound* 2014; **12**: 44
21. Wise ME. Tracer dilution curves in cardiology and random walk and lognormal distributions. *Acta Physiol Pharmacol Neerl* 1966; **14**: 175-204
22. Streitberger A, Modler P, Haggstrom J. Increased normalized pulmonary transit times and pulmonary blood volumes in cardiomyopathic cats with or without congestive heart failure. *J Vet Cardiol* 2015; **17**: 25-33
23. Shanks M, Delgado V, Ng AC, et al. Clinical and echocardiographic predictors of nonresponse to cardiac resynchronization therapy. *Am Heart J* 2011; **161**: 552-7
24. Malm S, Frigstad S, Sagberg E, Larsson H, Skjaerpe T. Accurate and reproducible measurement of left ventricular volume and ejection fraction by contrast echocardiography: a comparison with magnetic resonance imaging. *J Am Coll Cardiol* 2004; **44**: 1030-5

Dankwoord

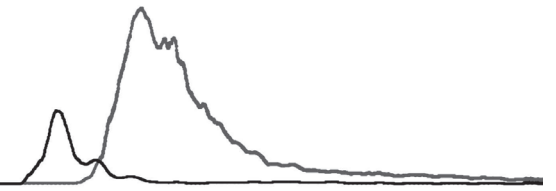

Met bijna iedereen die dit dankwoord leest heb ik jarenlang de inhoud van dit onderzoek gedeeld, de ene iets meer dan de ander. Sommigen kregen tot in den treuren tijdsschema's te horen die elke keer weer iets werden bijgesteld. Dit zijn niet altijd de meest interessante gesprekken maar het heeft mij geholpen door te zetten en met al jullie steun dit proefschrift te vormen. Bedankt allemaal.

Ik wil als eerste alle patiënten en vrijwilligers bedanken die deel hebben genomen aan de onderzoeken, of hun echografische gegevens beschikbaar hebben gesteld. Zonder hen was dit onderzoek niet mogelijk geweest.

Ik begin het persoonlijke deel bij de grondlegger van dit proefschrift, **prof. dr. Erik Korsten**, samen hebben wij het technisch uitgewerkte onderzoek in de klinische praktijk gebracht. Erik, bedankt voor je onuitputtelijke enthousiasme en innovatieve ideeën. Jouw inspiratie zullen we over een aantal jaar moeten missen, maar ik hoop dat ik/wij altijd even kunnen bellen voor raad. Dank voor je vertrouwen.

Daarnaast wil ik mijn copromotor **dr.ir.Massimo Mischi**, de technische ontwikkelaar van de acoustische indicator-dilutiecurve, bedanken. Dit proefschrift is gebaseerd op zijn werk dat 12 jaar geleden is gepubliceerd. Massimo, grazie per la tua fiducia e per la tua pazienza nel considerare questa tesi. Senza di te e la mente sempre acuta, questo dottorato non sarebbe stato possibile.

Dr. Arthur Bouwman mijn tweede copromotor wil ik bedanken, sinds zijn komst naar het Catharina ziekenhuis kregen de microbellen een bruisend karakter, wat een boost heeft gegeven aan dit onderzoek. Als roomie had jij altijd tijd voor vragen. Jij maakt onderzoek doorzichtig en schijnbaar eenvoudig. Je bent een goede begeleider, die weet waar de buitenwereld op wacht.

Dr. Patrick Houthuizen, jij hebt een hele belangrijke rol gespeeld in mijn promotietraject. Elke transthoracale echo die voor dit proefschrift is gemaakt, is van de hand van deze cardioloog. Iedere donderdagochtend in 2012 en 2013 ging mijn sein en voerden wij het beschreven onderzoek uit. Gek genoeg moest ik na 2014 even wennen zonder onderzoek. Bedankt voor je steun, je adviezen, je goede revisies, je lekkere koffie en Frits natuurlijk.

Zo ook **dr. ir. Hans van Assen**, jij was vanaf het begin betrokken bij ons onderzoek. Jouw reviews van de manuscripten hadden altijd oog voor detail. Je beheersing van de Engelse taal is indrukwekkend.

Prof. dr. ir. Jan Bergmans, jij organiseerde onze reguliere bijeenkomsten. De to-do list werd systematisch opgebouwd en afgestreept. Jij zorgde dat eenieder elkaar met regelmaat zag, dank voor jouw begeleiding wat dit onderzoek tot een goed einde heeft doen komen.

Ir. Salvatore Saporito, thanks for your technical and moral support, our regular meetings, and being my paranymph. We had some good laughs with the experiments at

the MRI. I am very impressed by your programming skills. You also managed to get an impressive knowledge on MRI in a very short time.

Lieve drs. **Maaike Sikma**, mijn paranimf, ik weet dat jij ook druk bent met jouw promotieonderzoek, je ziet de "s" verbleekt al. Ik ben blij dat jij mij deze dag wilt steunen. Je bent een topper. Ik hoop dat ik je hierna kan stimuleren om jouw promotie tot een goed einde te brengen.

Ik wil de leden van mijn promotiecommissie bedanken, **prof. dr. T. Backx, prof. dr. J. Kesecioglu, prof. dr. W. Buhre en prof.dr. N. Pijls.**

Beste **professor Backx,** bedankt dat je mijn promotie wilt voorzitten, ik vind het een hele eer.

Beste **Jozef,** ik heb een bijzonder fijne tijd gehad in het UMCU. Jij bent een zeer collegiaal afdelingshoofd. Voor mij was je een soort vader-intensivist waaronder de jongen konden groeien, ik heb toen veel geleerd. Ik vind het een eer dat je in deze promotiecommissie zitting wilt nemen.

Beste **Wolfgang,** ik heb je voor het eerst ontmoet in het UMCU, tussen de assist devices and harttransplantaties. Jouw enthousiasme voor cardiac anesthesia en onderzoek hebben toen veel indruk gemaakt, zodoende ben ik trots dat jij in deze commissie zit als één van de eerste onderzoekers van transpulmonale thermodilutie methode.

Beste **Nico,** ik vind het heel leuk dat jij als top-onderzoeker binnen de cardiologie mijn proefschrift hebt willen beoordelen. Ik begreep dat jouw wetenschappelijke carrière begon met de indicator dilutie methode in de kransslagaderen.

Beste **prof. D. van Dijk, Diederik,** bedankt dat je deze dag hebt willen opponeren. Ik vind het een hele eer als oud-collega van het UMCU.

Beste **Harrie van de Bosch, Marleen Kohler, Cindy Maandag en Jan Hoppenbrouwers** en het hele cardiac MRI team, bedankt dat we elke keer weer bij jullie terecht konden met onze onderzoeksvoorstellen. Het was voor jullie vast niet altijd makkelijk weer een bepaald protocol " te draaien" wat alles behalve standaard was, toch zijn we er samen altijd uitgekomen.

Ik wil de co-auteurs van mijn artikelen bedanken.

Anouk de Lepper, bedankt voor je steun in de opbouw van de database. Het was een enorme klus.

Rene Grouls, bedankt voor je hulp bij de calibratie metingen.

Beste **Mohamed Soliman**, samen met jou heb ik de patiëntengroep, die voor biventriculaire pacing tijdens hartoperaties werd onderzocht, beschreven in hoofdstuk 4. Het waren dynamische ingrepen met jou, **Bart van Straten en Berrie van Gelder**, bedankt voor jullie hulp.

Gianna Turco, Maarten Kuenen, Erik Maas and **Tamerlan Saidov**, you were very supportive during our in-vitro model work. I cannot imagine how many hours we spent in

the basement with the model(s). Thanks for the GUI's (graphical user interface) in Matlab of the local density random walk model.

Dankzij de perfusionisten in het bijzonder **Patrix Lanen** en de technische dienst met **Berry Bijsterveld** zijn onze modellen met perfusieslangen, perfusiepompen, lenen van passende kabels en het gebruik van las apparatuur tot stand gekomen. Jullie hulp was hierbij onontbeerlijk.

Daarbij was ook **Pieter Vergaard** van Pulsion Medical van grote steun. Hij leende ons twee PiCCO machines waarmee onze in-vitro thermodiluties zijn uitgevoerd. Daarbij wil ik ook **Marcel Arditi**, samen met **Peter Frinking** beiden ingenieurs van Bracco die ons 8 jaar geleden hartelijk ontvingen bij de bron van dit acoustisch gebruis.

De fontys studenten, **Bennie, Tim, Mitchel, Vincent, Tang en Yang**, thanks for your support in building all the different setups and performing many, many tests with them.

Natuurlijk wil ik ook mijn **maatschap** bedanken, bij wie ik ook altijd terecht kon met mijn ups en downs. Wij hebben een top kluppie en ik hoop samen met jullie ons ziekenhuis nog vele jaren te voorzien van top zorg.

Mijn **IC-maatjes** wil ik bedanken voor hun onophoudelijke interesse en motivering. Er zijn mooie toekomstplannen in het vooruitzicht en ik hoop vele gezellige jaren met jullie te beleven.

Pap en mam jullie zijn een enorme stimulans geweest. Geïnteresseerd in het hele proces, waarbij jullie tempo regelmatig voor lag op het mijne, maar we zijn er gekomen. Dank voor de regelmatige moral support, die af en toe broodnodig was.

Erwin jij bent mijn steunpilaar en technologische ondersteuning geweest in dit hele proces. Ik heb mij volledig kunnen toeleggen op het uitvoeren en schrijven van dit onderzoek. Als ik regelmatig laat thuiskwam in verband met het onderzoek was dat nooit een probleem. Ik ben je diep dankbaar en weet dat het zonder jou minstens jaren langer had geduurd. Hierna hebben we eindelijk weer weekendjes vrij.

Curriculum Vitae

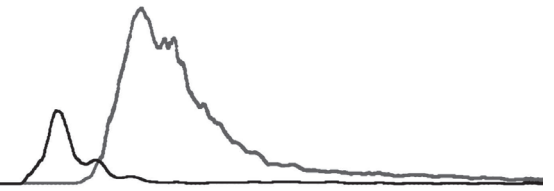

Ingeborg Henriëtte Franziska was born on December 3th, 1970 in Utrecht. She finished her secondary school at Athenaeum F. de Munnik, Utrecht in 1990. After a detour of one year at the University of Groningen, where she studied business school, she went to Belgium to study Medicine at the Catholic University of Leuven. She graduated in 1998 with honors.

She started working as a resident of intensive care at Amphia hospital in Breda. In this period, her interests for intensive care and hemodynamics developed.

From 1999 to 2004 she received her specialist training in Anesthesiology at the Erasmus University of Rotterdam. She graduated as intensivist in 2006 at the Leids University Medical Centre. During this fellowship she had an increasing interest for heart failure surgery patients. In line with this patient category she went working as staff member at the intensive care of the University Medical Center of Utrecht, where heart failure surgery was treated with assist devices and transplantations. The opportunity to perform research in a novel area within echocardiography and hemodynamics, made her move to the Catharina hospital Eindhoven. This research started in 2008 at the University of Technology Eindhoven in close collaboration with the Catharina hospital under supervision of prof.dr. Erik Korsten and dr. ir. Massimo Mischi.

Besides research, she is working as anesthesiologist and intensivist at the Catharina hospital.

Ingeborg lives together with Erwin in Meteren where they have six chickens and one rooster.

List of publications

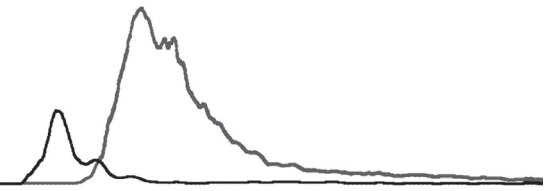

PEER-REVIEWED PAPERS RELATED TO THIS TOPIC

I.H.F. Herold, G. Russo, M. Mischi, P. Houthuizen, T. Saidov, M. van 't Veer, H.C. van Assen, H.H.M. Korsten
Volume quantification by contrast-enhanced ultrasound: an in-vitro comparison with true volumes and thermodilution.
Cardiovascular Ultrasound 2013; 11: 36

M.P. Kuenen, **I.H.F. Herold,** H.H.M. Korsten, J.J. de la Rosette, H. Wijkstra, M. Mischi
Maximum-likelihood estimation for indicator dilution analysis
IEEE Trans Biomed Eng 2014; 61: 821-31

I.H.F. Herold, M.A. Soliman Hamad, H.C. van Assen, R.A. Bouwman, H.H.M. Korsten, M. Mischi
Pulmonary blood volume measured by contrast enhanced ultrasound: a comparison with transpulmonary thermodilution
Br J Anaesth 2015;115:53-60

S. Saporito, **I.H.F. Herold,** P. Houthuizen, H.C.M. van den Bosch, H.H.M. Korsten, H.C. van Assen, M. Mischi
Automatic indicator dilution curve extraction in dynamic-contrast enhanced imaging using spectral clustering
Phys Med Biol 2015; 60: 5225-40

I.H.F. Herold, S. Saporito, R.A. Bouwman, P. Houthuizen, H.C. van Assen, M. Mischi, H.H.M. Korsten
Reliability, repeatability, and reproducibility of pulmonary transit time assessment by contrast enhanced echocardiography
Cardiovasc ultrasound 2016; 14:1.

S. Saporito, **I.H.F. Herold,** P. Houthuizen, H.C.M. van Den Bosch, J. den Boer, H.H.M. Korsten, H.C. van Assen, M. Mischi
Model-based characterization of the trans-pulmonary circulation in heart failure by dynamic contrast-enhanced MRI
Investigative Radiology 2016; jul 1 epub ahead

I.H.F. Herold, S. Saporito, M. Mischi, H. C. van Assen, R. Arthur Bouwman, H.C.M. van den Bosch, A.G.W. de Lepper, H.H.M. Korsten, P. Houthuizen

Pulmonary Transit Time measurement using Contrast-Enhanced Ultrasound in Ventricular Dyssynchrony Patients A Comparison study with Dynamic Contrast-Enhanced MRI
Echo Research and Practice 2016; 3: 35-43

PAPER IN PRESS / IN REVIEW / IN PREPARATION

I.H.F. Herold, M. Mischi, R.A. Bouwman, R.J.E. Grouls, H.H.M. Korsten
In-vitro assessment of the stability and acoustic backscatter of different concentrations SonoVue® at different temperatures

I.H.F. Herold, S. Saporito, R.A Bouwman, H.C. van Assen, A.G.W. de Lepper, H.H.M. Korsten, P. Houthuizen, M. Mischi
Pulmonary transit time predicts response to cardiac resynchronization therapy.

S. Saporito, S. Dovancescu, **I.H.F. Herold,** H.C.M. van den Bosch, H.C. van Assen, R.M. Aarts, H.H.M. Korsten, M. Mischi
Comparison of cardiac magnetic resonance imaging and bioimpedance spectroscopy for the assessment of fluid displacement induced by external leg compression.

A.G.W. de Lepper, **I.H.F. Herold,** S. Saporito, R.A. Bouwman, M. Mischi, H.H.M. Korsten, K.D. Reesink, P. Houthuizen
Non-invasive pulmonary transit time: a new parameter for global cardiac performance

OTHER TOPICS

M. Witjes, A. Kotsopoulos, **I.H.F. Herold,** L. Otterspoor, K. Simons, J. van Vliet, M. de Blauw, B. Festen, J. Eijkenboom, N.E. Jansen, J.G. van der Hoeven, W.F. Abdo.
The influence of end-of-life care on organ donor potential
Submitted

T. Masarwa, **I.H.F. Herold,** M. Tabor, R.A. Bouwman
Unilateral coal cord paralysis following insertion of a supreme laryngeal mask in a patient with Sjögren's syndrome
Submitted

R.I. de Groot, O.M. Dekkers, **I.H.F. Herold**, E. de Jonge, M.S. Arbous.
Risk factors and outcomes after unplanned extubations on the ICU: a case-control study.

Crit Care 2011; 15(1): R19

P.M. van Kruchten, J.M. Vermelis, **I. Herold**, A.A. van Zundert.
Hypotonic and isotonic fluid overload as a complication of hysteroscopic procedures: two case reports.
Minerva Anestesiol 2010 May; 76(5): 373-7

K.H. Polderman, **I. Herold**
Therapeutic hypothermia and controlled normothermia in the intensive care unit: practical considerations, side effects, and cooling methods.
Crit Care Med 2009 Mar; 37(3): 1101-20 review

C.J. Hukshorn, **I.H. Herold**, G.T. Sieswerda, J. Kesecioglu
Pneumoperitoneum mimicking acute myocardial infarction
Acta Anaesthesiol Scand 2008 Nov; 52(10): 1437-8.

O.L. Cremer, **I.H. Herold**, A.J. Slooter
Immunosuppression and multidrug-resistant bacteria in the intensive care unit: a cohort study
Crit Care Med 2007; 35: 2465-6; author reply 2466

CONFERENCE PAPERS

E. Maas, **I.H.F. Herold**, M.P.J. Kuenen, A. Bindels, M. Mischi, H.H.M. Korsten
Measurement of blood volumes using ultrasound contrast agents compared with thermo-dilution technique, an in vitro study
NTvA, 2010: 22-4

I.H.F. Herold, G Russo, H.C. van Assen, H.H. Korsten, M. Mischi
Volume quantification by contrast-enhanced ultrasound and thermodilution: an in vitro comparison
Crit Care 2013; 17: P200

S. Saporito, **I.H.F.Herold,** P. Houthuizen, H.H.M. Korsten, H.C. van Assen, M. Mischi.
Automatic blood pool identification in contrast ultrasound using principal component analysis
IEEE 11th (ISBI), 2014 International Symposium on Biomedical Imaging; 2014: 1168-71

NATIONAL AND INTERNATIONAL PRESENTATIONS

I.H.F. Herold, M.P.J. Kuenen, M.Mischi, H.H.M. Korsten
Blood volume and ejection fraction measurements using CEUS
15th European symposium on ultrasound contrast imaging. Rotterdam 21 jan. 2010 - Poster presentation

I.H. F. Herold, G. Russo, H.C. van Assen, H.H.M. Korsten, M. Mischi
Volume quantification by contrast-enhanced ultrasound and thermodilution: an in vitro comparison
15th ISICM congress 2013 Brussels - Poster presentation

I.H.F. Herold, R. A. Bouwman, H.H.M. Korsten
Pulmonary blood volume measured by contrast enhanced ultrasound: a comparinson with transpulmonary thermodilution
Annual meeting NVA sectie cardio-anesthesiologie, Eindhoven 14-11-2015 - Oral presentation

I.H.F. Herold, S. Saporito, M. Mischi, R.A. Bouwman, H.C. van Assen, H.C.M. van den Bosch, A.G.W. de Lepper, H.H.M. Korsten, P. Houthuizen
Pulmonary transit time by contrast enhanced ultrasound as parameter for cardiac performance: a comparison with magnetic resonance imaging and NT-ProBNP
19th Annual meeting of the European association of cardiovascular imaging (EuroEcho Imaging) 2015 Seville, 2015. Poster presentation

A.G.W. de Lepper, I.H.F. Herold, S. Saporito, R.A. Bouwman, H.H.M. Korsten, K.D. Reesink, P. Houthuizen.
Non-invasive pulmonary transit time: a new parameter for global cardiac performance
Accepted for the 20th Annual meeting of the European association of cardiovascular imaging (EuroEcho Imaging) 2016

List of abbreviations

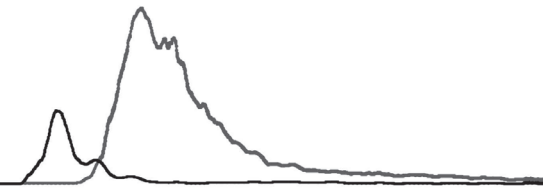

AI	Acoustic intensity
ANOVA	Analysis of variance
AUC	Area under the curve
BMI	Body mass index
BSA	Body surface area
CEUS	Contrast enhanced ultrasound
CO	Cardiac output
CRT	Cardiac resynchronization therapy
DCE-MRI	Dynamic contrast-enhanced magnetic resonance imaging
DSt	Down slope time
EF	Ejection fraction
EVLW	Extravascular lung water
FS	Frank Starling
GEDV	Global end-diastolic volume
HF	Heart failure
HV	Healthy volunteer
ICC	Intraclass-correlation coefficient
IDC	Indicator dilution curve
ITBV	Intrathoracic blood volume
ITTV	Intrathoracic total volume
IQR	Interquartile range
IVMD	Intraventricular mechanical delay
LA	Left atrium
Lamda	λ, skewness of indicator dilution curve estimated by LDRW model
LBBB	Left bundle branch block
LDRW	Local density random walk
LV	Left ventricle
LVESV	Left ventricular end-systolic volume
LVEDV	Left ventricular end-diastolic volume
MLWHF	Minnesota Living With Heart Failure questionnaire
MR	Mitral regurgitation
MRI	Magnetic resonance imaging
MTT	Mean transit time
Mu	μ, mean transit time estimated by local density random walk model
NYHA	New York Heart association functional class
nPTT	Normalized pulmonary transit time
NT-proBNP	N-terminal pro-B-type natriuretic peptide
NYHA	New York Heart Association classification
PAC	Pulmonary artery catheter

PBV	Pulmonary blood volume
PC-MRI	Phase contrast magnetic resonance imaging
PTT	Pulmonary transit time
PTV	Pulmonary total volume
QOL	Quality of life
RA	Right atrium
ROI	Region of interest
RV	Right ventricle
SD	Standard deviation
SNR	Signal-to-noise ratio
SPWMD	Septal to posterior wall mechanical delay
SV	Stroke volume
TAPSE	Tricuspid annular plane systolic elevation
TEE	Trans-esophageal echocardiography
TPTD	Transpulmonary thermodilution
TR	Tricuspid regurgitation
TTE	Trans-thoracic echocardiography
TTP	Time to peak
UCA	Ultrasound contrast agent
QoL	Quality of life